On the Potential of a Weather-Related Road Surface Condition Sensor Using an Adaptive Generic Framework in the Context of Future Vehicle Technology

Von der Fakultät für Ingenieurwissenschaften,

Abteilung Maschinenbau und Verfahrenstechnik der

Universität Duisburg-Essen

zur Erlangung des akademischen Grades

eines

Doktors der Ingenieurwissenschaften

Dr.-Ing.

genehmigte Dissertation

von

Thomas Weber

aus

Kamp-Lintfort

Gutachter:

Prof. Dr.-Ing. Dr. h.c. Dieter Schramm

Prof. Zsolt Szalay, Ph.D.

Tag der mündlichen Prüfung: 21. Dezember 2021

Abstract

Mobility is one of the fundamental and essential elements in our modern globalized society. The European Commission (EC) has formulated five main challenges for current and future transport systems: Further development of the European transport area, rising resource costs, pollution, infrastructure congestion, and road traffic safety. In this context, the present thesis deals with the question to what extent future vehicle systems can be examined a priori regarding their potential effectiveness concerning the dimensions: safety, efficiency, and comfort.

For this purpose, a general research method is derived based on a status quo analysis, which in principle makes it possible to consider various perspectives and impact dimensions in the complex environment of modern and future mobility. Since often only models or, at best, initial prototypes of future vehicle systems exist in the early development phase, an approach is required that is primarily based on simulations. The thesis combines existing approaches and extends them by various dimensions. Subsequently, this methodology is applied to a novel sensor system for detecting weather-related road surface conditions, which has been prototypically developed within the framework of a joint research project. An extended potential analysis is carried out based on this sensor system, whereby the impact dimensions frequently mentioned in vehicle technology - safety, efficiency, and comfort - are considered both at the individual vehicle level and at the traffic level. Since this sensor system only exists as a prototype so far, several new simulation models from the areas of driver assistance, driver behavior, and the environment are developed and evaluated in addition to a digital sensor model as part of this thesis.

The thesis shows that the applied research method addresses both the general and various specific research questions. It turns out that knowledge of the weather-related road conditions has excellent potential for the safety dimension. For example, on the vehicle level, a braking distance reduction between 2 % and 11 % and a lateral stabilization during braking maneuvers in curves can be achieved by reducing the lateral deviation of up to 5 % through the optimization of corresponding vehicle systems. Furthermore, a reduction between 46 % and 53 % of potentially critical driving situations at high vehicle equipment rates is determined for the traffic level. Concerning efficiency, both positive and negative effects are shown in the sense of a traffic-stabilizing effect and adverse effects due to longer distances and the associated higher energy consumption. In terms of comfort, the results suggest that by increasing the availability of automated systems through knowledge of the dynamic driving limits, a reduction of manual driving times by up to 60 % is possible.

Kurzfassung

Mobilität ist eines der wesentlichen Bedürfnisse unserer modernen globalisierten Gesellschaft. Die Europäische Kommission hat fünf große Herausforderungen für die derzeitigen und zukünftigen Verkehrssysteme formuliert: Weiterentwicklung des europäischen Verkehrsraums, steigende Ressourcenkosten, Umweltverschmutzung, Überlastung der Infrastruktur und Sicherheit im Straßenverkehr. In diesem Zusammenhang beschäftigt sich die vorliegende Arbeit mit der Frage, inwieweit zukünftige Fahrzeugsysteme a priori auf ihre potentielle Wirksamkeit hinsichtlich der Dimensionen Sicherheit, Effizienz und Komfort untersucht werden können.

Dafür wird zunächst auf Basis einer Status quo Analyse eine allgemeine Vorgehensweise abgeleitet, welche es grundsätzlich ermöglicht alle möglichen Blickwinkel und Wirkdimensionen im komplexen Umfeld moderner und zukünftiger Mobilität zu berücksichtigen. Da von zukünftigen Fahrzeugsystemen in der frühen Entwicklungsphase häufig lediglich Modelle oder allenfalls erste Prototypen existieren, bedarf es eines Ansatzes, der im Schwerpunkt auf Simulationen basiert. Die Thesis verbindet hierfür existierende Ansätze und erweitert diese um diverse Dimensionen. Anschließend wird diese Methodik auf ein neuartiges Sensorsystem zur Erfassung des witterungsbedingten Fahrbahnoberflächenzustandes angewendet, welches prototypisch im Rahmen eines Verbundforschungsprojektes entwickelt wurde. Für dieses Sensorsystem wird eine erweiterte Potenzialanalyse bezüglich der oben genannten Dimensionen durchgeführt. Da dieses Sensorsystem bisher nur prototypisch existiert, werden im Rahmen dieser Thesis neben einem digitalen Sensormodell auch eine Reihe von neuen Simulationsmodellen aus den Bereichen Fahrerassistenz, Fahrerverhalten und Umwelt entwickelt.

Es wird gezeigt, dass es durch die vorgestellte Methodik möglich ist sowohl allgemeine als auch spezifische Forschungsfragen in diesem Kontext zu bearbeiten. Es stellt sich heraus, dass die Kenntnis des witterungsbedingten Fahrbahnzustandes ein großes Potenzial für die Wirkdimension Sicherheit besitzt. Auf der Fahrzeugebene kann durch die Optimierung entsprechender Systeme beispielsweise eine Bremswegverkürzung zwischen 2 % und 11 % sowie eine laterale Stabilisierung bei Bremsmanövern in der Kurve, angezeigt durch eine Reduktion der lateralen Ablage von bis zu 5 %, erreicht werden. Für die Verkehrsebene wird eine Reduktion von potenziell kritischen Fahrsituationen bei hohen Ausrüstungsraten in den Fahrzeugen zwischen 46 % und 53 % ermittelt. Bezüglich der Effizienz werden sowohl positive Effekte im Sinne einer verkehrsstabilisierenden Wirkung aufgezeigt, jedoch auch negative Effekte durch verlängerte Wegstrecken und damit verbundenen höherem Energieeinsatz. Im Sinne des Komforts wird gezeigt, dass durch eine Erhöhung der Verfügbarkeit von automatisierten Systemen durch die Kenntnis der fahrdynamischen Grenzen eine Reduzierung der manuellen Lenkzeiten um bis zu 60 % möglich ist.

Acknowledgments

For me, as for so many others, the completion of my dissertation marks the end of an exceptionally rewarding and exciting phase in my career. My most sincere gratitude goes first to Prof. Dr.-Ing. Dr. h.c. Dieter Schramm. As an advisor and, in general, as a leader and boss, he was and is a shining example to me through his sheer tireless commitment, constant availability, and flexibility in problem and solution orientation. The freedom we enjoy at the chair in research and teaching is not self-evident and has also contributed significantly to the success of the work.

I would also like to thank my second examiner Prof. Zsolt Szalay, Ph.D., for his meticulous work and many valuable suggestions, especially in the final phase of the thesis. I remember with pleasure our personal meeting in Zalaegerszeg and hope that we can remain friendly and connected in joint projects in the future.

I would like to thank the chairman of the examination board, Prof. Dr.-Ing. Bettar Ould el Moctar, and the assessor, Prof. Dr.-Ing. Reinhard Schiffers, for the smooth running of the examination during this sometimes difficult pandemic period.

Not least, I would like to thank the many dear colleagues at the chair who, through the countless personal and professional discussions, always ensure an extremely pleasant atmosphere and the mental exchange and distraction necessary for the success of such work. Patrizia, Frank, Frédéric, Philipp, Patrick, Sebastian x2, Max x2, Kai, Christian, Patrik, Tobias, Roland, Markus, Martin, Niko, Ingmar, Michael x2 and all those I have overlooked my heartfelt thanks!

I thank my family for patiently enduring the phases of my mental absence, especially towards the end of the process. Finally, my special thanks go to Lisa; you are an essential support in all my undertakings.

Contents

List of Figures

List of Tables

List of Abbreviations

AAA	American Automotive Association
ABS	Anti-Lock Braking System
ACC	Adaptive Cruise Control
ADAS	Advanced Driver Assistance Systems
AIS	Abbreviated Injury Scale
BASt	German Federal Highway Research Institute (Bundesanstalt für Straßenwesen)
BSM	Basic Safety Message
CA	Certification Authority
CAM	Cooperative Awareness Message
CAS	Collision Avoidance System
CEN	Committee for Standardization
C-ITS	Cooperative Intelligent Transportation System
COG	Center Of Gravity
DDT	Dynamic Driving Task
DENM	Decentralized Environmental Notification Message
DSRC	Dedicated Short Range Communication
EBA	Electronic Brake Assistant
EC	European Commission
ESA	Electronic Steering Assistant
ESB	Electronic Steering and Braking
ESC	Electronic Stability Control
ETSI	European Telecommunications Standards Institute
EU	European Union
EVA	Emergency Vehicle Alert
FCC	Federal Communications Commission
FCD	Floating Car Data
FCP	Forward Collision Prevention
FCW	Forward Collision Warning
GIDAS	Gernam In-Depth Accident Study
GNSS	Global Navigation Sattelite System
GSM	Global System for Mobile Communications
HMI	Human-Machine Interface
IDIS	Intelligent Driver Information System
IEEE	Institute of Electrical and Electronics Engineers
IRF	Injury Risk Funktion
ISO	International Standardization Organization
ITS	Intelligent Transportation System
JSON	JavaScript Object Notation
KML	Keyhole Markup Language

LCA	Lane Change Assistant
LDM	Local Dynamic Map
LKA	Lane Keeping Assistant
LTE	Long Term Evolution
NGO	Non-Governmental Organizations
NHTSA	National Highway Traffic Safety Administration
ODD	Operational Design Domain
OEDR	Object and Event Detection, Recognition , Classification, and Response
OEM	Original Equipment Manufacturer
OSI	Open Systems Interconnection
PDU	Protocol Data Unit
PID	Porsche InnoDrive
PKI	Public Key Infrastructure
PSM	Personal Safety Message
RFC	Request for Comments
RSACC	Road Surface Condition Aware Adaptive Cruise Control
RSCA	Road Surface Condition Aware
RSU	Road Side Unit
SAE	Society of Automotive Engineers
SciL	Scenario-in-the-Loop
SPAT	Signal Phasing And Timing
TCP	Transmission Control Protocol
TCS	Traction Control System
TMC	Traffic Message Channel
TR	Technical Report
TraCI	Traffic Control Interface
TS	Technical Specification
UDP	User Datagram Protocol
UMTS	Universal Mobile Telecommunications System
V2V	Vehicle-to-Vehicle
V2X	Vehicle-to-X
VDA	German Association of the Automotive Industry
WAVE	Wireless Access in Vehicular Environments
WHO	World Health Organization
WRI	World Resources Institute
WLAN	Wireless Local Area Network
WRSCS	Weather-Related Road Surface Condition Sensor
WSMP	Wave Short Message Protocol
XiL	X-in-the-Loop
XML	Extensible Markup Language

1 Introduction

The automotive industry is facing increasing challenges in the course of ongoing social, economic, and political global changes. Future vehicle systems will be exposed to increasingly multifaceted and differentiated mobility solutions, while new products and services are likely to change the perspective on using means of transport. Therefore, manufacturers need to evaluate the potential of different options early to maintain competitiveness in the long term. This thesis aims to contribute to this by presenting an appropriate research methodology and applying it to a system for weather-related road surface detection. This Chapter describes the problem, raises the central research question, summarizes the main contributions, and gives an overview of the structure of the thesis.

1.1 Motivation

Mobility is one of the fundamental and essential elements in our modern global society. According to (Cornet et al. 2012), people spent 6.4 trillion Euros worldwide in 2010 for individual mobility and transportation of goods. In the private transport sector, no mode of transportation is as important as the automobile. In 2017 passenger cars made up 85 % of total passenger transport in Germany, amounting to a total distance of 642.4 billion kilometers. (Nobis and Kuhnimhof 2018) In this context, the European Commission (EC 2011) has formulated five main challenges for current and future transport systems in its White Paper "Roadmap to a Single European Transport Area - Towards a competitive and resource-efficient transport system: Further development of the European transport area, rising resource costs, pollution, infrastructure congestion, and road traffic safety".

Traffic safety is still a significant challenge worldwide today. While the number of road deaths reported by (Destatis 2020) has remained almost constant in Germany over the last five years at around 3,300 deaths annually, the World Health Organization (WHO 2018) reports that the global trend has been rising steadily to around 1.35 million deaths in 2016. Thus, it is not surprising that both the WHO and the EC have formulated declarations of intent to stabilize or reduce the number of road deaths (EC 2011; WHO 2018). In each case, different areas are mentioned in which specific measures can contribute to increasing road safety. These include traffic management, infrastructure, rescue management, and road users, including passenger cars. Many governments support industry and research institutions because of this, e.g., within the framework of publicly funded

research programs, to find new and innovative solutions for these challenges in future vehicle generations, especially in the context of the advancing automation and connectivity of passenger cars.

One of these projects was the publicly funded research project "Seeroad" (Weber and Schramm 2020b), which ran parallel to the writing of this thesis and whose goal was an innovative sensor system for autonomous detection of the weather-related road condition. With the derived values of the vehicle's static friction on the road, a higher level of safety for the vehicle occupants and other road users should be achieved, especially during demanding driving maneuvers in the transition to partially or fully automated driving. Several methods for road condition detection are already known from the literature, such as stationary systems, monitoring by special measurement vehicles, and indirect measurements via the chassis dynamics. However, all these approaches have individual weaknesses and until today no commercially available system for this purpose for direct measurement in the automobile is known (Krieger et al. 2020).

This thesis will mainly discuss this weather-related road surface condition sensor (WRSCS) as a technical system and exemplary application to increase the active safety of passenger cars that can help address individual and traffic safety issues. It also extends existing methods to assess the WRSCS' extended potential impact in the early stages of the system development to address some of the described challenges concerning safety, comfort, and efficiency.

1.2 Problem Definition and Research Question

The transportation sciences strive to create measures and framework conditions that ensure safe and congestion-free traffic conditions in their various disciplines. In addition to developing new systems and measures, testing and assessing their impact or effect are essential. The clear and valid determination of the potential of new technologies or measures supports and enables the target-oriented selection and implementation of promising innovations. The effects of new systems on the transportation system in terms of road safety and traffic efficiency often need to be determined in advance, meaning before the actual physical availability of these systems. Due to this unavailability of prototypes, experimental tests in the natural environment are often either not possible or highly cost-intensive and show only minor verifiable effects on the overall system. Additionally, the potentials of a new system often cannot be demonstrated in a clear, comprehensive, and comparable manner in the natural environment, whether due to uncontrollable complexity or unswayable external conditions.

Nevertheless, there are still possibilities to assess the effectiveness a priori. Data availability and quality strongly influence prediction accuracy, and existing approaches require a high level of effort and expert knowledge. Simulation models are standard and cost-efficient tools for supporting development and impact assessment. The most significant advantage of simulations is that individual model parameters can be changed ceteris paribus, and effects can be determined and

compared under otherwise identical boundary conditions. However, previous works in this field are often limited to individual aspects of a specific problem. They consider only certain functions or systems – often specific driver assistance systems (DAS) – and their effect in particular situations. Some studies also suggest generic processes and frameworks for an extended consideration of effectiveness. However, no approach unites all dimensions. A comprehensive summary of the state of research can be found in the following Chapter 2, which covers the fundamentals.

The main target of developing new and better assistance systems is often the improvement of road safety in general, as driver misconduct is still the leading cause for road accidents, with a share of over 90 % (Destatis 2018) in Germany. The problem in this context is that all assistance systems currently available in series production are based on the premise that it is the driver's responsibility to adapt the driving style to the prevailing environmental conditions. However, as systems are increasingly automated, this responsibility will increasingly have to be transferred from the driver to the system. It is essential to have an extended situational awareness, such as knowledge of the current state of the road's surface condition, to make system-led decisions about the type and extent of intervention in critical driving situations possible. Safety is only one of the possible dimensions that a new system may address when considering vehicle technology. Therefore, the **central research question** in this thesis is **whether and how it is possible to carry out a generalized a priori analysis and evaluation of the potential of future vehicle systems or functions**, which may initially only exist as an idea or concept. The mentioned system for detecting the current weather-related road condition (WRSCS) serves as an exemplary application for investigating this question, which will be further broken down into more specific and measurable research questions (RQs) after a systematic system analysis and stakeholder identification in Section 3.4.

1.3 Contribution and Thesis Outline

Based on an in-depth analysis of existing approaches and methods, a research method is presented, answering the central research question and all specific aspects raised in the following. The application of the method requires the design and development of some novel simulation models that form the notable contributions of the thesis:

- the derivation of a general method for a priori evaluation of future vehicle systems,
- the implementation of a framework for the simulation-based investigation of system influences on the vehicle and traffic level,
- the road surface-sensitive enhancement of several control systems,
  - Antilock braking system (ABS)
  - Emergency steer and brake assist (ESB)
  - Adaptive cruise control (ACC)
- the development of a road surface condition sensitive driver model,
- the design of a sensor model based on a road surface sensor prototype,

- the extension of a traffic flow simulation environment by a weather module,
- the application of the method and framework to investigate the potential of a weather-related road surface condition sensor (WRSCS).

For this purpose, the thesis is structured as follows. Chapter 2 covers the fundamentals of the current traffic and vehicle technology regarding the thesis's scope. On the one hand, the concepts of potential, safety, efficiency, and comfort are discussed, and on the other hand, the technical fundamentals of advanced driver assistance systems (ADAS), automated driving systems (ADS), and vehicle networking (V2X). This Chapter concludes by looking at the simulation models commonly used in this context, which in principle enable an a priori evaluation.

In Chapter 3, a method for the a priori evaluation of new transportation-related systems is derived from the fundamentals given in the previous Chapter 2 in the form of a general procedure model. The method is subsequently applied to a sensor for measuring and classifying the weather-related road surface condition. After analyzing this system comprehensively, further specific research questions are formulated regarding its potential. The Chapter ends with the selection of suitable tools for the investigation of these questions.

Chapter 4 describes the modeling and implementation of the selected tools and systems. The implementation includes an environment model, a vehicle model, assistance systems on the stabilization level, the guidance level, the navigation level, a driver model, and traffic models. It also covers the implementation of networking between them.

Chapter 5 forms the core of the simulation studies based on the specific research questions formulated using the very tools implemented. The chapter is subdivided into the vehicle and traffic levels, whereby several different simulations are carried out to estimate the potential, ranging from standardized individual driving maneuvers to complex traffic scenarios. It ends with a discussion of the main findings.

Finally, Chapter 6 summarizes the core of the thesis and gives a brief outlook on other possible application areas.

2 Fundamentals

This Chapter briefly describes the essential basics of the thesis. In addition to the introduction and definition of necessary terms, modern advanced driver assistant systems (ADAS) and automated driving systems (ADS) are examined in more detail. It presents the state-of-the-art in vehicle networking (V2X), a detailed introduction to existing approaches to prospective effectiveness assessment, and an overview of relevant simulation models for the scope of the thesis. The fundamentals provide a context for the subsequent derivation of an adequate research method as well as for the implementation and investigation of the research questions.

2.1 Potential

The Oxford English dictionary defines the noun "potential" as "the possibility of something happening or being developed or used" (Simpson et al. 1989). This very general definition should first be narrowed down for vehicle and traffic technology. In this discipline, the core elements are the entities driver, vehicle, and environment, which are always in a complementary relationship (Donges 1982; Winner et al. 2015). Any influence on one of these elements or sub-elements always impacts other elements. At first, these elements may be understood as rather abstract constructs.

For example, a vehicle can transport people or goods by land, sea, or air. In the further course of the thesis, however, the term will generally refer to passenger cars.

A driver is initially someone or something driving or operating such a vehicle. Given the increasingly networked and automated mobility of the future, this includes a human person and artificial systems that take over this task partly or entirely. The following Sections, 2.2 and 2.3, will deal explicitly with such systems.

In addition to the natural ecological environment, the term environment can generally mean infrastructure, static and dynamic objects, other traffic participants, or regulatory conditions.

The impacts or effects due to the complementary relationship are often divided into three categories or dimensions: safety, efficiency, and comfort. Table 2.1 shows a brief overview of the relationships between the core elements of mobility and their impact dimensions.

Table 2.1: Core elements of mobility and the prominent impact dimensions

	Vehicle	Driver	Environment
Safety	Active Passive	Health Attention Awareness	Accidents Policies Procedures
Efficiency	Energy Economic	Route Foresight Behavior	Sustainability Eco-Efficiency Level of Service
Comfort	Chassis Suspension Interior	Noise Vibration Driving Style	Quality of Life

For the scope of the thesis, the term potential ergo refers to precisely these dimensions of impact, which will now be examined in more detail.

2.1.1 Safety

In this thesis, the term safety refers to road safety and leaves areas such as air, rail, and sea traffic unconsidered. Safety is often intuitively equated with the number - or rather the absence - of countable accidents. Worldwide, the number of road deaths increased from 1.15 million deaths in 2000 to 1.35 million deaths in 2016, with a further increasing tendency. However, the (WHO 2018) reported a slight decline over the same period from 18.8 to 18.2 deaths per 100,000 population in relative terms. (WHO 2018) The trend is much more evident for most industrial countries, including Germany.

Figure 2.1 shows that the annual number of road deaths declined continuously from over 20,000 in the 1970s to just over 3,000 in recent years. (Destatis 2018) attributes the decline to various measures, such as introducing mandatory maximum speeds on country roads, introducing compulsory seat belts, or lowering alcohol limits, and the simultaneous improvement of active and passive vehicle safety systems such as the development of the anti-lock braking system (ABS) or the electronic stability control system (ESC). However, this number has remained almost constant over the last five years and that there is currently no trend for further improvement.

However, this pure consideration of road fatalities as a measure of road safety falls short for various reasons. (Schnieder and Schnieder 2013) state that this term conceals a complex network of social, financial, economic, technical, and, not least, legal aspects and that there can therefore be no uniform, all-encompassing definition of the term. Because of this, especially the effectiveness of new systems towards safety is relevant to various stakeholders for different reasons.

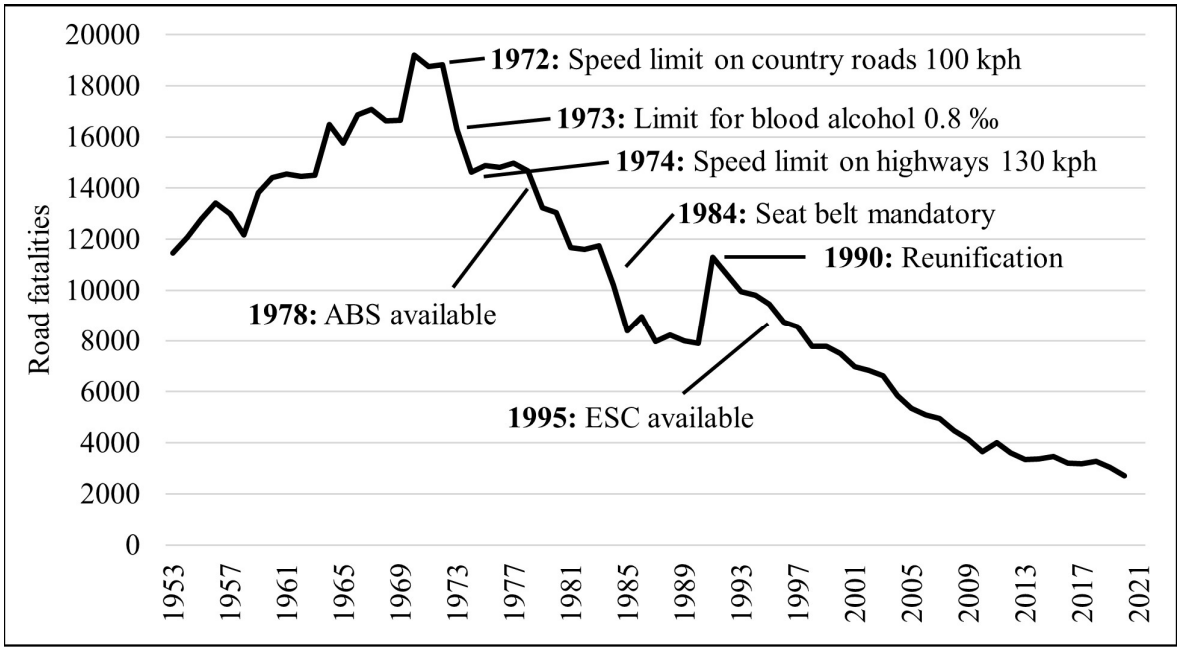

Figure 2.1: Number of road fatalities in Germany over the years (Schramm et al. 2020)

The legislation relies mainly on these figures to formulate its targets and decision-making, such as halving the number of road deaths in the EU by 2020 (EC 2011). It additionally relies on the research results and information from original equipment manufacturers (OEMs) on the effectiveness of a new system to bring about policy measures to improve road safety, such as the mandatory introduction of specific systems for new vehicles via the registration authorities. Regulation (EC) No 226/2009 (EC 2009) introduced an ESC and a tire pressure monitor system for new cars as mandatory requirements for the European market in November 2014, for example.

For vehicle manufacturers, the question of the effectiveness of technical systems on road safety tends to be dominated by economic aspects. Since significant investments always accompany new systems, the question arises as to whether these investments are justified. Especially in the early stages of development, costs must be included in the potential benefits of safety, customer acceptance, and willingness to pay.

Within research, the impact on traffic is particularly relevant in research projects that look at individual systems in isolation and consider the challenges facing society. This does not involve the development of systems to series maturity but rather the evaluation of technical feasibility and the identification of initial tendencies towards effectiveness. Especially regarding highly and fully automated driving systems, researchers must consider technical questions alongside social and legal ones. Some studies, such as (Pinter et al. 2021), focus on using onboard data recorders for accident reconstructions and liability investigations with respect to the changing responsibilities for highly automated vehicles (Pinter et al. 2017). But also larger projects such as AdaptIVe (Etemad 2017), ALFASY (Schweig et al. 2018), or Seeroad (Weber and Schramm 2020a) lay the

foundations. The results are available to other stakeholders, making the further development process more targeted on the one hand and driving the political framework process forward on the other hand.

There are also several other stakeholders, of whom only the insurance companies are mentioned here. According to figures from the Gesamtverband der Deutschen Versicherungswirtschaft e.V. (GDV) (Association of the German Insurance Industry), the gross claims payment of motor vehicle liability insurance in Germany in 2018 amounted to 14,885 million Euros. Systems that increase road safety by avoiding accidents or reducing the consequences of accidents can reduce overall damage costs and thus affect companies' business success. On the other hand, insurance companies can promote and support such systems without political pressure, for example, through discounts. In these considerations, less use is made of metrics that quantify the risk potential of a situation but instead of mathematically derived quantities of the consequences of accidents such as the amount of damage or severity of injuries.

Therefore, it is clear why the concept of road safety is a complex one. In the context of this thesis, road safety is to be understood as the absence of concrete accidents and the avoidance of risks and dangers when using the traffic infrastructure. This definition is based on the works of (Hoffmann 2013) and (Schramm et al. 2020). Accordingly, an accident-free traffic situation does not have to be inherently safe because a safe situation also implies the absence of danger. In this context, the term "danger" refers to a threat that potentially harms a person or an object. Of course, with this definition, there are no safe situations in road traffic, but a condition can be described as safe if all existing risks are below a justifiable border risk. In traffic safety research, situations that hold a higher risk are called conflict situations, and their probability of occurrence in road traffic is thus a measurement for safety. Especially with emerging automated driving functions, (Lengyel et al. 2020) and (Szalay et al. 2019) summarize several problematic situations and offer solutions to deal with the subject using simulation, scenario-in-the-loop, and proving ground approaches. A possible definition of a conflict situation is when two or more road users approach each other in place and time so that a collision would occur if their movement did not change.

For a qualitative and quantitative classification of these situations, especially in terms of criticality, substitute parameters are used in traffic safety research. They are usually derived based on physically measurable information of the participating vehicles. Those are, on the one hand, data about the actual state of motion such as position (s), velocity (v), acceleration (a), and characteristics derived from the relative movements of the vehicles. These include the net distance, the time headway, and the time to collision, as well as other use-case-dependent parameters. (Minderhoud and Bovy 2001)

The net distance d_{n}, which is the spatial distance from the front edge of a vehicle to the rear edge of the preceding vehicle:

$$d_{\mathrm{n}} = \left| s_{\mathrm{ego}} - s_{\mathrm{foe}} \right|. \tag{2.1}$$

The time headway t_{hw} as the amount of time a vehicle would need at its current speed v to cover the current net distance d_{n}. Suppose the time headway decreases to a value below the driver's reaction time or the intervention time of an automated system. In that case, it is no longer possible to appropriately react to changes in the motion of the preceding vehicle

$$t_{\mathrm{hw}} = \frac{d_{\mathrm{n}}}{v}. \tag{2.2}$$

The time to collision describes the time it would take for a crash between two consecutive vehicles to occur if both do not change their speed over this period, so the difference speed δv remains constant. Since this is only relevant if the following vehicle drives faster, the time to collision is defined as

$$ttc = \begin{cases} \frac{d_{\mathrm{n}}}{\delta v} & \delta v > 0 \\ \infty & \delta v < 0 \end{cases}. \tag{2.3}$$

For these parameters, threshold values are used to differentiate between safe and unsafe states or classify different criticality levels based on field observation tests as described by (Benmimoun et al. 2011). They proposed three increasing hazard levels based on different threshold values for some of the parameters introduced above as criteria for identifying safety-critical driving situations based on filed operational test data, summarized in Table 2.2.

Table 2.2: Criteria for safety-critical driving situations (Benmimoun et al. 2011)

Hazard Level	Identification Criteria
1	▪ $t_{\mathrm{hw}} < 0.35$ s $\wedge$ $\delta v < 20$ kph ▪ $t_{\mathrm{hw}} < 0.50$ s $\wedge$ $\delta v > 20$ kph ▪ $ttc < 1.75$ s
2	▪ $t_{\mathrm{hw}} < 0.35$ s $\wedge$ $\delta v > 20$ kph ▪ $ttc < 1$ s with brake deceleration
3	▪ $ttc < 1$ s without any brake deceleration

However, even these thresholds are not standardized at all. Critical values for the *ttc*, for example, range from 10 s derived from empirical data of natural driver preferences to a minimum value of 2.5 s identified by (Park and Won 2006). They used recorded information from actual vehicle accidents to derive typical safety indicators that have often been identified as the threshold for triggering an accident. These findings support the assessment of (Minderhoud and Bovy 2001), who place the threshold between 4 s and 2.6 s. Therefore, the use of absolute values may have to be critically examined. However, the relative differences between different scenarios and their

influence on traffic safety can provide a good insight into the effects of new systems, as shown in the further course of this thesis.

Studies on the effect of automated vehicle systems on road safety base their statements primarily on simulations conducted and assume that accidents caused by human error could largely be avoided using automation systems. In an exemplary study based on the simulation approach, different highway scenarios are calibrated using actual traffic data. Then the occurrence of conflict situations, depending on the share of self-driving vehicles in the total traffic, is measured. (Papadoulis et al. 2019) find the event of conflict situations in the different scenarios reduced by 12-47 %, 50-80 %, 82-92 %, and 90-94 % for proportions of 25 %, 50 %, 75 %, and 100 % automated vehicles, respectively. Studies like (Fagnant and Kockelman 2015) make the general assumption that 100 % penetration of automated vehicles will avoid all accidents attributable to human error assume a reduction in accidents of up to 90 %. Even if it is not possible to precisely assess how accurate the estimates of the studies presented are, the trend toward a reduction in accidents due to automated driving is nevertheless clearly emerging. For the qualitative assessment of potentials of automatic driving operation, it is considered that increased usability of the automation systems already creates an intrinsic added value in road safety. As a quantifiable and, above all, measurable variable, the driving time in automated driving operation is also defined as the benchmark for assessing this qualitative variable.

2.1.2 Efficiency

Efficiency is generally the relationship between effort and benefit and is often measured as a ratio of quantified energy to distance traveled, e.g., amount of fuel used per km or miles per gallon (Mohanadass 2020). From a driver's perspective, the aspect of time might also be of considerable importance rather than the energetic aspect of the term. Efficiency in road transport can thus be viewed from different perspectives. The number of vehicles in use worldwide has increased steadily over the years, leading to problems such as increased traffic congestion, longer commutes, and increased risk of accidents (Rabsatt 2018). In large cities, traffic congestion contributes to high economic costs in the form of increased time loss, additional fuel consumption, and associated air pollution (Wang et al. 2009). Traditionally, the response to increasing traffic demand has been to expand and widen the road network. However, these solutions are not practical at all, or only to a certain extent, due to extraordinary costs and the associated complex planning, especially in areas with high population density (Arnott and Small 1994).

Nevertheless, still, a considerable amount of road capacity is not used efficiently today. Drivers usually react to traffic incidents only as soon as they are in the line of sight. Especially in dense traffic, these delayed reactions of individual vehicles can influence the following vehicles in a shockwave-like propagation. Without direct knowledge of the driver, (Sugiyama et al. 2008) and (Rabsatt 2018) show that this can lead to stop-and-go traffic scenarios for the following traffic. Automated driving and vehicle networking promise to remedy or improve this phenomenon by

anticipating and damping any shock waves early. (Wu et al. 2018) find that this stabilizing effect on traffic flow can already be expected with mixed traffic of automated and manual vehicles. In addition to the increased efficiency resulting from the reduction of stop-and-go scenarios, other positive effects can be expected from automated driving. For example, the systems' fast reaction times allow for smaller vehicle distances or enable all vehicles to start simultaneously at traffic lights. In this way, with sufficient penetration of automated vehicles, the capacity of the existing road network could be better utilized, thus increasing overall efficiency in both ways: energy and time efficiency.

Thus, a general definition of transport efficiency can be summarized as the extent to which a given transport input can satisfy the travel demand of people or goods in a transport system. (Gaitanidou and Bekiaris 2012) describe, characterize, and quantify traffic efficiency by several parameters, such as travel times, average speeds, road users per route segment and time, or traffic composition. The corresponding traffic flow parameters are traffic volume q in vehicles/hour, traffic density k in vehicles/km, and the average speed $\bar{v}$ in kph. Their typical relationships have already been determined and confirmed by empirical studies such as (Brilon and Geistefeldt 2010). Figure 2.2 shows these well-known relationships that are often depicted in so-called fundamental diagrams in traffic research.

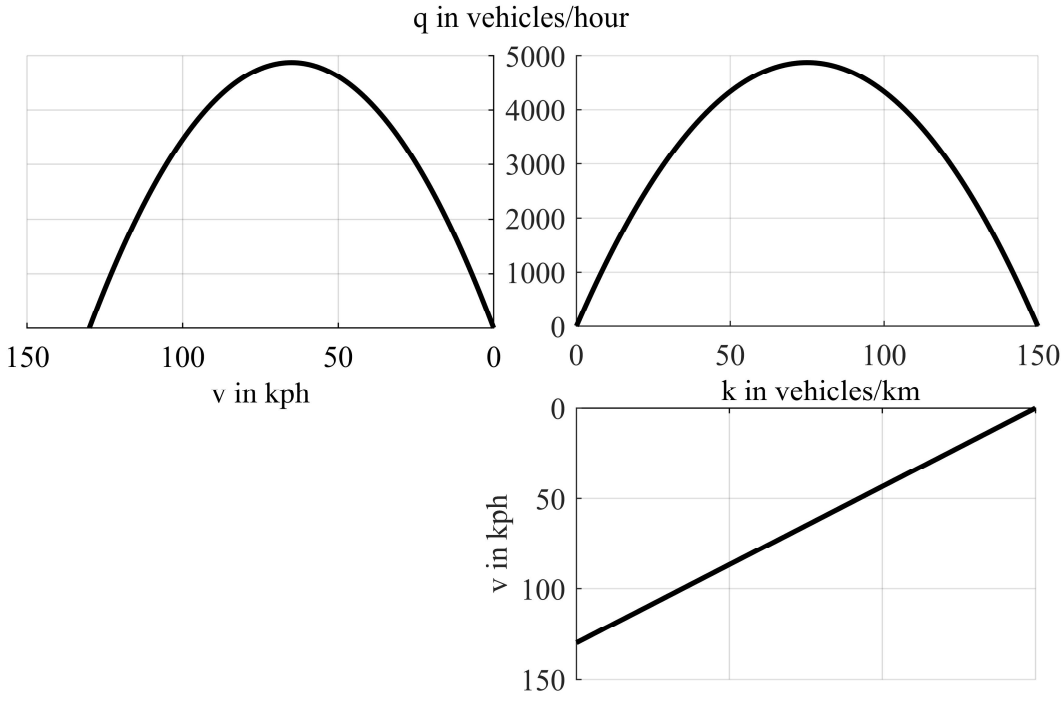

Figure 2.2: Fundamental diagrams of the traffic flow KPI relationship

The figure shows an established mathematical model of the traffic flow according to (Greenshields et al. 1935), applied to a two-lane highway with a maximum speed limited to 130 kph. The relationships according to this model are

$$v = v_f(1 - k/k_{max}), \tag{2.4}$$

$$q = v_f\, k(1 - k/k_{max}), \tag{2.5}$$

$$q = k_{max}\, v - (k_{max}/v_f)v^2, \tag{2.6}$$

where v_f describes the free traffic speed and k_{max} the maximum traffic density for a given road. With increasing traffic density (bottom right), the average drivable speed of all road users decreases. At the same time, there is a clear maximum in traffic volume (top right) at a traffic density of about 40 vehicles per kilometer, which corresponds to a stable flow of about 4,800 vehicles per hour and a safety distance of about 50 m. The diagram on the top left describes the relationship between the average speeds and the traffic volume. The parabolic nature of all the graphs is due to a distinction between stable and unstable traffic flows. There is hardly any obstruction from other road users in the former, while the latter means that free choice of speed or free overtaking is no longer possible.

Two crucial key densities of traffic flow are the critical density (k_c) and the jam density (k_j). The maximum density achievable under free flow is k_c, while k_j is the maximum density achieved under congestion. Figure 2.3 shows the location of those critical densities within the fundamental diagram of the flow density relationship.

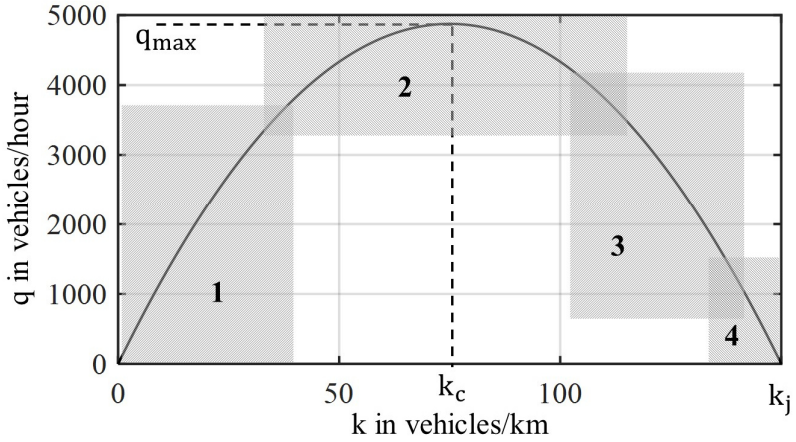

Figure 2.3: Critical and jam density in the flow density relationship

(Schnabel et al. 2011) introduce four distinct states of traffic flow based on these two parameters:

1. Free (unbound) flow ($k \ll k_c$), where the road user can choose his speed freely according to his wishes and the structural conditions. The condition is a very low traffic density.
2. Partially bound traffic ($k \approx k_c$), where there is a mutual influence as traffic density increases. Due to the decrease in overtaking opportunities, vehicles form groups of equal speed.

3. Bound traffic ($k_c < k < k_j$), where the further increase in traffic density leads to a further decrease in overtaking opportunities and, in extreme cases, to convoy traffic in which all vehicles drive at the same speed.
4. Traffic jam or "stop-and-go" ($k \approx k_j$), where the traffic density is too high to be handled in flowing traffic. Minor disturbances in the traffic flow cause a "traffic jam out of nowhere." The result is a bumpy traffic flow with constant changes between standing and driving at low speed. This traffic flow is unsatisfactory and leads to losses for the public, like higher emissions and loss of overall travel time.

2.1.3 Comfort

The human perceived sense of comfort in a defined environment is highly subjective, and an assessment of this can produce significant variations in respondents. (Corbridge 1987) divides driving comfort into three essential factors:

1. Dynamic factors (e.g., vibrations, shocks, and accelerations)
2. Environmental factors (e.g., air quality and conditioning, noise, pressure gradient)
3. Spatial factors (e.g., ergonomics of the passenger's position)

Although these factors are generally easy to measure and quantify, the difficulty lies in the objectification or transferability between different people, (Boyraz 2019; Festner 2019). According to (Hartwich et al. 2018), there is a further shift in relevance from ergonomic, vehicle-related factors to psychological ones regarding automated driving. Particularly in the early stages of market penetration, the occupants' perceived sense of safety and protection will represent basic needs. The driving style of autonomous vehicles could negatively impact comfort in this context, as shorter reaction times mean that they are practically able to make sharper turns or maintain smaller distances from other road users (Telpaz et al. 2018). Therefore, studies addressing this research question shift the focus from the pure technical implementation of autonomous driving to establishing comfortable driving styles and trajectories, (Bellem et al. 2018).

Other studies, like (van der Zwaag et al. 2012), show that even entertainment systems integrated into the vehicle, such as a music system, can increase driving comfort. In the scope of automated driving and the partial or complete transfer of the driving task, corresponding entertainment systems and alternative occupations will become increasingly relevant in the future. (Schiller et al. 2016) studied 2,100 German drivers on their willingness to use autonomous vehicles. The results showed that around 60 % of respondents see the additional time saved by relieving the driver of the driving task as the primary motivation for using an autonomous vehicle. From this point of view, the assessment of comfort can be directly related to the usability of the automation systems analogously to driving safety. Choosing this metric as the primary evaluation criterion for driving comfort is considered appropriate in this thesis since the usability of the automation systems also

represents the main optimization criterion for most investigated applications. Henceforth, increased driving time in automated driving mode is considered to influence driving comfort positively.

2.2 Advanced Driver Assistance Systems

With their functions, (advanced) driver assistance systems ((A)DAS) essentially address three core impact dimensions of the driving task, namely safety, comfort, and efficiency. The primary objective is to increase the quality and safety of modern mobility, on the one hand by reducing traffic accidents and environmental pollution, and on the other by increasing mobile efficiency in terms of energy, time, and resources. While these aspects are reflected in national (BMVI 2015) and international (EC 2011) political efforts – such as the above mentioned mandatory installation of electronic stability control systems within the EU in new vehicles since 2014 (EC 2009) – the focus in the area of increasing comfort is more on manufacturer-specific differentiation through the creation of individual customer benefits and the associated possibilities for monetization through specifically tailored products.

DAS today are generally divided into three categories to classify this complex and extensive field, with the central point of view being the division of tasks within the vehicle control between man and machine. A corresponding overview is shown in Table 2.3.

Table 2.3: Categorization of DAS based on (Winner et al. 2015)

Category A: Information and Warning Functions	**Category B: Continuously Automated Functions**	**Category C: Intervening Emergency Functions**
Only works indirectly via the driver on the vehicle guidance or navigation level.	Immediate influence on vehicle control (transmission by the driver; division of labor). It can always be overridden.	Direct influence on vehicle control in accident-prone situations, where the driver can no longer act.
Example: ▪ Traffic sign assistance (display of the speed limit) ▪ Lane departure warning (steering-wheel vibrations) ▪ Electronic horizon	Example: ▪ Adaptive cruise control ▪ Lane keeping assistance (LKA)	Example: ▪ Emergency Braking (system initiated) ▪ Evasion system (ESB)

The vehicle guidance tasks, in turn, are based on a 3-level structure model by (Donges 1982), which hierarchically divides the tasks into the stabilization task, the path guidance task, and the navigation task. Figure 2.4 shows the model schematically and assigns exemplarily some DAS to the corresponding levels. A stable driving condition shall be achieved at the stabilization level with high dynamics, which corresponds as closely as possible to the target condition specified by the

higher guidance level. It is irrelevant whether the command variables are set by the driver or by automated systems. The path guidance level forms the complex core of the vehicle guidance or dynamic driving task (DDT). The information about the route is transferred from the navigation level into a current target driving state concerning the lane, speed, and other dynamic properties, based on the prevailing surrounding conditions such as traffic, signage, and environmental conditions.

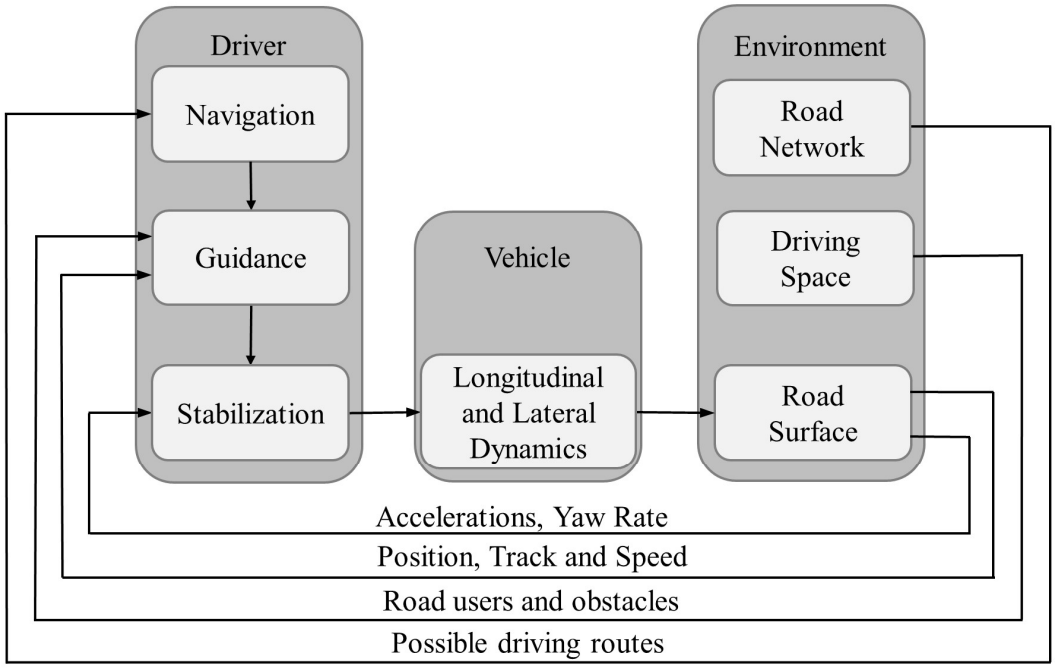

Figure 2.4: 3-level structure model of the driving task based on (Donges 1982)

The selection of an optimal route from the current position to any geographical target position forms the core of the navigation level, whereby optimal may be measured by individual parameters such as short, quick, or efficient. The increased availability and transferability of additional data, such as traffic and congestion information, enables increasing dynamization and linkage with the downstream levels. In addition to its function as an assistance system, navigation can also be understood as a sensor for other systems (Weber 2017). In the literature, terms such as “electronic horizon” (Winner et al. 2015) are frequently used for this purpose. At Porsche, for example, these functions are summarized under the term “Porsche InnoDrive” (PID), which at present essentially combines comfort and efficiency aspects through precise knowledge of the road network’s topography and translates them into a forward-looking driving strategy (Roth et al. 2011). The 3-levels of the driving task can also be characterized by their typical time horizons shown in Figure 2.5.

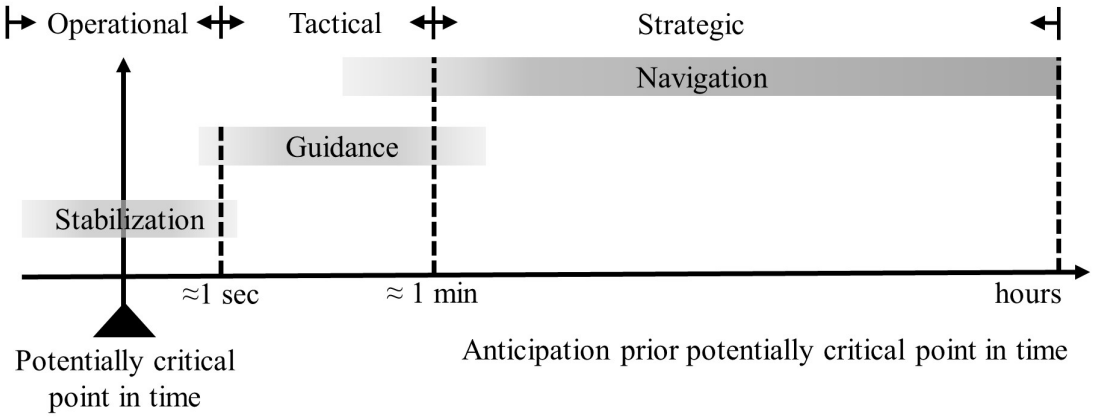

Figure 2.5: Typical time horizons of the driving task levels based on (Schramm et al. 2018)

The time horizon on the navigational level extends beyond the duration of a journey when including the preparation time from a few hours to the period of possible announcements of impending route changes in the range of a couple of minutes – as it is state-of-the-art for almost all popular navigation systems. This may also be referred to as the strategic level of the driving task, as it includes a considerable amount of long-term planning. The time horizon of the guidance level begins with the need to perceive the traffic and environmental situation and the road geometry to feed all information, warning, and intervention systems that require a kind of cognitive processing in a limited time. Timeframes typically range from a few seconds before a potential intervention to several tens of seconds, depending on the available sensors and spatial ranges. As this only permits a medium-term planning horizon, this level is referred to as the tactical level of the driving task.

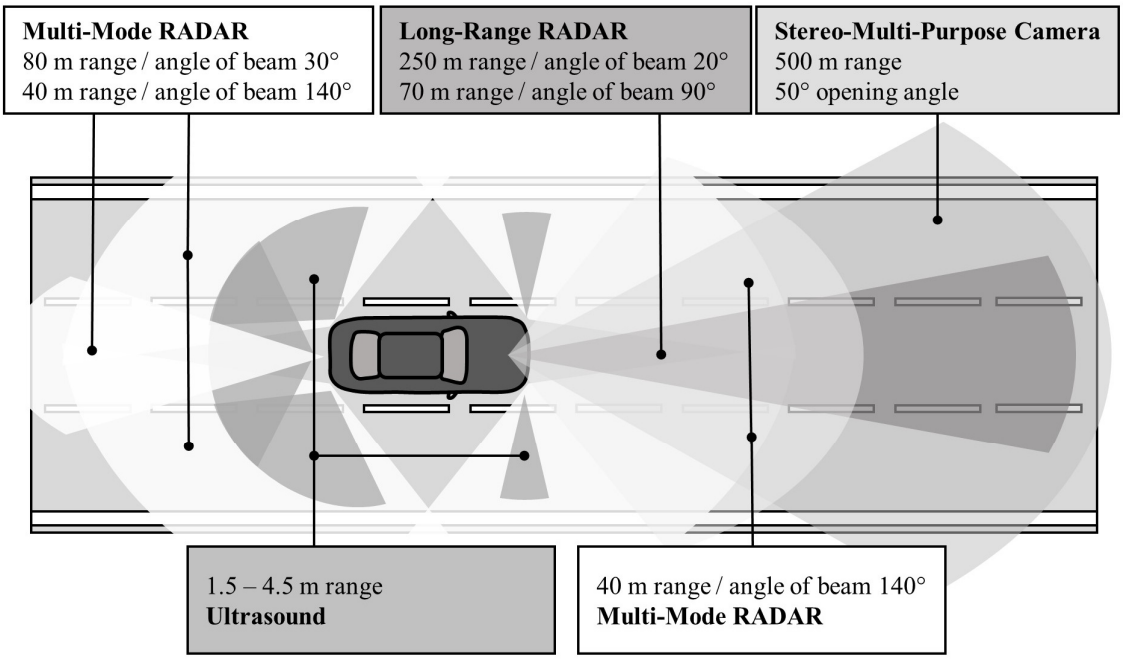

Figure 2.6: Typical sensor setup of modern ADAS equipped vehicles

Figure 2.6 shows the typical sensor equipment of a modern passenger car with their respective capabilities of reliable detection ranges. Translating the longer detection ranges of the long-range RADAR and camera to time horizons for the guidance task at typical inner-city low speeds of about 15 – 50 kph yields a couple of seconds to about a minute and a half.

Typical control interventions for compensation of control deviations on the stabilization level are carried out with a lag of several 100 ms, with the driver delay times in the closed control loop representing a lower limit as an indicator for skill-based action. Only technical control systems can realize cycle times in the range of milliseconds. Due to the short sample times at this level, it is referred to as the operational level of the driving task.

Figure 2.7 shows a history of past and possible future developments of ADAS from a technological perspective. Early ADASs were mainly based on proprioceptive sensors, i.e., sensors that measure internal vehicle conditions such as wheel speeds, acceleration, or angular speeds. These enable the control and regulation of vehicle dynamics, intending to follow the trajectory requested by the driver in the best possible way. Accordingly, antilock braking systems (ABS), traction control systems (TCS), and electronic stability control (ESC) were among the first series of products in this area.

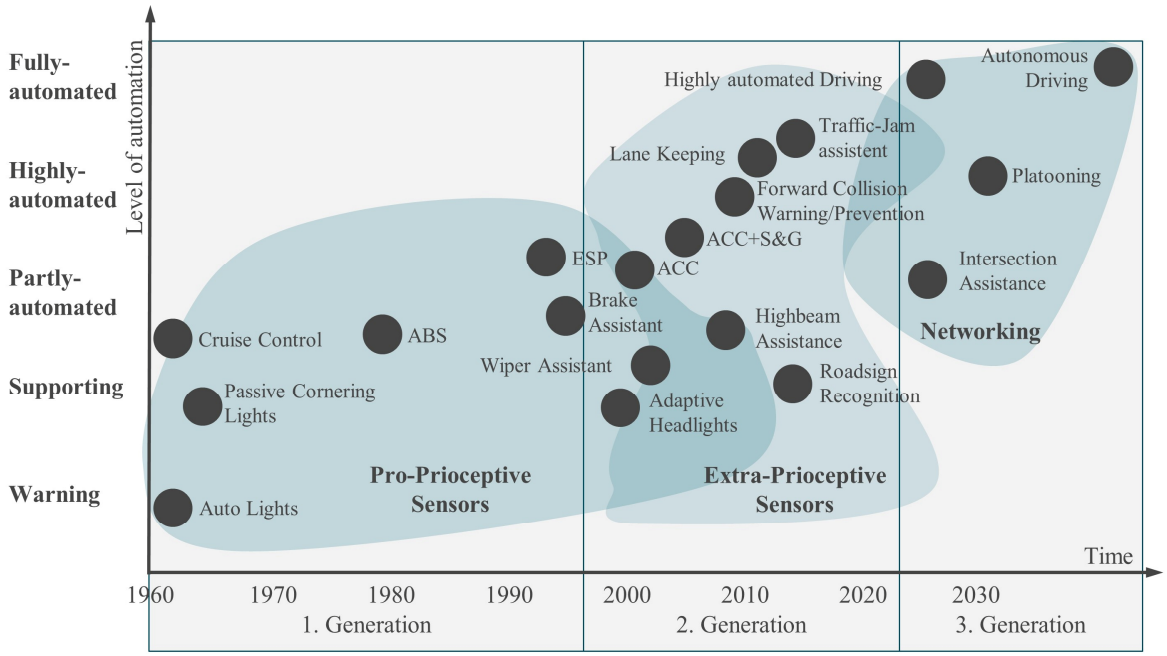

Figure 2.7: Past and possible future ADAS development based on (Schramm et al. 2020)

Since the second generation of DAS, introduced around 1990, its functions have increasingly been based on exteroceptive sensors, focusing on providing information and warnings to the driver and increasing driving comfort by reducing driver load. Exteroceptive sensors include ultrasonic, RADAR, video, and satellite sensors. In research and development, they also include LIDAR, infrared, and vibroacoustic sensors. These sensors provide information about the environment, particularly about the presence and condition of other road users and about the position of one's vehicle.

The development of adaptive cruise control (ACC) systems marked a further milestone in the field of ADAS. The use of electronic braking and drive control systems together with forward collision warning (FCW) and forward collision prevention (FCP) systems and lane departure warning (LDW) and lane-keeping systems (LKA) enabled semi-automated driving. Extensions of the system, such as already available traffic jam pilots, form the basis for the constantly progressing automation. This latest generation of ADAS selects and controls vehicle trajectories beyond the driver's current requirements. The high degree of safety requirements for such selection and decision processes is only possible through a common interpretation of all available sensor information, which is why approaches to collective sensor calibration and data fusion strategies are increasingly coming into focus, (Stiller et al. 2011).

Future systems may also require exchanging data between road users and the infrastructure via the so-called Vehicle-to-X (V2X) communication, introduced separately in Section 2.5. In parts of Europe, the term Car2X is used instead, with the same understanding of content. This approach promises an extension of the functions of a system through the extended availability of information to a collective of road users and thus supports automated and cooperative action.

2.3 Automated Driving Systems

The introduction of highly and fully automated driving systems (ADS) is an evolutionary process rather than a leapfrogging development (Proff and Proff 2008). Thus it is not surprising that these functions primarily base on the further development and coupling of already existing ADAS. As already mentioned in the introduction, however, technology is not the only driver of the current developments in this sector. The political, social, and legal aspects are just as central as the road safety objectives mentioned above. The same applies to factors such as ecological CO_2 emission targets (EU 2019), demographic change, and increasing traffic density due to increasing urbanization. ADS can offer a solution to all these challenges. They can significantly reduce harmful emissions through a forward-looking, consumption-optimized driving strategy combined with optimized traffic management. Existing infrastructure can thus be better exploited and blockages reduced. In addition, ADS can compensate for the individual mobility of citizens with age-related perceptions and reactions even more extensively than ADAS. (Bartels and Ruchatz 2015; Maurer et al. 2015)

Table 2.4: Overview of the levels for automated vehicle guidance

Institution	Level 0	Level 1	Level 2	Level 3	Level 4	Level 5
SAE	No Automation	Assisted	Partial Automation	Conditional Automation	High Automation	Full Automation
VDA						
NHTSA						

A study by the German Federal Highway Research Institute (BASt) on the legal consequences of increasing vehicle automation (Gasser et al. 2012) proposed a definition of the degrees of automation building on one another to advance a clear explanation of the terminology. This proposal was also supported by the newly founded working group “Automated Driving” of the German Association of the Automotive Industry (Verband der Automobilindustrie e.V. - VDA) and published in an extended version (VDA 2015). In addition, the efforts to further harmonize with the National Highway Traffic Safety Administration (NHTSA), which in turn had also proposed a corresponding categorization in 2013 (NHTSA 2013), came to a successful conclusion when it decided to adopt the SAE International® (Society of Automotive Engineers) Standard J3016 (SAE J3016:2021) with its federal automated vehicles policy in 2016 (NHTSA 2016). Table 2.4 gives an overview of the different views. One can see that as of today, SAE, VDA, and the NHTSA agree on the terms.

On the one hand, the classification is based on how the dynamic driving task (DDT) and object and event detection, recognition, classification, and response (OEDR) task are distributed between the system and the driver. On the other hand, it considers the requirements for the driver in each case concerning his ability to retake control if necessary. Since January 2014, when the (SAE J3016:2021) was first introduced, it has provided a detailed general definition given in Table 2.5.

Systems of the SAE Level 3 and above are henceforth considered automated driving systems, which pose particular challenges in executing the dynamic driving task and the automated testing and validation process. (Szalay 2021) points out new and future challenging aspects such as control loops without a human driver, cybersecurity, or AI-based control systems and introduces a next-generation X-in-the-Loop (XiL) validation methodology. He concludes that simulation will play an important and increasing role in the validation process of highly automated vehicles and automated driving systems to deal with these challenges in the future process. The following Section 2.4 deals with the topic of simulations in detail

Table 2.5: Automation levels of the Dynamic Driving Task according (SAE J3016:2021)

SAE Level	Name	Narrative Definition	Dynamic Driving Task (DDT)		DDT fallback	Operational Design Domain (ODD)
			Sustained lateral and longitudinal control	OEDR		
Driver performs part or all of the DDT						
0	No Automation	The performance by the driver of the entire DDT, even when enhanced by active safety systems.	Driver	Driver	Driver	N/A
1	Driver Assistance	The sustained and ODD-specific execution by a driving automation system of either the lateral or the longitudinal vehicle motion control subtask of the DDT with the expectation that the driver performs the remainder of the DDT.	Driver und System	Driver	Driver	Limited
2	Partial Driving Automation	The sustained and ODD-specific execution by a driving automation system of both the lateral and longitudinal vehicle motion control subtasks of the DDT with the expectation that the driver completes the OEDR subtask and supervises the driving automation system.	System	Driver	Driver	Limited
The system performs the DDT while engaged						
3	Conditional Driving Automation	The sustained and ODD-specific performance by an ADS of the entire DDT with the expectation that the DDT fallback-ready user is receptive to ADS-issued requests to intervene.	System	System	Fallback-ready Driver	Limited
4	High Driving Automation	The sustained and ODD-specific performance by an ADS of the entire DDT and DDT fallback without any expectation that a user will respond to a request to intervene.	System	System	System	Limited
5	Full Driving Automation	The sustained and unconditional (i.e., not ODD-specific) performance by an ADS of the entire DDT and DDT fallback without any expectation that a user will respond to a request to intervene.	System	System	System	Unlimited

2.4 Simulation Models

A model is always a simplified image of reality. The base for simulations is often a model described in mathematical formulas and can thus also be executed and solved by calculating machines. One tries to capture the essential parameters of natural phenomena and calculate them scientifically through the formal description. Calculability here means both the analytical investigation and the approximation utilizing numerical methods. As a rule, the so-called physical models are also mathematical models. However, they are always necessarily based on physical laws. This approach is also referred to as theoretical modeling.

In contrast, a purely mathematical model can achieve the same or similar results without needing knowledge of the physical relationships, as is often the case with the artificial neural networks frequently used today (black box). A valid model can predict future behavior, whereby "valid" in this case means that the output parameters of the simulation results correspond sufficiently accurately to any measurement on the real system. The term experimental modeling is often used to define this approach. (Schramm et al. 2018)

As already mentioned, all approaches aiming at a prospective assessment always use simulations as tools on different levels or in various steps of the respective processes. On the one hand, they describe vehicle movements - both at the individual driving level and the traffic level - and, on the other hand, represent the communication between vehicles, formulate the environmental conditions mathematically, or calculate the consequences of accidents. In this Section, some simulation models important for the thesis are presented.

2.4.1 Vehicle

For all investigations that deal with the effect of systems on road traffic, the corresponding road users must be modeled regardless of the chosen level of consideration. Since only passenger cars are considered on the vehicle level within this thesis, the following representation excludes other entities, such as pedestrians or cyclists.

In its simplest form, in which vehicles are described only as a whole uniform set of a summarized mass, the vehicle's description is limited to a pure description of its motion through Newton's second law. This means that the acceleration results from the ratio of the forces acting on the body to its mass:

$$\boldsymbol{a} = \frac{\sum \boldsymbol{F}}{m}. \tag{2.7}$$

This approach neglects the effects of individual components such as inertia in the powertrain or the brake system in its pure form. Due to its simplicity, this approach is often used on the traffic flow level since many vehicles can be simulated very computationally efficient. Whole collectives

are considered at this level, focusing on the general effects of interactions between individual vehicles rather than the behavior of individual vehicles or even their components. The model is usually extended by an elementary geometric description of the outer dimensions, e.g., via a rectangle to describe simple interactions between vehicles.

The simulation speed and the required accuracy always depend on the research question, the investigated problem, and the resulting necessary levels of consideration. Often it is required to find a compromise between these two opposing parameters. (Neubauer 2015)

At the level of driving situations or the functional level, where only individual vehicles and their components are considered, complex vehicle models are at the center of attention. Through explicit and detailed modeling of all essential parts, they permit a high degree of accuracy in describing vehicle dynamics. An actual motor vehicle is a continuous system consisting of spatially extended and vibrating components. This system has an infinite number of degrees of freedom f. It needs to be converted into an idealized discrete model to make mathematical calculations for this system. The model then consists of rigid blocks with masses and moments of inertia connected by springs and dampers. Through this simplification of reality, a concentration of the parameters occurs and reduces the models' degrees of freedom. Depending on the model requirements, different vehicle models, which differ in degrees of freedom and complexity, can be used for realistic simulation. Figure 2.8 gives an overview of a typical selection of vehicle models used in development and simulation. The complexity ranges from a simple single-track model with only two degrees of freedom, in which the tire forces acting to keep the car on course are combined in the axles, to the hybrid model with more than 500 degrees of freedom. (Schramm et al. 2018) offer a detailed description of such models.

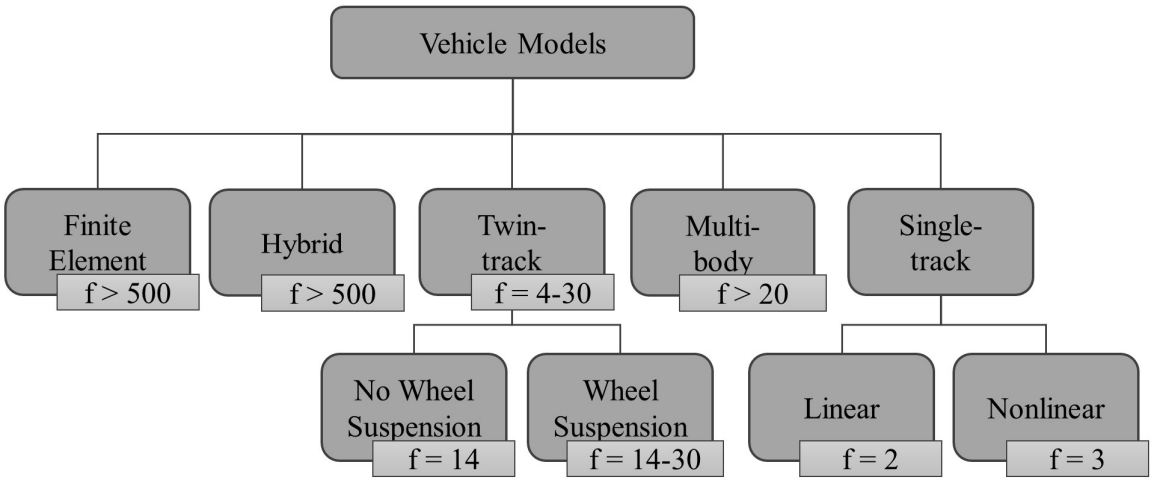

Figure 2.8: Overview over vehicle models and their degrees of (Schramm et al. 2018)

2.4.2 Traffic

Modern traffic simulation models and tools are used to investigate various issues. Classical applications investigate the effects of traffic lights or structural changes of the road network. The consideration of vehicle emissions, especially through the emergence of electric mobility, has also gained importance in recent years (Detering 2011; Driesch et al. 2019; Weber et al. 2020). Thanks to increasingly powerful computer systems and continuous development in simulation technology, traffic simulations are also increasingly used for traffic forecasts.

According to (Schnieder and Becker 2007), a traffic system consists of four units: traffic object, traffic means, traffic infrastructure, and traffic organization. In this thesis, the considered means of transport are mainly passenger cars. The road network forms the traffic infrastructure, traffic organization is the regulation by traffic rules, and traffic objects are drivers and passengers. Depending on the task, all these systems can be described by many parameters and different models. These models consequently show a typical overall behavior through their interaction when parameterized appropriately.

Traffic and traffic flow simulation models can additionally be divided into several levels of consideration. These are in the order of very detailed to aggregated data evaluation levels: nanoscopic or submicroscopic, microscopic, mesoscopic, and macroscopic approaches. (Treiber and Kesting 2013) give a comprehensive introduction to this topic.

Macroscopic models are very efficient in simulating extensive scenarios. This is achieved by describing aggregated parameters of traffic flow such as average speed $\bar{v}$ in kph, traffic density k in vehicles/km, and traffic volume q in vehicles/hour. These models are derived from analogies of fluid mechanics, and individual road users are not explicitly modeled, and therefore the interactions between them cannot be extracted precisely. However, approaches to represent automated vehicles at this level already exist, for example, in (Török et al. 2020).

Microscopic models are characterized through the explicit representation of each vehicle as a separate unit. They can interact with neighboring vehicles and are controlled by corresponding behavior models, i.e., driver models or car-following models. The entities are usually not modeled in detail but instead reduced to relatively simple equations of motion, as mentioned above, to maintain a high capacity and computational speed.

Mesoscopic models combine the macroscopic models that describe the traffic as a continuum flow and microscopic models describing the individual behavior, using more detailed models in specific regions or topics of interest. One can investigate a particular intersection with a microscopic model that includes vehicle interaction and traffic light dynamics, while the rest of a more extensive network is simulated via a macroscopic model.

In nanoscopic or submicroscopic traffic models, all entities are described by complex models such as single track or twin track models in the case of vehicles. The vehicle dynamics and the components or control algorithms of advanced driver assistance and automated driving systems,

for example, are evaluated in detail. The disadvantage is the high computational cost of this approach, so it is not often applied for larger-scale scenarios.

2.4.3 Driver Behavior

An essential and often challenging aspect of modeling road traffic is the reproduction of drivers and their behavior. There are many approaches in the literature since the requirements for the models based on their applications sometimes differ significantly. Since the driving task is usually divided into three levels (cf. Section 2.2) and into many subtasks, it is not surprising that there is no uniform consensus in the literature on how to model it in general. However, a typical subdivision on a still rather abstract level is the two-dimensional classification of (Michon 1985). On the one hand, it distinguishes behavioral (input-output) oriented models and internal-state (psychological) models, and on the other hand, taxonomic and functional models. In this way, he distinguishes four types: motivational models, adaptive control models, trait models, and task analysis models, as shown in Table 2.6.

Table 2.6: Driver behavior classification based on (Michon 1985)

	Taxonomic	**Functional**
Behavioral (input-output)	Task analysis models	Adaptive control models
Internal state (psychological)	Trait models	Motivational models

The functional models consider the dynamics of driver behavior by connecting model components. As part of these, Motivational models consider internal states of a driver, such as an attitude, subjective risk behavior, and insight as controlling factors. Adaptive control models deal with a driver's adaptation to his control to the characteristics of the controlled system. Taxonomic models are inventories of isolated facts. An essential aspect of trait models is that they assume it would be possible to identify a frequent accident driver through well-designed tests. Task analysis is the decomposition of the driving task into tasks and subtasks. The models usually incorporate three types of descriptions. They define task requirements, performance objectives, and enabling objectives. (Cacciabue 2007)

(Rasmussen 1983) first introduced a widely recognized model for goal-directed activity. Figure 2.9 distinguishes three levels of varying degrees of cognitive demand on people in the thesis process. This structure is also often applied in the literature to the three levels of the driving task (c.f. Figure 2.4). According to the model, people act on the knowledge-based behavior level when confronted with complex, previously unknown requirements. At this stage, mental processes are used to actively play through various alternative courses of action and examine their usefulness by comparing an intended goal before the best one is selected and, if successful, stored as a rule for future cases. Due to the lengthy process and the necessary transfer performance, a strategic approach can instead be assumed. Suppose a person has already been confronted with a given situation more

often. In that case, one can usually fall back on a pool of stored rules for its resolution and is thus at the rule-based level, which requires significantly less time and cognitive attention.

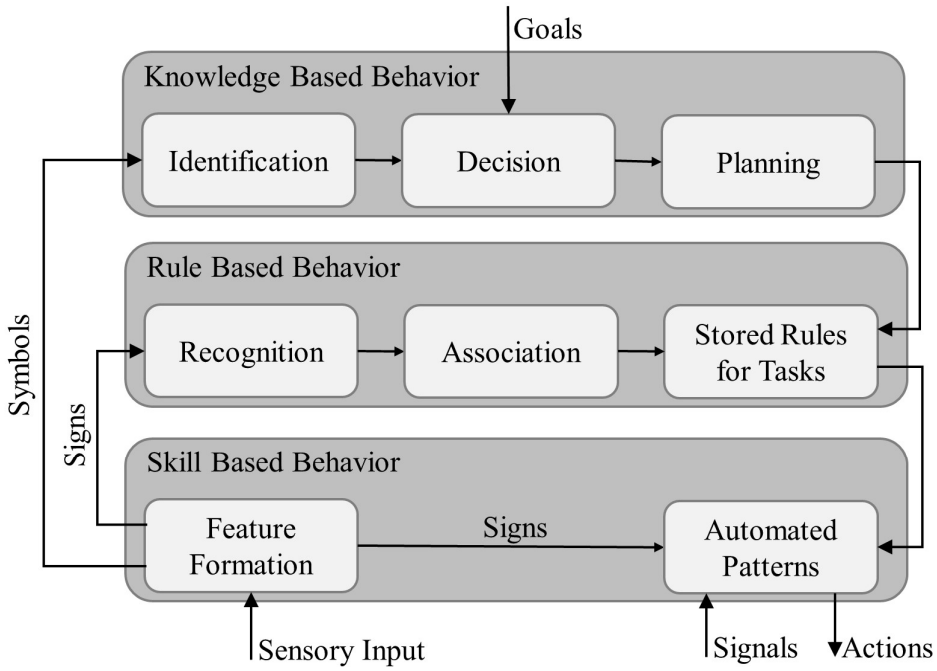

Figure 2.9: Three-level model for goal-directed activities of humans (Rasmussen 1983)

Regarding the driving task, this happens on the tactical level. Again, the operational level corresponds to the skill-based behavior level, characterized by reflex-like stimulus-response patterns, where processes can occur without conscious control. For example, in the context of vehicles, the shifting of gears in manual transmission can be mentioned here. They are, therefore, typical of routine recurring action sequences.

In the field of traffic simulation, and specifically microscopic traffic simulation (cf. Section 2.4.2), driver behavior is often modeled as the lateral and longitudinal movements under varying boundary conditions. Since only certain aspects are considered, the terms car-following model for the longitudinal movement and lane-change model for the lateral movements are often used instead, since the term driver model implies a broader approach. However, they can be categorized as functional models in the field of adaptive control models. More details on car-following models for traffic flow simulation will follow in Chapter 4 when describing the implementation and necessary adaptations for this thesis.

2.4.4 Environment

In the broadest sense, the environmental model in vehicle technology contains everything that can be relevant for the performance of the driving task (cf. Section 2.2) and directly or indirectly influences it. It contains and provides, among other things, information about traffic infrastructure,

other road users, static objects as well as the extended environment. Figure 2.10 shows examples of elements that may be mainly relevant for this context. The environment model is a collection of all models that must provide the necessary information and properties in different ways, depending on their type. Objects can, for example, contain shape models consisting of points, edges, lines, geometric models, surface models, and individual motion models. In addition to the geometric dimensions and the course, the road model can also contain information about the surface texture, the pavement, and the weather-related condition.

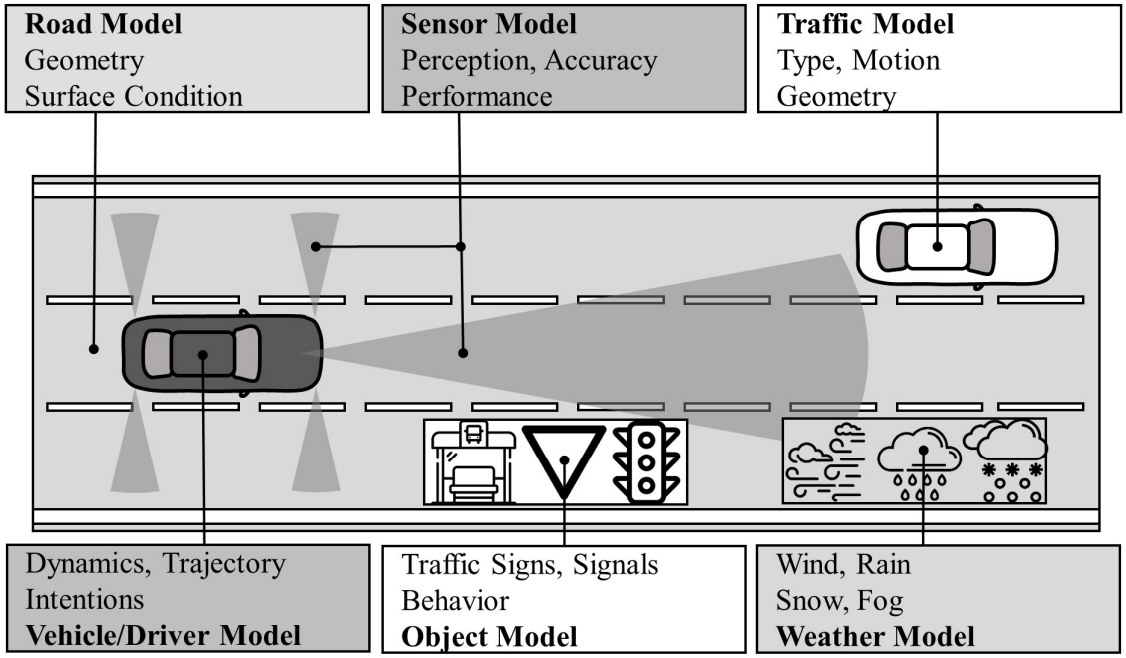

Figure 2.10: Environment Model for Traffic Simulation inspired by (Minnerup 2017)

The sensor models also play a central role as they specify how a vehicle perceives its environment. Ultimately, it is this information that is processed by the corresponding components of the vehicle model. Vehicle-specific sensors and their models can be directly assigned to the vehicle model, but this also includes other sensors, such as a global navigation satellite system (GNSS), which also influence other models in the simulation and should therefore be modeled at a higher level.

As with all simulation models, the investigated research question is particularly decisive for selecting the necessary models and their depth of detail and complexity for the environmental model. It must be ensured that all critical aspects are considered to represent a sufficiently complete scene for the respective investigation. In contrast, insignificant aspects can be neglected, which leads to a reduction in complexity and often a performance advantage of the entire simulation (Minnerup 2017).

This basic approach has two significant advantages in the analysis and investigation of ADAS and ADS. On the one hand, it is possible to achieve repeatable and reproducible preconditions and results in an economical way to reduce the number of necessary road tests. On the other hand,

maximum flexibility of the models is given so that they can also be created from data of past natural test drives. Otherwise, unconsidered influences can find their way into the simulation environment, e.g., with the help of statistical tools and probability distributions.

2.5 Automotive Networking

In the context of automotive networking, the term Vehicle-to-Everything (V2X) communication refers to both the direct wireless networking of vehicles (Vehicle-to-Vehicle, V2V) and the integration of the infrastructure (Vehicle-to-Infrastructure, V2I) or other road users. It forms part of an intelligent transportation system (ITS) where all participating entities and higher-level management systems intermesh. These are, for example, fleet management systems from logistics as well as inner-city and extra-city traffic management and safety systems aiming at using intermodal communication to achieve maximum synergy in terms of traffic performance and safety. This is also the understanding of the European Telecommunications Standards Institute (ETSI) and its cooperative ITS (C-ITS) approach (ETSI TR 101 607), which alongside the European Committee for Standardization (CEN), plays a leading role in European and international harmonization efforts. In the following, the focus will be on the European market, with some supplementary remarks on the US-American market, as this is where the most significant similarities already exist and where it is possible to equip the vehicles with a system to cover both regions.

Since the further course of the thesis is specifically looking at a system at the vehicle level, the following explanations concentrate predominantly on the vehicle environment. For linguistic differentiation, the term mobile platform is used in addition to the term vehicle, which also includes all conceivable mobile road users, such as trams, cyclists, or pedestrians, in addition to motor vehicles and trucks. For stationary communication units of the infrastructure, the common term roadside unit (RSU) is introduced, including appropriately equipped signs, beacons, traffic lights or public transport stops, and specially constructed facilities for this purpose.

Communication at the level of mobile platforms offers a future-oriented opportunity to improve all primary target dimensions of ADAS, namely: comfort, efficiency, and security. On the one hand, by extending the limited detection range of the environmental sensors and on the other hand by transmitting relevant traffic events from different sources. According to (Baldessari et al. 2007), the applications can be classified into corresponding categories: Comfort and infotainment, traffic flow optimization, and active safety.

Current research, development, and standardization take place mainly in the solid automotive markets of the USA, Japan, and Europe. The following is a brief overview based on (Festag 2015), with a focus on standardization. While in the USA and Europe, the process is already quite advanced, in Japan, near-field communication in the automotive sector is currently only used for the toll system, and there is presently no uniform standardization strategy for V2X communication. Therefore, the following Section concentrates on the regions USA and Europe. Three levels can

be distinguished in the architecture for V2X communication below the individual non-standardizable OEM-specific applications, as shown in Figure 2.11.

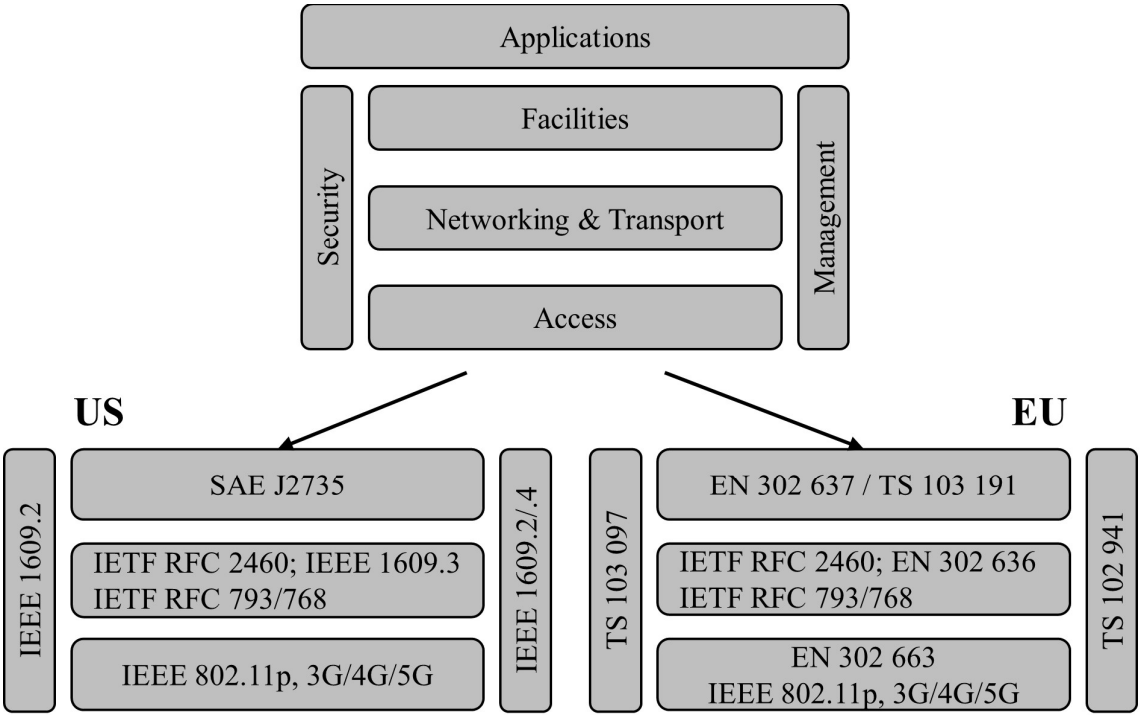

Figure 2.11: The level architecture of the V2X standardization US-EU

The accompanying security and management protocols and the radio standards (physical level) are almost identical in the regions considered. However, there are regional differences at the network and transport level as well as at the facility level, which are highlighted in the following subsections if necessary. However, since these are rather formatting issues and the underlying data do not differ significantly, the technical effort of a cross-regional implementation is neglectable. In the following, the individual levels are briefly described regarding content and the standards.

2.5.1 Access

The access layer defines the external communication protocols and logical links over which the V2X data is transparently transported. The access may be realized through complete, non-V2X specific communication systems such as GPRS/UMTS/LTE/5G or specific protocols such as the dedicated IEEE 802.11p standard. Both variants are briefly introduced in the following.

Cellular: UMTS/LTE/5G

The mobile network is already used as a standard for data exchange between vehicles and backends (OEM and third-party providers). The applications range from the transmission of vehicle status information to infotainment content and traffic information. (Daimler AG 2020)

The networks are operated by various commercial mobile network operators and have high coverage in the relevant markets. These networks can be used to establish connections to the backends via the Internet. The data rates depend on the mobile radio standards. In the case of LTE, network coverage in Germany is about 95 % (Forkel et al. 2020), with transmission rates of 100 Mbps and more, making it possible to transfer larger data volume in general. The proof of whether security-critical and real-time relevant data are transferable via this backend approach is still pending. In addition, the demand for fast and powerful mobile radio networks (e.g., for the use of entertainment services) will presumably continue to rise with increasing automation and the associated freedom to carry out non-driving activities. The next generation "5G" standard will support this with up to 10 Gbps transmission rates, and its feasibility has already been proven by (Szalay et al. 2020) through a successful series of 5G-supported autonomous driving demonstrations.

WLAN and Bluetooth

As early as 1999, the Federal Communications Commission (FCC) reserved a bandwidth of 75 MHz in the 5.9 GHz frequency band exclusively for the automotive sector for V2X communication devices. The new WLAN standard IEEE 802.11p specifies the radio channel access for this frequency band. This makes it possible to transmit data over medium distances of up to about 500 m within a few milliseconds, even at high relative speeds. In the USA, this type of communication is referred to as dedicated short-range communications (DSRC); in Europe, the term is further differentiated and is more commonly used as short-range wireless communication (ITS-G5). The maturity and functionality of the IEEE 802.11p basis have already been proven in various research projects, like simTD (Weiß 2017), Ko-FAS (Adameck 2011; Breuel 2014; Lankes 2014), and DRIVE C2X (Daimler AG 2017).

Via Bluetooth (IEEE 802.15.1), personal devices such as mobile phones, tablets, or other consumer electronics can be connected to the vehicle at close range, which is already common practice in series production today. For highly automated driving functions, this may be relevant because, in the event of a necessary driver intervention, the connected devices could also be used to draw the driver's attention to the situation. However, no application is planned for communication with other vehicles at close range thus far.

The main argument for the (additional) use of ad-hoc networks based on WLAN is the extremely low latency compared to a backend solution via mobile networks. Especially for safety-critical applications, e.g., warning of a vehicle braking strongly in front, information availability is an important influencing factor for the accident risk. Finally, it should be noted that both transmission paths will probably play an essential role in the future, depending on the application and the required data and information.

2.5.2 Networking and Transport

The networking and transport level also explicitly differentiate between the two application cases V2V and V2I. For the non-safety-critical applications, which are predominantly attributable to V2I communication, the use of IPv6 (Deering, Hinden 1998) with the standard transport protocols TCP (RFC 793) and UDP (RFC 768) is planned. For safety-critical applications, a regional distinction must be made at this point. In the USA, the transport level is based on the standards of the IEEE 1609 series, (Kenney 2011). The IEEE 1609.3 standard includes network services in vehicle communication and the Wave Short Message Protocol (WSMP). The WSMP is the core of a single-hop network protocol with a minimum header of a few Bytes. It offers the possibility of multiplexing messages, in which several messages are combined and transmitted simultaneously, leading to a further efficiency increase.

In Europe, the (ETSI EN 302 636) with the working term "GeoNetworking" is used in this area. The main feature of this protocol is the use of geographical coordinates for addressing and forwarding. Its use for addressing makes it easier for all vehicles located in a limited geographical area to become the packet's destination. While this is similar to sending a packet to all neighboring vehicles, geographic addressing makes parcel delivery independent of the communication area of a single jump. In addition, geographic coordinates are used to route packets locally based on vehicle knowledge of their position and neighboring positions, providing efficient multi-hop routing with low protocol overhead.

2.5.3 Facilities

At this level, processes and services are established which provide essential support services within the framework of the communication process. These, in turn, are divided into three areas: information support, communication support, and application support. In concrete terms, this also includes managing the message formats for V2X communication defined accordingly at this level. Messages are defined here as specific standardized data packages that can be created, received, processed, or prepared for further processing based on the data provided by various V2X applications.

(SAE J2945:2017) defines the system requirements in the USA, including the standard profiles and functional and performance requirements. (SAE J2735:2020) defines both the syntax and the semantics of the corresponding V2X messages. For this purpose, a whole series of messages are defined for different application cases, such as the "BasicSafetyMessage" (BSM), the "EmergencyVehicleAlert" (EVA), "MapData" (MAP), "Signal-PhasingAndTiming" (SPAT), "PersonalSafetyMessage" (PSM) and many more. Among the various defined messages, the BSM has the most significant relevance for traffic safety reasons. BSMs transmit core status information about the sending vehicle, including position, dynamics, status, and size. The BSM is designed for compactness and efficiency but can be expanded with additional data elements if required.

In Europe, this level is dealt with in detail in the Technical Specification (ETSI TS 102 637-1), including a list of all the typical services foreseen to date. The semantics and syntax of the message formats are also based on the standards EN 302 637. Part 2 (ETSI EN 302 637-2:1.3.1) specifies the “Cooperative Awareness Message” (CAM) and Part 3 (ETSI EN 302 637-3:1.2.1) the “Decentralized Environmental Notification Message” (DENM). The message types SPAT and MAP are also on the road to standardization being adopted from the (SAE J2735:2020) mentioned above.

2.5.4 Security and Management

In the USA, security is defined in the (IEEE 1609.2:2016) standard and enables authentication and optional encryption of DSRC messages based on digital signatures and certificates. The authentication scheme also implies a security and public key infrastructure (PKI), i.e., Certification Authority (CA) and PKI, and guidelines for certificate validity, certificate encryption, and certificate revocation. Accordingly, certificates protecting the privacy of drivers do not contain any information about them, although the certification authority can link the certificate to the identity of a driver. Furthermore, a vehicle only uses a certificate for a limited time and frequently changes it to make tracking more difficult.

In Europe, the ETSI has also developed standards for this purpose. Some go beyond the IEEE 1609.2 standard, which is explicitly used as a basis in the ETSI documents. In particular, these are the technical specifications (ETSI TS 102 941:1.2.1) “Trust and Privacy Management” and (ETSI TS 103 097) “Security header and certificate formats”. Here, too, a PKI authentication scheme is used. However, the implementation and explanation on the subject of data protection are more extensive.

2.6 Prospective Effectiveness Assessment

The fundamental problem with the question of effectiveness in a larger context is that it can usually only be measured after a more extended examination of their performance in real road traffic. These approaches are generally referred to as retrospective effectiveness assessment and are typically based on the analysis of afore collected relevant data about the subject matter of the investigation. For example, accident data in the context of traffic safety impact, as these are usually recorded in databases in one way or another and can be studied more closely later. Especially in the development of new types of systems, this is hardly possible. Even by testing prototypes, it is not possible - or very challenging - to deduce an effect in traffic due to the small sample sizes.

This is particularly true if the system is only to operate in certain situations where the probability of occurrence in real traffic is statistically extremely low. Therefore, other methods such as simulation-based approaches must be used. Some techniques and methods known from the literature are described, especially for prospective effectiveness assessment. In contrast, strategies for a

retrospective effectiveness assessment are not considered further in this thesis for the reasons given above.

The partial project “Traffic effects, legal aspects and acceptance” within the German Research Initiative INVENT (Benz et al. 2002) deals explicitly with advanced driver assistance systems. In the project, ADAS were modeled and integrated into traffic simulators to analyze the traffic effects of these systems. The understanding of the term “effect” in that context is comparing the behavior in certain situations between an equipped and unequipped vehicle. Even though this change is locally limited to the surrounding vehicles, they postulate that many individual changes lead to effects on a larger scale. By testing a Congestion Assistant, they suggest an iterative investigation approach for ADAS taking different levels of complexity into account. Figure 2.12 shows the suggested division of complexity levels. Due to the nature of the system, traffic efficiency and fuel consumption rather than traffic safety aspects were the centers of the investigations in this case.

According to the findings, it is feasible to start testing a function on its basic level to ensure desired system behavior for given demand values. The next step evaluates the system in certain driving situations that consist of a small number of vehicles before the ADAS can be studied in different, more extensive traffic situations. These include a large number of vehicles but are still limited in terms of space and time. The simulation on a large traffic scenario scale can only be carried out after ensuring the system’s usability in such an environment. Due to its iterative nature, findings on the upper levels may, in turn, be used to further enhance the base system under investigation.

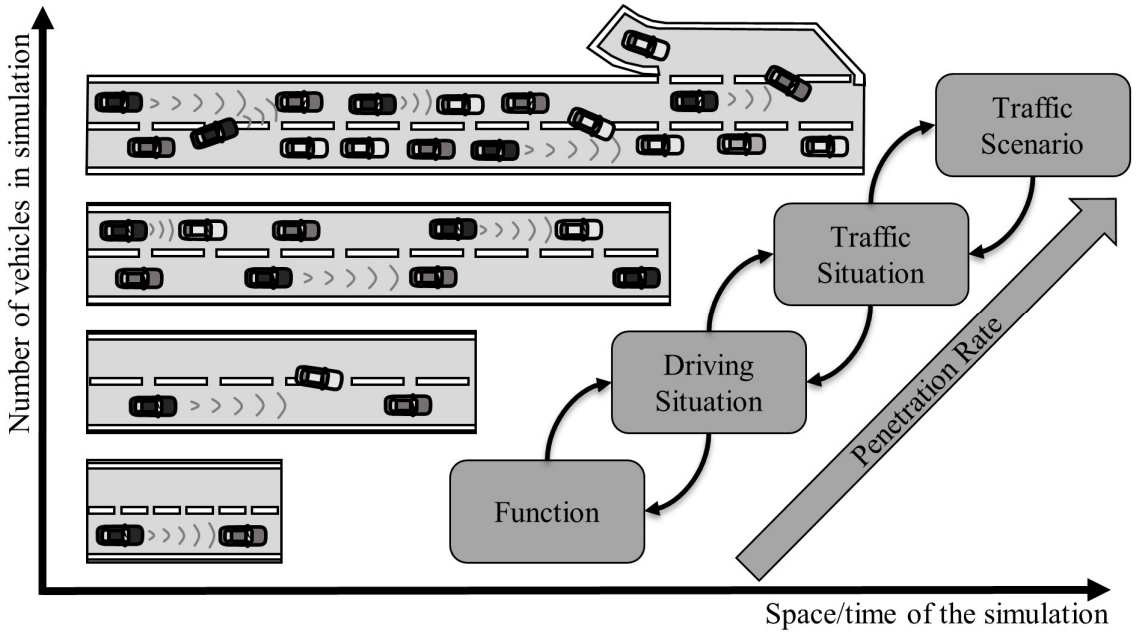

Figure 2.12: Levels of investigating ADAS based on (Benz et al. 2002)

(Baur 2015) introduces a generic modeling framework for intelligent transportation systems for the simulation-based analysis of their effects on road traffic. The system under consideration is a

dynamic and cooperative application that influences traffic on motorways employing modern communication technology. While it accounts for some aspects of networking between vehicles and the infrastructure, its characteristics are exclusively at the traffic level and here only at the highway traffic level. The modeling framework consists of three essential parts: a software framework for connecting ITS to various traffic simulation programs, a systematic process framework with recommendations for modeling and model optimization, and an analysis component to systematically evaluate the results obtained. Within the methodological process framework for modeling, the following three steps are proposed concerning an effectiveness analysis. First, a textual description of the system is to be made. Not only shall the functional processes of the system be recognizable, but also a complete description of effect situations must be included. These should contain concrete limitations regarding space, time, and boundary conditions for applying the system. One must also explicitly specify the desired effective dimension, such as traffic safety or traffic efficiency, and select corresponding metrics to measure this effective dimension. A series of simulation runs are carried out in the second step to evaluate the actual effect while varying the input parameters. The last step is the subsequent interpretation of the changes in the previously defined parameters.

(Ovcharova 2013) combines user-oriented experiments based on studies in driving simulators with accident analyses of actual accidents. However, the term “use” here only refers to the concrete avoidance of an accident. Based on the experiments in the driving simulator, a realistic driver model is developed to estimate general statements regarding the expected benefit of a driver assistance system on selected accidents with natural driver behavior under different boundary conditions. It is shown that an improved mapping of driver behavior leads to more valid results and can also be used specifically for the optimization of parameters such as warning or intervention time of an individual assistance system. However, this approach is limited to unique concrete situations and specific forms of accidents and does not provide a generalization to the overall traffic situation. Regarding the INVENT approach introduced above, this analysis remains at the lower two levels.

(Hoffmann 2013) investigates whether specially modified traffic simulations of critical traffic situations can contribute to the simulative impact analysis of intelligent traffic systems. The focus is on a generally applicable model for the simulation-based analysis of individual driving behavior in critical situations at the traffic level. Here, too, characteristic driver reactions are identified based on actual driving data. These are then used to modify the driver model of a traffic simulation to subsequently analyze the effect of driver behavior in other critical situations. It can be shown that also on this level, by improving models based on actual data, the simulation results in changed conditions are closer to the real referencing observations.

(Elyasi-Pour 2015) combines the situational level with the traffic level by describing a simulation-based framework to estimate the impact of advanced driver assistance systems on traffic. The framework suggests coupling a traffic simulation with a driving simulator to consider the interaction between driver, vehicle, and traffic system. The advantages of this approach are that the traffic simulation can support the vehicle simulation by supplying realistic (if available) driver models and a more realistic environment and surrounding traffic and that the vehicle simulation enhances

the traffic-simulated vehicle dynamics. One of the disadvantages is that the penetration rate of complex vehicles within the simulation is limited due to high computational costs. However, the investigation scope of this thesis is not concerning traffic safety but also environmental and traffic efficiency effects.

(Fahrenkrog 2016) develops the most comprehensive methodology to date for the effectiveness analysis of ADAS, specifically regarding traffic safety. The methodology is characterized on the one hand by the impact assessment on a local and global level and, on the other hand, by the comprehensive generalization of relevant driving and traffic situations. The methodology is divided into five main process steps. In the first step, a database of critical driving situations is created using actual traffic data, e.g., from field test studies. Based on this data, relevant driving situations and metrics for their description are determined to investigate the driver assistance system in the second step. In the third step, these simulations are carried out at the traffic level and the driving situation level, each level with and without the new system. Suppose special critical situations arise in the traffic flow simulation, which are not represented by the database from the first step so far. In that case, these should be examined here in an iterative process also on the situational level. In the fourth step, the results of the simulations are analyzed at their respective levels. For the traffic level, the frequency of occurrence of relevant critical driving situations, and for the level of driving situations, the criticality is based on previously defined metrics. The last step involves transferring the results obtained to the actual existing traffic based on a system proposed explicitly for this purpose. In this system, critical situations are first summarized in clusters and then compared as the sum of the products of frequency and criticality for the results with and without the investigated driver assistance system. However, even this methodology does not consider all aspects. For example, the connectivity of vehicles already implemented in parts is not even theoretically taken into account, or it does not give them a significant role, as in the case of environmental conditions.

3 Research Method

Chapter 3 describes the research method based on the problem definition and the overarching research question. It extends known approaches from literature to allows a generalized potential analysis for future vehicle systems. Subsequently, the first steps of the process are applied to a sensor for weather-related road surface condition detection, and specific research questions are formulated, which are to be answered at the end of the thesis by the complete application of the methodology. The Chapter concludes with the selection of the necessary simulation tools and models.

3.1 Concept

Based on the superordinate research question and the findings in Section 2.6, two basic levels of analysis are considered for investigating and evaluating the potential improvement of driver assistance and automated driving systems. As shown in Figure 3.1, this is, on the one hand, the consideration of the systems on vehicle level and, on the other hand, the question of the possible effects on the extended vehicle environment and the traffic situation in general.

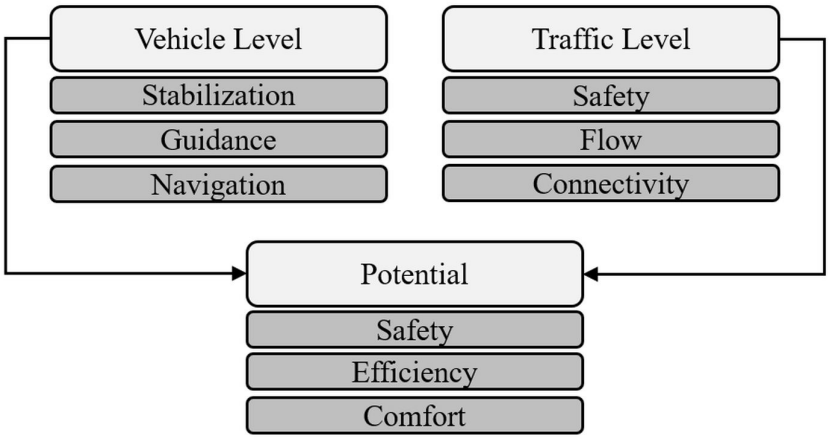

Figure 3.1: Scopes of consideration for the potential assessment of automotive systems

For the example of weather-related road surface condition detection, the investigation at the vehicle level may deal with the increase in safety through improved or faster compliance with driving dynamic limits. The investigation at the traffic level may deal with the development of average

distances, the frequency of potentially dangerous situations between vehicles, or other traffic relevant key performance indicators such as average speeds in the overall system.

Applying this division of levels to the results of the INVENT research initiative (Benz et al. 2002) (cf. Figure 2.12), the characteristic and functional test and the application in specific driving situations correspond to the vehicle level. The traffic level consists of the traffic situation and the traffic scenario. In this approach, the vehicle level and the traffic level are further subdivided depending on the number of simulated vehicles or the spatial and temporal extent. The advantage of this approach is that models of varying complexity and the required level of detail may be used within the respective observation levels, each of which is targeted at individual aspects of the investigated research questions. On the vehicle level, i.e., the level of functions and driving situations, complex vehicle models can be implemented with high precision to depict potentially dangerous or otherwise relevant situations straightforwardly and validly. In contrast, the occurrence probabilities of such relevant driving situations in large scenarios can be determined and investigated on the traffic level even with simple vehicle models. The only important aspect for a final holistic view is clear and meaningful interfaces between the models and levels of consideration.

As mentioned in Chapter 2, the procedural methodology of (Fahrenkrog 2016) consists of five main process steps, especially for investigating the effect of ADAS on road safety. The five main process steps, summarized in Figure 3.2, are in detail:

1. The analysis of real traffic situations

In this step, the current traffic situation is to be analyzed in its relevance for traffic safety for the system under consideration. Fahrenkrog proposes to distinguish between two types of input data, namely general information about traffic (e.g., based on national or international traffic statistics) and driving situation-specific input data (e.g., from field tests or corresponding databases such as the German In-Depth Accident Study (GIDAS) Database (Otte et al. 2003).

2. The derivation of relevant driving and traffic situations

Based on the previous step, relevant parameters for reduced scenarios are determined for the system under investigation and implemented with their help in the planned simulation environments. The number of scenarios to be created is directly dependent on the research question and the required general validity of the expected results. At the same time, this compromises simulation effort and validity, which must be considered critically.

3. Simulation of the system behavior in specific driving situations

This step aims to determine the changes in the criticality of individual driving situations and the frequency of occurrence of critical driving situations. The selection of the metrics (i.e., descriptive parameters) required for this purpose is again dependent on the research question and the target variable to be investigated.

4. The analysis of the simulation results regarding traffic safety

Step 4 introduces and derives a couple of road safety-specific metrics. Particularly concerning the ability to assess the hazard potential of driving situations and determine the severity of injuries as a comparative variable in the event of a possible accident.

5. Transfer of the simulation results to predict the effectiveness in the real environment

Once the simulations have identified those situations in which the new system brings about a verifiable improvement, a forecast of real traffic can be derived from the probability of occurrence of the overall traffic level. This step requires detailed statistical analyses and may be very extensive.

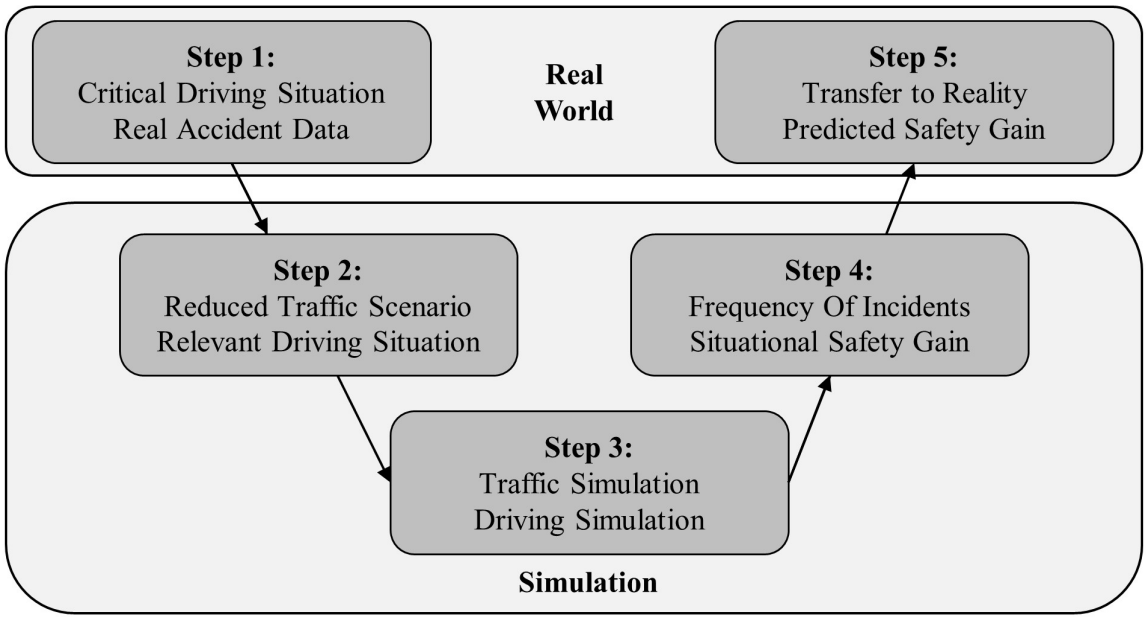

Figure 3.2: Methodology for the safety effect analysis of ADAS (Fahrenkrog 2016)

This approach might be sufficient if a specific driver assistance system is considered purely in terms of road safety. However, this presupposes that the system's mode of operation in the vehicle is already sufficiently known even in the first step and that the target variables are already entirely defined. The example of the sensor system for road condition detection quickly shows that this is not always the case. A supplier, for instance, can theoretically develop and offer such a system with the "detection" function without knowing in detail the concrete area of application or the type of downstream applications and functions in the vehicle, which the vehicle manufacturer himself may in turn develop. The benefit or function is therefore stakeholder-dependent, and the question of potential is thus ambivalent. Even an early restriction exclusively to road safety is not always expedient for the general case since other aspects of benefit may also be of interest for the reasons mentioned above.

Furthermore, (ISO 17287:2003) states that the usability assessment methods for Traffic Information and Control Systems (TICS), which include ADAS and intelligent driver information systems (IDIS), can be categorized into three levels. Figure 3.3 shows the three levels, whereby the transition from the first to the third level is associated with an increase in sensitivity while at the same time reducing generality in terms of validity. Even if the methods mentioned there do not directly aim at an a priori estimation of the system's effectiveness, the third level's representation underlines the necessity to consider the respective stakeholders in a holistic view explicitly. The third level methods concern the measurement of variables that are generally recognized as essential in the ADAS operation. These need to be identified and adapted for the respective stakeholders.

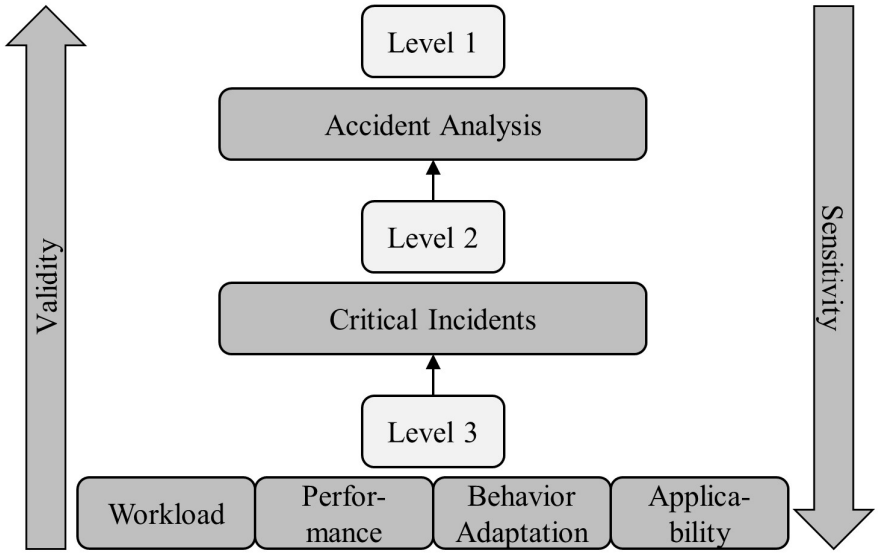

Figure 3.3: 3-levels of assessment methods for TICS according to (ISO 17287:2003)

The general research gap addressed by this thesis is the lack of a general methodology to systematically investigate the potential effectiveness of future vehicle systems. From the various existing approaches from research and literature, such a process is now being developed and then applied to the sensor system for detecting the weather-related road surface condition. As a first step, the thesis introduces an extension by an upstream, general, and comprehensive system analysis. The addition prevents the elimination of too many factors at an early stage of development and may be based on tools and methods known from system theory. The researcher needs to choose at various stages regarding the relevant elements and relationships of the system to reduce the complexity throughout the process. Initially, the system can be regarded as an arbitrarily abstract model, which can be used to make statements about the system's past and future developments and behavior in specific scenarios (see also (Krallmann et al. 2013)).

The basis of any analysis to determine the effect of systems is the potential or target analysis. According to (Zhurovskyj and Pankratova 2007), this analysis can reveal the individual purpose of a complex system with regard to various dimensions in order to be able to determine input and output variables for subsequent considerations. After the general objectives are clearly defined, a

stakeholder identification must follow. The different perspectives may lead to different approaches to solutions and functions or ways of working of the system to be implemented. A holistic picture emerges considering the three levels of the driving task introduced in Chapter 2 that allows the definition of specific research questions and individual aspects for further investigation.

In the next step, the concrete formulation of specific use cases and research questions enables a targeted selection of models, methods, and tools that can contribute to answering them in a targeted manner. This is particularly necessary because many different models and tools are already available, and not all of them are equally suitable in every case. In most cases, the selected methods and tools need an adjustment because, with new systems, it cannot be assumed that the existing implementations are already adequate. Only then can the investigation of the questions raised be carried out, e.g., through simulations or tests on prototypes, during which both the basic assumptions made initially can be checked, and more complex relationships can be investigated and uncovered. Finally, the results can be compiled, interpreted, and analyzed regarding their significance concerning the object of investigation defined initially. Figure 3.4 summarizes the novel general process.

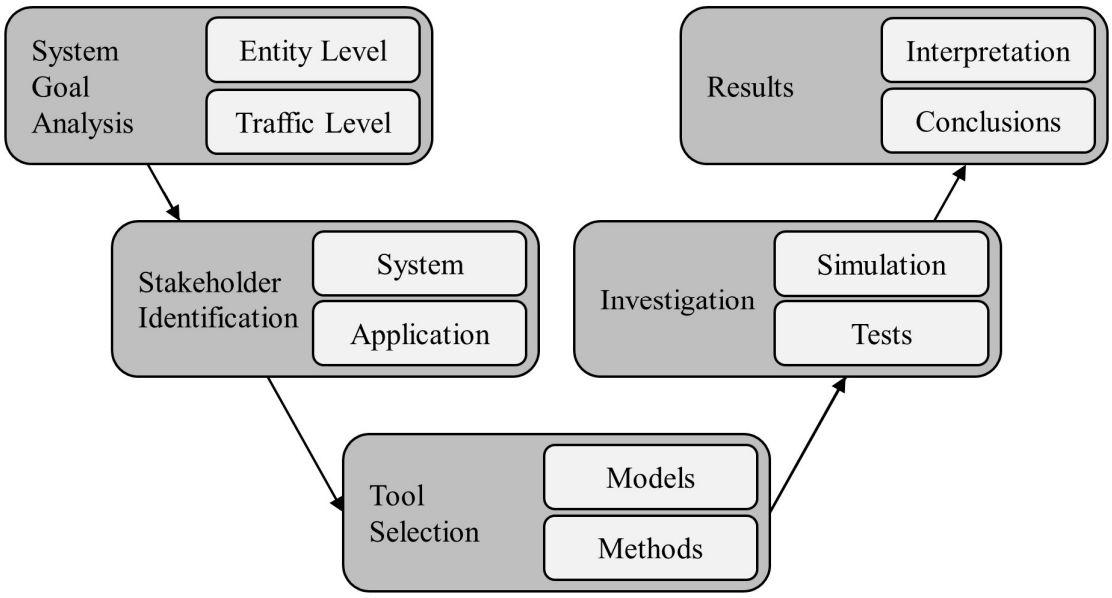

Figure 3.4: Holistic approach for the study of mobility-related systems

In contrast to the approaches known so far, this more general holistic approach can, in principle, be applied to all types of systems with relevance to the mobility and transportation sector. It thus combines the processes described in the literature to date into one by taking all dimensions into account as required. Accordingly, by omitting individual steps or dimensions, most existing approaches can be mapped again. This research concept is applied to a weather-related road surface condition awareness sensor in the further course of this thesis. The sensor serves as an example that includes different perspectives at each level of investigation to show the potential benefit of such a more general approach.

3.2 System Analysis

The system investigated in this thesis using the comprehensive methodology is a sensor for measurement and classification of the weather-related road surface condition, which was the center of the Seeroad research project (Weber and Schramm 2020a). Due to the complexity of this task, the overall system layout is not a single dedicated sensor but rather a network of sensors of different measuring principles (Krieger et al. 2020), whose measured values are combined and processed in a central electronic computing unit (ECU) as shown in Figure 3.5. In addition to the information available on the CAN bus, which includes data from the measurement technology installed as standard in the vehicle to control the chassis dynamics and a rain sensor located in the windshield, the data from the new developments in the Seeroad project are processed here. These include an optical infrared (IR) measurement array based on reflections, a wetness sensor in the wheelhouse (CAP) based on capacitive measurement technology, and structure-borne sound sensors (SHAKE), which are also installed there and are used, among other things, to detect spray water. Detailed information on the individual sensor development, the prototype vehicle integration, and results from measurement campaigns can be found in the final reports of the respective project partners (Krieger et al. 2020; Kanning 2020; Korte 2020; Unterreiner 2020) as well as exemplary in Section 4.3.2 and Appendix B. The ECU unit uses knowledge-based algorithms to calculate a probable range of values for the available coefficient of friction between the tire and the road surface (Korte 2020).

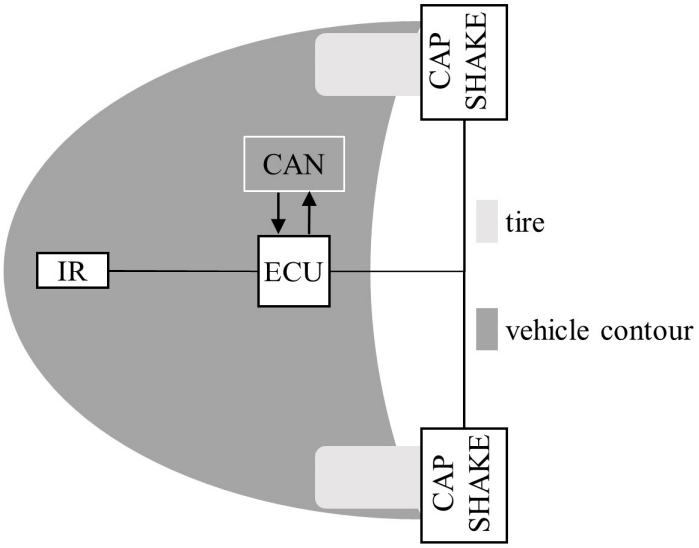

Figure 3.5: Sketch of the additional weather-related road surface condition sensor components

The term “road surface condition” can be classified both qualitatively and quantitatively. The qualitative classification, according to (BASt 2012), refers to the coverage of the road surface and distinguishes between them:

- Dry, free of snow and ice
- Moist or wet, snow or ice-covered

- Wetted with liquid water or aqueous solution (not frozen)
- Covered with snow/snow slush, a mixture of liquid and frozen water or aqueous solution.
- Covered with frozen water or an aqueous solution in solid-state
- Covered with ice (solid)
- Covered with ice deposits formed by sublimation from the air (“hoar-frost”)

Concerning stationary road condition information systems, (DIN EN 15518-3:2011) additionally offers a partial quantification:

- Dry: no moisture on the road surface
- Moist: from 0.01 mm water film thickness on the roadway
- Wet: from 0.2 mm water film thickness on the roadway
- Running water: from 2 mm water film thickness on the roadway
- Slick: detection of the partial or complete presence of frozen water/solution

Therefore, the fundamental goal that can be formulated for the system is the provision of appropriate information about the road surface condition at the vehicle level of an accordingly equipped vehicle. In the given context, this means that all levels of vehicle guidance are directly affected, at least theoretically, and must be investigated in more detail in the following. Based on the preceding considerations and the fact that each vehicle can also be understood as part of the overall traffic situation, the traffic level must also be examined regarding possible influences. To this end, a fundamental analysis of the impact of weather-related road surface conditions on the two levels under consideration is carried out first, followed by a closer look at the possible implications for each level of vehicle guidance task. With the resulting knowledge of the interrelationships, it is then possible to identify the stakeholders and, at the same time to select the corresponding functions or applications in more detail as well as to specify the research questions further.

3.2.1 Vehicle Level

Only specific characteristic values of individual vehicles are considered and evaluated at the vehicle level. In the context of weather-related road surface conditions, the contact patch between the road surface and the tire has a decisive influence on the vehicle’s dynamics. The contact patches transmit the friction forces for acceleration, deceleration, and directional changes of the vehicle. The maximum transferable friction forces, in turn, depend directly on the road conditions caused by the weather. A road grip reduced by wetness reduces adhesion, thus reducing stability and maneuverability.

The maximum transmissible longitudinal and transverse forces are proportional to the vehicle's maximum achievable transverse and longitudinal accelerations, which are limited by the respective coefficient of friction at the tires. The coefficient comprises the longitudinal friction value μ_x and the transverse friction value μ_y. The decisive influencing factors of the coefficient of friction are:

- the vehicle (wheel position, wheel loads, speed, mass),
- the roadway (material, micro/macrotexture, temperature),
- the tire (material, dimension, pressure, tread depth, temperature), and
- the intermediate medium (condition, dry, wet, snow, ice).

The condition and material of the road surface also have a significant influence on the behavior. In principle, tires can transmit greater forces in the longitudinal direction than in the transverse direction. Figure 3.6 shows the resulting approximate ellipse for the maximum transferable coefficient of friction μ_{max}. It shows that using a lateral friction value μ_y reduces the maximum acceleration capacity in the longitudinal direction $|\mu_x|$ and vice versa. The elliptical edge limits the current friction coefficient utilization, which represents the valid maximum friction coefficient μ_{max}. Since this value can be reduced to less than 10 % of the optimum value by the weather-related road condition, the elliptical edge is reached more frequently and earlier in degenerated road conditions, even in driving conditions that the driver supposedly perceives as uncritical. (Klempau 2003; Weber 2004)

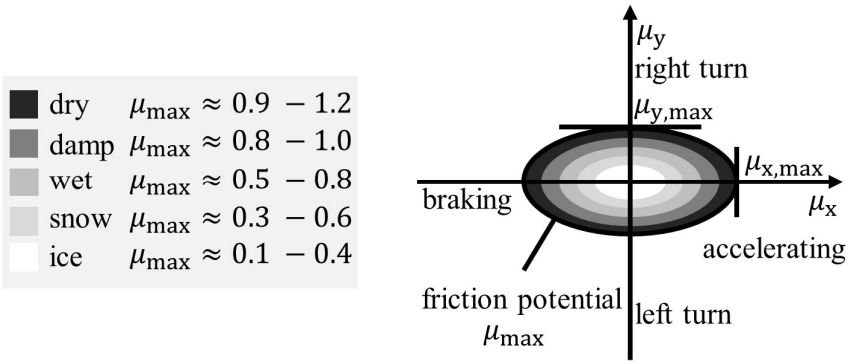

Figure 3.6: Friction potential ellipse according to (Weber 2004; Schramm et al. 2018)

3.2.1.1 Stabilization

For the stabilization level, the reduction in the transmissible forces between the vehicle tire and the road surface means that the vehicle tends to move in the physical limit range more often. Here it behaves increasingly nonlinear and can even become unstable. If the wheels are locked or spinning, the vehicle behavior can no longer be influenced or can only be controlled to a minimal extent. In extreme cases, the vehicle can skid, or steering may become impossible.

Nowadays, standard and, in many cases, mandatory assistance systems for new vehicles are the antilock braking system, the traction control system, and the electronic stability control system. Sometimes the latter is also used as a collective term for the previous ones. These systems ensure that the vehicle remains controllable, even under extreme braking, propulsion, and steering conditions. Since there is no sensor system for measuring the currently available adhesion limit, these systems work with estimation algorithms that only operate when the system is activated and are

only accurate when reaching the grip limit. However, especially regarding highly automated driving, it is desirable if both these and the higher-level control systems are aware of this value and the stability limits in general.

Other assistance systems of the stability level that are more commonly used in larger commercial vehicles include load-adaptive control (LAC), roll over mitigation (ROM), and the trailer sway mitigation system (TSM). In addition to these, several other systems influence the stabilization level according to similar principles. For example, torque vectoring applies braking and driving torque selectively to individual wheels. Some of these systems are discussed in more detail in (Bengler et al. 2014), (Winner et al. 2015), and (Schramm et al. 2020).

Table 3.1 gives a brief overview of selected systems relevant to the present thesis and shows their main effect and actuators mainly used for this purpose.

Table 3.1: Systems on the stabilization level with relevance to the road surface condition.

System	Main Effect Direction			Main Actuator		
	longitudinal	lateral	vertical	brake system	steering system	power train
Electronic stability control		x		x		
Antilock braking system	x			x		
Traction control system	x					x
Load-adaptive control		x		x		
Roll over mitigation			x	x		
Active roll stabilizer			x			x
Trailer sway mitigation		x		x		
Torque vectoring		x		x		x
Electric power steering		x			x	
Driver steering recommendation		x			x	

3.2.1.2 Guidance

As introduced in Chapter 2, the guidance level is the core of the dynamic driving task. At this level, the driver or automated driving system needs to assess and process the complex information about the vehicle's environment and translate these into an adequate driving state with respect to lane, velocity, and headway while ideally supporting the underlying stabilization level and adhering to the necessities of the navigational requirements, like changing lanes to enable a turn at the next intersection.

Numerous ADAS already exist at this level, the combination and further development of which often form the basis for ADS. Regarding the relevance for the improvement by a system providing road surface condition information, these include above all:

- Adaptive cruise control systems,

- collision avoidance systems (CAS), which include, e.g., emergency brake assistance (EBA) systems and emergency steering assistance (ESA) systems, and
- lane keeping assistance as well as lane change assistance (LCA) systems.

Some more systems, such as parking assistance or intersection assistance, will not be considered in more detail due to the given focus. Adaptive cruise control refers to speed control systems that adapt to the traffic situation. As long as the road is clear, the system maintains the desired speed set by the driver until the ACC system is switched off or a slower-moving vehicle comes up ahead. If this is the case, the ACC adjusts the vehicles' speed to that of the vehicle in front employing suitable braking system interventions, among other things, while maintaining the desired distance. As soon as the road is clear again, the system accelerates to the chosen speed.

Understandably, a constantly set distance to the vehicle in front can, under certain circumstances, lead to potentially dangerous driving situations when the chosen distance is within the range of the minimum safety distance. This may happen, e.g., due to the significantly longer braking distance caused by weather-related road conditions. The situation is similar to active collision avoidance systems, which often warn the driver at various escalation levels if specific criteria, such as distance and approach speed, are not met and actively intervene by braking or steering. However, as described above, the intervention threshold is also strongly dependent on the transmittable tire forces. Hence, such systems are also interesting for a corresponding improvement through appropriate information. LCA systems help the driver by monitoring neighboring lanes for the feasibility of lane changes on the one hand and, on the other hand, by actively executing these so that a corresponding release is issued. Here, the dependency of the feasibility assessment on the prevailing lane condition is apparent, which could significantly increase safety and performance in general. Table 3.2 gives a brief overview of selected systems relevant to the thesis' scope and shows their main effect and actuators mainly used for this purpose.

Table 3.2: A selected overview of vehicular systems on the guidance level with potential direct relevance to the road surface condition.

System	Main Effect Direction			Main Actuator		
	longitudinal	lateral	vertical	brake system	steering system	power train
Adaptive cruise control	x			x		x
Collision avoidance	x			x		
Emergency brake assist	x			x		
Emergency steer assist		x			x	
Lane change assistance		x			x	
Lane keeping assistance		x			x	

3.2.1.3 Navigation

On the one hand, the navigation level involves decisions made before the trip begins, such as the choice of route, which may depend on the time available, the volume of traffic, or, if available, the weather situation. On the other hand, it also includes dynamic reactions to unforeseen events such as traffic jams.

In terms of the individual vehicle level, the most common assistance system today is GPS-based geographic guidance. Especially in the development of electromobility and its increased demands on the energy efficiency of the driving strategy due to limited battery capacities, predictive information, e.g., about the topology, is increasingly coming into focus at this level. For the reasons mentioned above, this level might appear less relevant for the vehicle level in the given context of road surface condition detection. However, knowledge of the prevailing weather conditions is also quite interesting for an individual vehicle to support the downstream levels; one thinks of ADS, for example, which may only be activated under certain weather conditions due to their design. However, it would be more interesting to consider this at the overall traffic level since exchanging corresponding data across many vehicles could generate the necessary data for longer-term anticipation.

From all these considerations of the influences on the vehicle level, effects on the macroscopic level arise in the interaction of several vehicles regarding traffic safety and traffic flow, which will now be examined in more detail in the following Section.

3.2.2 Traffic Level

At the vehicle level, specific quantities are considered locally and primarily isolated from the extended environment. At the traffic level, the focus is more on general macroscopic quantities due to the emergent behavior resulting from the various microscopic interactions of the simulated entities. Even if it is possible to consider individual parameters, e.g., of the stabilization level, in submicroscopic and nanoscopic models, this would ultimately again be assigned to the vehicle level so that these are usually not considered separately at the traffic level. In principle, the influence of weather-related road conditions on traffic can initially be subdivided into two subject areas: the impact on traffic flow and road safety. While the effect of weather-related road conditions on traffic flow can be described using figures such as average speeds, travel times, and capacity, the influence on traffic safety is usually described using accident or criticality metrics in terms of headway distances or relative speeds. Since this will play a decisive role in selecting tools and implementation in Chapter 4, it is considered in more detail at this point.

Traffic Efficiency

As mentioned, weather-related road conditions can have a significant influence on traffic flow. Table 3.3 summarizes some USA-based studies to quantify the influence of weather-related road

conditions on traffic efficiency. The partly considerable variation of the values is due to the aggregated presentation of the different studies, which differ significantly in terms of the investigated scenario in each case. A more detailed categorization of the road conditions is omitted here due to better comparability and clarity. However, there is a correlation between the intensity of precipitation and a corresponding reduction in capacity and mean speeds, which is reflected accordingly in the scatter of values mentioned.

Table 3.3: Weather impact on traffic speeds from literature

Environmental Conditions	(Agarwal et al. 2005)	(Stern et al. 2003)	(TRB 2000)	(Goodwin 2002)
Rain (wet)				
Reduction:				
▪ Capacity	4-7 %	3-16 %	5-17 %	-
▪ Speed	10-17 %	10-30 %	0-15 %	10-25 %
Snow (slippery)				
Reduction:				
▪ Capacity	11-15 %	5-40 %	20-35 %	-
▪ Speed	10-17 %	12-27 %	25-30 %	13-40 %

The reduction in capacity is generally due to an increase in the average distance maintained between vehicles compared to dry conditions. Another reason for the large dispersion in the ranges is the different local conditions and the superposition of additional negative effects, such as twilight or darkness. Looking at the values of an older study by (Brilon and Ponzlet 1996), which also considers the influence of wetness on the average speed and capacity on German motorways, a transferability of the results of the American studies to the German traffic area can be established. Relative to a specific motorway Section with a general speed limit, this results in relative values of approx. 6 % - 12 % for speed reduction and approx. 17 % - 35 % for capacity reduction. This range is within the results of the other studies.

Traffic Safety

An analysis of accident figures for different weather-related road surface conditions can be used to illustrate the influence of these on road safety. Every year, the Federal Statistical Office presents a series of comprehensive traffic accident statistics (Destatis 2019), in which, among other things, traffic accidents, including the consequences of accidents according to the road condition, are recorded. In 2018, around 20 % of all accidents involving injuries occurred on wet or damp roads and approximately 2 % on slippery roads during the winter. This relatively low figure is on the one hand because the climate in Germany is relatively moderate, so these road conditions do not often occur even in winter. On the other hand, drivers adapt their driving behavior more strongly under such often unusual conditions. Looking at the time series of the last ten years in Figure 3.7, it becomes clear that there is neither a discernible tendency to improve nor worsen the values. The absolute accident figures of almost 310,000 accidents with injuries to people each year were almost

constant, as were the ratios in relation to road conditions. Each year, about 25 % of these accidents occur in wet conditions and about 3 % in slippery winter conditions.

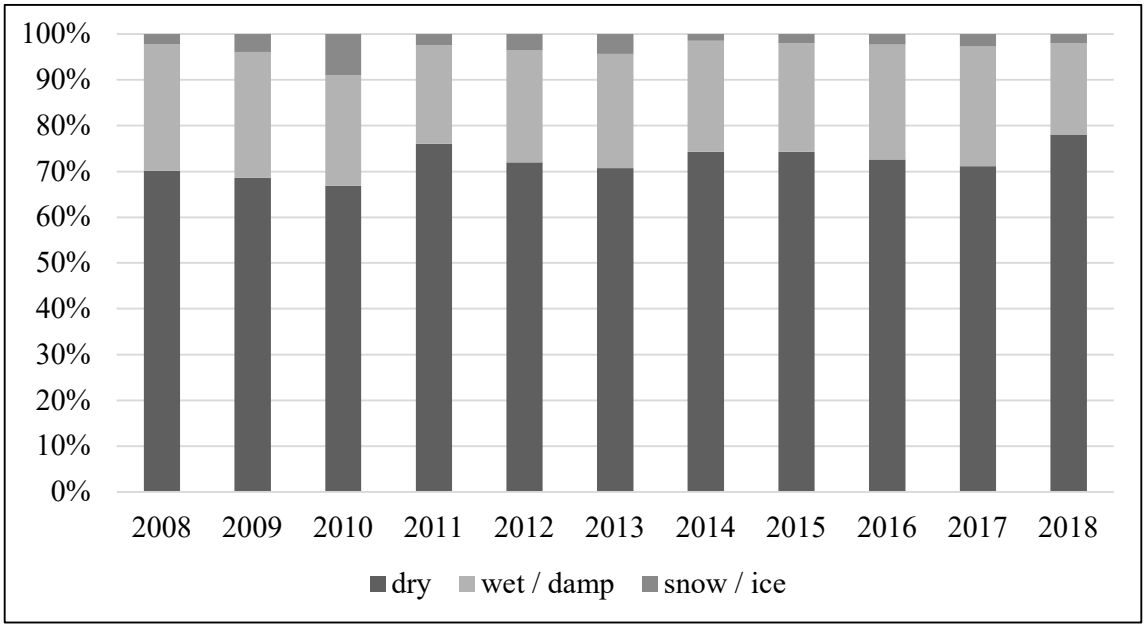

Figure 3.7: Relative numbers of accidents in different road conditions

Figure 3.8, on the other hand, indicates that the overall annual precipitation in Germany in the same timeframe has not significantly changed, even when looking at the average annual precipitation value since the start of recording such data in 1881. It implies that similar precipitation conditions lead to similar accident occurrences.

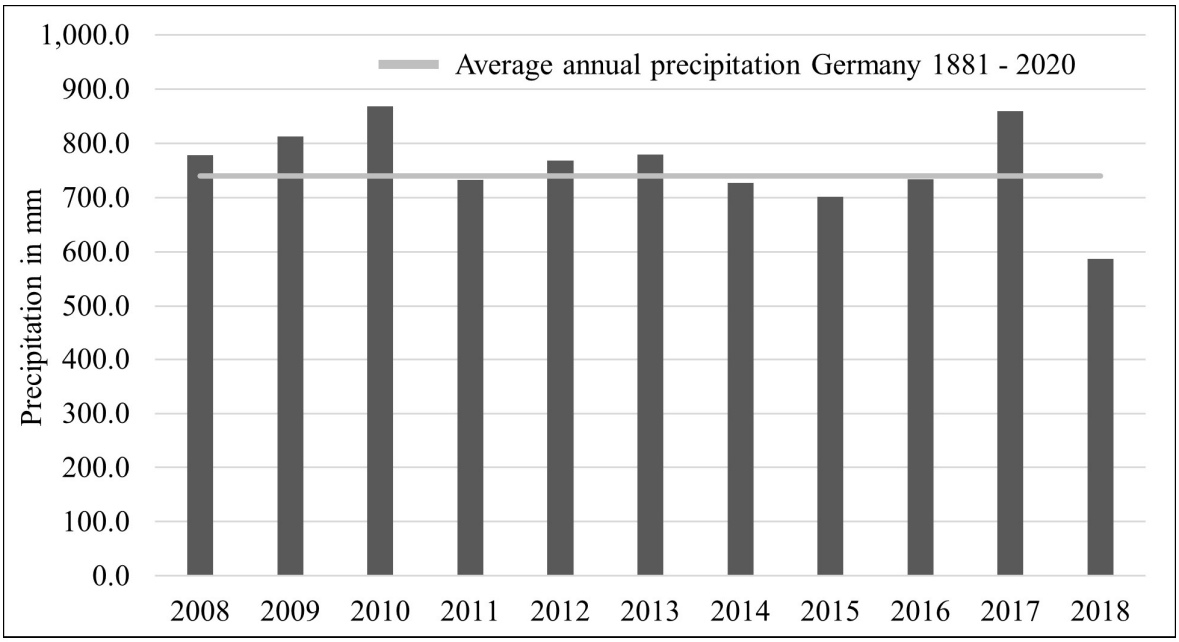

Figure 3.8: Annual precipitation in Germany (Umweltbundesamt 2021)

This illustrates the need to either warn road users of degenerated road conditions employing improved driver assistance systems or to support them in critical driving situations with appropriate interventions. The main potential lies in either significantly reducing the severity of accidents or even altogether avoiding them.

For the sake of completeness, it should also be mentioned that the number of traffic accidents with material damage of approximately 2 million per year has also hardly changed. The proportion of accidents attributable to the road condition is around 3.5 % and holds further potential for corresponding driver assistance or automated driving systems. However, the mere consideration of accident figures is not sufficient since the absence of accidents does not necessarily mean general safe traffic conditions. It is quite possible that critical or supposedly dangerous driving situations occur due to the weather-related road surface but are not recorded in any statistics.

3.3 Stakeholder Identification

The brief system analysis carried out previously shows that even a supposedly simple system can quickly reveal many new dimensions, depending on the angle of view, which might not otherwise be examined in detail. It helps to identify applications, individual systems, the associated impact dimensions, and the possible key performance indicators (KPIs) for a more detailed investigation depending on the task or research question. The stakeholder identification intends to reduce the amount of information obtained to the essentials in a targeted manner.

As mentioned in Chapter 2, stakeholders come from different areas of industry, service providers, civil society, or public authorities. One level below, the term can further be specified. In industry and among the service providers, we also speak of sectors, such as the automotive sector. Below that are, in turn, automotive manufacturers or the various tiers of automotive suppliers. These can be broken down into their organizational units and other corresponding stakeholders, from individual departments to individual products or product ranges, their functions, and value-creating elements, right through to the end customer. For example, in the case of service providers, the financial and banking sector should be mentioned, and below that, the insurance sector, as mentioned in Chapter 2. The term civil society can include all institutions of social coexistence, for example, communities of interest such as the American Automotive Association (AAA), but also non-governmental organizations (NGOs) such as the World Resources Institute (WRI) with their “Shared Mobility Principles for Livable Cities” initiative (Robin Chase 2021) or universities and other academic institutions. Public authorities include the regulatory authorities of societies, from transnational associations such as the European Union (EU) to states and regions to cities and municipalities. This includes the respective legislative responsibility and, for example, the construction, maintenance, and operation of public infrastructure and transport routes if these are not organized in the private sector.

The primary stakeholder of this thesis is the scientific community and is intended to provide an academic contribution. Since this thesis is the result of a research project at a university, and the aim of institutional science is usually more than just the consideration of individual singular aspects, several questions from different considerations and perspectives will be answered in the course of the thesis. The analysis of the system has revealed numerous possible applications, and corresponding specific research questions are formulated in the following subsection. However, it should be mentioned that the focus is generally limited to rather technical aspects since it is a technical thesis. However, the possibilities for linking to other research fields will be discussed in various sections and summarized in more detail in the outlook at the end of the thesis.

As previously discussed in the research concept, specific applications and systems are now selected based on the potential influence at both vehicle and traffic level, which can serve as examples for the application of the overall methodology in the following and at the same time provide quantifiable results. The focus is on integrating a road surface sensor into existing simulation models and using these data in existing or possible future vehicle systems. In this case, there are no special boundary conditions to be considered when selecting the corresponding methods and functions. Still, the thesis attempts to evaluate each potential dimension at least once to maintain the holistic approach. Table 3.4 summarizes the systems or applications selected for further consideration and their main impact dimensions.

Table 3.4: Applications for further consideration and their main impact dimensions

System Application	Driving Task			Potential Dimension		
	Stabilization	Guidance	Navigation	Safety	Efficiency	Comfort
Road surface condition sensor	x	x	x	x	x	x
Antilock braking system	x			x		
Adaptive cruise control		x		x	x	
Emergency braking and steering	x	x		x		
Local Dynamic Map			x	x	x	x

3.4 Specific Research Questions

The general system analysis, the stakeholder identification, and the initially formulated general research question form the frame to define specific research questions. The general research question targets the possibility of carrying out a holistic a priori analysis and evaluating the potential of new systems or functions.

This thesis aims to cover as many areas and levels as possible for the weather-related road surface condition sensor to underline the broad spectrum of applicability of the given research approach. Based on the applications selected in Section 3.3 above, the general research question is further particularized into specific research questions suitable for considering all levels of vehicle guidance and all impact dimensions of the WRSCS. One part, such as the stabilization level in the case of ABS adaptation, will be investigated in the further course of the thesis by focusing on the vehicle level. In contrast, another part will focus on the traffic level, particularly the navigation level, with the local dynamic map and routing. Doing so allows the described holistic approach of the methodology and keeps the thesis's scope manageable. In total, four specific research questions for the WRSCS regarding their potential are formulated:

- RQ1: Is a positive safety impact at the stabilization level achievable through the WRSCS?
- RQ2: Is a positive safety impact at the guidance level achievable through the WRSCS?
- RQ3: Can the use of such a WRSCS lead to an increase in efficiency?
- RQ4: Can the WRSCS be expected to have an impact on comfort?

Table 3.5 summarizes the reference of the questions to the selected applications and the impact dimensions considered in more detail. All three levels of the driving task, the vehicle and traffic levels, and all three potential dimensions are considered. In conducting the study and discussing the results in Chapter 4, the questions are taken up in each case where the results can contribute to answering them. Chapter 5 summarizes the partial results and answers the research questions in summary and conclusion.

Table 3.5: Specific research questions and their relation to the investigated systems and impact dimensions

Research Question	Driving Task			Potential dimension		
	Stabilization	Guidance	Navigation	Safety	Efficiency	Comfort
RQ1	x			V[1]		
RQ2		x		V/T[2]		
RQ3	x	x		V	T	(T)
RQ4			x	T	T	T

[1] V = Vehicle
[2] T = Traffic

3.5 Tool Selection

3.5.1 Adaptive Generic Framework

Before specific tools and models can be selected at the respective levels of investigation, it is necessary to take a closer look at and define the general framework of requirements. This is particularly important in the present case since most of the thesis is based only on computer simulations since no production-ready system for weather-related road surface detection exists to date. Thus possible potentials and influence possibilities can only be investigated in this way. The accuracy of the simulation results depends mainly on the underlying models, which is why the model selection and later implementation plays a central role in any simulation-based investigation. The question of sufficient model accuracy with the lowest possible model complexity concerning the investigated problem is always fundamental for model building. Depending on the available information about the actual process, different strategies of model building are generally considered. In practice, it often makes sense to combine or adapt the design and to run through the development cycle several times in a recursive or iterative process. (Schramm et al. 2018) Also, in the present case, a combination of the procedural models of theoretical and experimental modeling (David and Nolle 1982) is a helpful framework for the approach. Figure 3.9 shows the methodological procedure schematically.

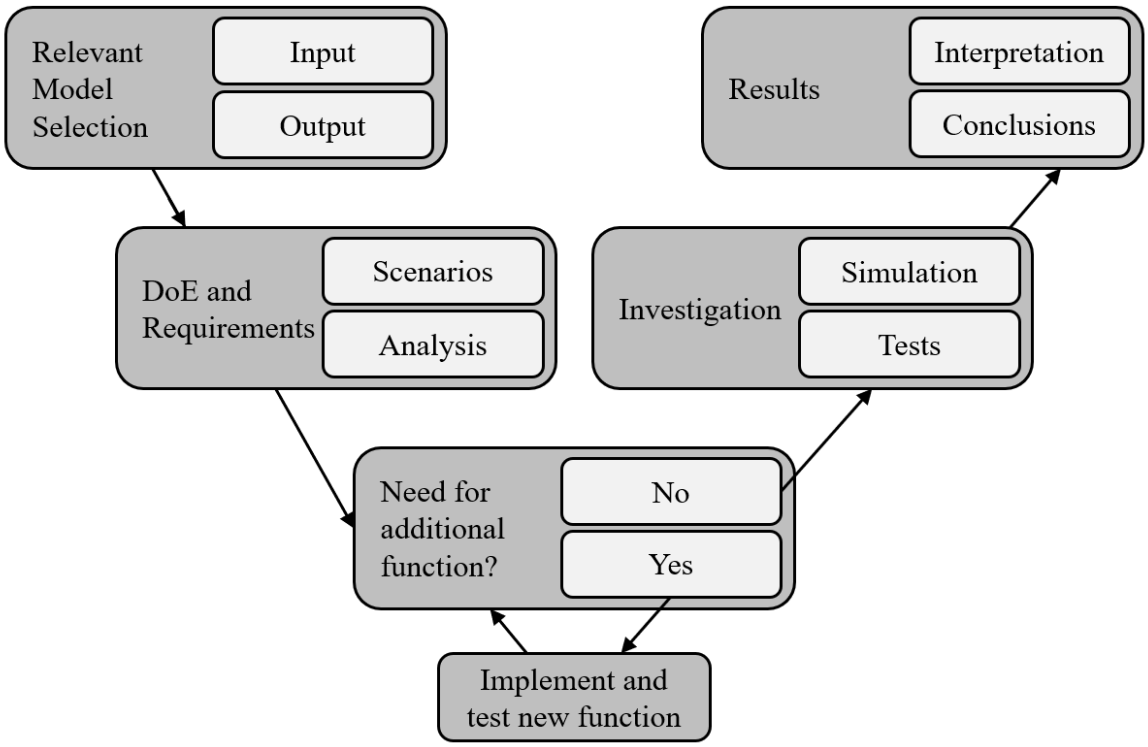

Figure 3.9: Methodological approach for the choice of appropriate tools and models

The essential prerequisite for this procedure is the possibility to collect data at the system inputs and outputs of the respective specific models at least in the simulations, even if real world measurements are not yet possible as mentioned above. Particular attention must be paid to ensuring that these also have the necessary relevance for the individual research questions. Once an appropriate model has been found, a corresponding experimental plan can be drawn up. This must be designed in such a way that, based on the measurable variables, knowledge about the effect of concrete influences on the target variables becomes recognizable while the complexity of the experiment is kept as low as possible. According to this principle, simulation scenarios must be designed so that the effect of the variable influencing variables on the respective previously defined potentials can be derived via the measurable simulation variables.

This is followed by the actual simulation runs and recording suitable measured values of the output variables. In the last step, the measured values obtained are evaluated and interpreted concerning the defined target variables. To enable reliable statements regarding a non-existent system, comparing already established and validated models with adapted, modified, or newly developed ones based on the overall premise is the approach here for all experiments. Even if there are hardly any absolute statements at the end of the process, it often allows to derive clear tendencies in the effect dimensions.

The adaptation, modification, and new development of technical models in the context of the computer-aided simulation analysis carried out here is a software development problem. An iterative and incremental development process can be used to make the overall complexity of the simulation scenarios and implementation necessities manageable. (Sommerville 2018) introduces several already existing processes. In this way, only core functionalities can be implemented in the first development step, while other functionalities can be added in later increments if required. This procedure has the advantage that there are always working solutions that typically already fulfill part of the requirements for the overall project or can even fully answer individual questions up to a certain extent. After an adequate set of functions is implemented to execute the following planned simulation scenario, the next simulation run and the further steps of the methodology for model building follow. It is no coincidence that the right arm of this methodology aligns with the general approach in Figure 3.4. The left arm is the further systematic elaboration of the tool selection. It already shows the flexibility and general applicability not only of the entire methodology introduced here but also of the sub-process steps in detail by their structural similarity. The following sections address the actual selection of specific simulation models and implementation tools with this outline in mind.

3.5.2 Vehicle Level

To analyze the impact of the road condition on the driving dynamics and the performance of individual systems of the vehicle, a model of sufficient complexity is required. As mentioned in Section 2.4.1, several models of different complexity exist, starting from a simple single track model

over rather complex twin track models up to very complex multi body system models. When selecting the model to be implemented, it is crucial to find a good compromise between computational complexity, fulfillment of boundary conditions regarding dynamics and absolute limits, and accuracy of the results concerning the variables of interest. Table 3.6 summarizes available vehicle models for consideration in this thesis, along with their average computational complexity.

Table 3.6: Vehicle model abilities and computational complexities

		STM		TTM	MBSM		
		linear	nonlinear		reduced	complex	FEM
Considerable motion	planar translation, yaw	x	x	x	x	x	x
	roll, pitch, vertical			x	x	x	x
	component motion			(x)	x	x	x
Computational complexity	low	x	x				
	medium			x	x	x	
	high					x	x

In principle, such models are possible in almost all programming languages. They can often be found in the literature, but the effort required to build and, above all, maintain them is not insignificant. Therefore, numerous commercial programs exist, which make appropriate implementations available. These include, for example,

- *CarMaker* from IPG,
- *DYNA4* from VECTOR,
- *ASM* (Automotive Simulation Models) from dSPACE, and
- *CarSim* from the company Mechanical Simulation,

to name just a few. The system dynamic vehicle models are often offered in different levels of detail or with a graduated range of functions. Even if it is possible with various commercial providers to replace multiple components or functions with one's own developments to test them, it is generally not possible to make significant adjustments to the existing software or the models as a whole. Beyond that, for the integration of own models, it is always necessary that appropriate interfaces are made available in the framework. Regarding the necessities of this thesis regarding the weather-related road surface condition, none of the considered commercial providers have appropriate solutions. Moreover, the acquisition of the licenses is often connected with relatively high costs. The block diagram-oriented simulation platform MATLAB/Simulink from *MathWorks*, which has become the industry standard in many areas of engineering over the past decades, is also not free, but is often available at much more favorable conditions in the context of

academic research and is also available at the University of Duisburg-Essen through a corresponding framework agreement. The advantage of an own implementation is the complete control of all interfaces and functionalities, while the increased software maintenance effort is opposed to this accordingly. However, at the Chair of Mechatronics, detailed descriptions of some complex models are already detailed based on previous works (Schuster 1998; Hesse 2011; Hiesgen 2011; Unterreiner 2014). In the context of this thesis, some functions in the dynamic and nonlinear limit range of the vehicle dynamics are examined. According to Table 3.6, only a twin track model or a multi body system model satisfy this requirement. Since many simulation runs are planned, a high computational complexity should be avoided, limiting the selection. Since the selection of the functions examined in the following does not necessarily require the consideration of individual component motions, the choice in this case for the complex vehicle model at the functional level is a variant of the TTM. The tool for implementing the vehicle model and all assistance systems and functions is MATLAB/Simulink due to its high flexibility, portability by code generation, and finally due to its availability.

3.5.3 Traffic Level

When selecting a suitable tool for the simulation of the traffic level, it is also of central importance that, on the one hand, all relevant parameters can be considered and, on the other hand, that it is possible to introduce own models if necessary, as in the present case, or to adapt the existing models accordingly. Furthermore, since functions that specifically influence the behavior of individual vehicles will also be investigated in the further course of the project, tools allowing consideration at the microscopic level must be selected for the traffic level (cf. Section 2.4.2).

A more extensive selection of common frameworks with this capability is summarized in Appendix C. It includes the integrated available longitudinal and lateral dynamics models of the individual vehicles. Although the commercially available programs all offer the possibility of integrating one's own models in one way or another, they are not further investigated here due to both the license requirement for use and the limited model flexibility. When considering the remaining open-source frameworks MITSIMlab (Ben-Akiva et al. 2010) and SUMO (Alvarez Lopez et al. 2018), the latter stands out for greater flexibility in different aspects.

In contrast to MITSIMlab, SUMO is, for example, cross-platform capable due to its implementation, which means that the framework can be compiled and executed on the common Linux and Windows operating systems. In addition, it already natively supports the mesoscopic approach in addition to the purely microscopic approach and provides a greater variety of longitudinal and transverse dynamic models, some of which can be considered significantly more modern and contemporary. In addition, SUMO offers a TCP-based client/server architecture, the so-called “Traffic Control Interface (TraCI)”, which allows the value retrieval and manipulation of simulated objects at runtime if necessary and is therefore very valuable for the further consideration of the connected mobility. Thus, in this thesis, the choice is the use of SUMO.

3.5.4 Automotive Networking

Considering the possibilities for the simulation of networking on both levels requires a tool for network simulation. Here, too, many frameworks are available, but only a few of them already consider the specific requirements of vehicle networking (cf. Section 2.4) so that they can be used for the present thesis without disproportionate effort. (Ben Mussa et al. 2015) compare some existing frameworks concerning usability for connected vehicular networks. Among these are OMNet++ (Varga 2010), NS-2 (Mahrenholz and Ivanov 2004) and NS-3 (Henderson et al. 2008), GloMoSim (Zeng et al. 1998), JiST/SWANS (Barr et al. 2004) and OPNET (Chang 1999). Table 3.7 summarizes their findings. They conclude that the presently most preferable solution for simulation-based studies of vehicular networking is the usage of OMNeT++, using the VEINS (Vehicles in Network Simulation) (Sommer et al. 2011) project for coupling SUMO via the aforementioned TCP interface TraCI. This approach will be used in this thesis since SUMO is the chosen tool for microscopic traffic simulation. VEINS does not yet natively support the ETSI V2X standardization, but this is achieved in this thesis by adding this functionality using additional libraries and is described in more detail in the implementation following in Chapter 4.

Table 3.7: Network simulation tools and their usability for V2X (Ben Mussa et al. 2015)

		OMNeT++ (VEINS)	NS-2/3	GloMoSim	JiST/ SWANS	OPNET
Software Criteria	▪ Open Source	x	x	x	x	x
	▪ Large Networks	x	x	x	x	x
	▪ Scalability	high	poor	high	high	high
	▪ Continuous Development	x	(x)	-	-	-
	▪ Ease of Use	x	x	x	x	x
V2X Criteria	▪ 802.11p	x	x	-	-	-
	▪ Obstacles	x	-	-	-	-
	▪ Traffic flow model	x	x	-	-	-

3.6 Summary

After deriving a general research method to investigate a generalized a priori analysis and evaluation of the potential of future vehicle systems, the target system, a weather-related road surface condition sensor, is thoroughly investigated regarding the potential impact dimensions on the vehicle level as well as the general traffic. For the vehicle level, a range of specific assistance systems is identified that allow which, in the further course, allow statements on all three target dimensions - safety, efficiency, and comfort. Since the interaction of a large number of vehicles basically forms

the traffic level, the foundations have already been laid for considering this level as well. However, since further aspects are important at this level, some extensions to the identified tool will be made here as well. Figure 3.10 summarizes the entire simulation framework for answering the research questions raised in Section 3.4, showing the tools, models, and intended target dimension for the following implementation and investigation.

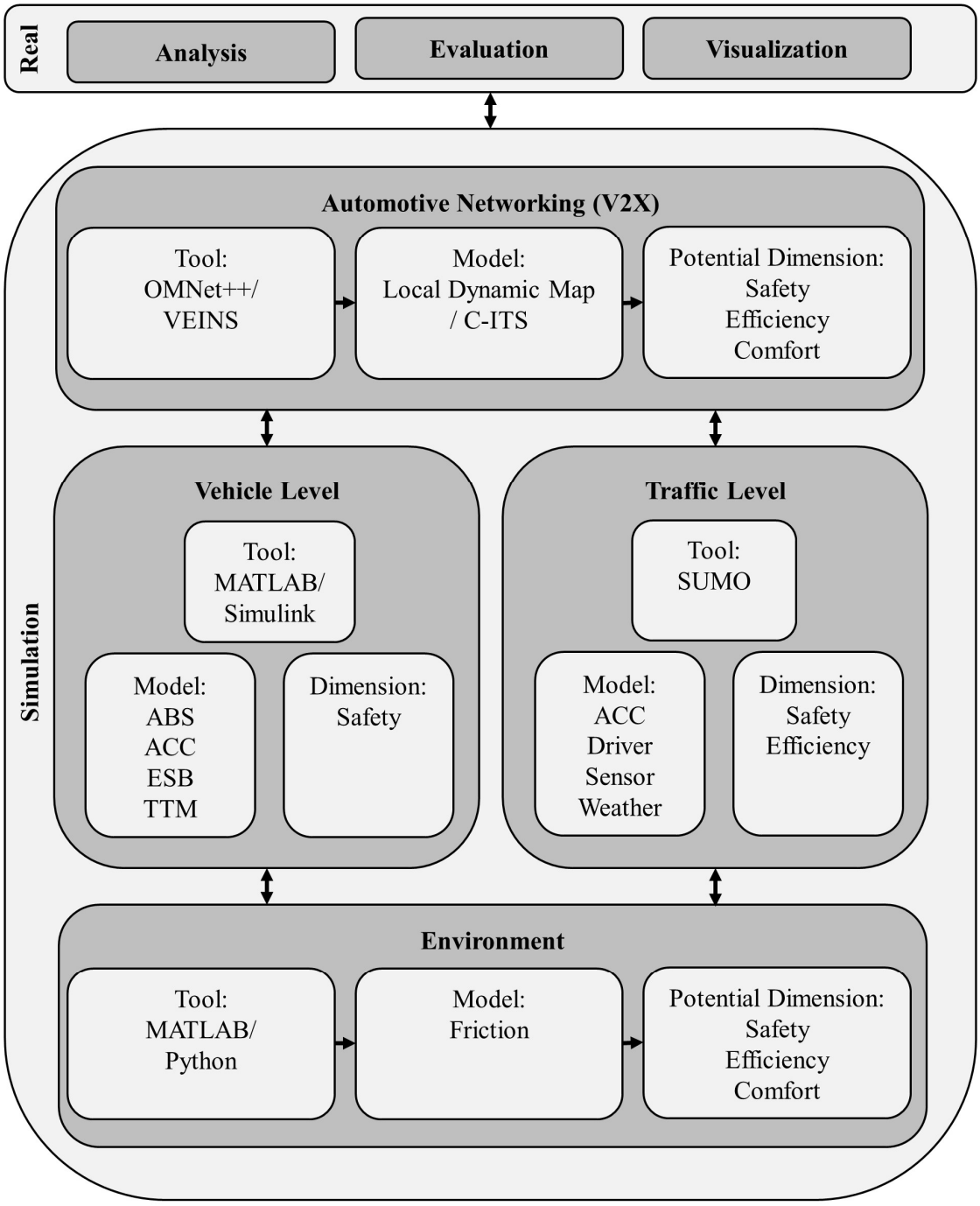

Figure 3.10: Framework for the investigation of the specific research questions

4 Framework Implementation

This Chapter gives a detailed description of the framework implementation. Based on the tool selection in the previous Chapter 3, the implementation of the selected specific simulation models, e.g., the environmental model, sensor model, and vehicle model, is described in detail, as well as the necessary adaptations to the various open-source software modules used and the software modules developed by the author during the integration into the integrated approach for investigating vehicle-related mobility-relevant research questions. The modular approach ensures the necessary flexibility to investigate all levels and various dimensions.

The tools and models selected in Chapter 3 are now combined in an overall simulation environment starting from the given real-world-based analysis of the problem. The concept allows each model to exchange their respective partial results online via an appropriate socket connection or offline through appropriate log files. Depending on the given requirement, they can already be analyzed, evaluated, or visualized online at runtime. This framework also allows performing hardware-in-the-loop tests by exchanging simulated components with real components - from already existing algorithms on electronic control units (ECUs) to complete vehicles. Some of these possibilities will be discussed and demonstrated through examples in this Chapter. It starts with implementing the fundamental environmental model, making the factor weather-related road surface condition available to the other modules on the vehicle and traffic level. Descriptions of these two levels and the implementation and adaption of the respective models and systems follow, and the Chapter concludes with the connection of the levels via automotive networking. The vehicle and the traffic level start with a short overview of the specific optimization approaches of all implemented modules.

4.1 Environmental Model

It is necessary to identify a way to numerically describe the weather-related road surface condition to implement it as a mathematical model for the tools and models on the vehicle and traffic level. In the automotive context, as discussed in Section 3.2.1, the road surface condition is one of the main influencing factors on the coefficient of friction between the tire and the road surface and thus on the transmittable longitudinal and lateral forces (c.f. Figure 3.6) (Klempau 2003; Weber

2004; Schramm et al. 2018). Figure 4.1 shows a graphical approximation of this relationship concerning the transferable longitudinal forces, based on empirical studies by (Yi et al. 1999), (Weber 2004), and (Koskinen and Peussa 2009).

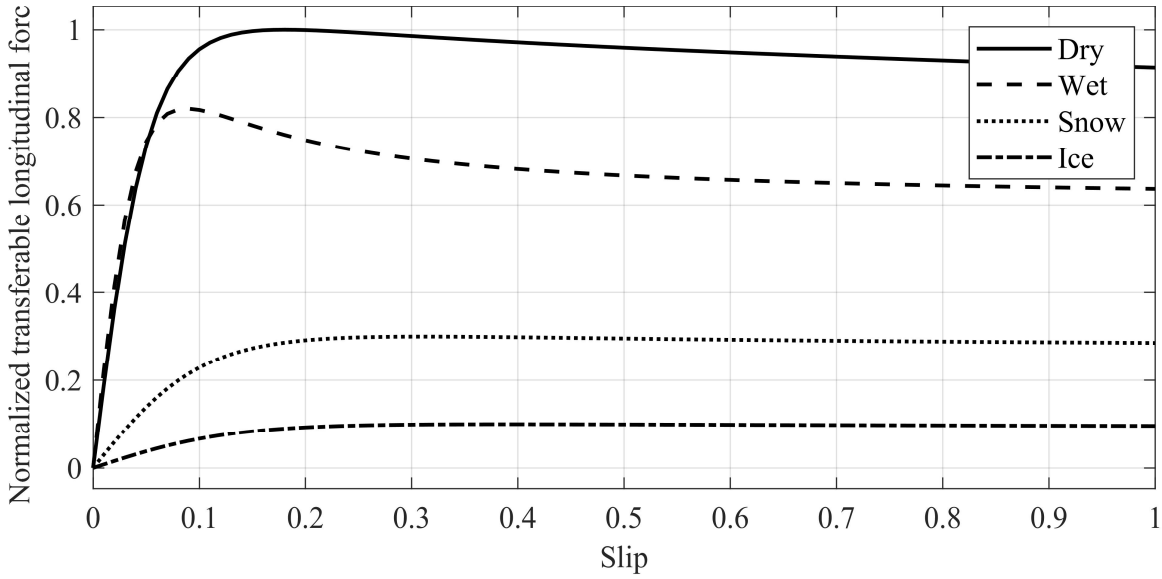

Figure 4.1: Normalized longitudinal force/slip relation in different road surface conditions based on (Koskinen and Peussa 2009)

The interface for the implemented complex vehicle model, which will be introduced in the following Section 4.2.1, is written in MATLAB and provides inputs of the road's vertical coordinate, e.g., to consider slopes or the roughness of the road and the prevalent friction coefficient at the tire level. Figure 4.2 shows the implementation exemplary with four 10x10 meter areas of different road surface conditions used as input for the complex vehicle model simulations

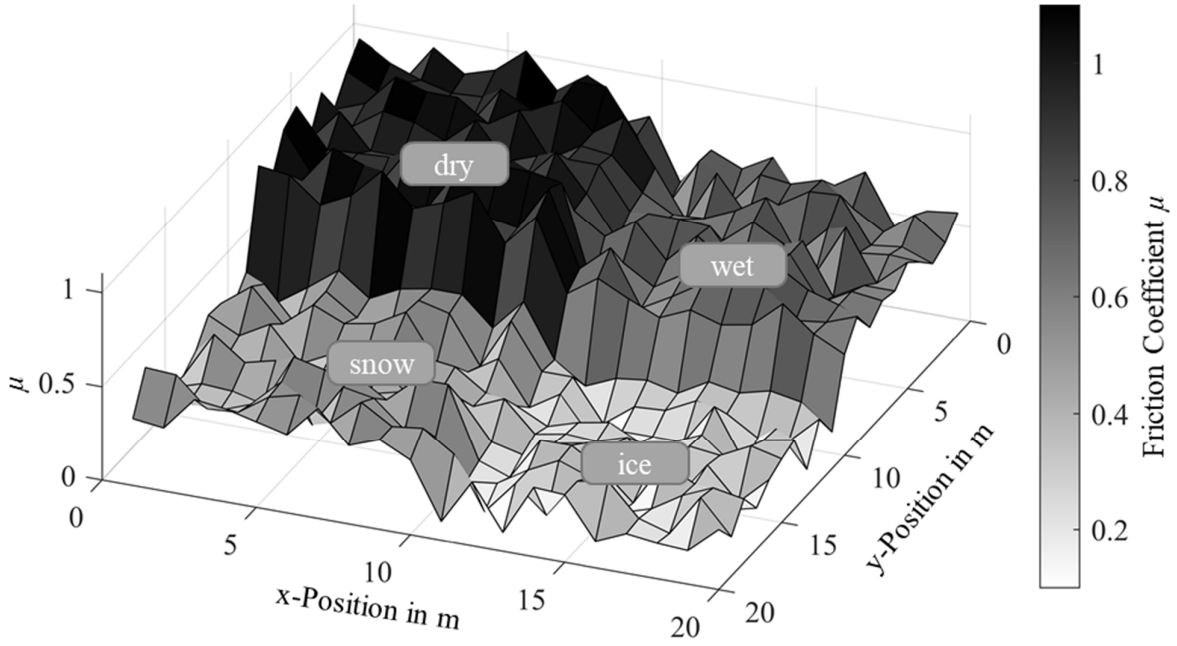

Figure 4.2: Road surface condition model output

4.2 Vehicle Level

As derived in Chapter 3, several different models must be implemented for the investigation of the vehicle level, the chosen tool for this level is MATLAB/Simulink. Next to a modular twin track vehicle model, several relevant ADAS for the vehicle's stability and guidance level are implemented and examined regarding their potential regarding safety. The investigated ADAS on the vehicle level are the antilock braking system, the adaptive cruise control, and the emergency braking and steering system.

The ABS is designed to ensure driving stability and steerability in all driving situations by controlling wheel slip at the maximum friction potential value. Current systems estimate the prevailing friction coefficient only in active operation, which leads to the characteristic 'stuttering' of the systems during emergency braking due to the inaccuracies during estimation and the associated departure from this range.

The operational parameters of current ACC systems are standardized. Nevertheless, short following times at higher speeds in scenarios with reduced friction coefficient conditions can quickly lead to latent critical driving situations.

For the ESB system, the last points to brake and steer are directly dependent on the real available coefficient of friction due to its influence on the overall braking distance and the lateral dynamics during a steering intervention.

Table 4.1 summarizes the optimization approach using the information provided by the weather-related road surface condition sensor for each of the investigated ADAS.

Table 4.1: Summary of the optimization approach for ADAS on the vehicle level

ADAS	Approach	Explanation
ABS	▪ Braking distance minimization ▪ Mastering special driving situations (braking in a turn).	Knowing the maximum current friction coefficient using the information provided by the WRSCS, the system can react faster and control more stable because the brake pressure can be adjusted so that the system always operates within the optimal range.
ACC	▪ Velocity adjustment ▪ Safety distance increase	By knowing the current state through the WRSCS, a system is implemented that adjusts both speed and distance depending on the road condition to reduce such situations and contribute to road safety.
ESB	▪ Last braking point ▪ Last point to steer	By knowing the weather-related road surface condition through the WRSCS, an optimized system can determine these points more precisely and make better decisions for release in case of doubt.

4.2.1 Vehicle Model

In Section 3.5.2, a modular twin track model (Schramm et al. 2018) is selected as a good compromise between complexity and performance. This subsection deals with a respective implementation. Together with a structural variant tire model based on (Schuster 1998), it meets the additional accuracy requirements for specific investigations of the road-tire contact. Specific values for the parameters are summarized in Appendix A.

The advantage of a modular overall vehicle model is that individual vehicle components such as tires, brakes, drive train, steering system, and even the ADAS and control systems can be modeled and replaced independently of one another and, if necessary, with varying degrees of complexity. In this vehicle model, the wheel suspension kinematics are not modeled. It is further assumed that the camber angles do not change during deflection to simplify matters. The wheels can only move vertically relative to the vehicle body in the model, but the suspensions are connected via springs and dampers for the dynamics. This results in 14 degrees of freedom for the twin track model used, listed and described in Table 4.2. The input variables for this system are the steering wheel angle δ_{H} specified by the driver (model), the accelerator pedal position p_{a}, the brake pedal position p_{b}, the engaged gear G, and the road topology in the form of the $z_{\mathrm{T}i}$ -coordinate as well as the road surface condition in the form of the coefficient of friction $\mu_{\mathrm{T}i}$ on the four wheels.

Table 4.2: DOF of the vehicle model by (Schramm et al. 2018)

DOF	Description
$x_{\mathrm{V}}, \mathrm{Y}_{\mathrm{V}}, z_{\mathrm{V}}$	Position of the vehicle COG in the inertial system
$\psi_{\mathrm{V}}, \theta_{\mathrm{V}}, \varphi_{\mathrm{V}}$	CARDAN angle of the vehicle chassis
$z_{\mathrm{T}i}(i = 1..4)$	Vertical position of the i$^{\mathrm{th}}$ tire in the vehicle system
$\rho_{\mathrm{T}i}(i = 1..4)$	Rotation angle of the wheels around their axle

The input vector is:

$$\boldsymbol{u} = [\delta_{\mathrm{H}}, p_{\mathrm{a}}, p_{\mathrm{b}}, G, z_{\mathrm{T}i}\,, \mu_{\mathrm{T}i}]^T, i = 1..4. \tag{4.1}$$

The system generates its dynamic behavior from these input variables in the form of the translational and rotational output variables. As shown in Figure 4.3, the sub-model “tires” represents the central model of the overall system. On the one hand, it describes the translational and rotational wheel movements and, on the other hand, the contact between tire and road surface.

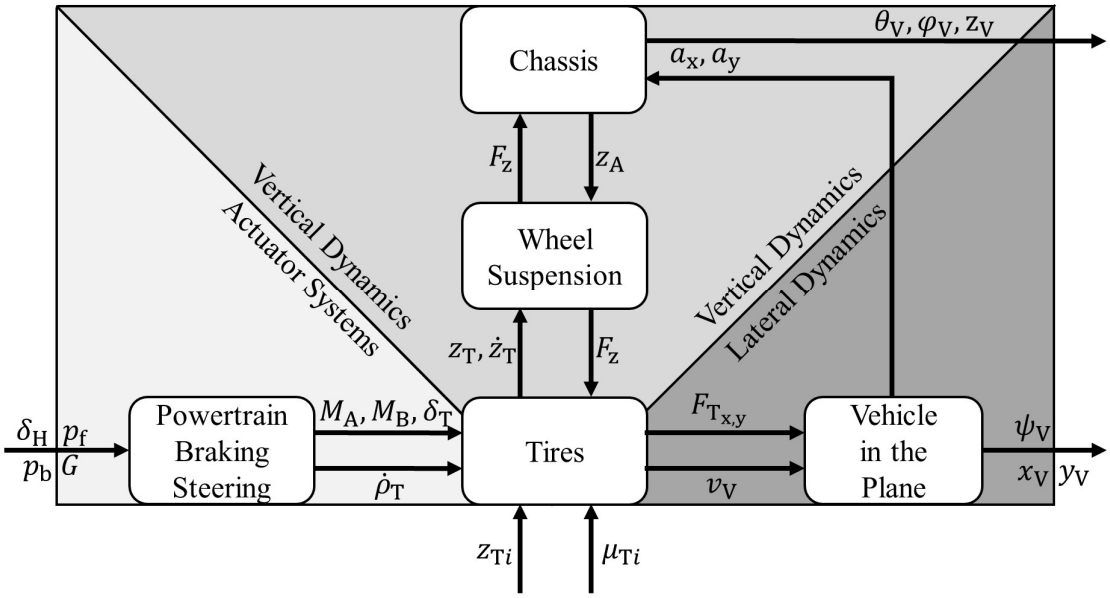

Figure 4.3: Structure of the vehicle model based on (Halfmann and Holzmann 2013)

To describe the movement of the vehicle in space, a spatially fixed Cartesian coordinate system is first defined as an inertial system:

$$\mathrm{K_E} = \{O_\mathrm{E}; x_\mathrm{E}, y_\mathrm{E}, z_\mathrm{E}\}. \tag{4.2}$$

A vehicle fixed coordinate system is defined for the center of gravity (COG) of the vehicle:

$$\mathrm{K_V} = \{O_\mathrm{V}; x_\mathrm{V}, y_\mathrm{V}, z_\mathrm{V}\}. \tag{4.3}$$

For each of the four wheels, a tire fixed coordinate system is defined:

$$\mathrm{K}_{\mathrm{T}i} = \{O_{\mathrm{T}i}; x_{\mathrm{T}i}, y_{\mathrm{T}i}, z_{\mathrm{T}i}\}. \tag{4.4}$$

The rotation of the vehicle fixed coordinate system relative to the inertial system is described by the CARDAN angles ψ_V (yaw angle), θ_V (pitch angle), and φ_V (roll angle), (Hiller 1983). The transition between these coordinate systems can be expressed mathematically by transformation matrices. For simplicity, the trigonometric functions sin (s) and cos (c) are abbreviated in the following formulas. The rotation into the inertial coordinate system $\mathbf{K_E}$ from the vehicle fixed coordinate System $\mathbf{K_V}$ can be achieved with the transformation matrix ${}^{\mathrm{E}}\boldsymbol{T}_\mathrm{V}$:

$$
\begin{aligned}
{}^{\mathrm{E}}\boldsymbol{T}_\mathrm{V} &= \boldsymbol{T}_\mathrm{z}(\psi_\mathrm{V}) \cdot \boldsymbol{T}_\mathrm{y}(\theta_\mathrm{V}) \cdot \boldsymbol{T}_\mathrm{x}(\varphi_\mathrm{V}) = \\
&\begin{bmatrix}
c\theta_\mathrm{V} c\psi_\mathrm{V} & s\varphi_\mathrm{V} s\theta_\mathrm{V} c\psi_\mathrm{V} - c\varphi_\mathrm{V} s\psi_\mathrm{V} & c\varphi_\mathrm{V} s\theta_\mathrm{V} c\psi_\mathrm{V} + s\varphi_\mathrm{V} s\psi_\mathrm{V} \\
c\theta_\mathrm{V} s\psi_\mathrm{V} & s\varphi_\mathrm{V} s\theta_\mathrm{V} s\psi_\mathrm{V} + c\varphi_\mathrm{V} c\psi_\mathrm{V} & c\varphi_\mathrm{V} s\theta_\mathrm{V} s\psi_\mathrm{V} - s\varphi_\mathrm{V} c\psi_\mathrm{V} \\
-s\theta_\mathrm{V} & s\varphi_\mathrm{V} c\theta_\mathrm{V} & c\varphi_\mathrm{V} c\theta_\mathrm{V}
\end{bmatrix}.
\end{aligned} \tag{4.5}
$$

The angular velocity of the rotation of the vehicle-fixed coordinate system relative to the inertial system can be determined in vehicle-fixed coordinates via the kinematic CARDAN equations:

$$ {}^{\mathrm{V}}_{\mathrm{E}}\dot{\rho}_{\mathrm{V}} = \begin{bmatrix} \dot{\rho}_{\mathrm{V,x}} \\ \dot{\rho}_{\mathrm{V,y}} \\ \dot{\rho}_{\mathrm{V,z}} \end{bmatrix} = \begin{bmatrix} \dot{\varphi}_{\mathrm{V}} - \dot{\psi}_{\mathrm{V}} s\theta_{\mathrm{V}} \\ \dot{\theta}_{\mathrm{V}} c\varphi_{\mathrm{V}} + \dot{\psi}_{\mathrm{V}} c\theta_{\mathrm{V}} s\varphi_{\mathrm{V}} \\ -\dot{\theta}_{\mathrm{V}} s\varphi_{\mathrm{V}} + \dot{\psi}_{\mathrm{V}} c\theta_{\mathrm{V}} c\varphi_{\mathrm{V}} \end{bmatrix}. \tag{4.6} $$

4.2.1.1 NEWTON-EULER Equations of the Chassis

For the general spatial, translational, and rotational movements of the vehicle body, the NEWTON-EULER equations are applied to the body in all directions of movement. With $\mathrm{r_V}$ being the vehicles position vector in the inertial system, the NEWTON equation for the chassis yields:

$$ m_{\mathrm{v}} \ddot{\mathrm{r}}_{\mathrm{V}} = \sum_{i=1}^{4} \boldsymbol{F}_i + \boldsymbol{F}_{\mathrm{G}} + \boldsymbol{F}_{\mathrm{W}} , \tag{4.7} $$

where m_{v} denotes the chassis mass without the mass of the wheels. The vector $\boldsymbol{F}_i$ consists of the horizontal reaction forces $\boldsymbol{F}_{\mathrm{H}i}$, the spring and damper forces $\boldsymbol{F}_{\mathrm{S}i}$ and $\boldsymbol{F}_{\mathrm{D}i}$, and the stabilizer forces $\boldsymbol{F}_{\mathrm{St}i}$, which are transmitted between the wheel suspensions and the vehicle body:

$$ \boldsymbol{F}_i = \boldsymbol{F}_{\mathrm{H}i} + \boldsymbol{F}_{\mathrm{F}i} + \boldsymbol{F}_{\mathrm{D}i} + \boldsymbol{F}_{\mathrm{St}i}. \tag{4.8} $$

Vector $\boldsymbol{F}_{\mathrm{G}}$ contains the gravitational force, and the vector $\boldsymbol{F}_{\mathrm{W}}$ denotes the air resistance and wind forces that act on the chassis. For the rotatory movement of the vehicle, the EULER equation in the vehicle fixed coordinate system yields:

$$ \boldsymbol{\Theta_V}\ddot{\boldsymbol{\rho}}_{\boldsymbol{V}} + \dot{\boldsymbol{\rho}}_{\boldsymbol{V}} \times (\boldsymbol{\Theta_V}\dot{\boldsymbol{\rho}}_{\boldsymbol{V}}) = \sum_{\boldsymbol{i=1}}^{\boldsymbol{4}} {}_{\boldsymbol{V}}\boldsymbol{r}_{\boldsymbol{S,i}} \times \boldsymbol{F}_{\boldsymbol{i}} + \boldsymbol{r}_{\boldsymbol{W}} \times \boldsymbol{F}_{\boldsymbol{W}}. \tag{4.9} $$

The inertia matrix $\boldsymbol{\Theta}_{\mathrm{V}}$ expresses the inertia of the vehicle body for rotations about the x-, y- and z-axis. $\ddot{\rho}_{\mathrm{V}}$ denotes the absolute angular velocity of the chassis. The vector ${}_{\mathrm{V}}\boldsymbol{r}_{\mathbf{S,i}}$ describes the position from the center of gravity of the chassis to the respective suspension point and the vector $\mathrm{r}_{\mathbf{W}}$ is the position vector from the chassis' COG to the resulting aerodynamic forces.

4.2.1.2 Steering

The steering system converts the rotation of the steering wheel into a rotation of the wheels around their vertical axis. In the passenger car segment, the steering is usually designed as front axle steering. Sometimes, rear-axle steering is also used to improve driving dynamics, as implemented in the Porsche 911 GT2 RS.

Within the scope of this thesis, the modeling of complex steering kinematics is omitted. Instead, it assumes that the steering angles of the two front wheels δ_T are always identical and depend linearly on the steering wheel angle δ_H via the steering ratio i_S. The steering angles are:

$$\delta_T = \frac{1}{i_S}\,\delta_H\,. \tag{4.10}$$

4.2.1.3 Drivetrain

Drive torque is generated in the drive train and transmitted to the vehicle wheels. Figure 4.4 shows the schematic structure of the drive train for a four-wheel drive. The combustion engine generates for the current engine speed n_M an engine torque M_M as a function of the accelerator pedal position p_F. This engine torque is translated into the four drive torques transmitted to the vehicle wheels by a transmission with the gear ratio $i_G(G)$, a central differential with the ration i_D, and the front and rear axle differentials i_{Df} and i_{Dr}.

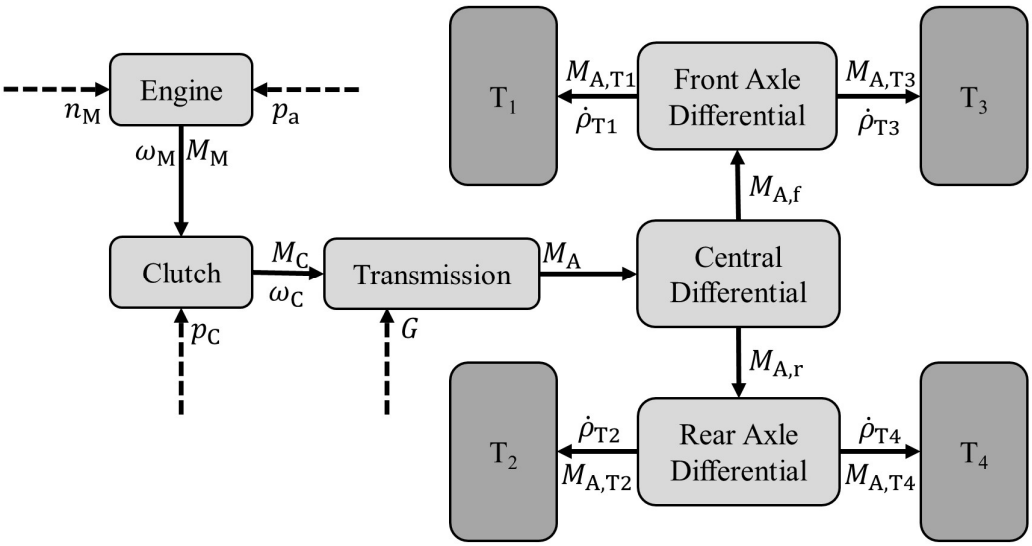

Figure 4.4: Schematic structure of a drivetrain with four-wheel drive

The motor angular speed ω_M is kinematically coupled to the wheel speeds $\dot{\rho}_{Ti}$ (i =1..4) and can therefore be determined. Parameter ξ_a determines how the drive torque is distributed between the front and rear axle. For front-wheel drive $\xi_a = 0$, for rear-wheel-drive $\xi_a = 1$ and for all-wheel-drive $0 < \xi_a < 1$. The motor angular speed is therefore calculated to

$$\omega_M = i_D i_G(G)\left((1-\xi_a) i_{Df}\left(\frac{\dot{\rho}_{T1}+\dot{\rho}_{T3}}{2}\right) + \xi_a i_{Dr}\left(\frac{\dot{\rho}_{T2}+\dot{\rho}_{T4}}{2}\right)\right). \tag{4.11}$$

By conversion, the motor revolutions per minute n_M can be calculated to

$$n_M = \frac{30}{\pi}\omega_M \tag{4.12}$$

and used to determine the engine torque based on an engine map shown in Figure 4.5.

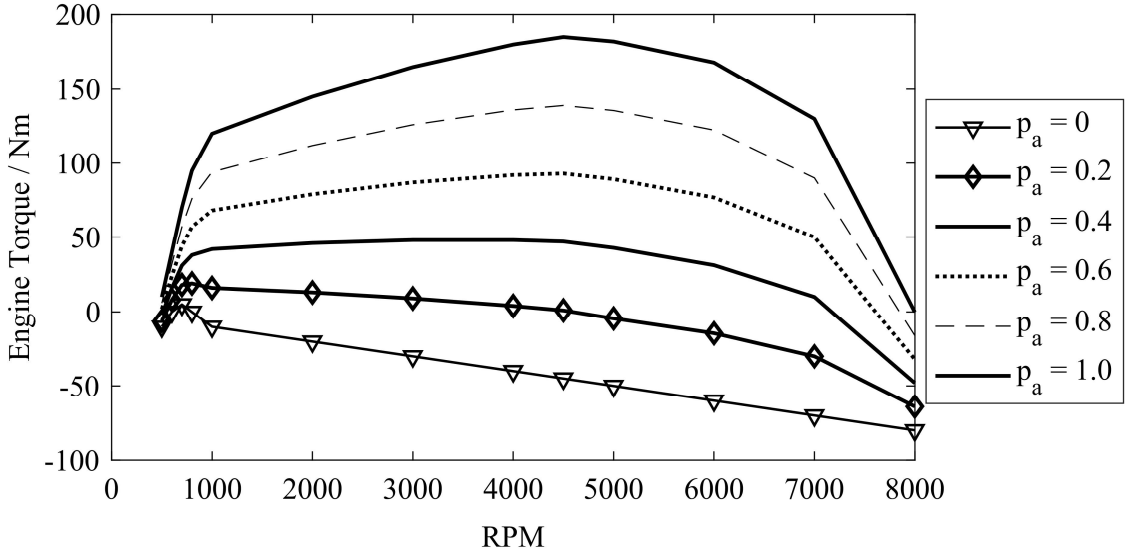

Figure 4.5: Engine torque map derived from ADVISOR (Markel et al. 2002)

The transmittable torque at the coupling is M_{C} with the motor angular acceleration $\alpha_{\mathrm{M}} = \dot{\omega}_{\mathrm{M}}$ considering the motor inertia θ_{M}:

$$M_{\mathrm{C}} = M_{\mathrm{M}} - \theta_{\mathrm{M}}\alpha_{\mathrm{M}} . \tag{4.13}$$

This torque is transmitted if the clutch is closed, i.e. $p_{\mathrm{c}} = 0$ (pedal is released). However, the transmitted torque is reduced when the clutch becomes opened, i.e., $0 < p_{\mathrm{C}} \leq 1$, expressed by:

$$M_{\mathrm{C}} = (M_{\mathrm{M}} - \theta_{\mathrm{M}}\alpha_{\mathrm{M}})(1 - p_{\mathrm{C}}). \tag{4.14}$$

For simplification, it is assumed that the speeds of the clutch discs are always synchronous and that the transmittable torque only changes at decoupling. Considering the inertia of the gearbox input shaft θ_{GI} and the gearbox output shaft θ_{GA} as well as the gear ratio i_{G} and the differential ratios i_{D} , i_{Df}, and i_{Dr}, the total drive torque is calculated:

$$M_{\mathrm{A}} = (i_F\,(1 - \xi_a\,) + i_B\,\xi_a\,)i_{\mathrm{D}}\left[i_G M_C - \frac{1}{i_g}(\theta_{GI} i_G^2 + \theta_{GA})\alpha_M\right]. \tag{4.15}$$

This equation shows that no rear Differential is required for front-wheel drive ($\xi_{\mathrm{a}} = 0$) and no front Differential for rear-wheel drive ($\xi_{\mathrm{a}} = 1$). The drive torques of the individual wheels are identical for each axle.

4.2.1.4 Braking System

When the brake pedal is actuated, the braking system generates a braking torque applied to the vehicle wheels. Passenger cars usually employ a brake booster, significantly reducing the muscle

power required to operate the brake pedal. (Breuer and Bill 2012) Figure 4.6 schematically shows the structure of the implemented hydraulic brake system.

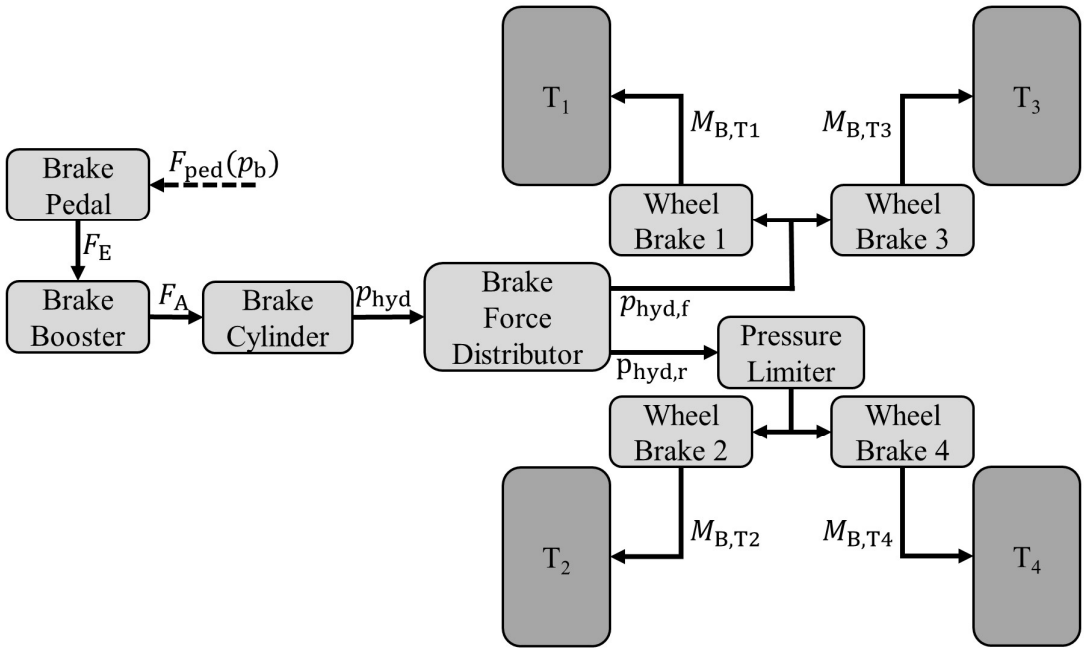

Figure 4.6: Schematic structure of the hydraulic brake system

The main components of the brake system are the brake pedal, the brake booster with the master brake cylinder, the wheel brakes with the brake pistons, and the brake disks. The input variable of the brake system is the relative brake pedal position p_b. The position is converted into a pedal force F_E via a progressive force-displacement characteristic curve shown in Figure 4.7, which is subsequently converted by the linear amplification ratio i_AR into the input force of the brake booster.

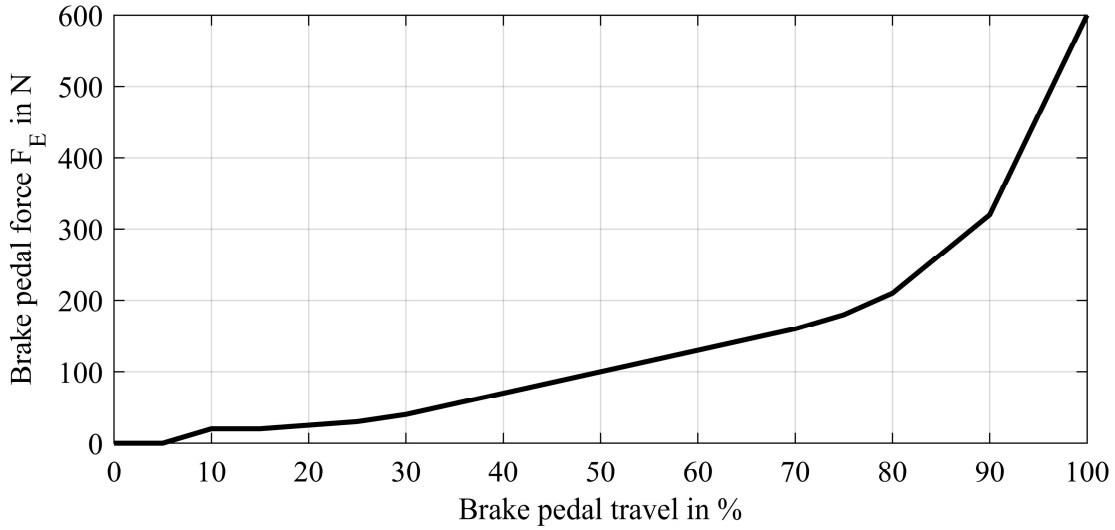

Figure 4.7: Progressive brake pedal travel-force relation based on (Breuer and Bill 2012)

A supporting force F_{A} is generated in the brake booster depending on the force F_{E}. The maximum possible brake support is achieved at the modulation point and is determined by the brake booster's design features and the quality of the vacuum. Below the so-called trigger point, the braking force is amplified with the linear amplification ratio i_{AR}:

$$F_{\mathrm{A}} = i_{\mathrm{AR}} F_{\mathrm{E}} - F_{\mathrm{F,AR}}, \tag{4.16}$$

where $F_{\mathrm{F,AR}}$ denotes the counteracting force of the compression spring, which is calculated from the counteracting force resulting from brake pedal units' return spring.

Above the trigger point, the additional support force remains constant because the differential pressure between the atmosphere and vacuum p_{vac} is applied to the entire membrane area A_{AR}. Thus F_{A} yields:

$$F_{\mathrm{A}} = F_{\mathrm{E}} + p_{\mathrm{vac}} A_{\mathrm{AR}} - F_{\mathrm{F,AR}}\,. \tag{4.17}$$

The force of the return spring $F_{\mathrm{F,AR}}$ counteracts the increase in braking force in both cases.

The master brake cylinder converts the force F_{A} into the hydraulic pressure p_{hyd} of the brake system via its effective area A_{BC} according to:

$$p_{\mathrm{hyd}} = \frac{F_A}{A_{\mathrm{BC}}} = \frac{1}{A_{\mathrm{BC}}}\left(i_{\mathrm{ped}} F_{\mathrm{ped}} + p_{\mathrm{vac}} A_{\mathrm{AR}} - F_{\mathrm{F,AR}}\right). \tag{4.18}$$

The brake lines transmit the hydraulic pressure to the brake pistons of the wheel brakes. Finally, the wheel brakes generate the braking torque $M_{\mathrm{B,T}i}$. With the effective brake radius r_{eff} and the brake piston area, A_{Bp} one gets the braking torque:

$$M_{\mathrm{B,T}i} = r_{\mathrm{eff}}\, A_{\mathrm{Bp}}\, p_{\mathrm{hyd}}\, C^*\,. \tag{4.19}$$

This standardized calculation formula applies to all brake types. The dimensionless brake characteristic C^* considers the differences in the characteristics of the various designs. The various C^* values are summarised in (ISO 611:2003) as a function of the brake design. The clamping force acts on the brake shoes with disc brakes and presses the brake linings against the brake disc. The braking force is thus the friction force between the brake linings and the brake disc with the friction coefficient μ_{lin}:

$$C^* = 2\,\mu_{\mathrm{lin}}\,. \tag{4.20}$$

The braking force between the tire and the road surface is calculated with the dynamic tire radius as follows:

$$F_{\mathrm{B,T}i} = \frac{M_{\mathrm{B,T}i}}{r_{\mathrm{dyn,T}i}}\,. \tag{4.21}$$

The axle load shift due to the vehicle's pitch leads to higher transmittable braking forces at the front wheels. To prevent over-braking, i.e., exceeding the maximum braking force of the rear

wheels, the aim is to distribute the braking pressure so that the rear wheels utilize their braking force potential of the rear wheels optimally. The implemented model applies a fixed brake force distribution

4.2.2 Tire Model

Tires are among the most critical vehicle components because they form the interface between the wheels and the road. The task of the tires is to carry the weight of the vehicle and transmit the longitudinal forces for braking and accelerating and the transverse forces for cornering. The tires thus have a major influence on the driving dynamics of a vehicle. In addition, their spring and damping properties contribute to driving comfort. The contact between the tire and the road surface is a very complex system due to the unique characteristics of a tire. Within simulations, the forces in the patch cannot be determined analytically without further effort. Therefore, the tire behavior is approximated by tire models that can be divided into mathematical, physical, and partially physical models. (Leister 2015)

Because this thesis also focuses on a system for detecting the condition of the road, a tire model is required in which the contact between road and tire is approximated more closely and allows non-linear observations. In order to fulfill all requirements, a structure variant tire model is implemented according to the approach of (Schuster 1998). Structure variant meaning that three states of motion of the tires are distinguished, the adhesion or adhesion and sliding, the blocking, and the standstill of the tire. For standstill, an additional distinction is made as to whether the tire is decelerating or accelerating.

4.2.2.1 Model for tire adhesion or adhesion and gliding

The tire model is based on the Highway Safety Research Institute (HSRI) model, initially developed by (Dugoff et al. 1969). The HSRI model is a physical tire model in which the horizontal forces in the patch are determined by approximating the resulting deformations. The horizontal forces F_x and F_y are determined by approximating the deformations in the patch and calculating the resulting stresses. Figure 4.8 gives an overview of the model structure and the required calculation parameters described in detail below.

The relevant parameters for the EULER equation are the braking and drive torque, the longitudinal force in the patch, and the dynamic tire radius. Due to the radial compression of the tire, the dynamic wheel radius r_{dyn} is smaller than its design radius r_0 and is calculated inside the vertical dynamics block for the respective driving condition with the aid of the vertical tire forces F_x by modeling the tire as a very stiff spring for this purpose. Thus, the EULER equation yields:

$$\ddot{\rho}\theta = M_A - sign(\dot{\rho})M_B - F_x r_{dyn}. \tag{4.22}$$

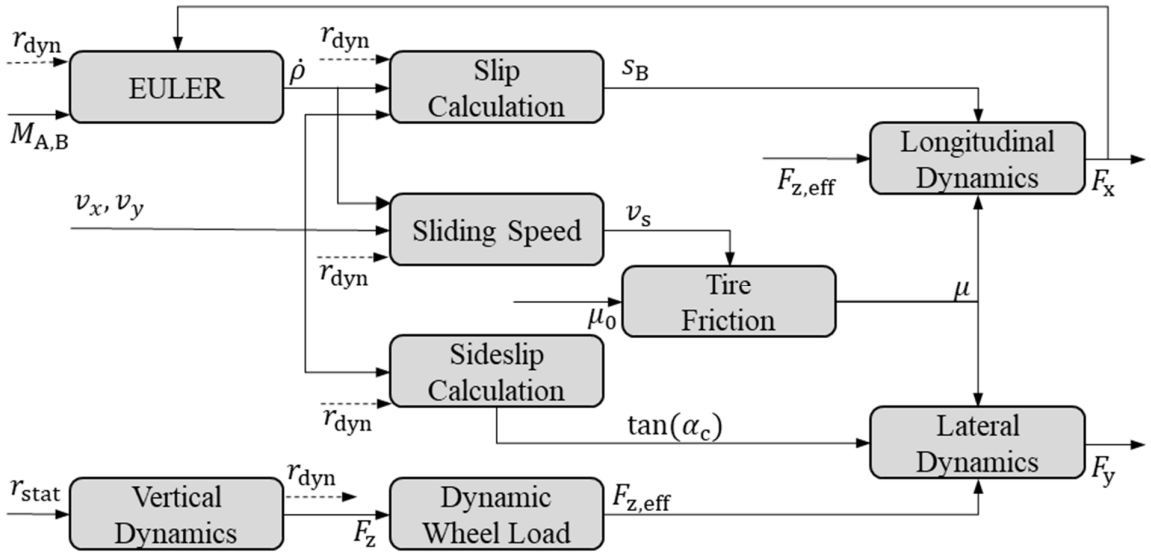

Figure 4.8: Schematic model structure for adhesion and gliding

With the help of the wheel speeds and the vehicle speed vector, the slip, the sideslip angle, and the sliding speed in the patch can be calculated. A distinction between drive slip $s_D$and brake slip s_B is made:

$$s_B = \frac{v_x - \omega r_{dyn}}{v_x}, \tag{4.23}$$

$$s_D = \frac{v_x - \omega r_{dyn}}{\omega r_{dyn}}. \tag{4.24}$$

In contrast to most models in the literature, the tire model presented is also used to calculate the brake slip on the driven wheel and describe the forces physically. In the simulation, some variables can be combined to the drive slip s_D. The calculation of the drive slip can be described as follows as a function of the brake slip:

$$s_D = \frac{s_B}{1 - s_B}. \tag{4.25}$$

This can reduce the number of parameters transferred from the slip formation sub-model to the force calculation sub-model and the calculation time required for the slip calculation at low speeds. The sideslip angle is usually described as the angle between the longitudinal direction of the wheel and the direction of wheel movement in the xy-plane and is calculated according to:

$$\alpha = \tan^{-1}\left(\frac{v_y}{v_x}\right). \tag{4.26}$$

According to (Schuster 1998), these values can be used to determine the sliding speed in the patch

$$v_s = |v_p|\sqrt{s_B^2 + \tan^2\alpha}\,, \tag{4.27}$$

where $|v_\mathrm{p}|$ denotes the magnitude of the speed in the longitudinal direction of the patch. This can be used to calculate the coefficient of friction between the tire and the road surface

$$\mu\,(\mu_0) = \mu_0(1 - k_\mathrm{R}\tanh(a v_\mathrm{S})^2). \tag{4.28}$$

The parameters k_R, a and μ_0 depend on the surface texture of the road. For the calculation of the tire forces, an effective wheel load is needed. The specific tire design determines the influence of the wheel load on the horizontal force in the contact patch. According to (Ammon 1997), the transmissible tire forces in normal operating conditions are linearly related to the vertical load. After exceeding the constructive operating load $F_\mathrm{z,stat}$ the force potential in the patch shows a weakly decreasing behavior, which can be explained by the decrease of the friction bond with increasing contact pressure. A wheel-specific characteristic curve function can consider this behavior. Here, a parabolic influence of the wheel load according to (Schramm et al. 2018), is used:

$$F_\mathrm{z,eff} = F_\mathrm{z}\left(1 - e_\mathrm{z}\left(\frac{F_\mathrm{z}}{F_\mathrm{z,stat}}\right)\right)^2. \tag{4.29}$$

For the calculation of the resulting longitudinal and transverse forces on tires F_x and F_y, knowledge of the adhesion and sliding condition in the contact patch is required in addition to the effective wheel load. According to (Schramm et al. 2018), the dimensionless quantity $\bar{s}_\mathrm{R}$ serves as an indicator for the occurrence of slippage, F_tot being the sum of transferred forces at the tires:

$$\bar{s}_\mathrm{R} = \frac{F_\mathrm{tot}}{\mu F_\mathrm{z,eff}} = \frac{\sqrt{\left(\frac{1}{2}c_\mathrm{S}s_\mathrm{B}\right)^2 + \left(\frac{1}{2}c_\alpha\tan(\alpha)\right)^2}}{\mu F_\mathrm{z,eff}(1 - s_\mathrm{B})^2}. \tag{4.30}$$

If $\bar{s}_\mathrm{R} < 0.5$, no sliding occurs between the contact patch and the road's surface. As soon as this value is exceeded, a sliding area forms behind the adhesion area in the patch. The longitudinal force F_x and the transverse force F_y result from integrating the longitudinal and transverse stresses across the adhesion and sliding areas. (Schuster 1998) gives a detailed derivation of the force equations. Depending on the conditions indicated by $\bar{s}_\mathrm{R}$, the forces yield:

$$F_\mathrm{x} = \begin{cases} -\dfrac{c_\mathrm{S}s_\mathrm{B}}{1 - s_\mathrm{B}} & \bar{s}_\mathrm{R} \le 0.5 \\ c_\mathrm{s}s_\mathrm{B}\dfrac{\bar{s}_\mathrm{R} - 0.25}{\bar{s}_\mathrm{R}^2(1 - s_\mathrm{B})} & \bar{s}_\mathrm{R} > 0.5 \end{cases} \tag{4.31}$$

$$F_\mathrm{y} = \begin{cases} -c_\alpha\tan(\alpha_\mathrm{C}) & \bar{s}_\mathrm{R} \le 0.5 \\ -c_\alpha\tan(\alpha_\mathrm{C})\dfrac{\bar{s}_\mathrm{R} - 0.25}{\bar{s}_\mathrm{R}^2} & \bar{s}_\mathrm{R} > 0.5 \end{cases} \tag{4.32}$$

4.2.2.2 Locking Wheels

The model for locking wheels is applied when the brake slip $s_\mathrm{B} \geq 0.99$. In the locked state, the deformation of the profile elements is assumed to be constant over the entire contact patch. Due to the homogeneous tangential stress in the patch, the wheel-road contact can be described independently of it. This results in the horizontal tire force:

$$F_\mathrm{h} = \mu F_\mathrm{z,eff}. \tag{4.33}$$

It works against the direction of movement of the wheel center, and with (4.26), the individual tire forces yield:

$$F_\mathrm{x} = -F_\mathrm{h}\cos(\alpha) \tag{4.34}$$

$$F_\mathrm{y} = -F_\mathrm{h}\sin(\alpha) \tag{4.35}$$

For the sliding speed of the profile elements of the locked wheel, the wheel center speed is:

$$v_\mathrm{S} = \sqrt{v_x^2 + v_y^2}. \tag{4.36}$$

As a rule, locking wheels transmit less longitudinal force than strongly braked rotating wheels. The braking force must be loosened for some elements of the wheel's profile to stick. An adhesion area occurs when the torque resulting from the tire forces exceeds the torque from the drive and braking torque:

$$M_\mathrm{F} > M_\mathrm{A} - sign(\dot{\rho}_\mathrm{T}) M_\mathrm{B}. \tag{4.37}$$

4.2.2.3 Tire Standstill from Braking

Reaching a standstill with the models presented so far leads to numerical problems in the tire force calculation when dividing by slip values near zero. Realistic modeling plays only a secondary role in the standstill models for vehicle dynamics investigations. The numerical problems are avoided by considering the wheel contact point as fixed after falling below a standstill transition speed v_s. This means that the further movement of the wheel center only results from the deformation of the tire's profile elements. The deformation is simplified by modeling a spring-damper system.

Before switching to the standstill model, the deformation is required, which is equivalent to the spring/damper system's initial deflection, to achieve a continuous transition of the forces between the motion models. The deformation can be determined from the last calculated tire forces and tire speeds in the longitudinal and transverse directions F_x and F_y, v_x and v_y, as well as the spring and damper constants c_s and d_s:

$$\Delta x = \frac{F_\mathrm{x} - v_\mathrm{x} d_\mathrm{s,x}}{c_\mathrm{s,x}}, \tag{4.38}$$

$$\Delta y = \frac{F_{\mathrm{y}} - v_{\mathrm{y}} d_{\mathrm{s,y}}}{c_{\mathrm{s,y}}}. \tag{4.39}$$

The tire forces until the standstill is reached are calculated to:

$$F_{\mathrm{x}} = c_{\mathrm{s,x}} x - d_{\mathrm{s,x}} v_{\mathrm{x}} \text{ with } x = \Delta x + \int v_{\mathrm{x}}\, dt. \tag{4.40}$$

$$F_{\mathrm{y}} = c_{\mathrm{s,y}} y - d_{\mathrm{s,y}} v_{\mathrm{y}} \text{ with } y = \Delta y + \int v_{\mathrm{y}}\, dt. \tag{4.41}$$

4.2.2.4 Tire Standstill to Start-up

As soon as the drive torque M_{A} on the wheel exceeds the applied braking torque M_{B} during standstill, the tire standstill to driveaway model is activated. Only longitudinal force transmission occurs until reaching the transition speed, neglecting the wheel's moment of inertia at start-up to simplify matters. Thus, the longitudinal force yields:

$$F_{\mathrm{x}} = \frac{M_{\mathrm{A}} - sign(\dot{\rho}_{\mathrm{T}}) M_{\mathrm{B}}}{r_{\mathrm{stat}}}. \tag{4.42}$$

When the transition speed v_{s} is exceeded or if the applied braking torque M_{B} exceeds the drive torque M_{A}, the model is deactivated.

4.2.2.5 Interaction of the Models

Event-oriented switching between the described partial models realizes the interaction of the tire model. Figure 4.9 shows an overview of the different model states and the respective switch-over criteria. Several parameters are used for the recognition of the different model states. A total of five different model states can occur, whereby the determination of slip for pure adhesion and adhesion and sliding is divided into normal speed ($v_{\mathrm{x}} \geq v_{\mathrm{x,l}}$) and low speed ($v_{\mathrm{x}} < v_{\mathrm{x,l}}$).

The parameter $\bar{s}_{\mathrm{R}}$ indicates whether pure adhesion ($\bar{s}_{\mathrm{R}} \leq 0.5$) or adhesion and sliding ($\bar{s}_{\mathrm{R}} > 0.5$) is present in the contact patch. Locking of the wheel is detected by the brake slip s_{B}. From a physical point of view, a wheel blocks when the brake slip is $s_{\mathrm{B}} = 1$. To avoid numerical problems, the criterion for wheel locking within the tire model is $s_{\mathrm{B}} \geq 0.99$.

If the torque resulting from the tire force exceeds the torque applied to the wheel, ($M_{\mathrm{F}} = F_{\mathrm{x}} r_{\mathrm{stat}} > M_{\mathrm{A}} - sign(\dot{\rho}_{\mathrm{T}}) M_{\mathrm{B}}$), the locked wheel is released, and the model for adhesion or adhesion and gliding becomes active again. If the vehicle speed falls below the transition speed v_{s}, the model for tire standstill due to braking is activated. This remains active until the drive torque applied to the wheel exceeds the braking torque ($M_{\mathrm{A}} - sign(\dot{\rho}_{T}) M_{\mathrm{B}} > 0$), thus fulfilling the criterion for activating the model for standstill during acceleration. When the transition speed v_{s} is exceeded, the model for adhesion or adhesion and gliding is activated again.

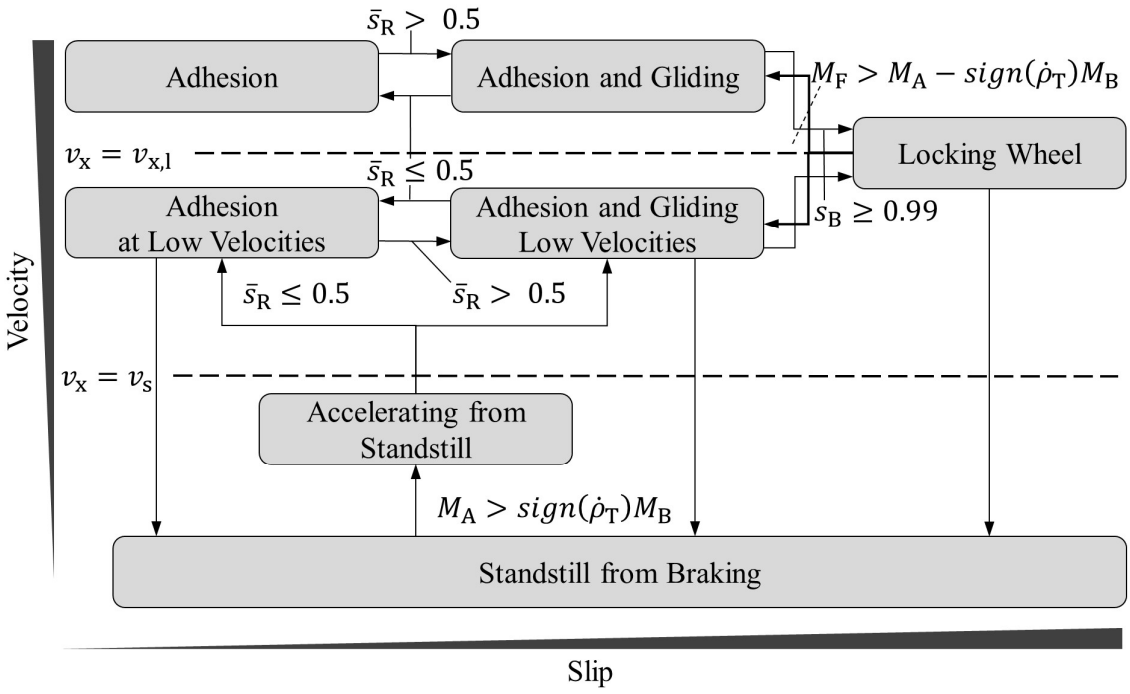

Figure 4.9: Switchover criteria for the tire model states

4.2.2.6 Dynamic Tire Force Generation

The equations described so far assume a stationary or quasi-stationary state of motion. Thus, the quantities used for force calculation must be constant or change only gradually. However, this is generally not the case as many maneuvers or safety systems such as the antilock braking system, the traction control system, or the electronic stability control system can cause sudden changes in the required parameters such as slip, slip angle or applied torque. As described above, the build-up of tire forces depends directly on the deformation of the tire's profile elements and thus on the movement of the tire. Therefore, the build-up of forces is always subject to a time delay. (Schramm et al. 2018) approximate this behavior by a PT1 transmission element:

$$F_{x,stat} = T_x \frac{dF_x}{dt} + F_x, \tag{4.43}$$

$$F_{y,stat} = T_y \frac{dF_y}{dt} + F_y. \tag{4.44}$$

The partial models determine the stationary tire forces $F_{x,stat}$ and $F_{y,stat}$. The forces F_x and F_y on the other hand, contain the dynamic force build-up and are passed on by the tire model as output values. The time constants are:

$$T_x = k_T \frac{c_s}{c_x v_x}, \tag{4.45}$$

$$T_y = k_T \frac{c_\alpha}{c_y v_x}. \tag{4.46}$$

4.2.3 Stabilization

An antilock braking system is adapted and optimized to work with the information given by the road surface condition sensor to investigate the possible improvement of systems by knowing the prevalent weather-related road surface condition on the stabilization level. State-of-the-art systems apply the maximum brake pressure and build up the longitudinal tire force F_x starting in the adhesion area as depicted in Figure 4.10.

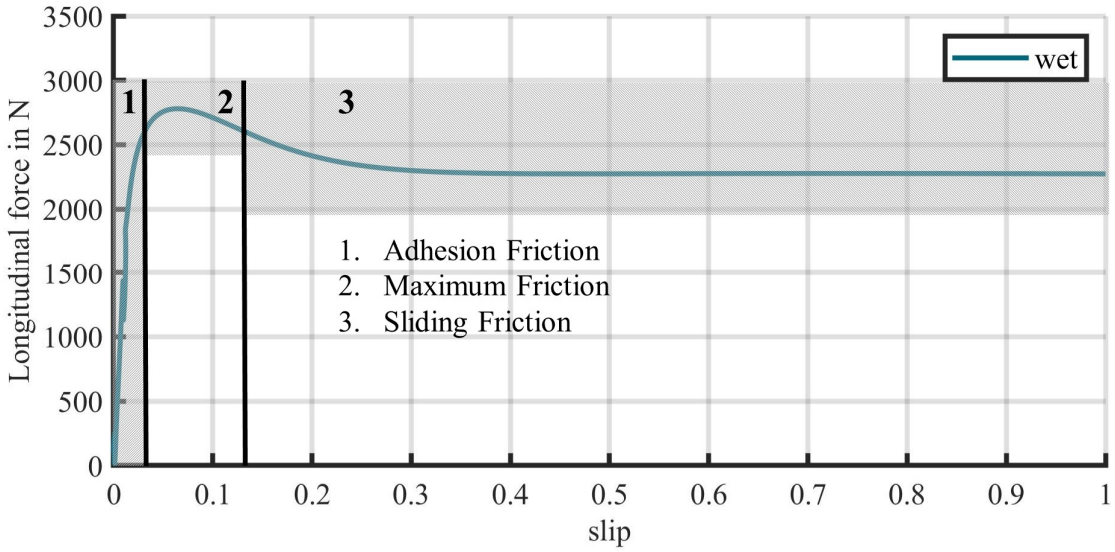

Figure 4.10: Friction areas in the force/slip curve based on (Koskinen and Peussa 2009)

Not knowing the prevailing weather-related road surface condition, braking continues until reaching the end of the sliding friction area, where the wheel starts locking up. An observing algorithm can now estimate the maximum friction region based on this information. If the maximum friction area is already known utilizing the information of the WRSCS, a weather-related road surface condition awareness (RSCA) optimized system can immediately apply the respective brake pressure and maintain it within the maximum friction region. The implemented controller does not intervene in the braking system by regulating the braking pressure, as is the case in an actual vehicle, but simplifies matters by reducing or increasing the braking torques for the individual wheels within the limitations of the overall system.

The ABS model is based on (Burckhardt 1993), combining control of acceleration and slip. The angular acceleration of the wheel and the slip are multiplied by dimensionless weighting factors K_Z and K_λ to determine a switching criterion

$$S_K = K_\lambda \, s_B - K_Z \, \frac{r_{eff} \, \ddot{\rho}}{g}, \tag{4.47}$$

where r_{eff} denotes the effective wheel radius, and g denotes the gravitational acceleration. The upper and lower switching criteria S_{KU} and S_{KL} cause the following system reaction for the braking torque M_B:

$S_{\mathrm{K}} < S_{\mathrm{KL}}$ Braking torque is increased

$S_{\mathrm{KL}} < S_{\mathrm{K}} < S_{\mathrm{KU}}$ Braking torque remains constant

$S_{\mathrm{K}} > S_{\mathrm{KU}}$ Braking torque is reduced

Figure 4.11 shows a schematic of the ABS model.

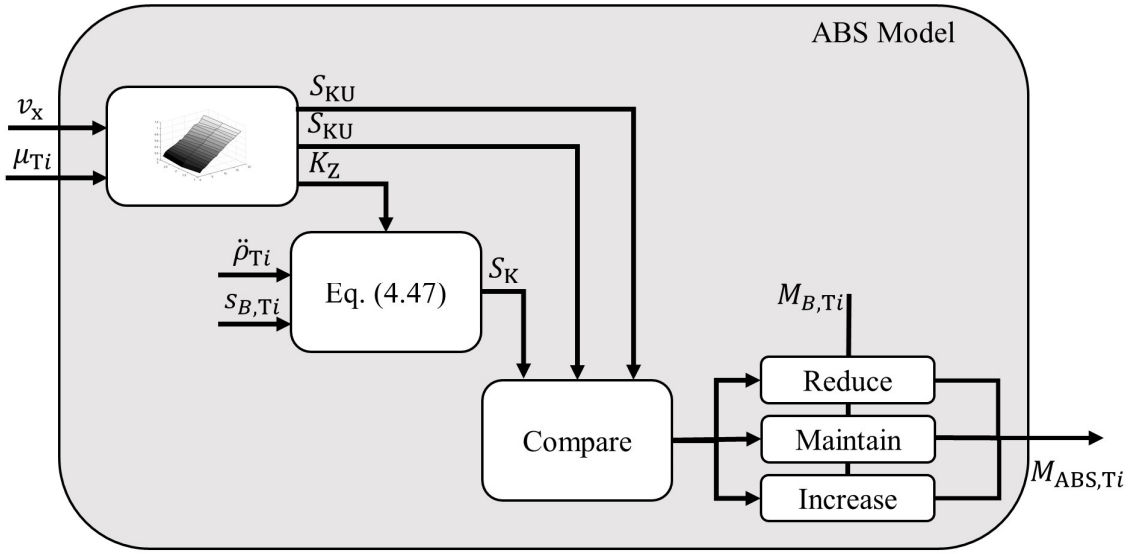

Figure 4.11: Schematic structure of the ABS model integration

Initially, the values suggested by Burckhardt for the state switching criterion are $S_{\mathrm{KU}} = 1.2$ and $S_{\mathrm{KL}} = 1$. This value can be used to estimate values for the deceleration weighting factor K_{Z} and the weighting factor for slip K_{λ}.

The lower threshold is calculated for a higher than the maximum possible deceleration to avoid premature control intervention. As an empirical value a = 14 m/s^2 can be considered according to Burckhardt. This yields an approximation for K_{Z}

$$S_{\mathrm{KL}} = 1 = -K_{\mathrm{Z}} \frac{r_{eff}\,\dot{\omega}}{g} = K_{\mathrm{Z}} \frac{14}{g} \approx 1.4 K_{\mathrm{Z}} \implies K_{\mathrm{Z}} \approx 0.7 \tag{4.48}$$

and the weighting factor for slip K_{λ}

$$S_{\mathrm{KL}} = 1 = K_{\lambda}\, s_{\mathrm{B}} \implies K_{\lambda} \approx \frac{1}{0.2} = 5. \tag{4.49}$$

As these values are derived from literature, they serve as a reference for the implemented system. These values are optimized to improve the RSCA optimized system's performance under deteriorated road surface conditions. A sensitivity analysis for the individual parameters showed that the influence of K_{λ} on the braking distance is only in the order of a few millimeters. Figure 4.12 shows the braking distance development at an initial speed of 80 kph.

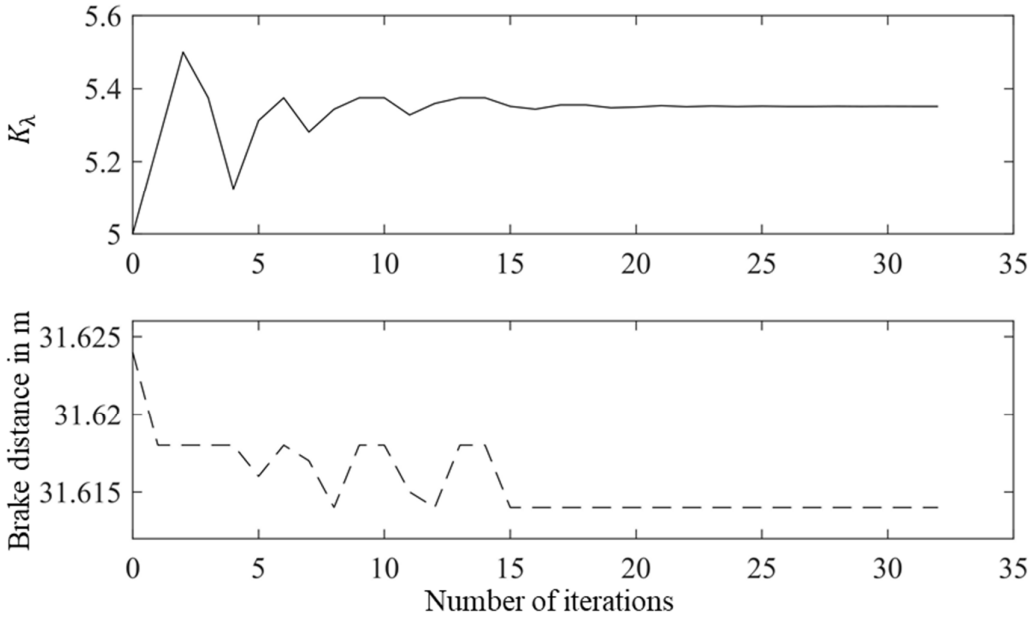

Figure 4.12: Braking distance development with the variation of K_λ

A similar development is equally evident for all investigated initial velocities, so the value suggested in the literature for this parameter is kept constant in the following. The number of optimization parameters reduces from four to three variables and the complexity and effort of the optimization problem. Two methods are tested to perform parameter optimization, a genetic algorithm (GA) (Whitley 1994) as a representative of global optimizers and the Nelder-Mead algorithm (NM) (Nelder and Mead 1965) as a representative of a local optimizer. As shown in Figure 4.13 and Figure 4.14, both approaches yield useable results as they converge to the same values.

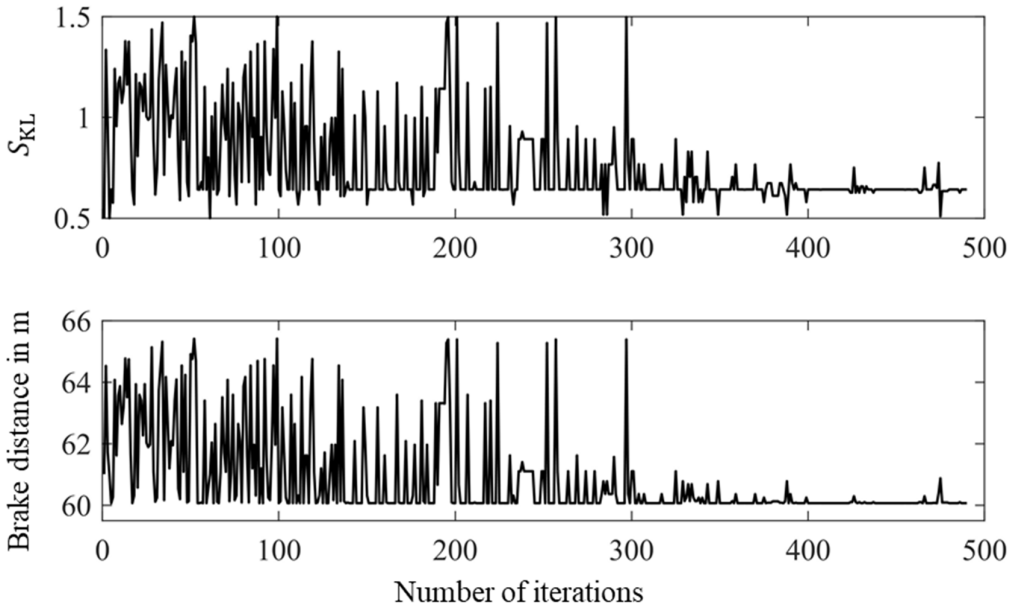

Figure 4.13: Example behavior of the GA when optimizing a single parameter

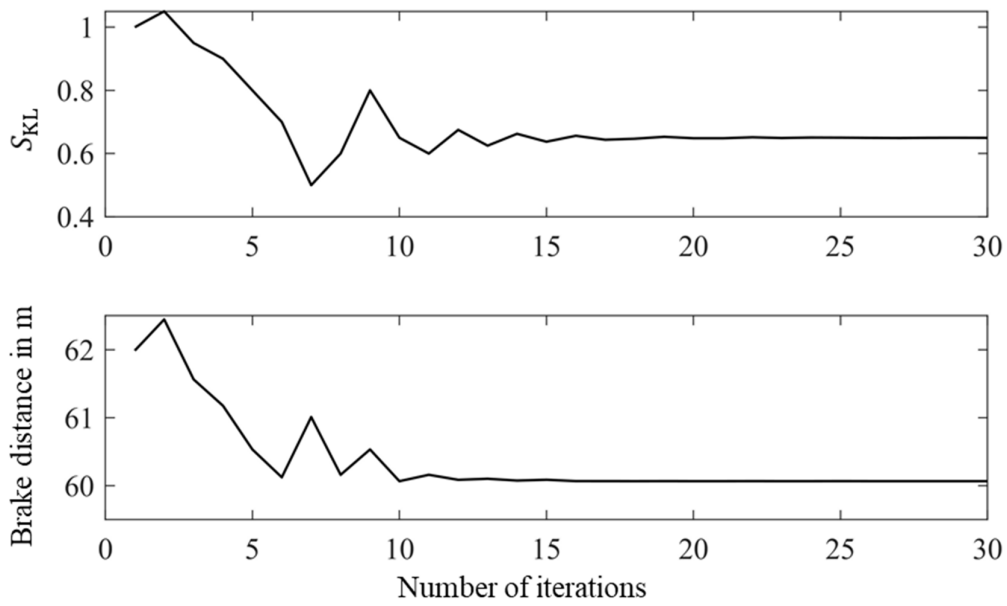

Figure 4.14: Example behavior of the NM algorithm when optimizing a single parameter

The latter, however, is the better option for the problem at hand since it shows promising results with faster convergence. This is due to the different nature of the approaches since good starting values are known from the literature, and the search space was accordingly limited. The fact that the genetic algorithm can optimize all parameters simultaneously and thus delivers a complete set of parameters, as a result, cannot compensate for the performance disadvantage of convergence and is therefore dismissed. A sufficiently stable value to stop the process is reached after about 20 iterations for each parameter.

For performance reasons of the entire simulation, optimized values are determined for all parameters at different speeds and road conditions and stored in a multi-dimensional Look-Up Table, from which these values are taken during the actual simulation within the ABS model according to the respective driving and environmental conditions, as shown in Figure 4.11.

4.2.4 Guidance

On the guidance level, two ADAS are implemented for the potential investigation of the weather-related road surface condition sensor. An adaptive cruise control system is implemented in the following subsection that adjusts both speed and distance depending on the road condition to reduce safety-relevant situations. Following this, an emergency braking and steering system is optimized to determine adapted last points to brake steer to make better decisions for the systems' activation.

4.2.4.1 Road Surface Condition Aware Adaptive Cruise Control

The first ADAS chosen on the guidance level to investigate the safety improvement potential by the WRSCS is the adaptive cruise controller. (ISO 15622:2018) standardizes the general performance requirements for modern ACC systems, such as limitations for speed, accelerations, and the time gaps to the leading vehicle. Figure 4.15 depicts a typical driving situation using an ACC, where the following vehicle is equipped with that system. The net distance d_n denotes the spatial distance from the front edge of the following vehicle to the rear edge of the leading vehicle.

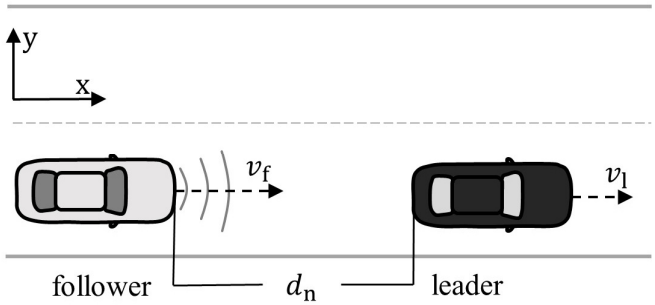

Figure 4.15: Typical driving situation for an adaptive cruise control scenario

In ACC systems, however, the so-called time headway t_hn is used as the controlled variable instead of the net distance. The time headway is the amount of time a vehicle would need at its current own speed v to cover the current net distance d_n:

$$t_\mathrm{hn} = \frac{d_n}{v}. \tag{4.50}$$

Equation (4.50) shows that the net distance increases linearly with the driven speed. However, without considering the usable friction coefficient due to the road surface condition, the resulting distance between the vehicles may potentially be unsafe in state-of-the-art ACCs, because of the assumption that the maximally possible deceleration rate is always reachable.

The critical distance between vehicles can be derived from the equation of motions and the conditions for braking to a standstill. The indices l, f denote the leading and following vehicle respectively:

$$d_\mathrm{crit} = \frac{1}{2}\left(\frac{v_\mathrm{l}}{a_\mathrm{l,max}} - \frac{v_\mathrm{f}}{a_\mathrm{f,max}}\right) \tag{4.51}$$

Figure 4.16 shows the general control loop structure of both implemented ACCs. The structure applies to the state-of-the-art version as well as the weather-related road surface condition aware version (RSACC).

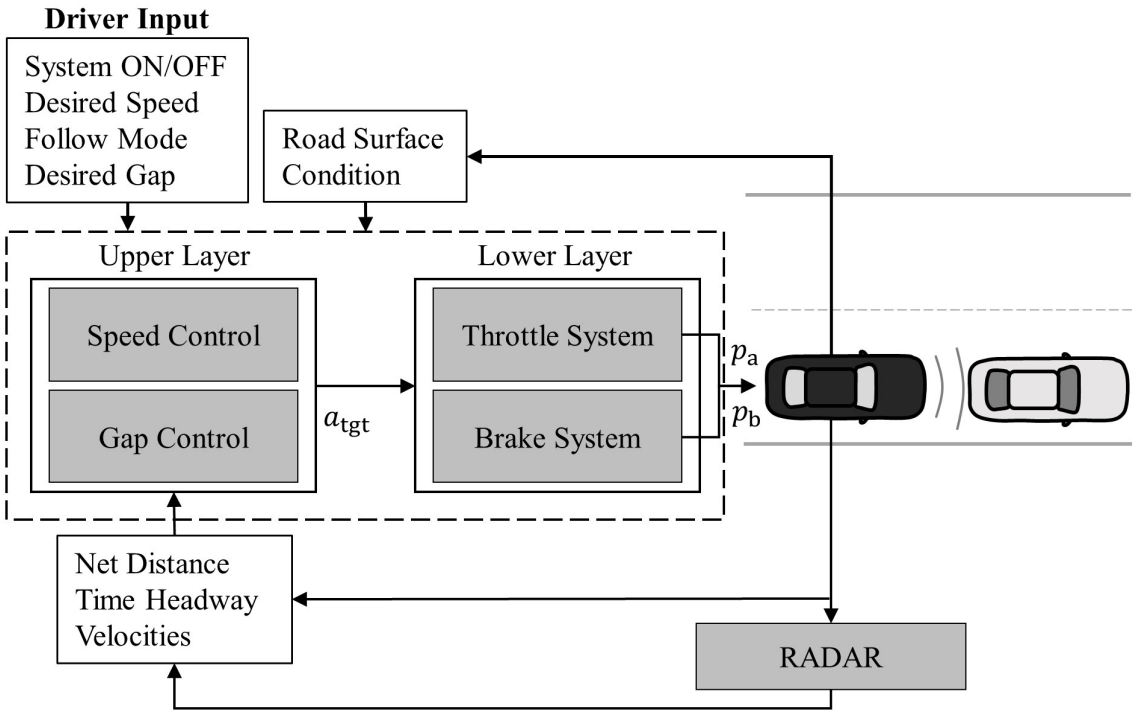

Figure 4.16: Control loop structure of the implemented ACC/RSACC

The system input is given either by a human driver or by the responsible system in a highly or fully automated vehicle. As it is usual, the ACC system includes multiple sub-controllers for different motion purposes. The speed controller is designed to keep the vehicle at a constant velocity (desired speed input) when there is no preceding vehicle present. The general formula for this control loop is given by

$$a(t) = k(v_{\mathrm{set}} - v_{\mathrm{act}}), \tag{4.52}$$

where k is the control gain factor for the speed error determined by the desired speed input v_{set} and the actual speed at a given time v_{act}. The gap controller is active in car following situations and aims to keep the desired gap constant. In some cases, the gap controller is further enhanced with a subset of gap-closing parameters for the transition from the speed controller to the gap controller. The general formula for the gap control loop is

$$a(t) = k_1(d_{\mathrm{des}} - d_{\mathrm{n}}) + k_2(v_{\mathrm{l}} - v_{\mathrm{f}}), \tag{4.53}$$

where the vehicle's acceleration depends on the gap error between the desired gap, the net distance, and the speed difference between the ego vehicle and the preceding vehicle. The control gain factors $k_{1,2}$ are the variable parameters determining the system's performance. (Xiao et al. 2017) provide initial values for the control gain. For the complex vehicle model simulations, the calculated target accelerations are handed down to the second control loop consisting of a reduced transfer function model of the drive train to generate the necessary inputs for the gas or brake pedal.

For the RSACC, an adaptation of the selected safety speed in case of speed control mode and adaptation of the safe distance or time gap respectively in gap control mode via scaling functions, as exemplarily shown in Figure 4.17, is implemented, similar to the work of (Yi et al. 1999).

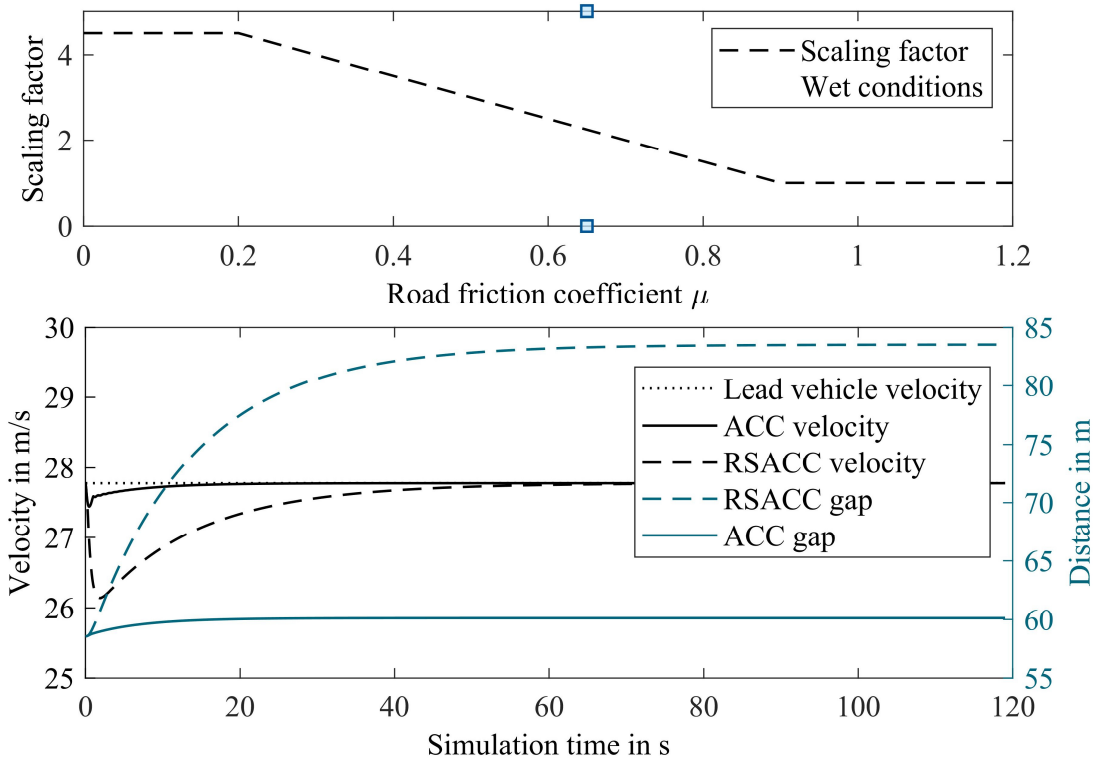

Figure 4.17: Scaling function for friction depended safety gap adaptation (above), Resulting systems behavior with (RSACC) and without (ACC) adaptation mode (below)

The bottom picture in Figure 4.17 shows the resulting system behavior for a following situation in wet road surface conditions and a desired speed of 100 kph (27.7 m/s). Without the scaling factor acting on the gap control loop, the distance to the leading vehicle is about 60 m. This gap is increased to about 84 meters by the RSACC due to the prevailing conditions. At the time t = 0, the distance to the lead vehicle is set to be slightly too small for both systems, which explains the reduction in the speed of the systems that can be seen at the beginning of the simulation. In both cases, the respective system regulates the speed of the lead vehicle after the desired distance has been reached.

4.2.4.2 Emergency Steer and Brake Assistant

The second, which is considered in the context of this thesis due to its dependency on transmittable forces between a vehicle and the road, is an emergency steer and brake assistant. Such a system is interesting concerning highly automated driving because even automated systems should execute a maneuver in an impending collision, which transfers the vehicle into a risk-minimized state. In many cases, this maneuver represents an emergency stop. Due to the exponential relationship of the braking distance with speed, emergency braking can only reduce the accident's severity at high

relative speeds because the braking distance is too long to avoid a collision. An extended system to include an evasive maneuver can avoid some of these accidents (Reinisch 2013). The basis of an ESB is the continuous calculation of the distances for an evasive maneuver d_S or braking d_B maneuver to a detected obstacle. Figure 4.18 shows this relationship and the corresponding variables. The last point to brake and the last point to steer depend on the weather-related road surface condition due to its influence on the vehicles' dynamics. Knowing the prevailing conditions through the WRSCS can enhance the decision and activation procedure.

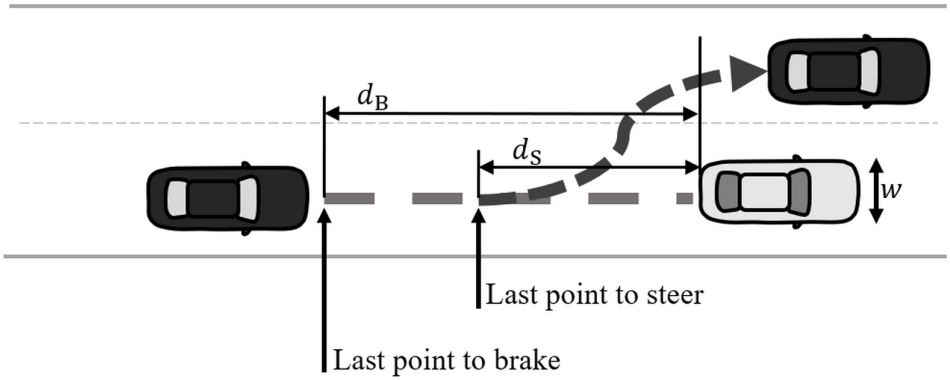

Figure 4.18: Last points to brake and steer based on (Eckert et al. 2011)

Due to the intervention characteristics of an ESB assistant, it can be classified as category C: "intervening in emergency situations". The evasive maneuver tends to be the preferred action plan for out-of-town areas, where vehicles travel at high speeds. The emergency braking maneuver is always suitable, especially in inner-city areas at lower speeds and where the probability of oncoming traffic is significantly higher. The avoidance maneuver can also be the better choice in the inner city area with a low friction coefficient or a small obstacle width to achieve a risk-minimized driving condition (Eckert et al. 2011). Figure 4.19 shows a schematic of an ESB system.

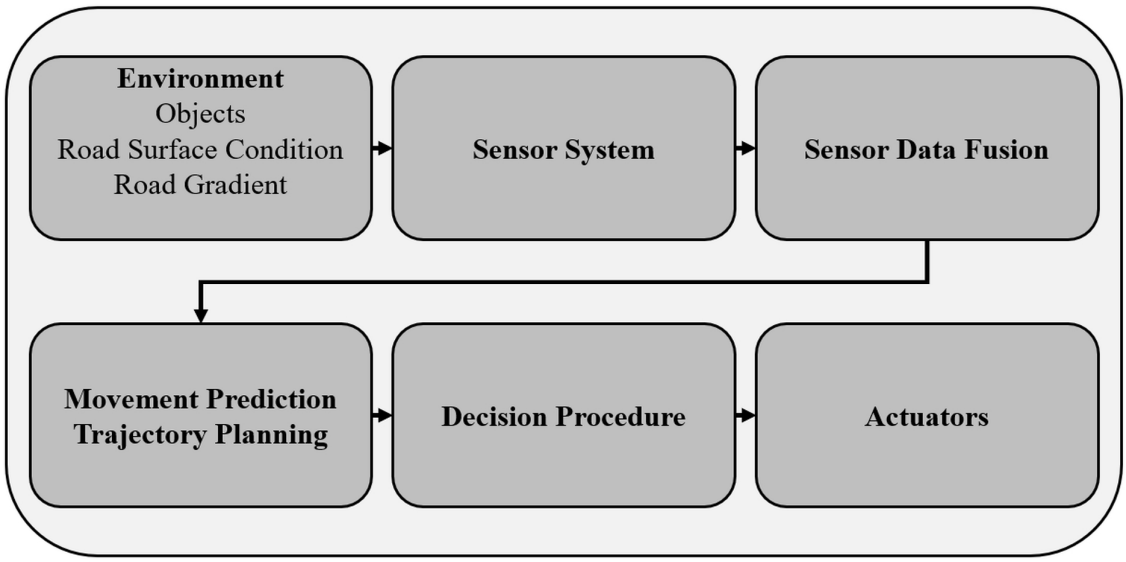

Figure 4.19: System architecture of an ESB assistant according to (Maurer et al. 2012)

The required distance d_{B} for a braking maneuver of a point mass can be calculated using the possible braking acceleration a_{x} and the relative speed v_{rel} between the vehicle and the obstacle

$$d_{\mathrm{B}} = \frac{v_{\mathrm{rel}}^2}{2a_{\mathrm{x}}}. \tag{4.54}$$

The width w of the obstacle and the possible lateral acceleration a_{y} are required in addition to the relative velocity to calculate the required distance for an avoidance maneuver through steering d_{S}

$$d_{\mathrm{S}} = v_{\mathrm{rel}} \sqrt{\frac{2w}{a_{\mathrm{y}}}}. \tag{4.55}$$

Figure 4.20 shows the time-dependent build-up process of the longitudinal and lateral accelerations.

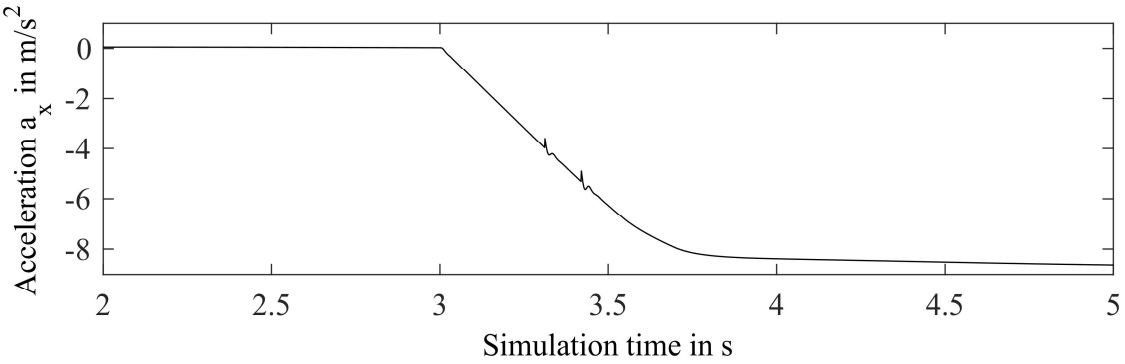

Figure 4.20: Time-dependent deceleration build-up

The equations (4.56) and (4.57) for the calculation of the required distance for a braking or evasive maneuver for the decision making of the ESB are extended by a corresponding time-dependent safety term. The factor τ is set to one second and includes both the reaction time of the system and the corresponding delay in the acceleration build-up.

$$d_{\mathrm{B}\tau} = \frac{v_{rel}^2}{2a_x} + \tau v_{\mathrm{rel}} \tag{4.56}$$

$$d_{\mathrm{S}\tau} = v_{\mathrm{rel}} \left(\sqrt{\frac{2w}{a_y}} + \tau \right) \tag{4.57}$$

The influence of the road surface condition on the maximum accelerations is taken into account for the design of the corresponding system variant as a friction coefficient factor as shown in the equations (4.58) and (4.59), where g denotes the acceleration due to gravity:

$$a_{\mathrm{x}} = \mu g, \tag{4.58}$$

$$a_y = 0.8\,\mu g. \tag{4.59}$$

The relationship of the required distance for a braking or evasive maneuver via the relative speed and the respective thresholds is qualitatively shown in Figure 4.21.

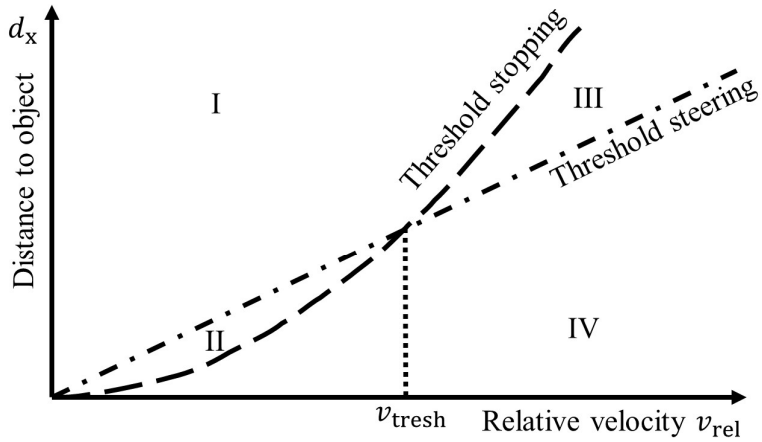

I: Steering & braking possible II: Only braking possible

III: Only steering possible IV: Steering & braking impossible

Figure 4.21: Relationship between braking and evasive maneuvers based on (Weber 2012)

However, the course of thresholds is also dependent on the friction value, which is considered in the decision-making process in the case of the road surface condition aware variant of the ESB. Figure 4.22 shows, for example, the different courses of the respective threshold values for dry and wet road conditions.

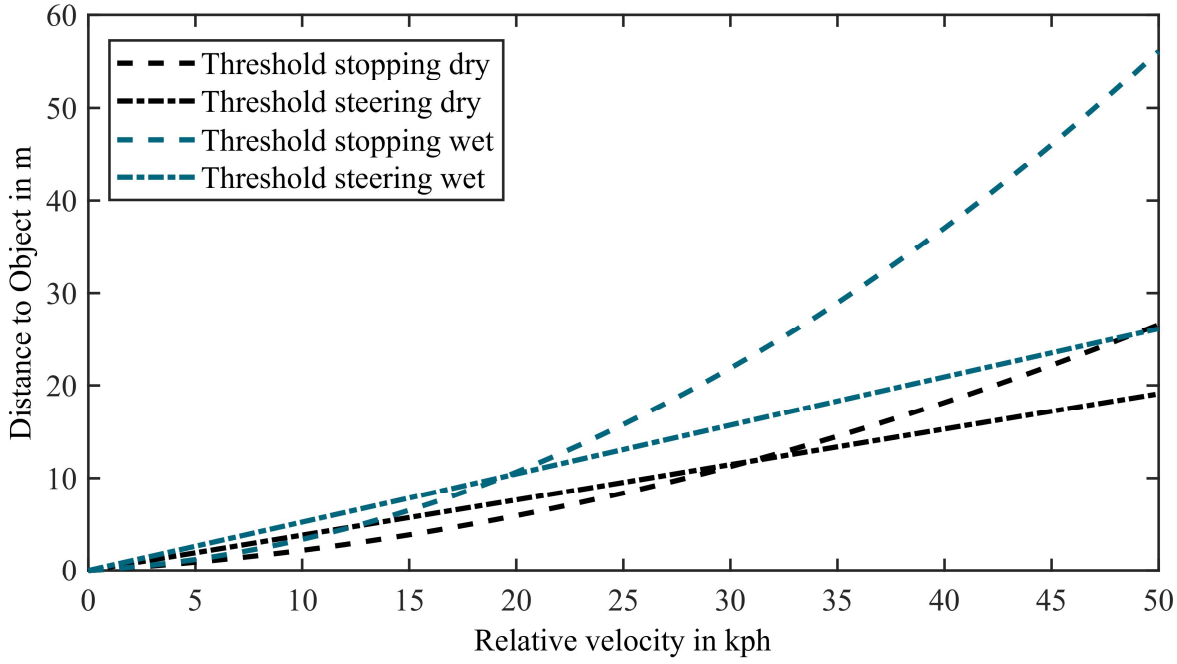

Figure 4.22: Road surface condition dependence on thresholds for braking or steering decision

The steering angle controller for the evasive maneuver is developed based on the (Fiala 2006) model for vehicle guidance in the transverse direction. According to this, the steering wheel angle δ_H is composed of the lateral offset q and the product of the maneuver distance d_S and the angle α and is multiplied by a linear scaling factor c

$$\delta_H = c(q + d_S\alpha). \tag{4.60}$$

As shown in Figure 4.23, the angle α results from the direction vectors of the vehicles heading $\boldsymbol{r}_V$ and the direction vector $\boldsymbol{r}_P$ to the desired passing point P

$$\alpha = \cos^{-1}\left(\frac{\boldsymbol{r}_V \cdot \boldsymbol{r}_T}{|\boldsymbol{r}_V||\boldsymbol{r}_T|}\right). \tag{4.61}$$

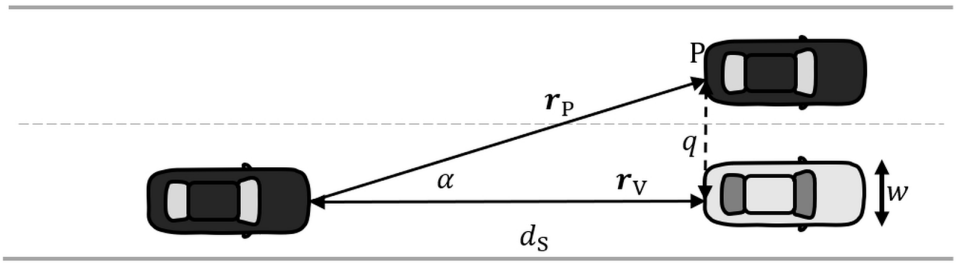

Figure 4.23: Variables for calculating the steering angle according to (Fiala 2006)

For the lateral offset q the simulation uses the obstacle width w plus a safety distance of 0.5 meters. The maneuver distance d_S is equal to the value from equation (4.57) at maneuver initiation. Figure 4.24 shows lateral acceleration, speed, and offset progression for a controlled evasive maneuver under dry road conditions at a starting velocity of 50 kph.

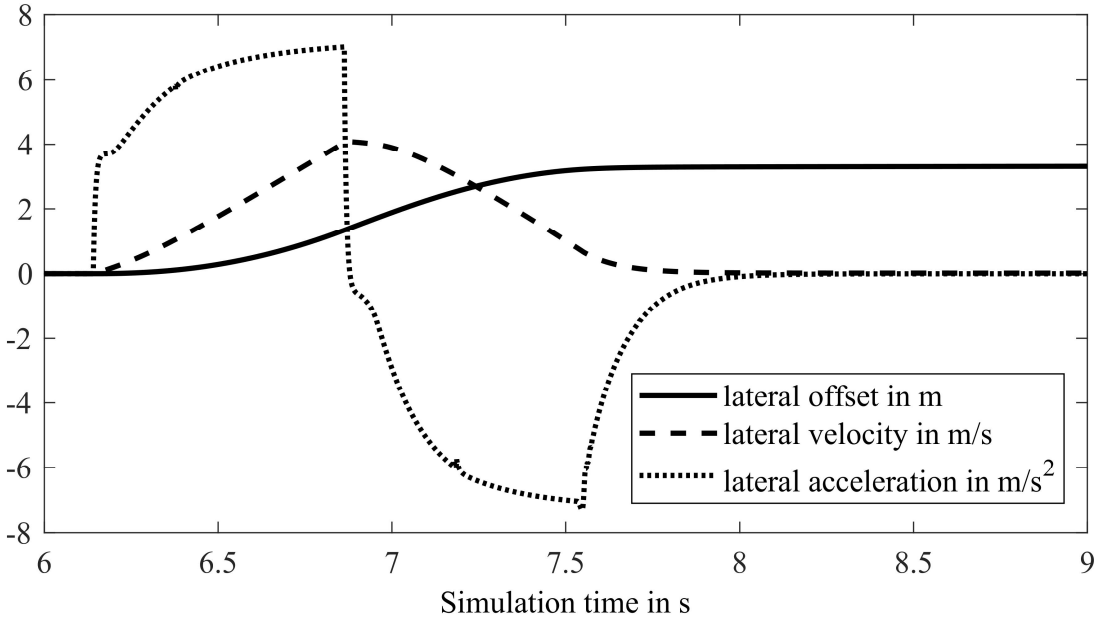

Figure 4.24: Lateral dynamics during a controlled evasive maneuver

Both versions of the ESB are implemented in six structural elements, as shown in Figure 4.25. The first three elements work while the ESB is inactive and are necessary for decision making and activation. If the ESB intervenes in the vehicle guidance, the corresponding system block is activated, and the maneuver is executed. Except in state area III (only evasive maneuver possible), emergency braking is generally preferred to a lateral maneuver, as in this case, no additional potential danger to road users in an adjacent lane is caused.

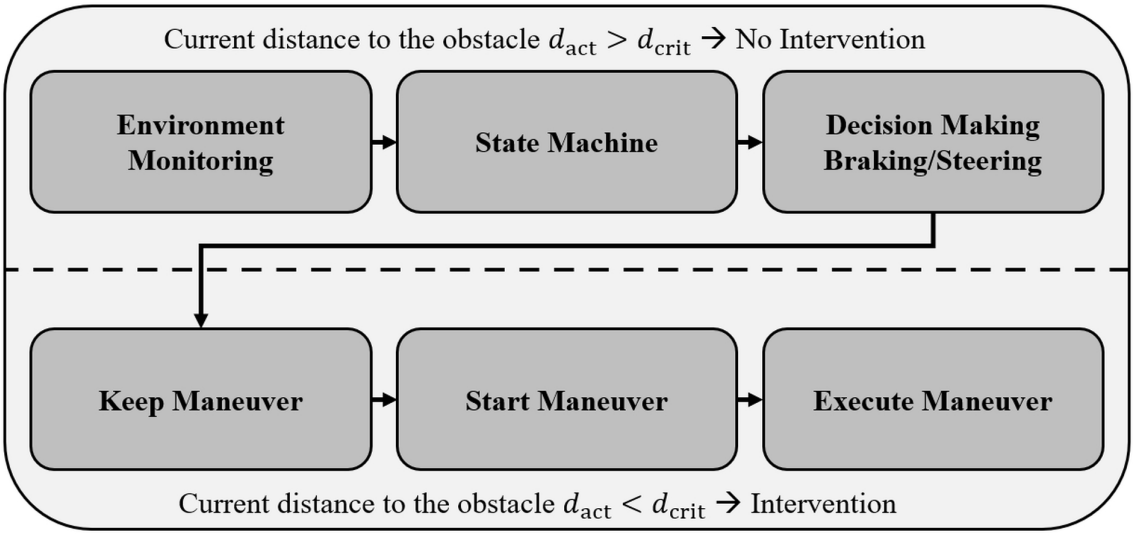

Figure 4.25: Sequence and elements of the ESB

4.2.5 Navigation

The essential prerequisites on the navigational level include digital road and environment maps and sensors for determining position. Once the driver has entered the destination, suitable routes are determined, and visual and acoustic information is generated that the driver can utilize to guide the vehicle to the desired destination. Modern devices dynamize the route guidance process by considering certain boundary conditions such as traffic information or environmental events. This can involve dynamic data with a low update rate, such as traffic information via TMC (Traffic Message Channel) broadcasted by radio signal, or, with a corresponding connection to the Internet, also via data that various providers transmit, usually for a fee, in near real-time. A prominent example of a free version with data of short latency is the traffic situation consideration in the navigation extension of Google Maps.

According to (Winner et al. 2015), the basic functionality of vehicle navigation can be divided into a scheme, as shown in Figure 4.26. The individual elements listed there can also be understood as software modules, which are implemented according to the requirements of this thesis. Firstly, in addition to a fundamental database, three core components are required:

- Positioning: determination of the current (geographical) location,
- Routing: calculation of an optimal route to the desired destination, and
- Guidance: en-route guidance from the current position to the desired destination.

Secondly, elements for human-machine interaction

- Destination input: selection of the desired destination and
- Map display: information feedback from the system to the driver,

and thirdly, optional auxiliary functions such as the

- Dynamization: consideration of traffic and environment.

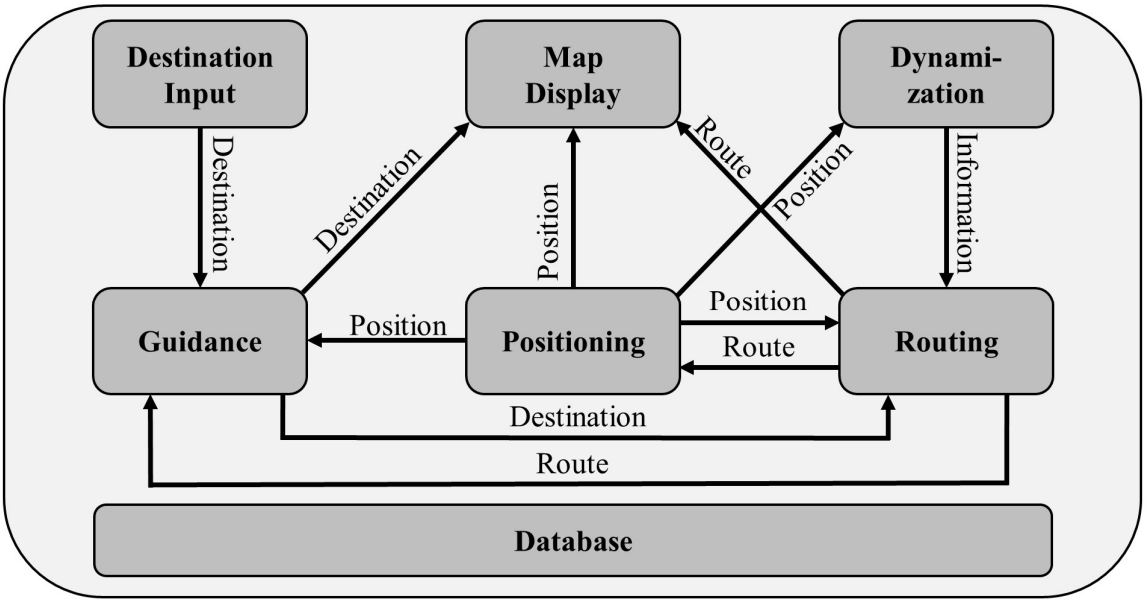

Figure 4.26: Functional scheme of vehicle navigation based on (Winner et al. 2015)

Specific requirements can be defined for the respective components considered during implementation for use in the real world and used in an extended simulation environment. These are described in more detail in the following sections.

4.2.5.1 Database

The requirements for the database for the application in navigation can be divided into two areas: the data storage properties and the data structure. In terms of storage, factors such as data volume, access times, and data transfer rates are relevant because even if the calculations to be performed are not usually time-critical, requirements for the HMI may well be. A vector-based structure is appropriate for the data representation because it can subsequently be extended and used in this form for further modules of navigation since information on geometry and topology can be integrated. Nodes, defined by their coordinates, essentially represent the geometry, and lines, defined by their start and end nodes. The edges are usually additionally described by ordered sets of points to map the road course more precisely. With these elements alone, it is already possible to represent a georeferenced network if geographic coordinates are used in the description of the nodes.

The topology, in turn, describes the connection between the nodes and edges and is thus essential for route search in said networks. They are often modeled with the help of graphs, whereby unique properties such as one-way streets or height and weight restrictions and an individual

weighting of the edges can be taken into account, which is used in the further course, for example, to dynamize the routing.

An open data source and project that fulfills all requirements is (OpenStreetMap 2020). The OSM data format inherently fulfills the requirements for further processing in navigation, namely the vector-based representation of geometry and topology. Another primary reason for choosing OpenStreetMap as a database is to provide interfaces for ongoing and planned projects of the Chair of Mechatronics at the University Duisburg-Essen and seamlessly enable its use in real-world environments and further projects and its use in simulations. In addition, scenarios based on real are generated in the further course on the traffic level, in which OSM data are used for road network generation based on the same considerations. Several open-source modules building on the OSM data exist, some of which are applied in the course of the thesis. To save and provide the data for the following processes, they are stored in a PostgreSQL database. It is an object-relational database (ORDB) whose SQL implementation complies with the (ISO/IEC 9075:2016) standard. It offers interfaces to many programming languages, including Python, PHP, and C/C++, and is well documented. Due to its open-source philosophy, PostgreSQL also contains a framework that allows user-defined data types and supporting functions and operators to be defined. In order to use the database optimally for the project at hand, extensions of this kind are used, namely (PostGIS 2020) and (pgRouting 2020). (PostGIS 2020) adds support for geographic objects, allowing both location- and network-based operations, such as environment searches or distance calculations, as well as spatial projections, as may be relevant for various representations, to be performed directly in SQL. The (pgRouting 2020) project is based on the PostGIS extended PostgreSQL and provides several routing algorithms, including the Dijkstra (Dijkstra 1959) and the A* (Hart et al. 1968) algorithm, explained in more detail in the following Subsection 4.2.5.3 on dynamic routing.

4.2.5.2 Positioning

In the literature such as (Winner et al. 2015), location determination is often divided into two subareas. A distinction is made between positioning, the determination of absolute coordinates of the vehicle on the earth's surface, and localization, the determination of the relative position with respect to the road network. Methods that realize the latter are also called "map matching". In almost all vehicles, positioning is performed via GPS (Global Positioning System) measurement, serving as the input variable for localization.

Particularly regarding highly and fully automated driving, there are high requirements for the possible use of navigation in assistance functions concerning the accuracy of this module, including the determination of the current lane. To achieve this, in addition to the GPS signal, other vehicle sensors such as gyroscopes, acceleration sensors, steering angle sensors or cameras, and even connected or installed GSM (Global System for Mobile Communications) devices can be used for localization. Overall, map matching must be robust to measuring noise from the input sensors and inaccuracies in the digital map. Ideally, the localization error should always be small

enough to ensure that destination guidance still works even in rapidly successive driving maneuvers. After a few adjustments, a corresponding algorithm based on a supervised bachelor thesis (Zhao 2017) and an adaptation for a subsequent publication (Tewiele et al. 2018) is available for this thesis. Suppose the position comes from other simulation elements instead of real-world data and is not itself provided by a virtual sensor with similar error behavior as an actual sensor. In that case, the latter requirement does not apply and significantly increases the performance of the map matching.

4.2.5.3 Dynamic Routing

The route search can be performed both before the start of the journey and during it, whereby the speed requirements of the process usually range from several tens of seconds to several minutes. The purpose of a search is to find the optimal connection between the current position and a given target position in the given road network. Optimal in this context means related to criteria or conditions that are also predetermined. In vehicle navigation, such conditions are, for example, to calculate the shortest, fastest, or also most economical connection. Static information can also be regarded as costs for a corresponding algorithm, such as section lengths, maximum permissible speeds, and similar restrictions. These are often already contained in the road networks. Dynamic information, which is also suitable for consideration in a cost function for route search, such as congestion information or information on the roadway condition, must be made available to the system later via suitable channels. In practice, cost functions are often multi-criteria. For this problem, algorithms from graph theory such as the (Dijkstra 1959) or the A* (Hart et al. 1968) algorithm are particularly suitable since they have advantages in the required computing power, especially in memory requirements. In these algorithms, the neighboring nodes are traversed step by step from start to end, and the alternatives are evaluated according to cost functions and discarded if necessary. The A* algorithm applies a priori knowledge by using a heuristic to visit only those nodes that most likely lead to the goal and thus influence the search direction. If no a priori knowledge is available, the algorithm degenerates to the Djikstra algorithm (Cormen et al. 2013). As mentioned above, the database extension pgRouting is the core of this function. The extension provides implementations of the Dijkstra and A* algorithms, which require at least the starting point, the endpoint, and the cost to be considered for execution. In the present thesis, these are either provided by other modules of the simulation environment or can be submitted through a specially designed HMI (cf. Figure 4.27), implemented as a web frontend to the web server, which communicates with the PostgreSQL database through a created PHP script and provides the result. In order to be able to consider different options and boundary conditions for the route search, corresponding SQL functions have been implemented in the databases, which in turn make use of the aforementioned routing algorithms. The main extension here is the use of road condition information as a factor in the cost function. In the further course of the thesis, this information is transmitted by appropriately equipped vehicles in a traffic-flow simulation via a V2X interface to a backend and thus made available to the navigation systems of the other vehicles as required.

4.2.5.4 Guidance

Based on the current information about the position from the positioning, instructions or hints about upcoming driving maneuvers can be generated for the driver in the destination guidance to stay on the selected route. These driving maneuvers must then be communicated to the driver at the appropriate time via the HMI. This can be done visually by superimposing them on a screen or acoustically. Finally, compliance with the maneuvers must be checked to provide appropriate information in the event of deviations and, if necessary, to initiate the search for a new route, on which destination guidance can then be provided. The maneuvers determined in this way can ideally be passed on to the downstream level together with the determined route as input variables for concrete path planning.

For destination guidance, an overall list of driving maneuvers is first generated on the server based on the determined route and the current orientation of the vehicle concerned according to the following three-step model:

1. Individual route segments are combined into sections based on the street names and extended by information on the starting angles at the beginning and end of the sections,
2. if necessary, an initial maneuver is generated to follow the route,
3. the necessary maneuvers on and between the sections are calculated and stored in a list.

In the web frontend, this list is used to implement a dynamic display based on the current driving situation; in the backend, this list is used to follow the virtual driver along the dynamic route if required. After initialization, the first maneuver to be executed is displayed, and a process for monitoring is started. The main criteria on which this process is based are the distance to the next maneuver and the vehicle heading compared to the maneuver specification. When the distance to the next maneuver decreases below a specified threshold, this is shown on the display until the criteria for its execution or the conditions for recalculation of the route are met. The maneuver is considered executed when the vehicle has reached the target heading near the maneuver point. Subsequently, the next upcoming maneuver is shown in the display, and the process starts from the beginning. The conditions for recalculation are also continuously monitored and consist of a combination of the distance to the specified route and the vehicle's orientation. Driving around obstacles, for example, does not lead directly to a recalculation but only a straightforward continuous motion away from the specified route.

4.2.5.5 Map Display

The map display forms the central optical HMI of the navigation. It serves to display the necessary information of the connected modules in a suitable manner (Mittlböck and Atzl 2015). From the database, this is, e.g., the map of the road network superimposed in the background and the built-up areas, the bodies of water, and, if necessary, other landmarks. The positioning provides the current position, represented by a marker, and can also represent the vehicle movement. The track

to be taken from the routing module is highlighted, and information about upcoming driving maneuvers is displayed.

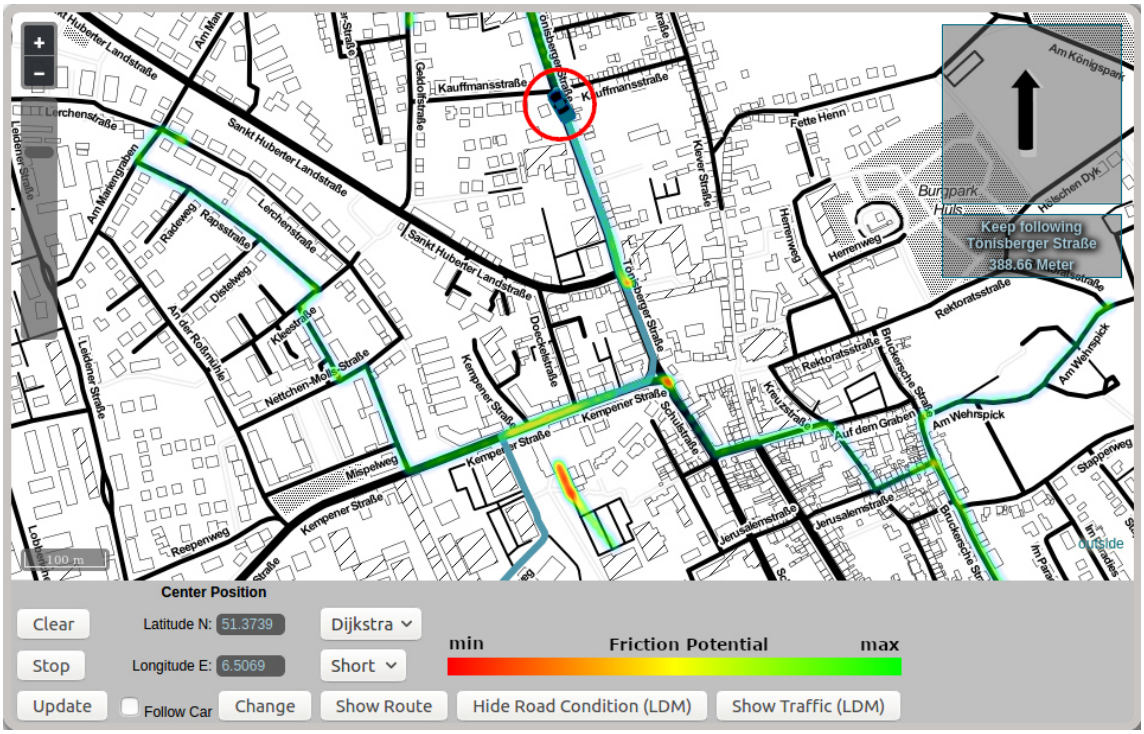

Figure 4.27: Map display for the navigational level

Figure 4.27 shows a summary of the final map display implementation with all available elements. Containing the ego vehicle (top center), the desired route (petrol line), routing directions (top right), available road surface condition data (heatmap), and several HMI components (bottom) such as buttons to toggle visibility of elements and selection of routing algorithm and cost function.

As already mentioned, the representation is done via a web-based approach for maintaining a high degree of flexibility and adaptability. In the overall simulation framework, a dedicated OpenStreetMap server is operated. It provides the map material and allows the implementation of the necessary extensions for the modules described above and the offline operation of the system. Using the JavaScript library (OpenLayers 2020) realizes the visualization in the front-end browser. It efficiently displays tiles from dedicated servers, in this case, the Apache Web Server, and any number of additional layers from different sources, such as vector data from GeoJSON (an extension of the JavaScript Object Notation JSON) or KML (Keyhole Markup Language) files. This functionality is used in the following, e.g., to display routes and vehicles.

4.3 Traffic Level

The primary tool selected in Chapter 3 for the investigation of the traffic level is the microscopic traffic simulation software SUMO (Alvarez Lopez et al. 2018). Several modules summarized in Table 4.3 are adapted or newly implemented to assess the potential of the WRSCS.

Table 4.3: Summary of the implemented modules at the traffic level

Module	Approach	Explanation
Weather	▪ Georeferenced Network adaptation	Modul for applying georeferenced environment weather data to large-scale simulation networks for the subsequent processing of the WRSCS model.
Sensor	▪ Model from real-world data	A realistic WRSCS model based on real-world measurement data to enable the vehicles to measure within the simulation framework enables the driver models to react accordingly and distribute the information in automotive networking scenarios.
Driver	▪ Human behavior adaptation ▪ RSACC	Human drivers react to the prevailing weather-related road surface conditions primarily by adapting their speed. As the state-or-the-art models do not reflect this behavior, an adaptation is needed. As for the behavior of an automated system, a driver model according to the RSACC is implemented.
Navigation	▪ Sharing data via V2X transmission	Sharing weather-related road surface conditions via V2X is used to enable the navigation system to avoid areas of reduced friction to enhance the availability of the automated driving mode.

Next to the actual weather condition as part of the environment model, this includes a sensor model, an adaptation to the existing driver behavior model, an automated driver model based on the RSACC described in the previous Section 4.2.4.1, and an adapted navigation module to include the WRSCS information into the strategic planning process.

4.3.1 Weather-Related Road Surface Condition

At the traffic level, the implementation bases on the environment model introduced in Section 4.1. Unlike at the vehicle level, vehicles cannot move freely within the used microscopic traffic simulation software SUMO but are bound to those edges and lanes of the network used.

Thus, it is consistent with implementing this value as an additional attribute of the edge and lane elements. A default value of 1.0 representing dry conditions is set upon parsing when using network XML files without prior specified friction values to ensure overall compatibility with older versions and networks. A specific value is defined within these XML files like other attributes through a newly defined and implemented key-value pair for the friction value within the respective tags. It is defined as a dynamic attribute that can be changed online while the simulation runs either through the TraCI (Traffic Control Interface) or via a trigger object that can be specified within an additional file. While the direct manipulation of network files might be feasible for smaller networks with only a few edges and a limited number of lanes, it becomes very tedious for

larger scenarios quickly. Therefore, SUMO's graphical network editor (NETEDIT) is also amended to accommodate and manipulate the new attribute on the one hand. On the other hand, a weather module is implemented in order to be able to recreate weather conditions as realistically as possible in the investigated scenarios. With the help of the weather module, individual clouds or entire rain and snow areas can be mapped in the simulation environment. The actual process of the module consists of four steps.

In the first step, rain areas are defined in a configuration file. Analogous to all other configuration files, which need to be created in the preparation of a simulation scenario in SUMO, this one also follows the XML format and contains the description of the individual rain clouds, which are assumed to be circular in a simplified way. This simplified representation has the particular advantage that only the radius of the circle and the X and Y coordinates of the center point, measured in the coordinate system of the SUMO road network, are needed to describe the clouds. Precipitation areas or clouds whose shape cannot be holistically approximated as circular can be subdivided into smaller segments for increased accuracy or mimicked by overlapping multiple circular segments. When using georeferenced output data for the network, it is possible to convert weather data, such as from rain radar measurements, from appropriate service providers to appropriate format.

In the second step, polygons are generated in the SUMO network based on the previously defined definitions. These are mainly used to visualize the precipitation areas at simulation runtime and allow user visual validation. The shape of polygons in the simulation is determined using a list of coordinates. Therefore, to approximate the radial shapes by the polygons, 360 pairs of coordinates are computed at one-degree intervals on the edge of each circle based on the available cloud definition. Only those points are used for approximated areas from several circle segments, which do not lie in the circle segment of another circle, whereby finally, an outer contour of the total area is created.

In the third step, all roads of the SUMO network located within the defined area are retrieved. The fourth and last step consists of generating and assigning a friction value to the lanes via the TraCI according to the conditions defined in the weather module. However, the value can only be changed for the entire length of an edge so that in the case of very long contiguous road sections, inaccuracies may occur, as shown in Figure 4.28. The problem can be solved by additional segmentation, which can be automated during the pre-processing or post-processing of the road network. The entire process can also be performed online at runtime, which means that in larger scenarios, a moving weather front can also be displayed and simulated.

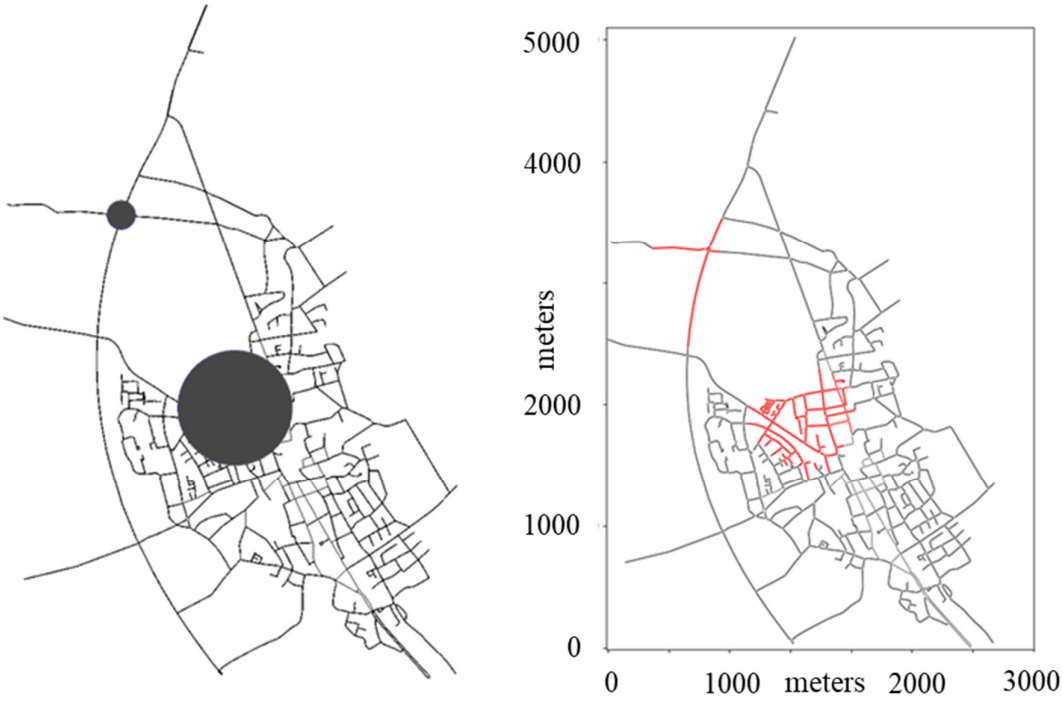

Figure 4.28: Inaccuracy in the automated assignment of precipitation areas

For example, Figure 4.29 shows a progressively advancing precipitation front moving from north to south varying in the total area.

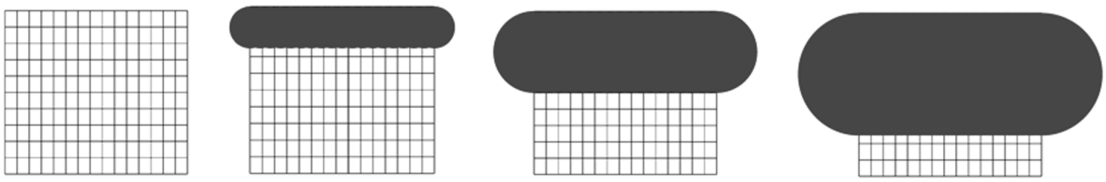

Figure 4.29: Moving area of rain on a generic chessboard road network in SUMO

A more detailed description of the implementation can be found in a conference paper by the author (Weber et al. 2021). The weather-related road conditions generated in this way can then be picked up and used by the vehicles' other systems, models, or functions. In the further course, this concerns, for example, a sensor model, a driver model, and ADAS at the guidance and the navigational level.

4.3.2 Sensor Model

The implementation in the previous subsections covers the introduction of the road surface condition as a property of the simulation network. The next step in the implementation process is to enable individual vehicles in the simulation to pick up and interact with this attribute in the manner of its intended reflection of the weather-related road surface condition sensor. This was done primarily for the subsequent investigation in terms of the feasibility of V2X based distribution of the data. For purposes like this, SUMO has a designated class called a device, which may be equipped for individual vehicles or a class of vehicles. In this case, a new device is derived and designed to simulate the WRSCS and to be able to hold various mathematical models if necessary.

The implemented model is based on collected measurement data from the actual experiments of partners from the project Seeroad (Weber and Schramm 2020a). After completing winter test runs in Norway and Sweden, the Dr. Ferdinand Porsche AG partners provided some data sets collected with a commercial reference sensor system MARWIS (Lufft 2021), also used in various other studies (Brustad et al. 2020). The model is based on Data of a day-long trip of about 442 km collected throughout 6 h 23 min 31 s.

Figure 4.30 shows that all relevant road conditions, dry, moist, wet, and slick, were recorded during the journey. First, it is examined to what extent the measurement characteristics for the different defined categories differ to assess whether a single mathematical description is enough or whether a separate one should be preferred for each cluster. For this purpose, the data from Figure 4.30 are clustered according to the classification presented in Section 3.2. Figure 4.31 exemplary shows the measured values of the data cluster “dry”.

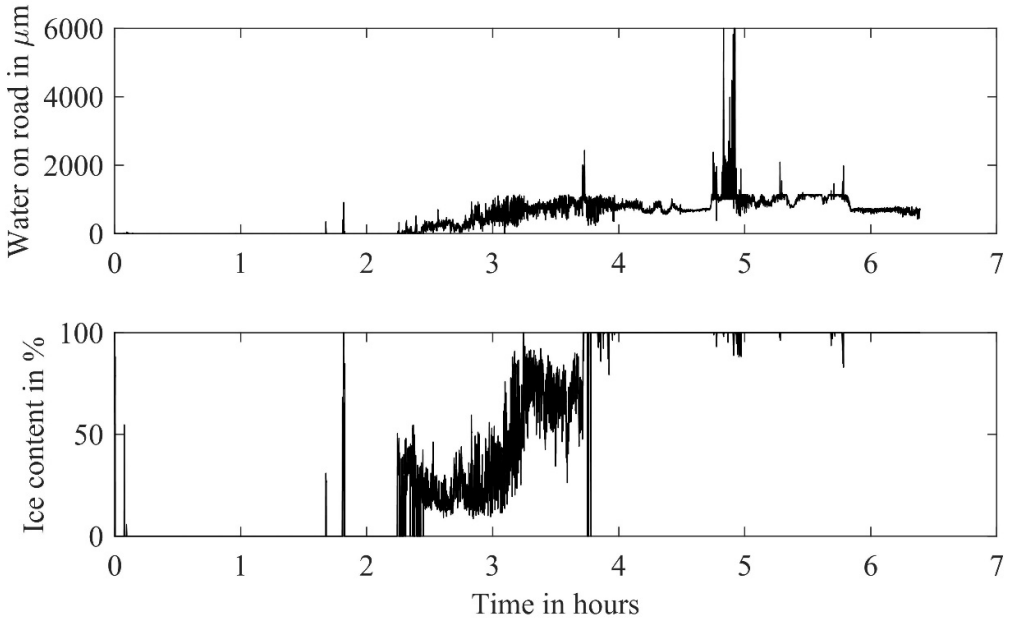

Figure 4.30: Measurement profiles for water height and ice content for the entire trip

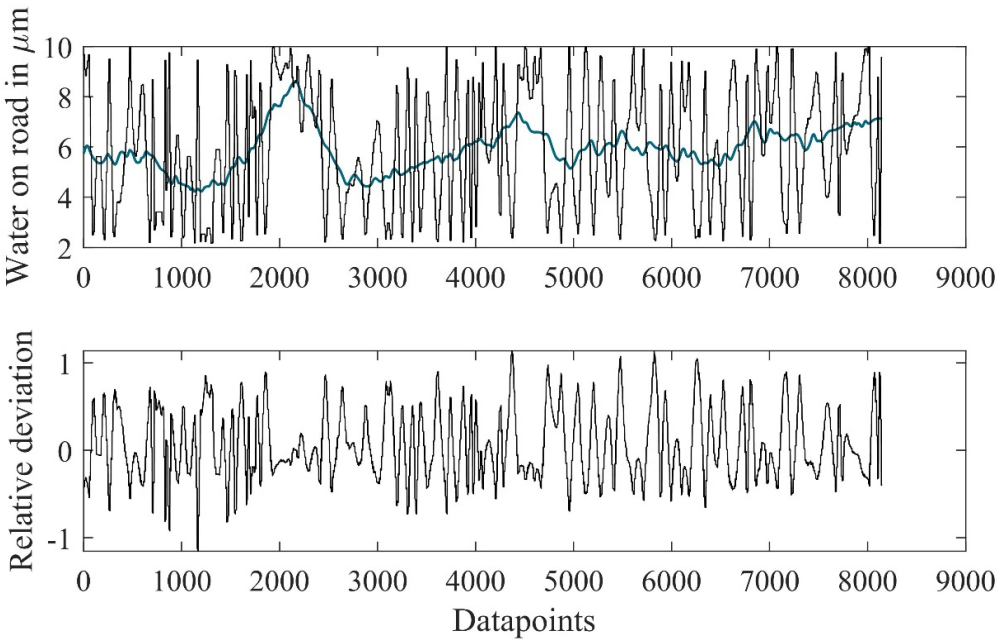

Figure 4.31: Measured value analysis of cluster “dry”

A moving average filter is applied to the raw data with a window width of 500 Datapoints. This value then serves as a reference for determining the relative deviation of the individual measured values. It also normalizes the data, making it easier to compare them over time. The frequency distribution of the relative deviations is the chosen dimension for the characterization of the sensor that can later be compared with the simulation for the different clusters.

The relative deviation of the two curves is given in Figure 4.32. The frequency distribution is plotted, and a fitting of probability functions is performed to characterize these. In this case, a generalized extreme value distribution is the best approximation, while the normal distribution also offers an acceptable solution and is in line with the expectation for measurement inaccuracies.

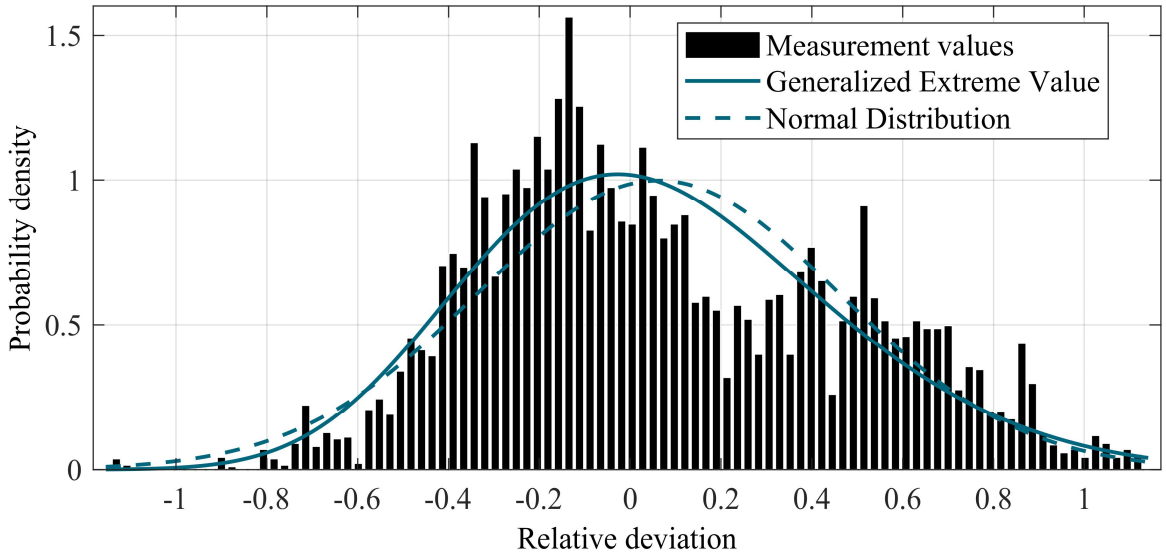

Figure 4.32: Distribution fitting of the relative measured value deviations of the cluster “dry”

The probability density function for the generalized extreme value distribution (GEV) is of the form

$$y = \left(\frac{1}{\sigma}\right) exp\left(-\left(1 + k\frac{(x-\mu)}{\sigma}\right)^{-\frac{1}{k}}\right)\left(1 + k\frac{(x-\mu)}{\sigma}\right)^{-1-\frac{1}{k}} \tag{4.62}$$

with location parameter μ, scale parameter σ, and shape parameter k ≠ 0. In this case the distribution parameters yield k = -0,1760, $\sigma = 0.3668$, and μ = -0.0970. The normal distribution with the parameters means value μ and standard deviation σ is of the form

$$y = \frac{1}{\sigma\sqrt{2\pi}} exp\left(\frac{-(x-\mu)^2}{2\sigma^2}\right). \tag{4.63}$$

In the present case the values μ = 0.0622 and σ = 0.3998 are determined.

The other clusters are processed in the same way, and the results are given in Appendix B. The simulated measurement data thus generated is added to the existing floating car data (FCD) output format. The implementation is such that the friction key-value pair appears within the attribute list of the output tags only of those vehicles that are equipped with a WRSCS.

Furthermore, SUMO's existing TCP-based control interface TraCI is adapted to fully support online access to the actual measurement data point through the selective generic parameter retrieval call and subscriptions to the respective vehicle variable. This becomes necessary when using the data in a larger V2X co-simulation environment, as used in Chapter 5.

4.3.3 Driver Model

It is necessary to adapt a driver model within the simulation to emulate a realistic driver behavior under adverse road surface conditions to satisfy the approach of using a realistic base traffic scenario as a reference for describing and estimating the influence of road surface condition aware systems in future scenarios. Some studies regarding the influence of weather-related road surface conditions on traffic can also be found in Section 3.2.2. and the respective Table 3.2.

The considerable variations in the study results come from the difference in the severity of the precipitation and in various types of measuring stations and different road types. Another reason is the overlapping of different additional effects, such as twilight, darkness, or other visual impairments. However, together with the information from Table 3.3, the relevant findings from research in terms of observed speed reductions in different forms of precipitation are used to estimate a model relationship between the condition of the road surface and the reduction of speed.

Figure 4.33 shows two possible models based on a first and second-degree polynomial fitting of the data derived from Figure 3.6 and Table 3.3. According to the linear model, a wet road, described by the range $\mu \approx 0.5 – 1.0$, leads to a speed reduction of 0 – 22.4 %, and a snowy road,

represented by the friction value range $\mu \approx 0.3 – 0.6$, leads to a reduction of 17.9 – 31.4 %. While the quadratic model reduces the speed within the wet road range by 1 – 19.2 % and in the snowy road range by 14.1 – 31.5 %.

$$f(\mu) = 0.4481\mu + 0.5720 \tag{4.64}$$

$$f(\mu) = -0.3491\mu^2 + 0.8922\mu + 0.4493 \tag{4.65}$$

Equations (4.64) and (4.65) describe the derived speed reduction factor of the fitted relative speed reduction models. Both equations are implemented into an augmented standard (Krauß 1998) car-following model to more accurately simulate a driver's behavior under adverse weather conditions.

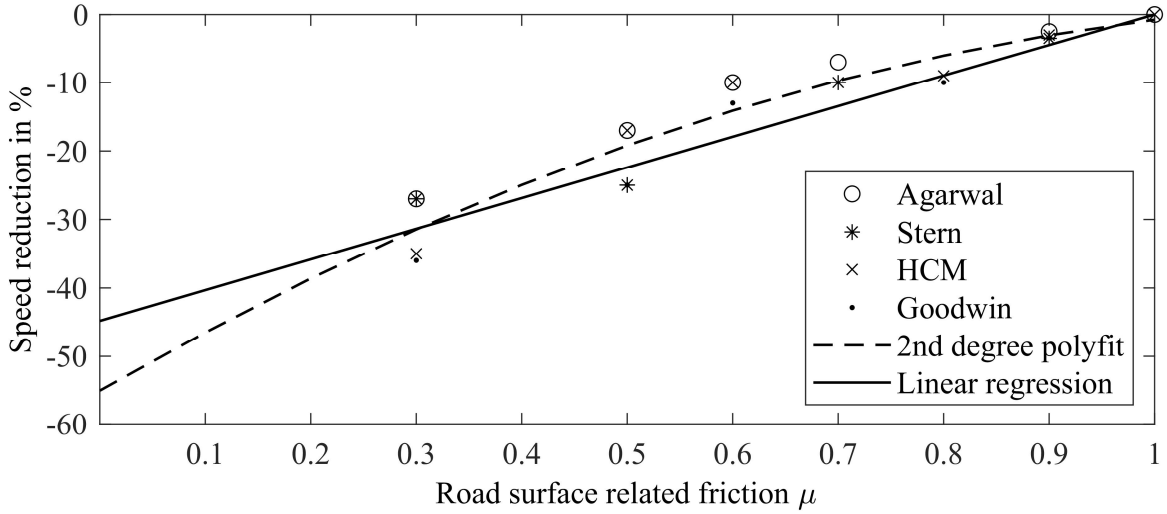

Figure 4.33: Speed reduction model for the car-following model adaptation

4.3.4 Stabilization

Since it is not common in microscopic traffic simulation environments to use more complex vehicle models that allow a direct, explicit consideration of this level (Detering 2011; Treiber and Kesting 2013), no corresponding adaptation of the software is made in this thesis. Instead, the modularity and flexibility of the described overall approach are used, if necessary, to simulate situations on the vehicle level with complex models, based on findings from relevant situations from the traffic flow simulation, and thus also to investigate them on the stabilization level. Furthermore, this approach avoids the disadvantage of unnecessarily increasing the complexity of traffic simulation by introducing nanoscopic elements. Although this is technically possible, such a detailed and time-consuming calculation in larger scenarios is neither sensible nor goal-oriented for performance reasons.

In contrast, the proposed methodology only takes up situations classified as particularly interesting or important for the object of investigation based on the respectively defined characteristic values. The necessary start and input variables for executing the complex simulation on vehicle level can be extracted, transferred, and used directly from the traffic flow simulation.

4.3.5 Guidance

In addition to the road surface condition aware extension of the standard car following model as described in Section 4.3.3, an implementation of the road surface condition aware ACC as introduced in Section 4.2.3 is also carried out on the traffic level within SUMO as an extension of an already existing ACC approach based on the work of (Milanés and Shladover 2014) and (Xiao et al. 2017). Since the standard simulation step size within SUMO is one second, the system was not adopted without further review but was subjected to a detailed sensitivity analysis beforehand. The analysis was published in the International Journal of Advanced Mechatronic Systems (Weber and Schramm 2020b) due to its novelty value. The result shows that it is generally possible to recreate the controller's behavior with the increased step size in the traffic simulation environment, but only after optimizing the respective control parameters.

4.3.6 Navigation

As introduced in Chapter 3, the navigational level mainly deals with the choice of routes either before starting a trip or dynamically adapting to dynamic events such as traffic jams or changing weather conditions. After implementing the weather module and different driver and car-following models, another function is introduced into SUMO to consider these factors on the navigational level of the traffic simulation. This is based on the dynamic routing considerations of Section 4.2.5.3 above. Since various routing algorithms are already included in the SUMO distribution, only a corresponding adaptation to the new conditions is necessary. The algorithm chosen for this purpose in this thesis is based on the depth-first search method and allows a numerical evaluation of the route sections by the so-called effort value, which is added up in the cost function for all sections. In a first approach, the evaluation is carried out based on the coefficient of friction of the road sections.

If the friction value of a road section is $\mu \leq 0.5$, this section shall by definition no longer be considered as autonomously drivable and is conditionally evaluated with a very high-cost value ε_n. Road sections with a friction value of $\mu > 0.5$ initially remain cost-free. In the optimization based on this evaluation, the roadway sections on which autonomous driving is not possible are avoided, provided that the route destination and the road network allow this. According to this approach, the mathematical formulation of the cost function f_c and the optimization results in equation (4.66), which sums up the costs of all roadway sections from the starting point $n = 1$ to the last roadway section of the route where $n = m$ and then minimizes them.

$$\min f_c = \min \sum_{n=1}^{n=m} \varepsilon_n \tag{4.66}$$

$$\varepsilon_n := \begin{cases} 0 & \mu_n > 0{,}5 \\ 1000 & \mu_n \leq 0{,}5 \end{cases} \tag{4.67}$$

This approach alone is insufficient because unnecessary long detours can sometimes occur to avoid undesirable sections, as shown in Figure 4.34

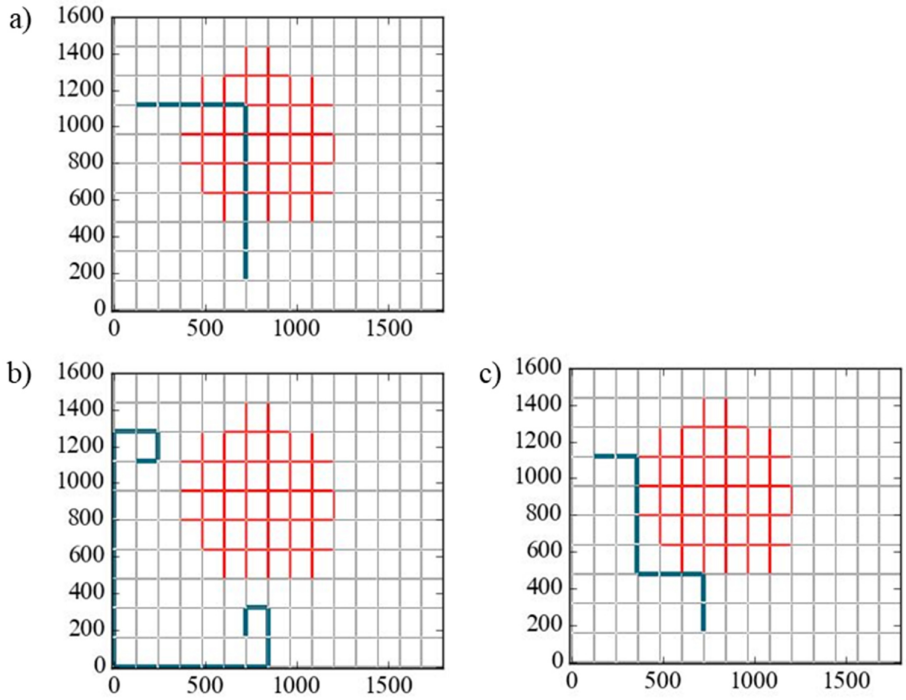

Figure 4.34: Route selection with different cost functions. a) Routing based on shortest time only b) Routing by effort only, with identical effort values for unaffected areas c) Routing by minimizing effort and travel time Eq. (4.68).

This behavior is due to SUMO's linking of the routing algorithm with the stored street IDs. These are often random and usually not sorted in an ideal or shortest order in the database, leading to such problems with depth-first search procedures. To avoid this without having to change the actual underlying routing algorithm, in a second iteration of the cost function, the estimated travel time in seconds τ_n is added to the numerical evaluation of the route sections in addition to the costs ε_n for traveling on the route sections to be avoided. The travel time is estimated as the length of the route section divided by the maximum permissible speed. This slight adaptation leads to a narrow bypass of undesirable areas.

$$\min f_c = \min \sum_{n=0}^{n=m} (\tau_n + \varepsilon_n) \tag{4.68}$$

Thus far, the premise is that the data is available before starting the trip. However, especially with weather-related road surface conditions, changes can be abrupt or temporary, making it an ideal target for investigating dynamic conditions by sharing the information in a V2X connected driving environment, which is dealt with in the following Section 4.4.

4.4 Integration Automotive Networking

One premise for this thesis is to analyze the impact and potential of emerging systems and trends such as the growing connectivity of vehicles on present-day and future traffic scenarios. The VEINS (Sommer et al. 2011) project is used to cover this area which uses TraCI to connect a network simulation performed by OMNeT++ (Varga 2010) to the traffic simulation SUMO using the vehicles as nodes. The adaptations to TraCI during the implementation of the models and functions on the traffic level thus far make it possible to access all aspects of the road surface condition itself and the sensor device. This Section deals with the technical aspects and implementation within the framework using current and future standards of V2X.

As part of the ongoing standardization of V2X communication, a concept for the consistent exchange of environmental data has already been developed based on various projects (Eichhorn 2014), the so-called Local Dynamic Map (LDM) as described in (ETSI EN 302 895:V1.1.1). The concept of the LDM is now briefly explained, and the form in which data generated in this thesis can be integrated is shown.

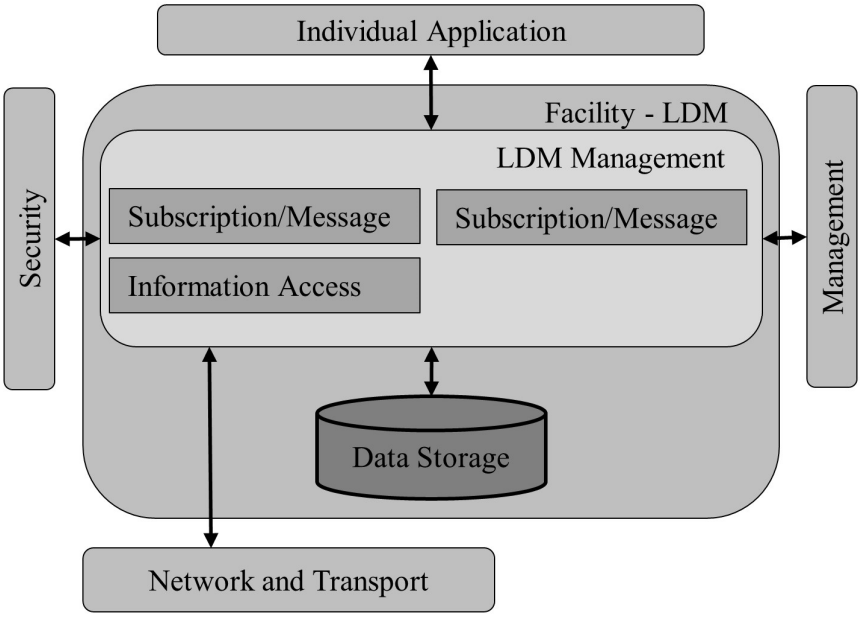

Figure 4.35: Architecture of a Local Dynamic Map

The LDM is located at the facilities layer (cf. Section 2.5.3), and it assumes essential tasks for data management, i.e., in addition to collecting and forwarding relevant messages. It also consolidates, localizes, verifies plausibility, and makes the data available to all network participants in line with the situation. Based on the available information within the LDM, appropriate applications can be implemented. In the present case, these are, for example, a visualization of the road condition for the driver, the generation of warning notices or speed recommendations, right up to use in control systems such as longitudinal dynamics control (such as the RSACC) or a brake system.

Architecturally the LDM consists of two elements, the LDM management and the database for the storage of relevant data, schematically shown in Figure 4.35. The data within the LDM is assigned to four different layers, two static and two dynamic layers. These are defined as follows:

- Layer 1: Permanent static data (e.g., extended information on the infrastructure),
- Layer 2: Transient static data (e.g., temporarily changed signage),
- Layer 3: Transient dynamic data (e.g., traffic information or road conditions),
- Layer 4: Highly dynamic data (e.g., safety-relevant information).

The categorization is helpful for targeted storage and processing within the database. Figure 4.36 displays a corresponding overview.

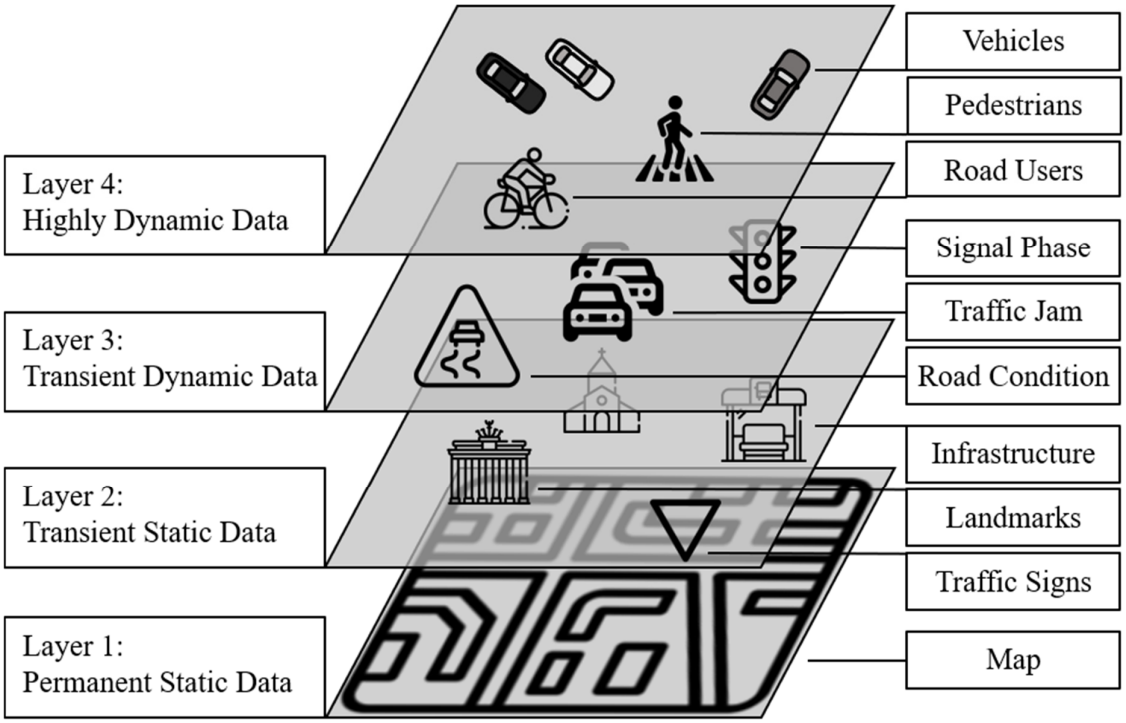

Figure 4.36: The four layers of an LDM based on (Shimada et al. 2015)

The LDM is designed in such a way that an instance runs on each communicating platform. The relevant information that each platform receives can vary greatly depending on its nature. This means that, in addition to vehicles, roadside units also send and receive corresponding data or forward it. At a central location (or several locations), large aggregating databases can be set up to store all information. Since the information in the LDM is always position-bound data, the load on mobile platforms can be reduced because only data in a specific area is relevant. A further advantage at central locations where data from many sources are collected is the better possibility to check the plausibility of incoming data, e.g., through cross-comparisons or the comparison with weather information in the case of road condition data.

A dynamic road condition map concept can be developed if the available information is combined, as shown in Figure 4.37. First, mobile platforms, i.e., vehicles with a corresponding system,

record the road conditions in their immediate vicinity or on the sections they drive on. Then, after appropriate processing by the platform's LDM, this information can be used for platform applications. In addition, this information is transmitted via Decentralized Environmental Notification Messages both to vehicles and RSUs in their environment.

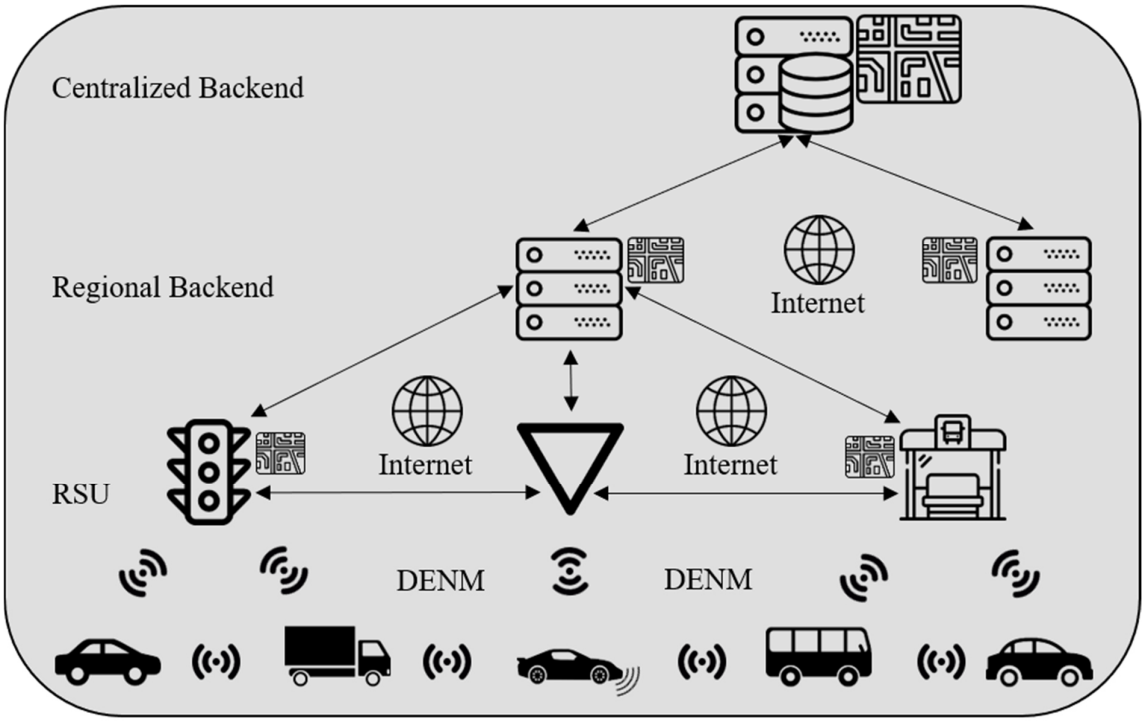

Figure 4.37: Concept of a distributed dynamic road condition map

It can be assumed that with the increasing availability of vehicles with an acquisition system, the information density already at the RSU level is so high that an improvement of the information quality by data fusion in the LDMs of the RSUs is possible. Even if the backend units were unavailable, such a system could already be used. All RSUs, in turn, send their data to so-called regional backends, on which consolidation can then be carried out with the aid of other sources, such as weather data from corresponding services. Finally, a central backend collects all regional data and merges them into an overall picture.

The data and information processed in this way are simultaneously propagated backward to the RSU level, where it can be queried and processed locally by mobile platforms if required. Platforms with appropriate sensors can improve their perception in this way or check their plausibility, while platforms without a road condition detection system of their own can still benefit from the recorded road condition data.

Next to the distribution of Cooperative Awareness Messages, which hold specific data about the respective road users state and make up the highly dynamic data of layer 4, Decentralized Environmental Notification Messages are used transmission of road condition data. For this application, the corresponding service offers several advantages. On the one hand, the local limitation of the information is already planned, and on the other hand, it can be triggered, updated, and

rescheduled as required. In addition, the available message definition already contains classes that can be used for the transmission of road conditions. Figure 4.38 outlines the general structure of a DENM as defined in (ETSI EN 302 637-3:1.2.1). For data transmission efficiency reasons, the information of the containers is usually encoded. A detailed code list of the containers is available in the first three parts of the technical specification (ETSI TS 101 539-1:V1.1.1).

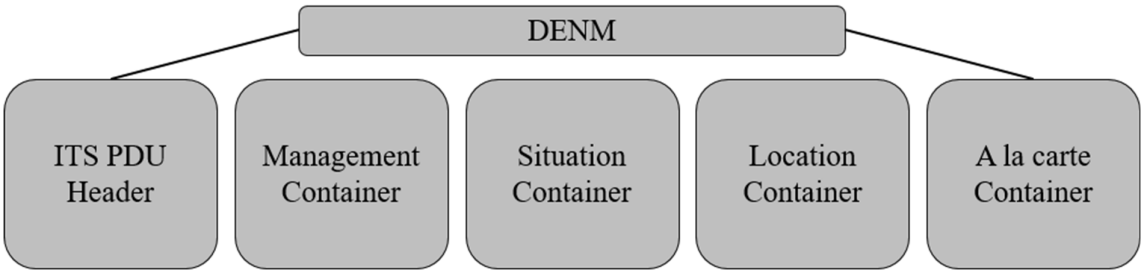

Figure 4.38: Decentralized Environment Notification Message

In the situation container, the cause of the message is transmitted in such an encoded form. Code 6: “Adverse weather condition - adhesion” is an obvious option here. Even if the available substantiating “subCauseCodes” may not correspond directly to the data provided by the system, this further information can be transmitted as required within the so-called “a la carte” container. In this thesis, this goes for the specific measurement value provided by WRSCS equipped vehicles.

As mentioned above, the VEINS project does not natively support the ETSI Cooperative Intelligent Transport System (C-ITS) and specifically the V2X protocols, so the Vanetza project (Riebl et al. 2017) is integrated, which provides an open-source implementation of the entire protocol suite as a C/C++ library. After making the necessary adjustments to process the road surface condition information in the a la carte container of DENMs, ETSI V2X standard-compliant messages are exchanged and processed in the simulation environment.

A self-developed facility server (FaciSrv) takes over the management function for the LDM in the framework, including the encoding and decoding of messages, the processing, and the connection to the PostgreSQL storage database (cf. Section 4.2.5.1), while meeting the ETSI requirements. Figure 4.39 shows the integration of V2X connectivity as a module is into the overall modular framework concept introduced at the end of Chapter 3 (cf. Figure 3.10). This way, the facility layer can be expanded or replaced as needed, and additional applications can be implemented and investigated.

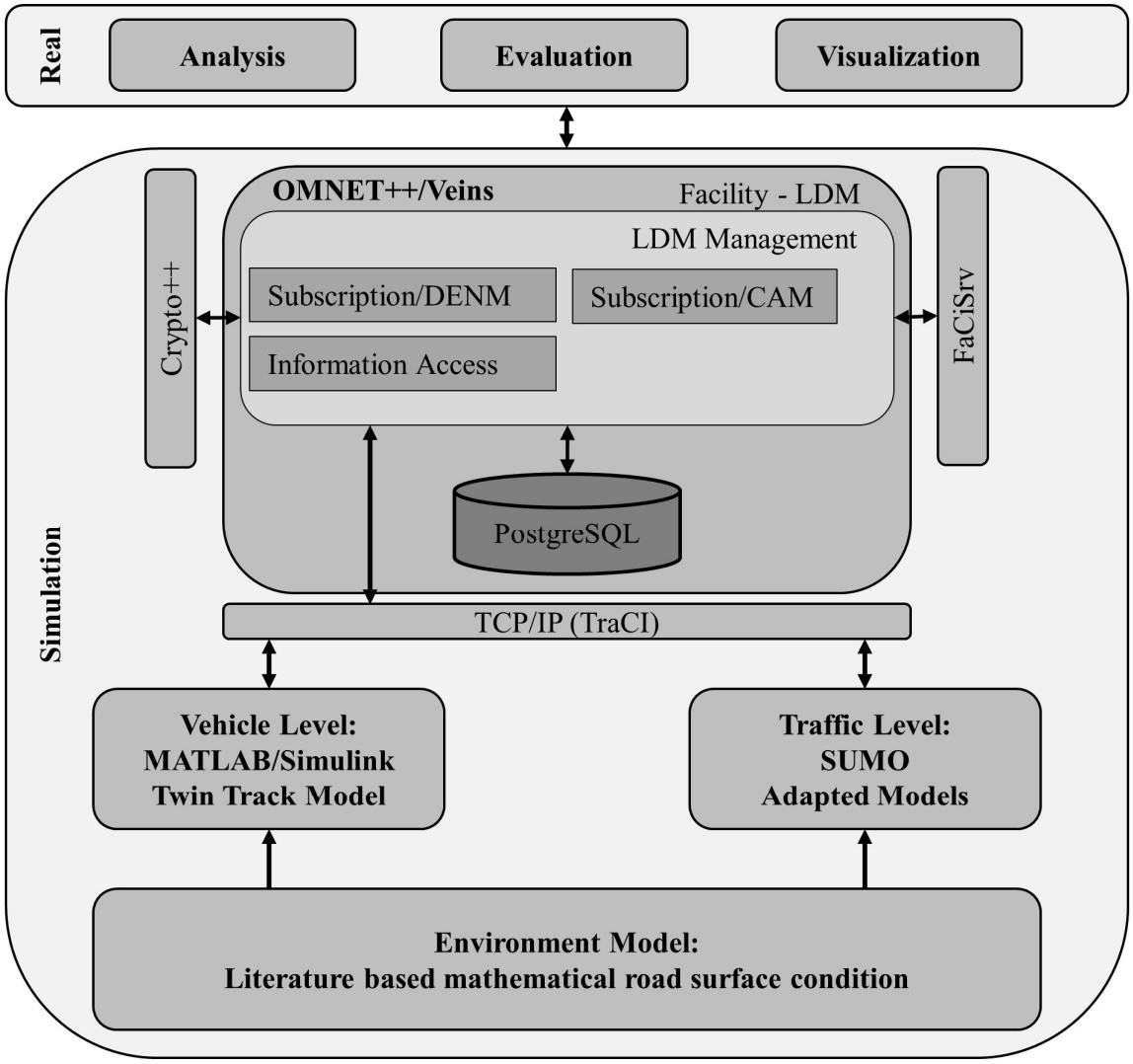

Figure 4.39: V2X integration into the overall framework

5 Simulation

This Chapter forms the core of the thesis, as it describes the various simulation studies that finally serve to answer the specific research questions. The Chapter's core is divided into two parts: the vehicle level and the traffic level, in line with the overall research concept. The former focuses on the stabilization and guidance level, the latter on the guidance and navigation level. In both cases, the various tools and systems selected are examined in a series of different scenarios. In each case, a state-of-the-art system is compared with a new weather-related road surface condition aware version to determine concrete potentials not only qualitatively but also quantitatively. The selection and introduction of the necessary metrics are always made at the beginning of the subsections. The Chapter concludes with a discussion of the results from the studies.

5.1 Vehicle Level

For exclusive simulations on the vehicle level, the complex twin track vehicle model implemented in MATLAB/Simulink as described in Section 4.2 is used. In industry and research, typical driving maneuvers are often used to evaluate the driving dynamics properties of a vehicle, some of which are also specified in international standards, such as braking in a turn according to (ISO 7975:2019) or lane change behavior according to (ISO 3888-1:2018). (Zomotor et al. 1998) has arranged these typical driving maneuvers in the so-called “driving dynamics circle”. According to his classification, driving behavior is principally subdivided into different categories for evaluation. The classification distinguishes between straight driving behavior, cornering or turning behavior, alternating cornering, and transition behavior.

(Weber 2004) has extended this circle to include typical characteristic road conditions concerning the available friction coefficient μ, under which these driving maneuvers may be carried out for comparative studies. He also proposed a three-point rating scale to further evaluate driving maneuvers regarding their respective relevance in terms of safety, frequency, and road condition (friction value), given in Table 5.1. The selection of the specific driving maneuvers for the following analysis is based on the one hand on this rating scale and on the other hand on the scope of the previously selected ADAS for the detailed investigation of the vehicle level in Section 4.2. As these are an antilock braking system, an adaptive cruise control, and an emergency braking system and their optimization through the information provided by a weather-related road surface condition sensor, the selection on the vehicle level focuses mainly on maneuvers at the driving dynamic stability limits.

Table 5.1: A relevance rating scale for driving maneuvers (Weber 2004)

Criterion		Relevance/Points		
No.		1	2	3
1	Safety	low	medium	high
2	Frequency			
3	Road condition			

Table 5.2 ranks the dynamic driving maneuvers following (Weber 2004) accordingly. The ranking is based on the combination of literature research and own assessment. Regarding the selected ABS and ESB systems (cf. Section 3.5.2), three maneuvers are selected (highlighted in grey), which appear particularly suitable for answering the specific research questions RQ1 and RQ2 that deal with the potential safety impact of the WRSCS at the stability and guidance level. Furthermore, maneuvers from three different classes are selected in order to consider the different dynamic load scenarios longitudinal dynamics (braking straight ahead), lateral dynamics (evasion test), and combined longitudinal and lateral dynamics (braking in a turn).

Table 5.2: Ranking of the dynamic driving maneuvers

No.	Class	Maneuver	Safety	Frequency	Road cond.	Sum	Rank
1	Straight	Braking	3	3	3	9	1
2		Accelerating	1	3	2	6	4
3		Load changing	2	2	2	6	4
4	Cornering	Stationary	1	1	2	4	6
5		Instationary	2	2	2	6	4
6		Braking in a turn	3	3	3	9	1
7		Accelerating	2	3	3	8	2
8		Load changing	2	1	2	5	5
9	Alternating	Evasion test	3	1	3	7	3
10		Weaving	3	1	3	7	3
11	Transition	Simple lane change	3	3	2	8	1
12		Steering angle step	3	1	3	7	3

Figure 5.1 shows an adaption of the original driving dynamics circle on the left-hand side and the adaptions regarding possible scenarios for the weather-related road surface conditions and their implication for the friction coefficient during the test runs on the right-hand side. The selected maneuvers are again highlighted in dark grey.

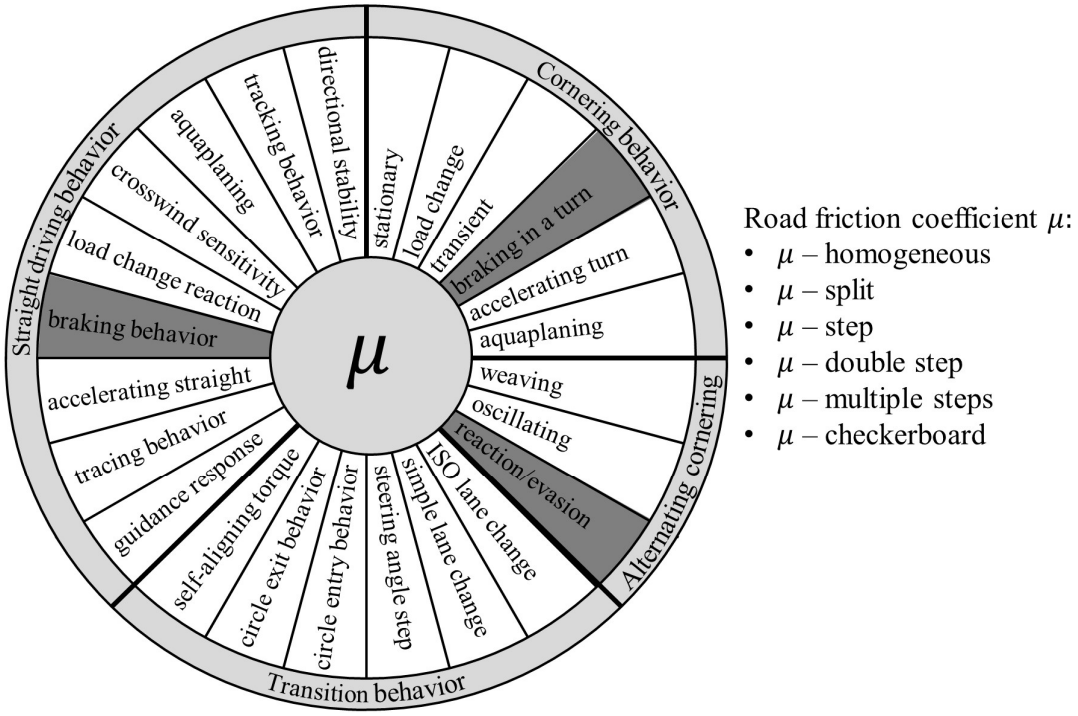

Figure 5.1: Driving dynamics circle following (Zomotor et al. 1998; Weber 2004)

5.1.1 Stabilization

RQ1 (cf. Section 3.4) addresses the safety impact of the weather-related road surface condition awareness system on the stabilization level. Criteria for evaluating relevant parameters for the performance of the systems at this level can be derived from the driving maneuver standards described in more detail in each of the considered driving maneuvers. In each case, these are variables relating to the vehicle's longitudinal and lateral dynamic properties, which can be compared when considering the system’s performances. In the case of longitudinal dynamics for a braking maneuver, these are, for example, a rapid deceleration buildup, the highest possible average deceleration over the entire braking process, and the shortest possible braking distance. Variations such as the sideslip angle, the yaw rate, or the lateral deviation from the reference path are essential when considering lateral dynamics.

5.1.1.1 Braking Straight-Ahead

(DIN 70028:2004) standardizes “measuring the stopping distance with ABS in straight-ahead stops”. For this purpose, a procedure is specified for determining the braking distance covered by a vehicle during ABS-controlled braking (in full braking condition) from straight ahead. The procedure described is initially only valid for measuring braking distances on a straight, level, dry road with a high level of grip. It is concerned explicitly with emergency braking, which with maximum deceleration always means emergency braking in regular driving operation, in contrast to comfort-oriented deceleration braking. For appropriately equipped vehicles, this means continuous

ABS control. The process relates exclusively to the steady-state condition to minimize individual influences caused, for example, by different types of pedal actuation. For this purpose, after a transient phase, the distance covered between a defined trigger speed and a defined final speed is measured. At the start of braking, the target speed is 113 kph with a maximum permissible deviation of ±2 kph. If the speed falls below the initial speed of 100 kph (27.78 m/s), the mean deceleration and the so-called normalized braking distance are calculated. Since these are simulations, the specifications regarding measurement accuracy, data processing, and boundary conditions can be complied with in any case when carrying out the test. The variables to be evaluated for this test maneuver under the standard are the mean deceleration, the normalized braking distance, the speed curve, and the brake pedal force. Figure 5.2 shows a comparative standard-compliant graphical representation of the measured variables in the time sequence of a braking operation under moderately wet road conditions ($\mu = 0.8$) and a brake-relevant initial speed of 100 kph for the reference system and the optimized road surface condition aware system. The results for the state-of-the-art ABS (reference) are depicted in black, while the results for the optimized RSCA system are given in petrol.

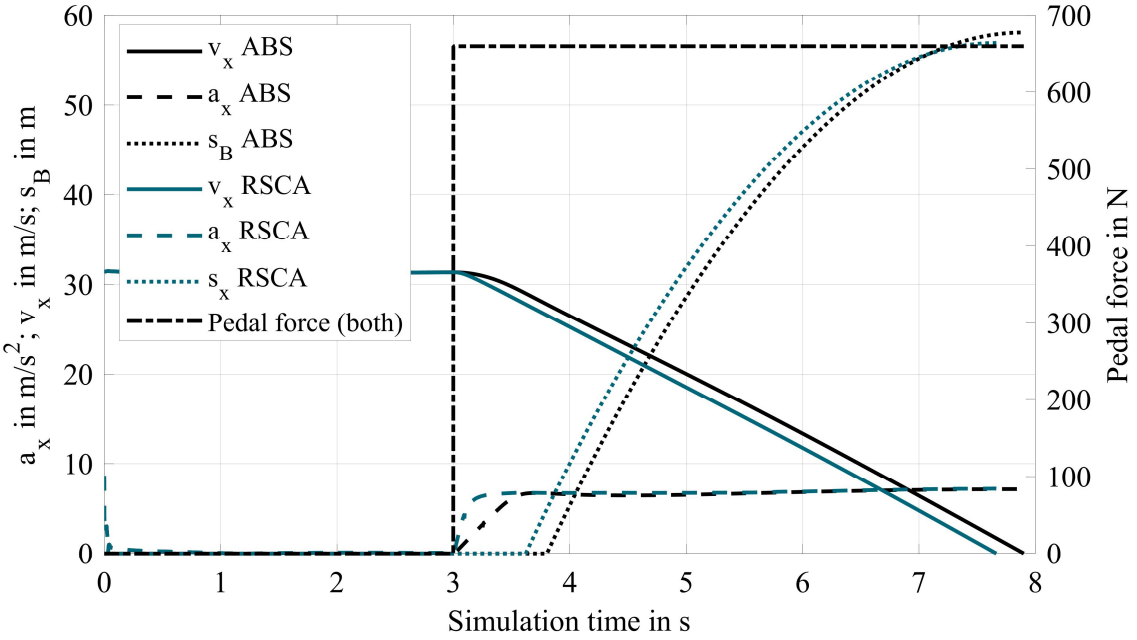

Figure 5.2: Graphical representation of the measured variables in the time sequence of a braking operation following (DIN 70028:2004)

The same conditions prevail for both systems in the first three seconds (start-up and constant speed range) before braking is initiated at $t_B = 3\ s$. The RSCA system builds up the maximum braking deceleration significantly faster than the reference ABS, which reduces the speed earlier. The measurement of the normalized braking distance begins in each case at the initial speed of 27.78 m/s relevant for the test, in the case of the RSCA system after 3.6 s, and for the reference ABS after 3.8 s. For the normalized braking distance, this translates from 58.09 m to 56.93 m. The applied pedal force is equal to 660 N in both cases.

A total of 36 simulations with different road conditions and braking-relevant initial speeds are carried out to compare the systems under the different conditions. Table 5.3 summarizes the results of standardized braking distances in meters for different road surface conditions and initial speeds.

Table 5.3: Summary of comparative simulation results for different conditions

	50 kph		70 kph		100 kph	
μ	**ABS**	**RSCA**	**ABS**	**RSCA**	**ABS**	**RSCA**
0.3	36.92	35.68	74.88	69.66	158.72	140.60
0.5	22.07	21.72	44.60	42.80	95.17	87.52
0.8	13.85	13.83	27.57	27.50	58.09	56.93
1.0	11.43	11.17	22.37	22.25	46.34	46.34
1.0 / 0.3	25.63	23.13	48.99	45.17	100.05	92.46
1.0 / 0.5	20.68	18.14	38.97	35.29	78.42	72.13
1.0 / 0.8	16.77	13.76	30.67	26.60	60.77	55.26

It can be seen here that optimization is particularly worthwhile for poor road conditions since the reduction in the normalized braking distances increases progressively. Figure 5.3 and Figure 5.4 illustrate this trend.

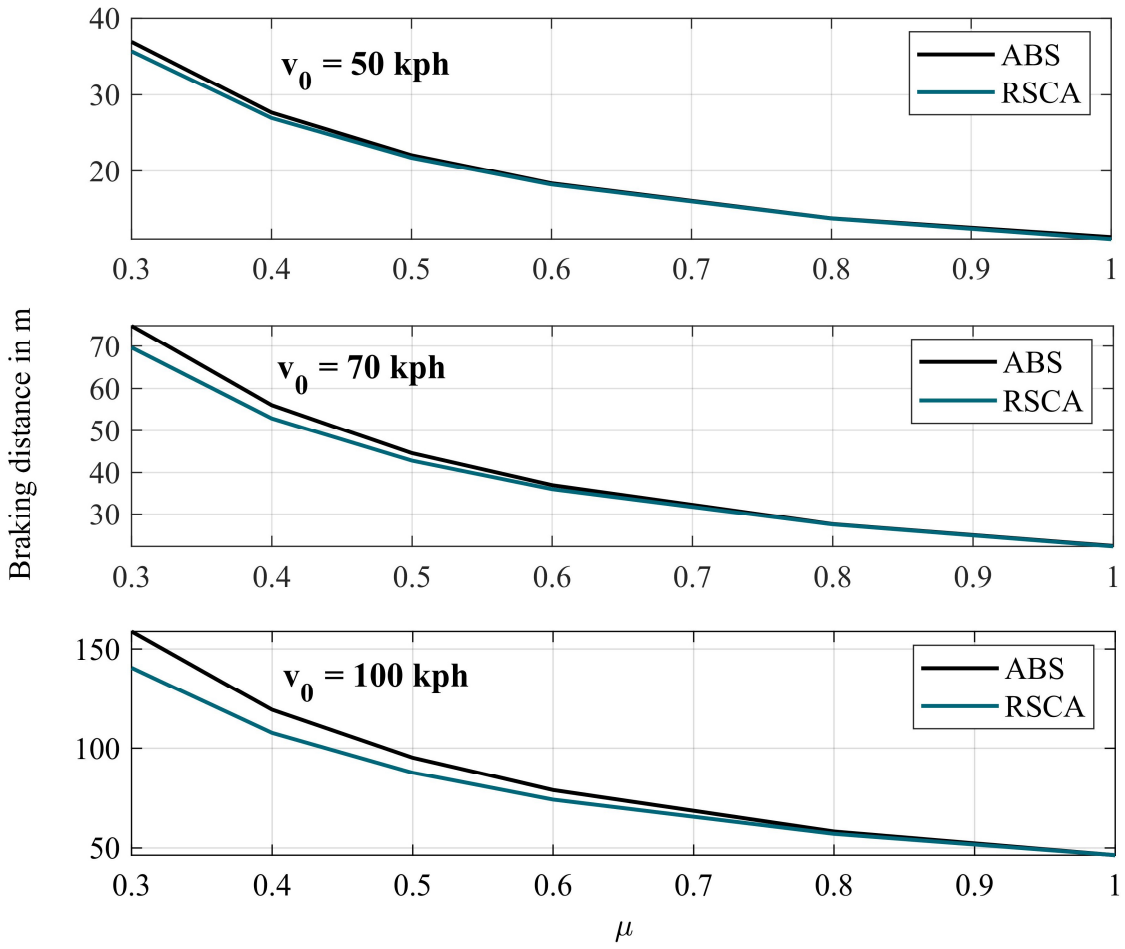

Figure 5.3: Absolut normalized braking distance comparison under different conditions

The former shows comparatively the courses of the absolute normalized braking distance comparison under different road surface conditions. The latter depicts a graphical representation of the absolute braking distance improvement of the RSCA system as a function of the prevailing road surface condition. The results show that a weather-related road surface condition sensor can positively impact safety by reducing braking distance when used appropriately in vehicle stabilization assistance systems. The simulations show that a braking distance reduction of up to 2 % can be achieved on damp road surfaces, up to 8 % on wet road surfaces, and even up to 11 % on icy road surfaces. (Weber 2004) demonstrated a braking distance reduction of 8.6 % on wet road surfaces, which again speaks for the plausibility of the achieved results.

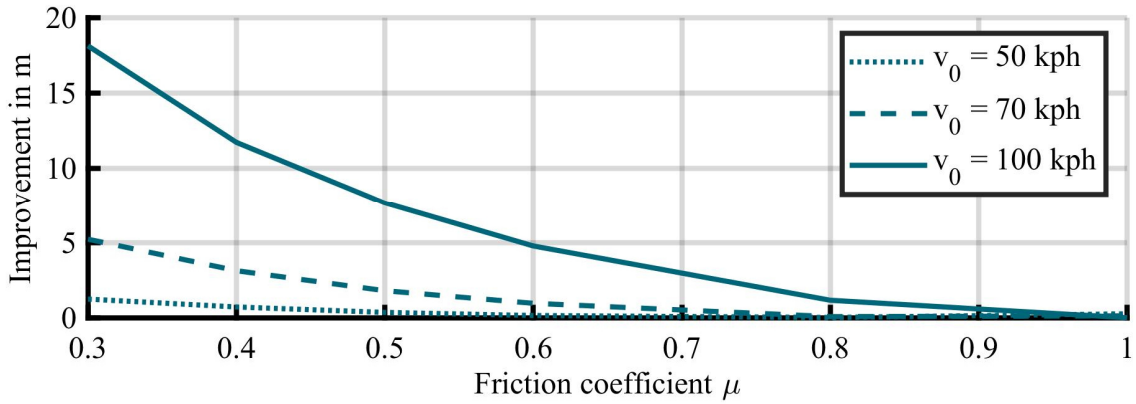

Figure 5.4: Absolute braking distance improvement of the RSCA system as a function of the prevailing road surface condition

5.1.1.2 Braking in a Turn

The maneuver “braking in a turn” is particularly interesting for the investigation of vehicle stability. Longitudinal and lateral dynamics are combined here, and, depending on the conditions, the stability edge of the friction coefficient ellipse (cf. Section 3.2.1) may be reached. (ISO 7975:2019) standardizes a test procedure for investigating “the effect of braking on course holding and directional behavior of a vehicle”. Specifically, it defines initial conditions, mandatory recording variables, and a series of characteristic values and their evaluation and presentation. For comparability and reproducibility, the following results are created in compliance with the corresponding regulations and the same initial conditions of the respective systems with and without optimization through a priori knowledge of the prevailing weather-related road condition by the sensor system.

Table 5.4: Initial test conditions (ISO 7975:2019)

Condition	Curve radius	Lateral acceleration		Longitudinal velocity	
	m	m/s^2	tolerance %	kph	tolerance %
Standard	100	5	±10	81	±5

Table 5.4 shows the requirement of the standard regarding the initial test conditions for a standard execution of the maneuver. The conditions are the same as those for a steady-state circular run as specified by (ISO 15037-1:2019). After reaching steady-state conditions, the brake can be applied to slow the vehicle down to a standstill. The steering wheel angle must be kept constant during the entire maneuver, which is not a problem in the simulation. The standard also explicitly allows deviation from the given values if the boundary conditions do not permit compliance. This is the case, for example, with deteriorated road conditions due to the weather, when accelerations of around 5 m/s^2 are not possible simply because of the available coefficient of friction, which theoretically already applies as of $\mu \approx 0.51$. However, since this restriction in the boundary conditions affects both systems equally in the comparative analysis, the investigation is also possible for these areas. Furthermore, Figure 5.5 shows the effect of decreasing road surface conditions on the vehicle path in constant steering wheel and steady-state conditions.

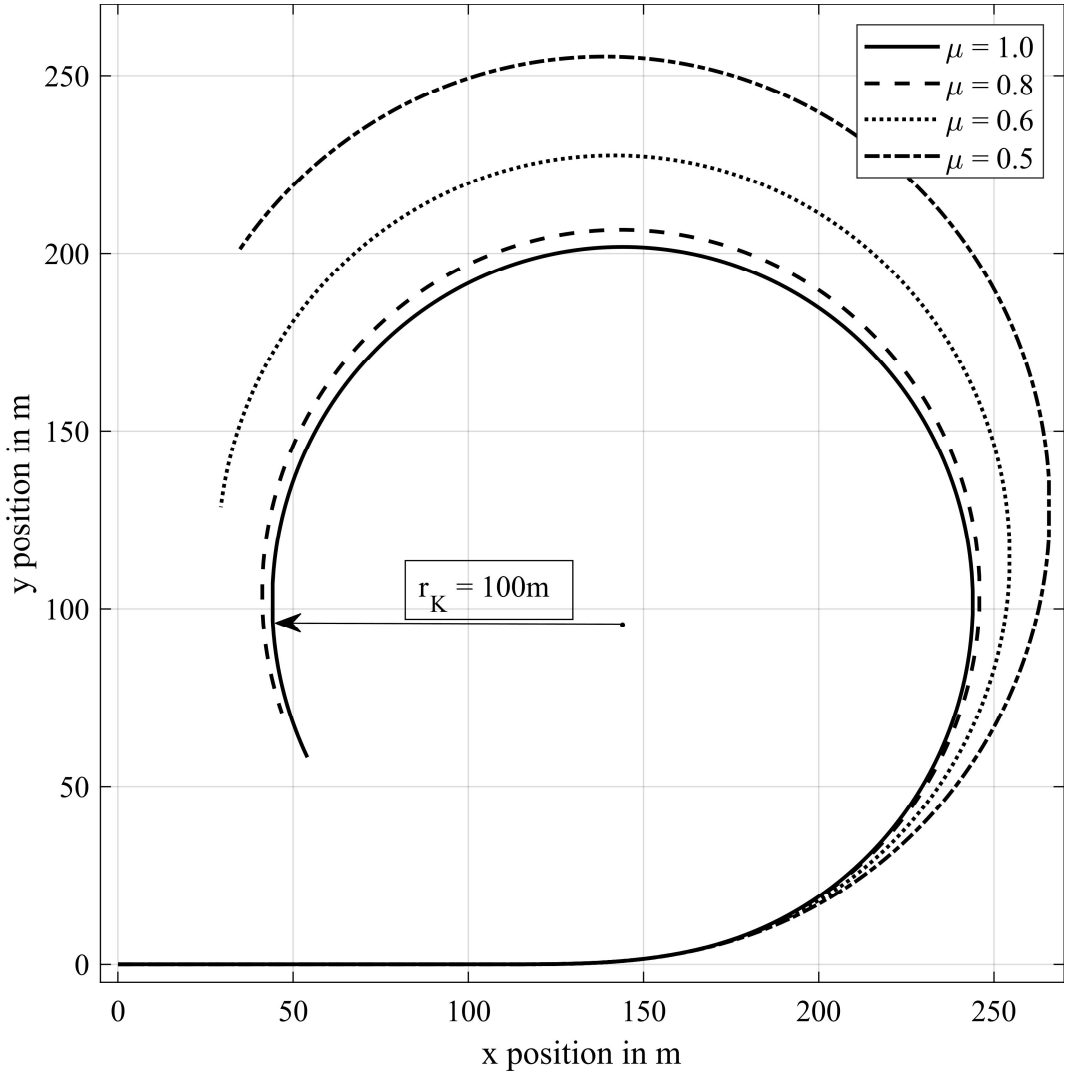

Figure 5.5: Effect of decreasing road surface conditions for a constant steering wheel angle resulting in a 100m curve radius in dry conditions

The change in the frictional connection conditions at the tires due to the decreasing road surface conditions leads to decreasing lateral forces for the same steering wheel angle and increasing the driving radius. This effect can be compensated by increasing the steering wheel angle accordingly until the tire force limit is reached and a circular radius can be driven that the ultimately available lateral acceleration permits. It must be considered that the theoretical value of $\mu \approx 0.51$ cannot be achieved at an initial speed of 80 kph, since a certain proportion is already used to compensate for the driving resistance forces to maintain the speed, and the remaining potential available for building up lateral acceleration is reduced accordingly. Figure 5.6 shows the corresponding reference curves for the different road conditions used to evaluate the following braking maneuvers.

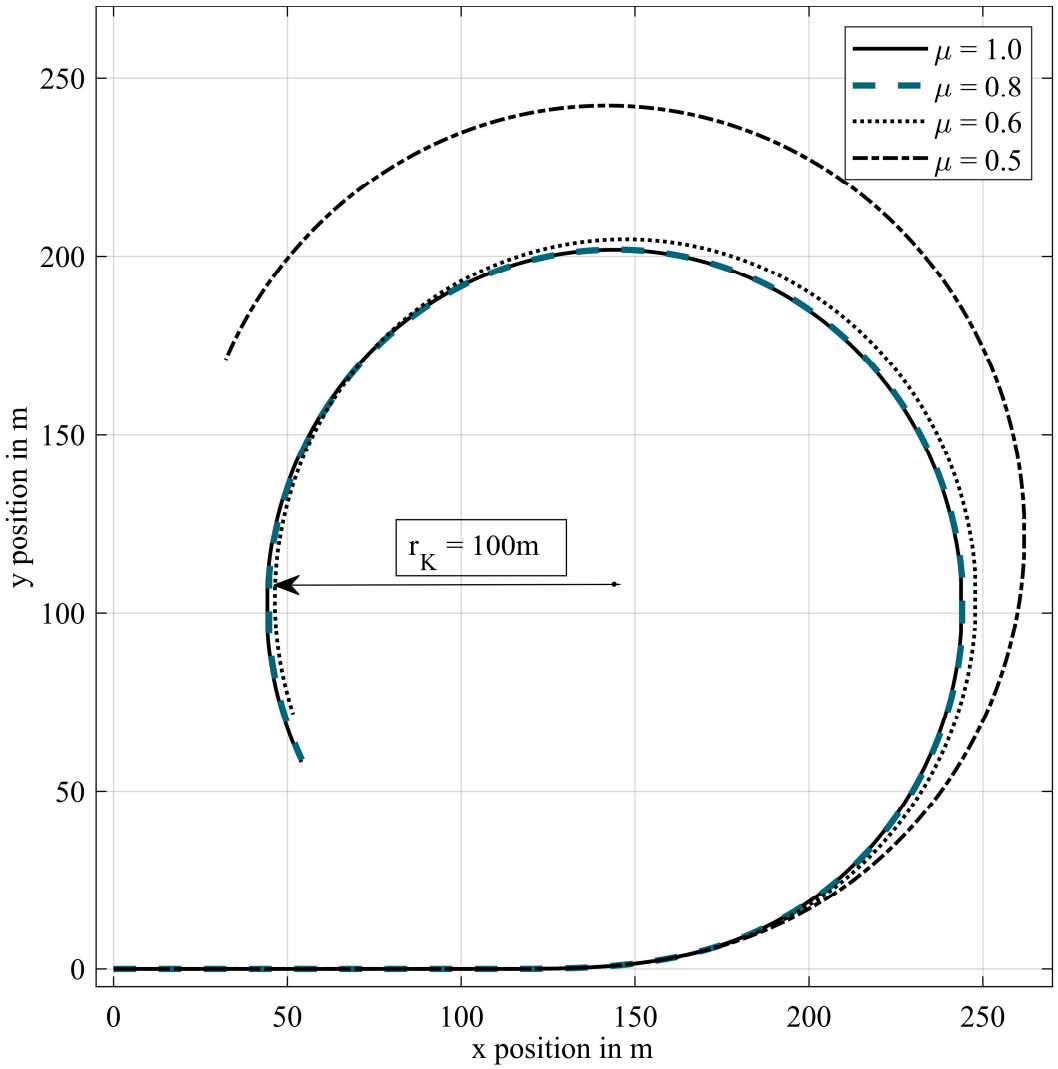

Figure 5.6: Drivable radii for decreasing road surface conditions by increasing the steering wheel angle until reaching the (ISO 7975:2019) requirements or the tire force limits

After establishing the respective steering wheel angles for each road surface condition, the braking maneuvers are performed according to the ISO execution specification. Generally, after reaching the steady-state, the steering wheel is fixed, the gas pedal is released, and the brake is applied as quickly as possible. Several test runs are to be performed with increasing levels of longitudinal

acceleration. The test runs are performed as follows to complete all simulation-related transient processes and achieve a corresponding steady-state. First, the test vehicle drives straight ahead for five seconds at a speed of v_0= 81 kph. At time t_s = 5 s, the steering angle is increased at a rate of 10 °/s until a lateral acceleration of a_y = 5 m/s^2 is reached. This is followed by a short period of constant cornering under these conditions before braking is initiated at the fixed time t_0 = 15 s, at which the steady-state was reached in each case. For each road surface condition, the brake pedal position was increased from 20 % to 100 % in steps of 10 %. The values of all test runs are recorded in each case and, following the requirements of the standard, also processed and stored with regard to the characteristic values, which are described in detail below. The time t_n is defined in the standard as $t_n = t_0$+1 s, where t_0 is the time of brake initiation as mentioned above.

For vehicles with ABS, as in this case in the two versions with and without road surface awareness optimization, the test should be continued at least until "the peak value of mean longitudinal acceleration at time t_n is detected" (ISO 7975:2019). Although this value was also achieved for brake pedal positions well below 100 %, particularly in more unsatisfactory road surface conditions, all test runs were nevertheless performed and recorded for all conditions.

The presentation of the characteristic values should be done as a function of the mean longitudinal acceleration $\bar{a}_{x,t_n}$ in the time interval t_0 until time t_n. Only in one case is the mean longitudinal acceleration $\bar{a}_x$ over the entire braking process from time t_0 to standstill t_{end} used, namely for the ratio of the maximum yaw rate $\dot{\Psi}_{max}$ achieved to the reference yaw rate $\dot{\Psi}_{Ref,t_{max}}$ at that very instance (t_{max}) since this does not occur within the first second of the maneuver in most cases. The standard takes this into account. In the following, a series of corresponding characteristic values for the maneuvers with the reference ABS and the optimized system for a road surface condition of μ = 0.5 are presented and briefly explained since the consideration under these conditions is particularly interesting for the reasons mentioned above.

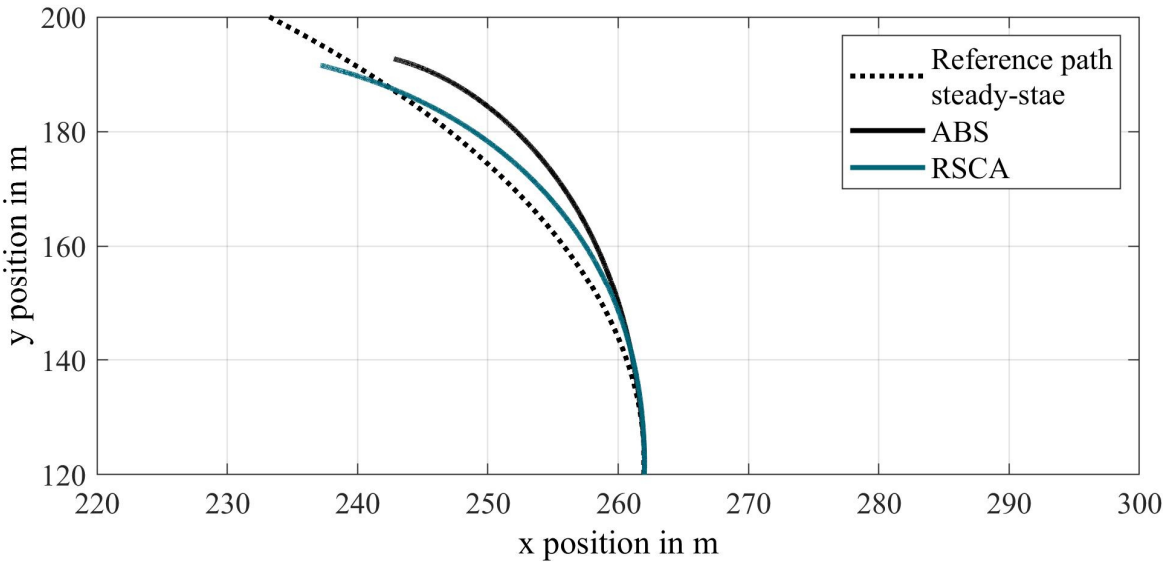

Figure 5.7: Path comparison for full braking in a curve under wet road surface conditions

The goal of stabilizing assistance systems must be to realize the driver's instructions or those of an automated driving system as well as possible. In the case of (full) braking in a curve, this means minimizing the braking distance and, if possible, the lateral deviation from the reference curve. Figure 5.7 shows the comparison of the path during full braking. It is immediately apparent that the RSCA optimized system follows the reference curve better, and both the absolute and the mean deviation are smaller over the entire braking process. Under these conditions, however, this is at the cost of a slightly increased absolute braking distance of $s_{\mathrm{B,opt}} = 78.41$ m compared to $s_{\mathrm{B}} = 76.76$ m since a slightly increased lateral acceleration is preferred over the longitudinal acceleration to achieve this effect. Evaluating the characteristic parameters, which focus on the lateral dynamic properties, also reflects this observation.

Figure 5.8 shows the comparison of the first characteristic value in the standard, which is the ratio of the yaw rate $\dot{\Psi}_{\mathrm{t_n}}$ to the value of the reference yaw rate $\dot{\Psi}_{\mathrm{Ref,t_n}}$ as a function of the mean longitudinal acceleration $\bar{a}_{\mathrm{x,t_n}}$. Values close to one indicate better tracking behavior and thus relatively better overall lateral dynamic behavior. The RSCA optimized system reaches a slightly higher mean longitudinal acceleration in the first second of the maneuver for higher brake pedal positions. In contrast, both systems perform almost identical for small brake pedal positions and small deceleration values concerning this characteristic value.

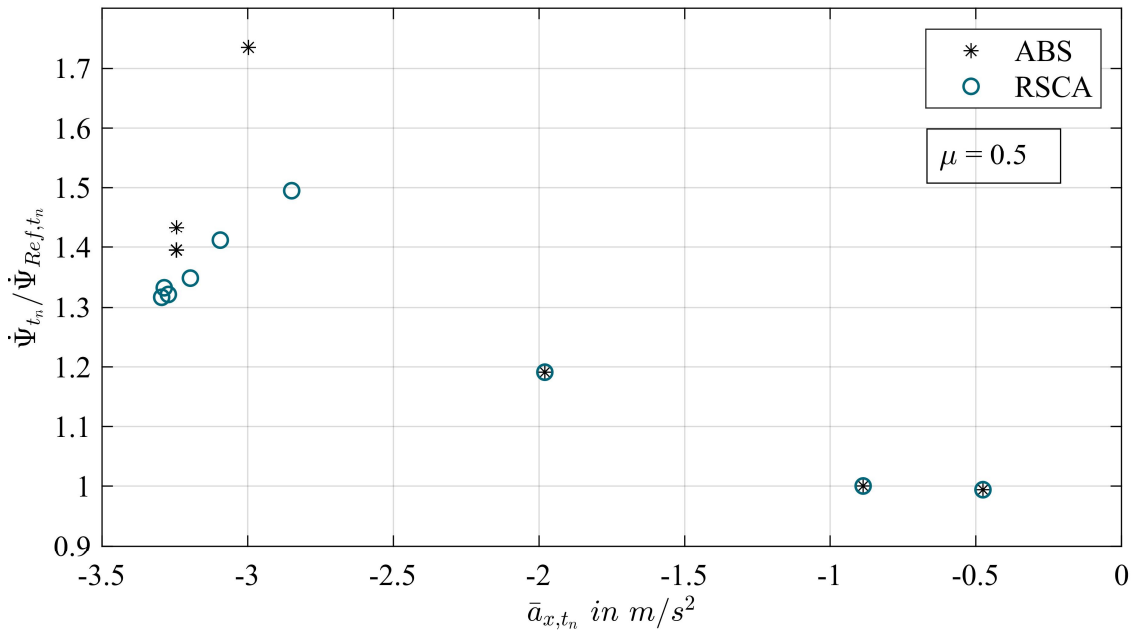

Figure 5.8: Ratio of the yaw rate $\dot{\Psi}_{\mathrm{t_n}}$ to the value of the reference yaw rate $\dot{\Psi}_{\mathrm{Ref,t_n}}$ as a function of the mean longitudinal acceleration $\bar{a}_{\mathrm{x,t_n}}$

The comparison of the second characteristic value of both systems in Figure 5.9, which depicts the ratio of the maximum yaw rate attained during braking $\dot{\Psi}_{\mathrm{max}}$ to the reference value $\dot{\Psi}_{\mathrm{Ref,t_{max}}}$ as a function of the overall mean acceleration $\bar{a}_{\mathrm{x}}$, shows a similar result. The RSCA optimized system can complete the maneuver with lower maximal yaw rates at higher decelerations.

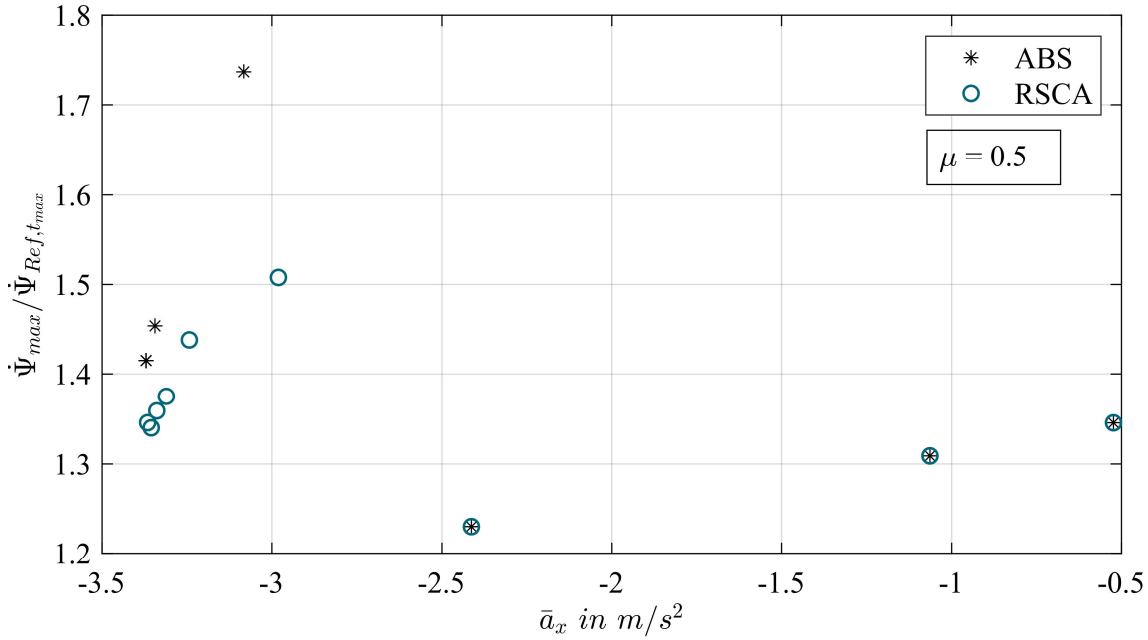

Figure 5.9: Ratio of the maximum yaw rate attained during braking $\dot{\Psi}_{max}$ to the reference value $\dot{\Psi}_{Ref,t_{max}}$ as a function of the overall mean acceleration $\bar{a}_x$

Figure 5.10 depicts the closely related characteristic ratio of the lateral acceleration a_{y,t_n} to the steady-state reference lateral acceleration a_{y,Ref,t_n} as a function of the mean longitudinal acceleration $\bar{a}_{x,t_n}$.

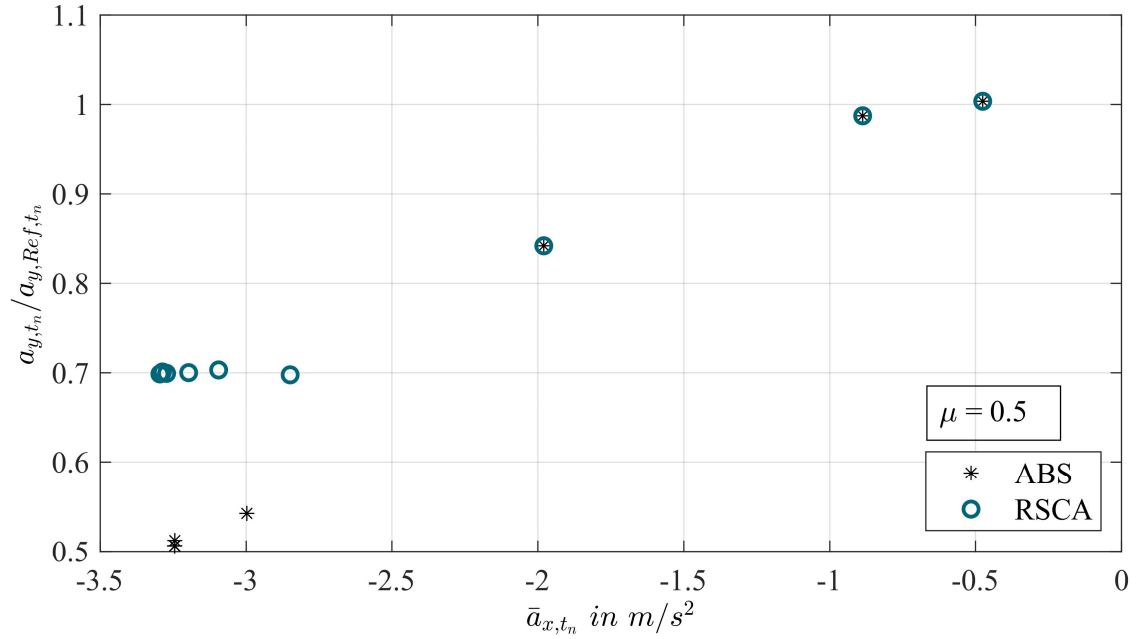

Figure 5.10: Ratio of the lateral acceleration a_{y,t_n} to the steady-state reference lateral acceleration a_{y,Ref,t_n} as a function of the mean longitudinal acceleration $\bar{a}_{x,t_n}$

For higher decelerations, the RSCA optimized system maintains an almost constant ratio of about 0.7, while the ratio further deteriorates to about 0.5 for the reference system. This behavior follows the observation in Figure 5.7, where this leads to a better path tracking behavior of the vehicle equipped with the RSCA optimized system in terms of global positioning.

The following two characteristic values the standard calls for deal with the vehicle's sideslip angle during the maneuver. Figure 5.11 shows the maximum value of the sideslip angle $\beta_{\max}$ during the entire braking maneuver as a function of the mean longitudinal acceleration. Since the entire tire potential is already utilized under these road surface conditions in the steady-state case before brake initiation, the sideslip angle for higher brake pedal positions is rather large as the vehicle tends to start losing grip.

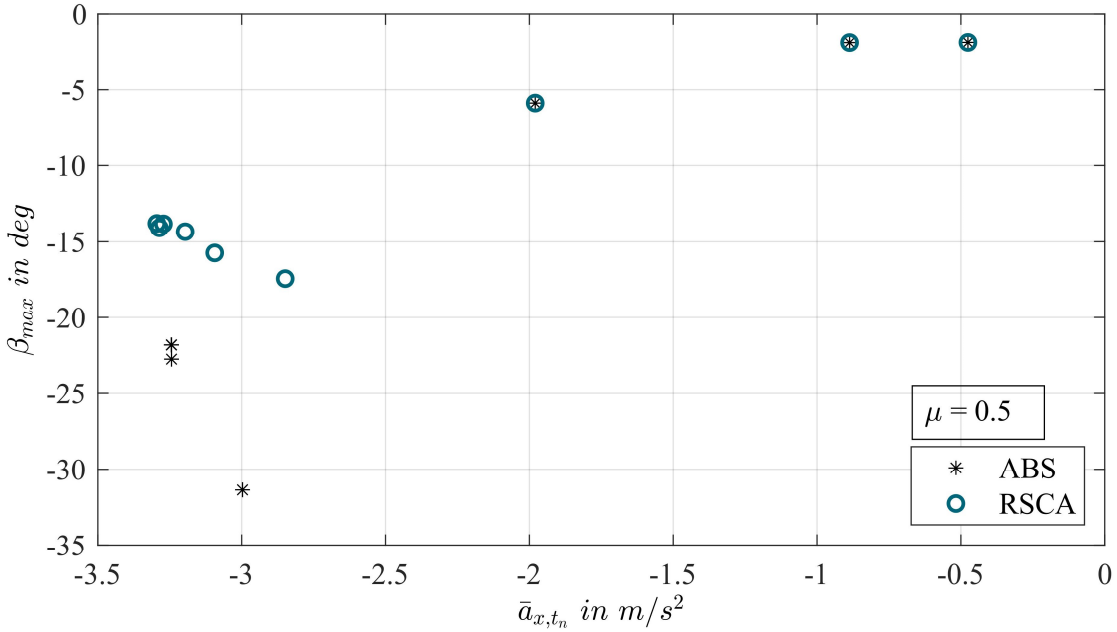

Figure 5.11: Maximum sideslip angle $\beta_{\max}$ during the braking maneuver as a function of the mean longitudinal acceleration $\bar{a}_{\mathrm{x,t_n}}$

Meanwhile, the systems intervene to establish a new longitudinal to lateral force balance to meet the braking requirements, where the RSCA optimized system works more efficiently as the maximum value is considerably smaller at higher deceleration rates. The same applies to the difference between the sideslip value $\beta_{\mathrm{t_n}}$ and the steady-state value β_0, shown as a function of the mean longitudinal acceleration $\bar{a}_{\mathrm{x,t_n}}$ in Figure 5.12. For all the values shown, it is always necessary to find a compromise between lateral and longitudinal movement in the limit range of the theoretically possible force transmission between tire and road, depending on the requirements of the driving situation. However, it is also evident that a system optimized for knowledge of the prevailing road condition can achieve better values, in this case, more stable lateral dynamics, for the combined load case than a corresponding reference system based on the classic approach. Following the definition, this is equal to a positive safety impact at the stabilization level due to the knowledge of the prevailing weather-related road surface condition.

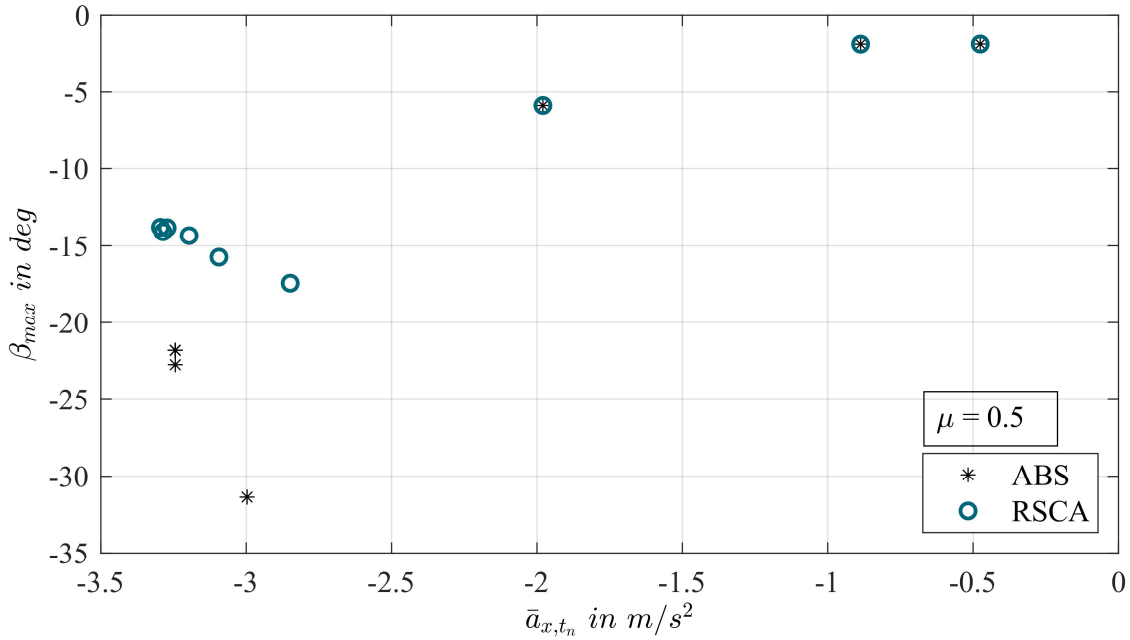

Figure 5.12: Difference between the sideslip angle value β_{t_n} and the steady-state sideslip angle value β_0 as a function of the mean longitudinal acceleration value $\bar{a}_{x,t_n}$

5.1.1.3 Summary Stabilization

The goal of stabilizing assistance systems must be to realize the driver's instructions or those of an automated driving system on the guidance level as well as possible. For an antilock braking system, this means minimizing the braking distance and, if possible, the lateral deviation from the reference curve of steady-state circular driving upon braking at the tire-road friction limit.

The results from the straight braking scenario study show that a weather-related road surface condition sensor can positively impact safety by reducing braking distance when used appropriately in an ABS. The simulations show that a braking distance reduction of up to 2 % can be achieved on damp road surfaces, up to 8 % on wet road surfaces, and even up to 11 % on icy road surfaces.

The simulations of braking in a turn reveal an increased lateral stability for the RSCA optimized system. This is reflected in the yaw rates as well as the maintained lateral accelerations. Even at high decelerations, the RSCA system still achieves approx. 70 % of the reference lateral acceleration from steady-state gyration, while the state-of-the-art ABS drops to a value of only 50 %. The maximum sideslip angle, another indicator of lateral stability, is also more than 40 % lower at high decelerations for the optimized system compared with the reference ABS. However, this increase in lateral stability is at the expense of longitudinal performance, which results in an approx. 1.65 m increase in absolute stopping distance.

5.1.2 Guidance

5.1.2.1 Road Surface Condition Aware Adaptive Cruise Control (RSACC)

The speed controller and the distance behavior are investigated in more detail to verify the desired behavior of the RSACC compared to the reference system. The scenarios are chosen so that both control modes can be tested and compared under various road surface conditions. For this purpose, a highway section is modeled with equal sections of different road surface conditions and corresponding friction coefficients. For the speed controller, the vehicle is simulated by itself without the influence of a preceding vehicle. The friction coefficient ranges within the sections are modeled according to the environment model in Section 4.1.

In the generic case, to test the effect of the implemented speed control algorithm, the desired speed is set to 120 kph, and the vehicle drives subsequently through the different sections from dry to icy road surface conditions, where the transitions occur after every 30 seconds of simulation time. The controller is expected to consider the new surface condition and adapt the speed accordingly. Figure 5.13 shows the behavior of the road surface condition adapted speed controller. The system overrides the desired speed input of the driver by applying the aforementioned linear scaling function.

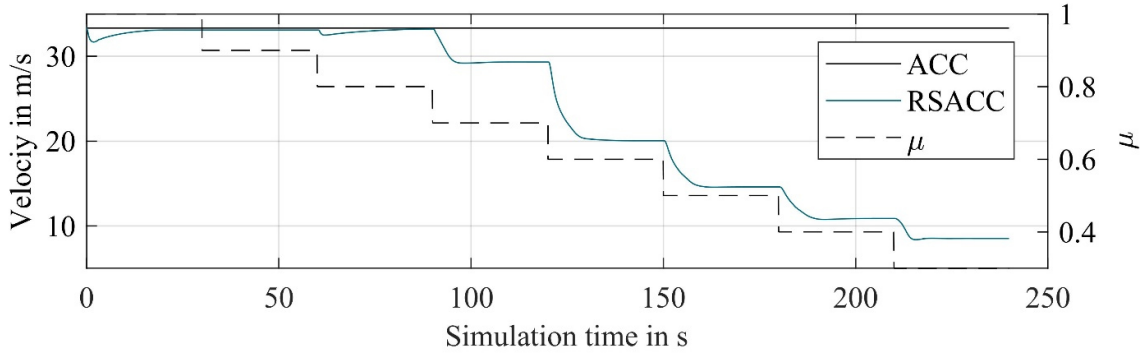

Figure 5.13: Adaptive Cruise Controller response comparison

Based on this implementation, it is possible to reach a complete stop within the range of the system's RADAR detection capabilities (here assumed to be 300 m) within the system's deceleration limits. One must point out that this leads to relatively small velocities under highly deteriorated road surface conditions and that this might pose a problem in the context of customer acceptance. However, the safety margin with this approach is relatively high, and it might be feasible to overcome this problem by applying different systems for different conditions, such as a different collision avoidance system that allows for higher decelerations than the ACC's system limits, which is limited by (ISO 22179:2009) to a maximum continuous deceleration value of 3.5 m/s^2. The dashed line of the set μ value decreases by 0.1 every 30 seconds. While the unaware ACC system maintains a constant velocity of 120 kph (33,33 m/s), the road surface condition variant (RSACC) only does so until a value of 0.7. Under these conditions, the system would not be able to come to a complete stop under the mentioned conditions of a front RADAR detection capability of 300 m

and its allowed maximum continuous deceleration rate, which results in a reduction of the driven velocity. This continues further as expected with further decreasing conditions.

A real-world highway driving profile from the portfolio of the Seeroad project (Weber and Schramm 2020a) is used as input for the virtual leading vehicle to verify the gap (front spacing) controller behavior, and the road surface condition is set to a corresponding friction coefficient of $\mu = 0.8$. As shown in Figure 5.14, the RSACC can follow the given input profile under these conditions. Even speeds up to 30 m/s are not yet relevant for the velocity control part of the system, as can also be seen in Figure 5.13 above.

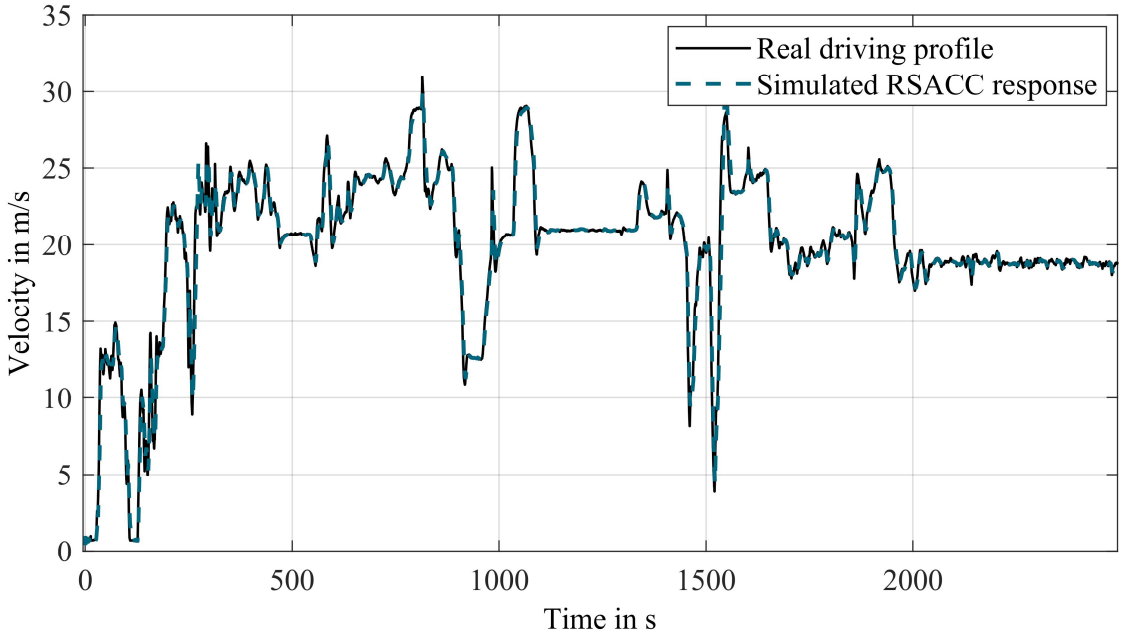

Figure 5.14: RSACC velocity control response for a real-world driving profile

However, the difference between the two investigated versions of the system becomes apparent when looking at Figure 5.15. While the reference ACC system maintains a constant front-spacing relation corresponding to a time headway of two seconds, the RSACC does this only for speeds that do not infringe the above-stated safety criteria. The RSACC increases the maintained distance to the lead vehicle for higher driven speeds to increase the safety margin and enlarge the reaction and execution time for relatively moderate intervention in difficult driving conditions. As greater distances translate to increased safety margins in space and time, the shown results imply a positive safety impact of a weather-related road surface condition sensor on the guidance level. How this system behavior plays out in a larger traffic scenario is closely related to the consideration in the following Section 5.2.4 dealing with the traffic level simulation with the mentioned variant of this system.

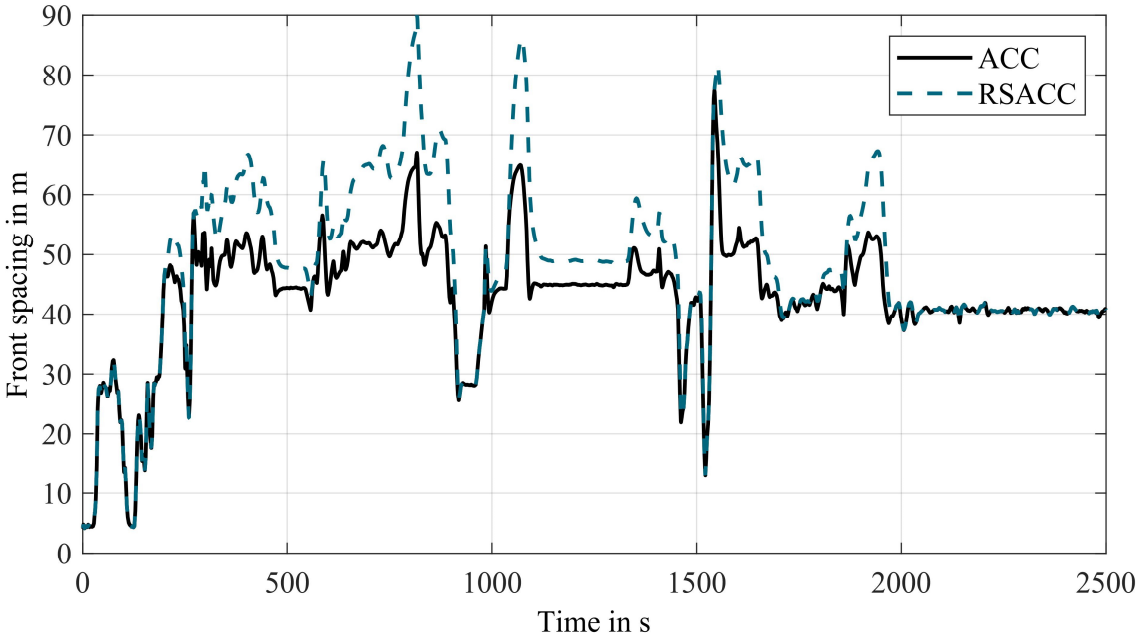

Figure 5.15 Gap control performance comparison between a standard unaware ACC and the road condition aware RSACC version

5.1.2.2 Emergency Steer and Brake Assist

As a second ADAS on the vehicle guidance level, an emergency steer and brake assist is considered. As an emergency system, it intervenes only in case of a pending collision, deciding to either initiate an evasive maneuver or an emergency braking based on the vehicles and objects state variables. As shown in the implementation (cf. Section 4.2.4.2), an optimized system can determine the last point to steer and the last point to brake more precisely and make better decisions for release by knowing the weather-related road surface condition through the WRSCS

Four use cases are simulated to compare and evaluate the performance of the ESB and the road surface condition awareness enhanced system. The differences in the systems are the calculation and selection of the execution maneuver and the corresponding time of intervention. In the following, the simulation results of the RSCA improved system are summarized in detail to show the remaining system limits. Subsequently, the performance of both systems is compared to show the existing potential with knowledge of the weather-related road condition.

Use case: Inner-city low velocity

The first use case chosen was an inner-city scenario. The equipped vehicle drives past a row of parked vehicles in a zone with a speed limit of 30 kph. From between the parked vehicles, a person steps out onto the road. The distance between the object person and the vehicle is d_x = 8.5 m. To avoid an accident with the person, the ESB must intervene and take over the vehicle guidance. The obstacle width in this scenario is w = 0.5 m. Figure 5.16 depicts such a traffic situation.

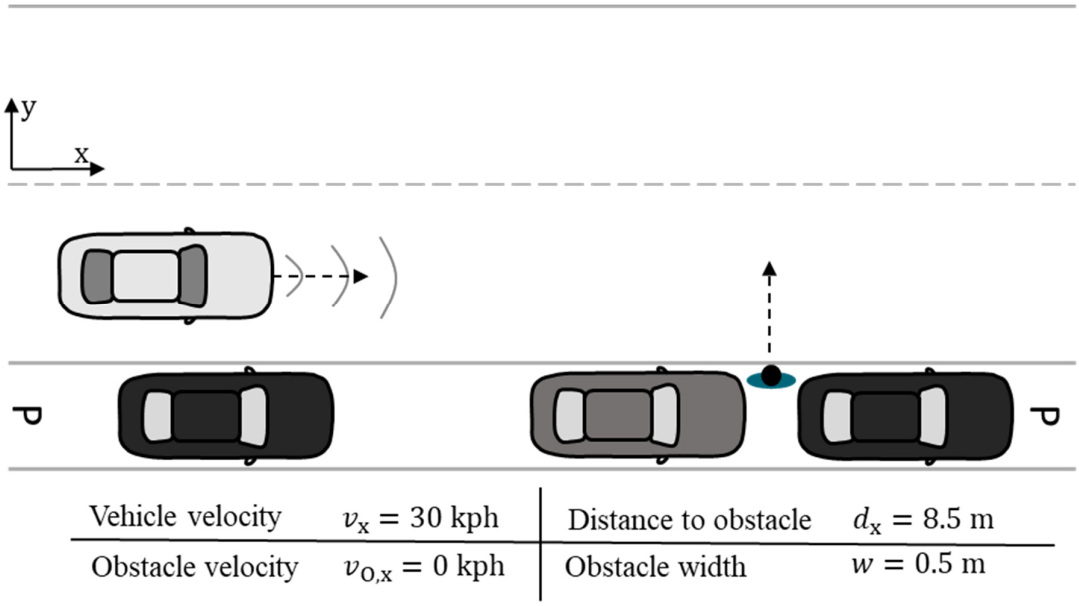

Figure 5.16: Use case: Inner-city scenario at 30 kph

In this use case, the ESB prevents the vehicle's collision with the obstacle for the first three simulation runs. In the first two simulations, the vehicle is in state area I when the ESB intervenes, and a collision could be prevented by both driving maneuvers, either steering (S) or braking (B). In the third simulation, the state changes from I to III, making collision-free braking impossible and leaving only an evasive vehicle maneuver. In the last simulation, the given distance of 8.5 m is insufficient to perform either of the two driving maneuvers without a collision. This is because the remaining time was insufficient under the given icy road surface conditions to build up sufficient longitudinal or lateral accelerations. Upon collision with the obstacle, the vehicle still has a remaining velocity of 7.41 m/s (26.68 kph). Table 5.5 gives a summary of the results of the use case, where d_M denotes the distance required to complete the selected maneuver in the simulation.

Table 5.5: Simulation result summary of use case inner-city low velocity

Road Surface Condition	Dry		Wet		Snow		Ice	
System	ESB	RSCA	ESB	RSCA	ESB	RSCA	ESB	RSCA
State	I	I	I	I	I	III	I	IV
Maneuver	B	B	B	B	B	S	B	B
Collision	No	No	No	No	Yes	No	Yes	Yes
d_M in m	6.0	6.0	8.4	6.57	(11.47)	5.33	(39.32)	(39.32)

However, the braking maneuver initiated reduces the severity of the collision. If the obstacle had been detected 3.25 m earlier by the vehicle's environment detection system, the collision could

still have been prevented by an evasive maneuver. In comparison, for a collision-free braking maneuver, over 30 additional meters are missing in case of icy road surface conditions.

Use case: Inner-city medium velocity

The second use case is an inner-city scenario with a speed limit of 50 kph. Figure 5.17 depicts the scenario where a cyclist rides on the roadside in front of the vehicle. The cyclist tumbles at a distance of d_x = 15 m and thus makes the intervention by the ESB necessary.

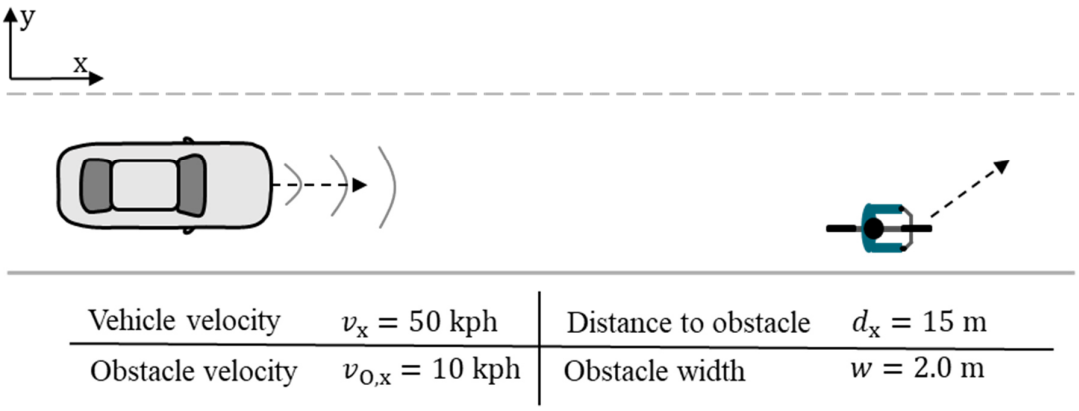

Figure 5.17: Use case: Inner-city scenario at 50 kph

The result summary of the second use case simulation in Table 5.6 shows that the ESB can only prevent a collision in two of the four investigated cases. For the cases of dry and wet road conditions, the vehicle is in state range III according to the calculations of ESB, which can prevent the collision by an evasive maneuver.

Table 5.6: Simulation result summary of use case inner-city medium velocity

Road Surface Condition	Dry		Wet		Snow		Ice	
System	ESB	RSCA	ESB	RSCA	ESB	RSCA	ESB	RSCA
State	I	III	I	III	I	IV	I	IV
Maneuver	B	S	B	S	B	B	B	B
Collision	No	No	Yes	No	Yes	Yes	Yes	Yes
d_M in m	11.7	10.7	(16.8)	11.7	(23.8)	(23.8)	(118.7)	(118.7)

In the two cases of the reduced friction coefficient by snow and ice, even the ESB can no longer solve the traffic situation without collision. The respective collision speeds are 36 kph and 46 kph. This again underlines the previously mentioned insight that under adverse road surface conditions,

an overall adapted driving style is crucial for the assurance of safety so that the emergency systems can still react adequately in case of doubt. This is particularly true in the transition to highly automated driving when drivers are increasingly relieved of their responsibility. Any system can only make such an adjustment if it always has appropriate information about the prevailing conditions.

Use case: Country road medium velocity

The third use case deals with a country road scenario at 70 kph initial speed. In this scenario, a slow-moving agricultural machine oversees the equipped vehicle and turns off a dirt road onto the main road. The agricultural machine has a speed of 20 kph. The relevant distance after the turn is d_x = 30 m. Because of the high relative speed of 50 kph, the ESB must intervene. The lateral offset w required for a safe evasive maneuver is set to be four meters in this case. Figure 5.18 summarizes the use case.

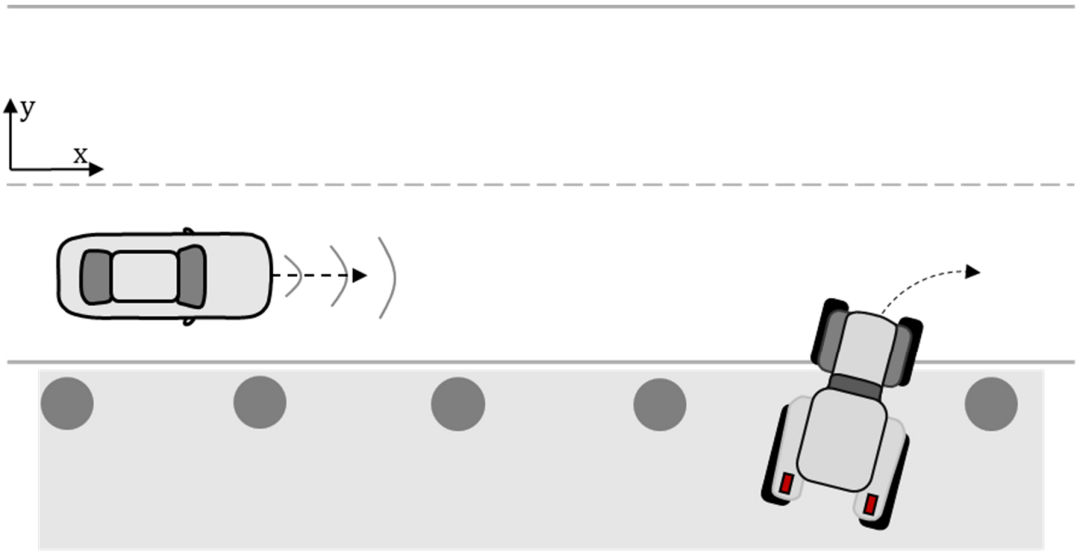

Vehicle velocity	$v_x = 70$ kph	Distance to obstacle	$d_x = 30$ m
Obstacle velocity	$v_{O,x} = 20$ kph	Obstacle width	$w = 4.0$ m

Figure 5.18: Use case: country road scenario at 70 kph

The ESB prevents collisions in three of the four examined conditions. The ESB uses the braking maneuver to achieve a risk-minimized driving condition for the vehicle for dry and wet roads. In the third simulation, the state range changes from I to III according to the calculated distances, and the steering maneuver is executed and successfully prevents a collision. Only for the icy road condition is the ESB unable to prevent a collision for the same reasons as above. Table 5.7 summarizes the simulation results again.

Table 5.7: Simulation result summary for use case country road medium velocity

Road Surface Condition	Dry		Wet		Snow		Ice	
System	ESB	RSCA	ESB	RSCA	ESB	RSCA	ESB	RSCA
State	I	I	I	I	I	III	I	IV
Maneuver	B	B	B	B	B	S	B	B
Collision	No	No	No	No	Yes	No	Yes	Yes
d_{M} in m	29.9	26.9	31.4	31.4	41.4	31.5	(225)	(225)

Use case: Highway high velocity

The last use case deals with a highway scenario where the equipped vehicle approaches the end of a traffic jam at 130 kph. The relevant distance for the system, in this case, is d_{x} = 100 m. For a successful avoidance maneuver, both lanes must be crossed up to the shoulder, resulting in an obstacle width of w = 7 m.

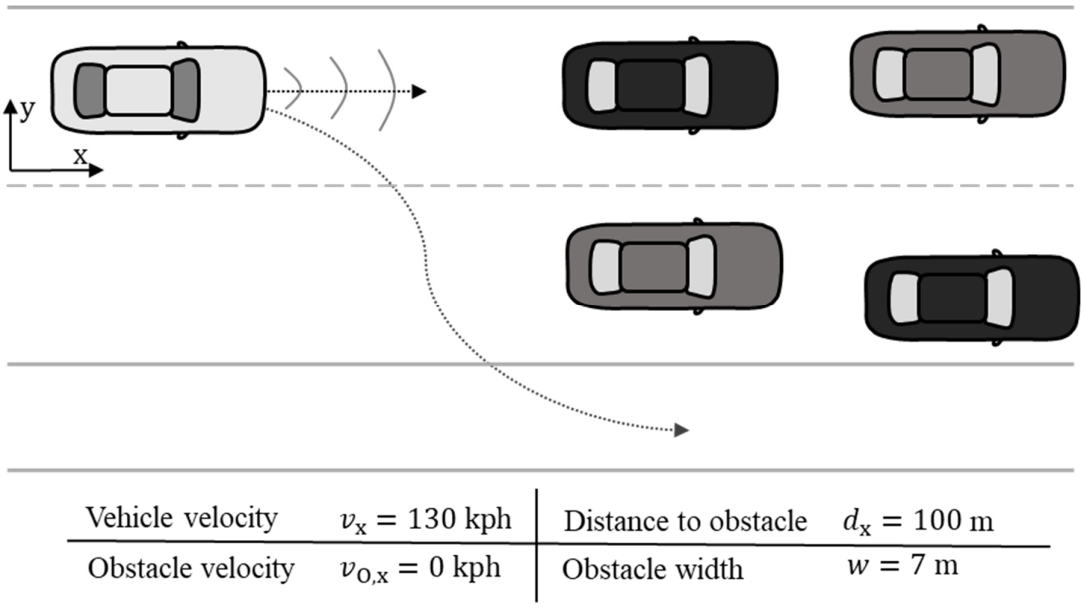

Figure 5.19: Use case 4 – highway scenario at 130 kph

In the simulation under dry road conditions, the ESB successfully performs a braking maneuver because the vehicle is in state area I. The situation can be resolved by a steering maneuver starting from state area III in the second and third simulation with wet or snow-covered road surfaces. Under icy conditions, the initial speed cannot be maintained in the fourth simulation since the tire forces that can be transmitted are lower than the driving resistances to be overcome. This leads to the fact that when the braking maneuver is triggered, the output speed is only 120 kph, but the

remaining distance to the end of the traffic jam is insufficient to bring the vehicle to a complete standstill.

Table 5.8: Simulation result summary for the highway use case

Road Surface Condition	Dry		Wet		Snow		Ice	
System	ESB	RSCA	ESB	RSCA	ESB	RSCA	ESB	RSCA
State	I	I	I	III	I	III	I	IV
Maneuver	B	B	B	S	B	S	B	B
Collision	No	No	Yes	No	Yes	No	Yes	Yes
d_{M} in m	86.5	86.5	109.9	69.7	(167.2)	88.28	(643)	(643)

5.1.2.3 Summary Guidance

The weather-related road surface condition aware system versions for the ADAS on the guidance level show considerable safety potential. The RSACC increases the maintained distance to the lead vehicle for higher driven speeds to increase the safety margin and enlarge the reaction and execution time for relatively moderate intervention in difficult driving conditions. As greater distances translate to increased safety margins in space and time, the shown results imply a positive safety impact of a weather-related road surface condition sensor on the guidance level.

Figure 5.20 compares the performance of ESB without road surface awareness with the system with awareness for the four simulated use cases.

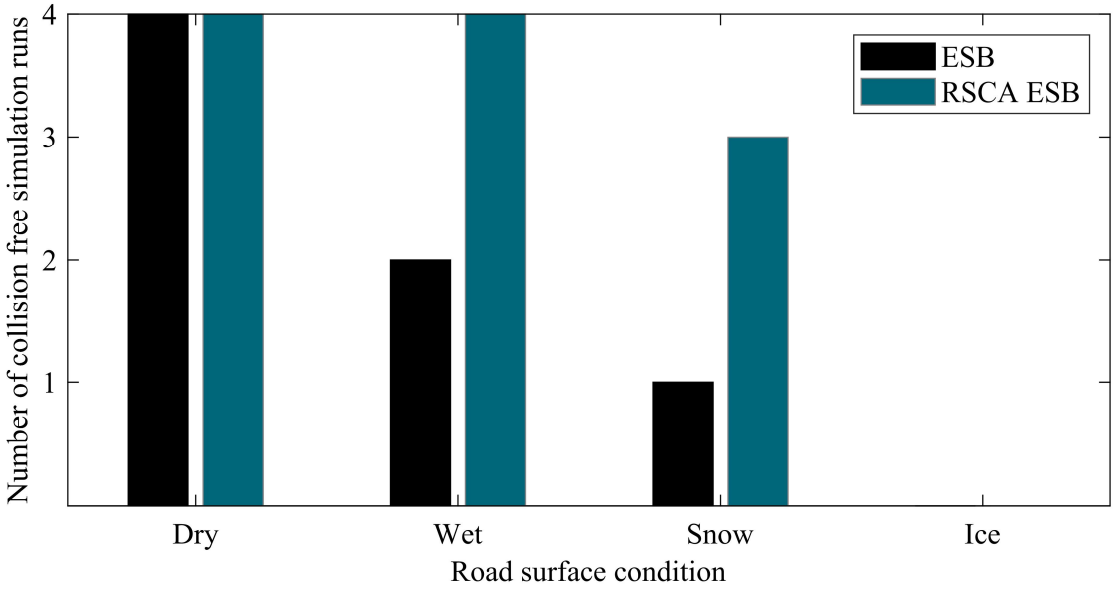

Figure 5.20: System performance comparison for the given use cases

While the former of the 16 runs only successfully intervenes in 7 cases under the given conditions, the latter prevents a collision in 11 situations by correct intervention. The figure also shows that the number of accidents increases when the road condition deteriorates. The vehicle must have a higher-level control system with a comprehensive, weather-related understanding of the situation to prevent these weather-related accidents in highly automated operations. It must adapt the driving condition (e.g., speed or distance) to the given road condition even before a critical traffic situation occurs. This adjustment must be within the system boundaries where the ESB system can work collision-free. Overall a positive safety impact at the guidance level results from enhancing an ESB through a weather-related road surface condition sensor, leading to an increase in collision-free scenario resolutions by 25 %.

5.2 Traffic Level

The simulation study for the WRSCS potential analysis on the traffic level starts with describing and evaluating the reference traffic scenarios. The goal is to create several calibrated, more extensive networks to investigate the effect of different penetration rates of vehicles with WRSCS optimized systems onboard and the potential benefit of sharing data in a connected V2X environment. The reference scenarios are used to evaluate the implemented sensor (cf. Section 4.3.2) and driver model (cf. Section 4.3.3) adaptations of the framework. After the evaluation, the entire framework is applied to investigate the guidance and navigational level in the scenarios regarding the WRSCS' potential regarding safety, efficiency, and comfort.

5.2.1 Reference Scenarios

All essential functions for the variation of influencing variables and the acquisition of relevant variables for the traffic level have been implemented in Chapter 4. This Section describes the preparation of the simulation scenarios to be investigated. Aspects that are particularly relevant in preparing these scenarios include: preparing the road network, modeling the weather conditions, and calibrating the traffic volume. The challenges of creating reference scenarios are mainly based on the trade-off between the complexity of the scenarios and sufficient simulation accuracy concerning the investigated research questions. The investigations of the traffic level in this thesis are primarily based on two simulation scenarios and the combination of the different influencing parameters. In the first scenario, the complexity of the road network is deliberately kept low, and simulation results are analyzed for discernible trends and tendencies. A second and third more elaborate scenario aim at increasing comparability to more complex actual traffic events.

5.2.1.1 Highway Scenario

For verifying the effectiveness of all parts of the implementation on this level, a reference Scenario consisting of a highway section is created and calibrated with traffic data collected from induction

loops provided by the German Federal Highway Research Institute (BAST 2021). A highway interchange in the vicinity of the city Suhl is used because several induction loops and their data are available in a relatively small area, simplifying calibration. Figure 5.21 depicts the chosen section in the form of the (OpenStreetMap 2020) source and the result after its import into NETEDIT and the corresponding placement of induction loops based on the position of their counterparts in the real world. Each lane at each location is equipped with a loop, resulting in 16 measurement points in total.

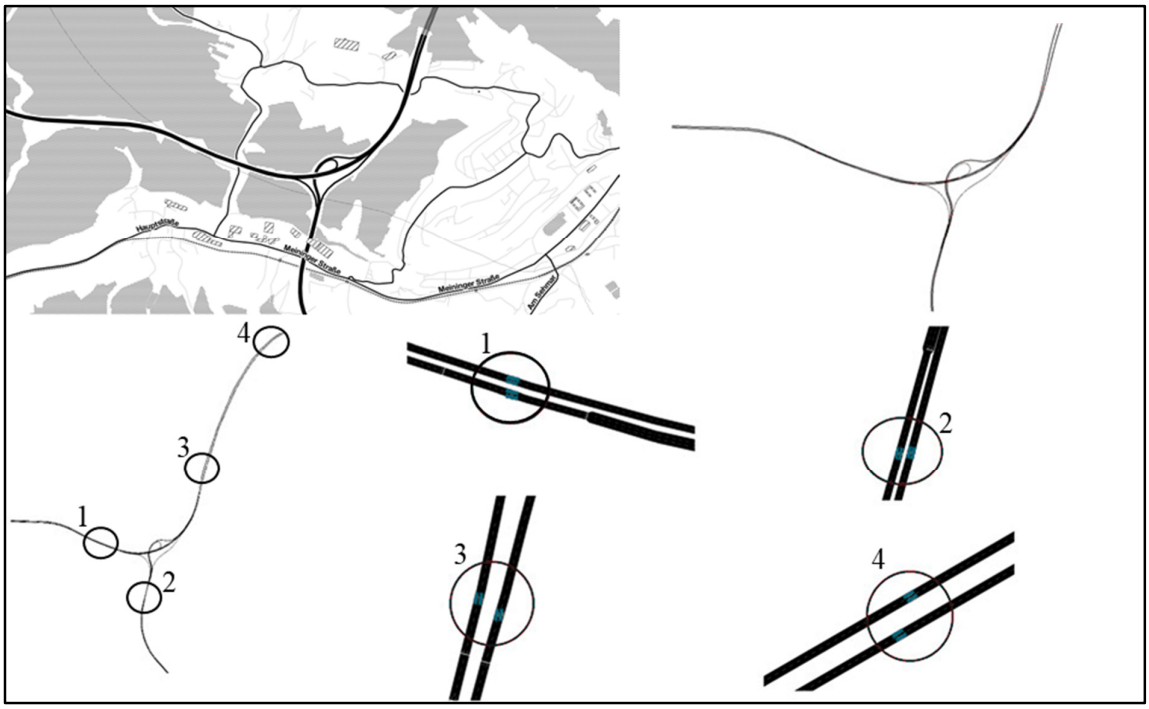

Figure 5.21: Suhl highway interchange network and induction loop placement

The traffic data are available hourly in an aggregated form and describe the macroscopic value of traffic flow Q (Eq. 5.1), which is generally defined as the number of vehicles ΔN that have passed through the cross-section at point x in time interval Δt:

$$Q(t,x) = \frac{\Delta N}{\Delta t}. \tag{5.1}$$

(Treiber and Kesting 2013) state that the flow is usually expressed in terms of vehicles per minute or vehicles per hour. The calibration of a reference traffic scenario, in this case, is a constrained optimization problem. With a highway network with detectors at all entrances and exits, it can first be assumed that all entering vehicles are equal to the sum of the leaving vehicles. At measurement points where vehicles enter the network, there is only one possibility of how the measurement data is composed because, at these points, all counted vehicles come from the same direction. Counting at network exits becomes more difficult. Here, the number of vehicles consists of all potential routes leading from the entrances to this exit. With this premise, it is possible

to represent the present optimization problem as a linear equation system with additional requirements to the constraint parameters. In matrix notation, a linear system of equations can first be divided into a coefficient matrix $\boldsymbol{A}$, the parameter vector $\boldsymbol{x}$, and a result vector $\boldsymbol{b}$:

$$\boldsymbol{A}_{n,k} * \boldsymbol{x}_{k,1} = \boldsymbol{b}_{k,1}, \tag{5.2}$$

$$x_1 * \boldsymbol{a_1} + x_2 * \boldsymbol{a_2} + \cdots + x_{\mathrm{k}} * \boldsymbol{a_{\mathrm{k}}} = \boldsymbol{b}. \tag{5.3}$$

The system of equations is solvable if the result vector $\boldsymbol{b}$ can be represented as a linear combination of the column vectors $\boldsymbol{a}$. In other words, the system of equations can only be solved if the result vector lies in the column space of the coefficient matrix. In natural systems, however, it is often the case that measurements are subject to perturbations. Due to inexact data in the coefficient matrix or the result vector, it can quickly happen that the result vector no longer lies in the column space of the coefficient matrix, and thus no unique solution for the equation system exists. The least-squares method (Abdulle and Wanner 2002) assumes that there must be one or more linear combinations within the column space that come closest to the result vector. This approach thus minimizes the distance from the result vector to the column space:

$$\min_{\boldsymbol{x} \in \mathbb{R}^n} \|\boldsymbol{b} - \boldsymbol{A}\boldsymbol{x}\| = (b_1 - x_1\boldsymbol{a_1})^2 + (b_2 - x_2\boldsymbol{a_2})^2 \ldots + (b_n - x_n\boldsymbol{a_n})^2. \tag{5.4}$$

All vectors that are perpendicular to column space belong to the zero space of the transposed coefficient matrix, so for the unique solution, $\boldsymbol{x}^*$ must hold:

$$\boldsymbol{A^T}(\boldsymbol{A}\boldsymbol{x}^* - \boldsymbol{b}) = \boldsymbol{0}, \tag{5.5}$$

$$\boldsymbol{A^T}\boldsymbol{A}\boldsymbol{x}^* = \boldsymbol{A^T}\boldsymbol{b}. \tag{5.6}$$

The special solution $\boldsymbol{x}^*$ yields the solution according to the least square's method since the distance squares are minimized according to equation (5.4). According to (5.5), the system of equations can now be solved with a suitable method for linear systems of equations. In this case, the Sequential Least-Squares Programming (SLSQP) algorithm (Kraft 1988) is applied. Although the available data allows for a more detailed subdivision in vehicle types, only two classes are used for simplicity. Those two classes are a passenger car vehicle type and a heavy truck type. Their attributes, such as length, acceleration and deceleration capabilities, and maximum speeds, define their differences. Figure 5.22 shows the summarized result for the scenario based on a random excerpt from the real-world induction loop data records from Monday, 25.01.2016, aggregated for each hour over the twelve hours from 7 a.m to 7 p.m. The optimization targets the nodes, i.e., the correct number at each hour and the best overall result concerning the total numbers. It can be asserted from the simulation results that this approach produces an accurate scenario of a highway section of a random weekday.

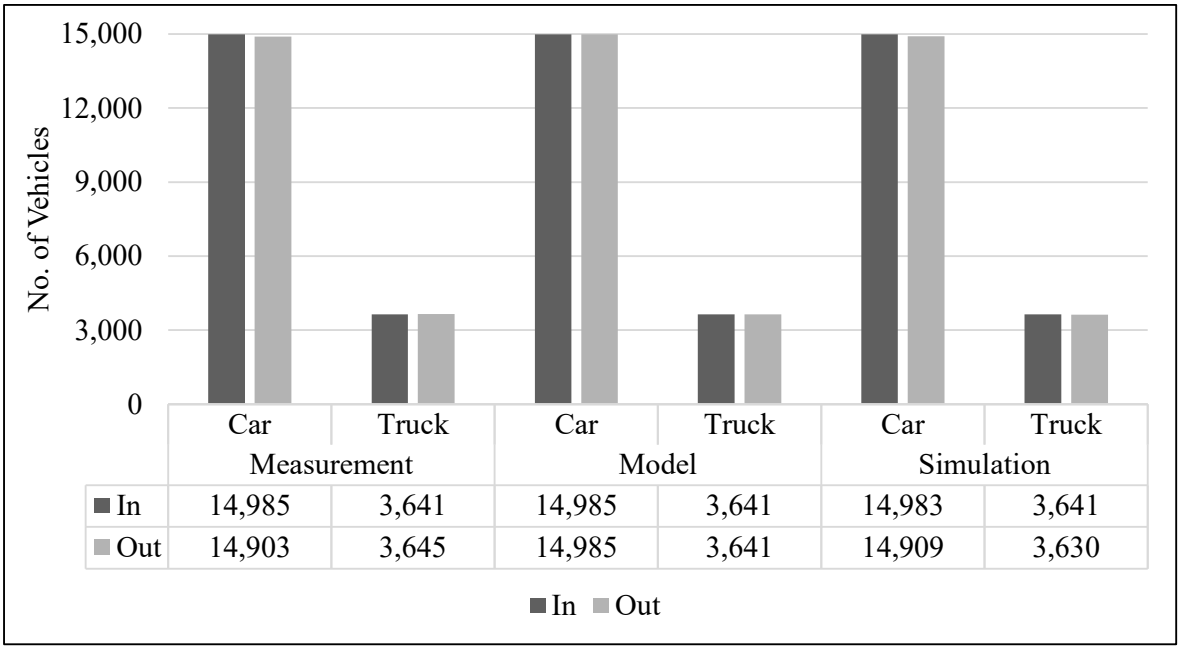

Figure 5.22: Traffic volume of the highway scenario

5.2.1.2 Generic City Scenario

The generic city scenario is created based on several street blocks in a major Canadian city. The composite corresponds approximately to a rectangle with edge lengths of 1.8 km by 1.6 km. Idealized, cross streets are assumed to be 120 m apart in the horizontal direction, while a crossing street is drawn every 160 m in the vertical direction. The roads within the network can each have a single lane in either direction. In this way, the SUMO network shown in Figure 5.23 is created, which is created manually in the network editor NETEDIT.

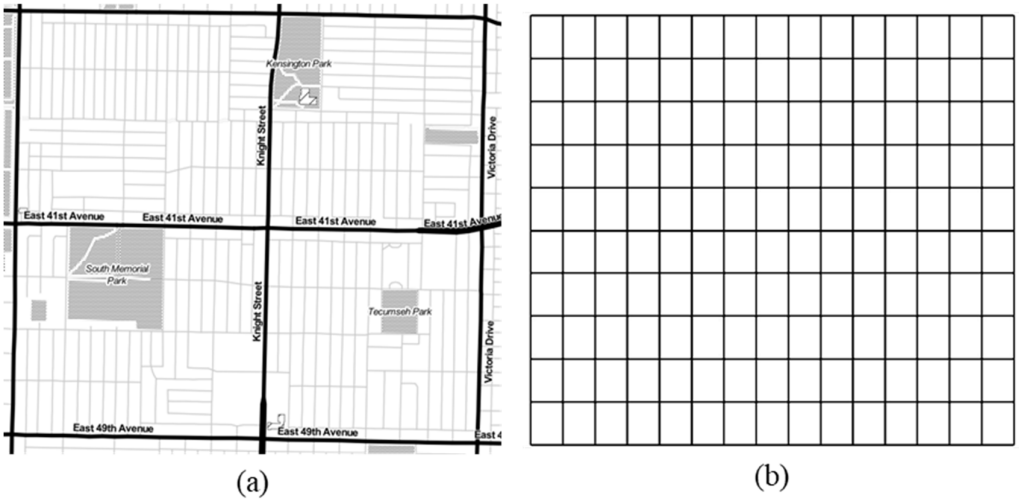

Figure 5.23: (a) OSM by (Stamen Design 2016); (b) Idealized SUMO road network

To prepare the measurement series, the traffic volume in this scenario is then modeled. A series of measurements is defined as a sequence of simulation runs based on the same simulation scenario

and the same number of simulated vehicles despite varying influencing variables. In the first test series, the number of vehicles is 100, so that only a small interaction between the vehicles in traffic is to be expected. In the subsequent series of measurements, the number of vehicles increases up to 1,000. For reference generation, the initial vehicle routes are randomly generated once and adjusted by the respective systems in the further course only at runtime.

5.2.1.3 Real City Scenario

The real city scenario depicts the small town of Hüls, which was incorporated as a district of the independent city of Krefeld under the "Act on the Reorganization of the Municipalities and Districts of the Reorganization Area of Mönchengladbach/Düsseldorf/Wuppertal" of September 10, 1974. As of 2018, Hüls has a population of approximately 16,400 (Krefeld 2021). Due to the excellent connection to the next larger city of Krefeld, there are many commuters in addition to the traffic within the city. For this scenario, map data is extracted from the (OpenStreetMap 2020) format and converted into a road network file format suitable for simulation using the NETCONVERT routine included in SUMO (cf. Figure 5.24). The scenario covers a traffic area of ca. 15 km^2 with a north-south extension of approximately 5 km and a west-east extension of about 3 km.

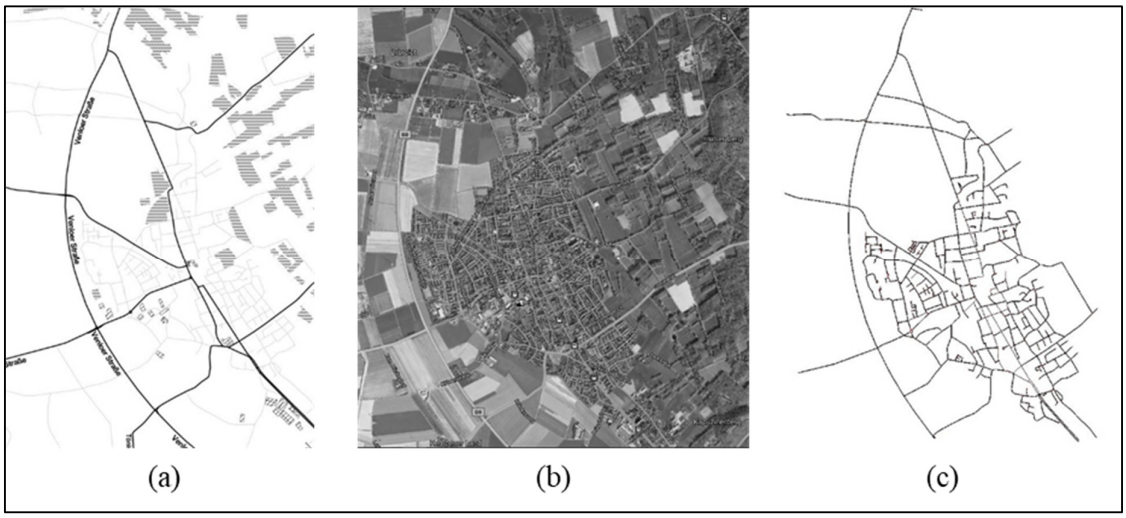

Figure 5.24: (a) OSM by (Stamen Design 2016); (b) Geobasis NRW (Mirgel and Wruck 2021); (c) SUMO

When examining the converted map data, it is still noticeable that some elements such as traffic lights are not included in the map data. However, since traffic light systems play an essential role in stabilizing traffic volumes, the converted road network is manually supplemented with the traffic light systems available by default in SUMO. Even though inaccuracies occur at this point due to the traffic light system deviating from reality, a better approximation of the natural traffic conditions is achieved. The traffic volume itself is modeled for 24 hours. The activity generator included in the SUMO distribution is used for this end. It calculates an estimated traffic volume based on statistical characteristics, such as the number of inhabitants and households, average

working hours, and demographic characteristics (DLR 2021). Experiences with creating simulation scenarios this way for the city of Duisburg have been published with the collaboration of the author in the meantime (Ma et al. 2021). Figure 5.25 shows the generated activity profile between 6 a.m. and 10 p.m. The characteristic peaks in the early hours and the afternoon are due to the thesis, schooling commuter rushes, and errand trips in the afternoon.

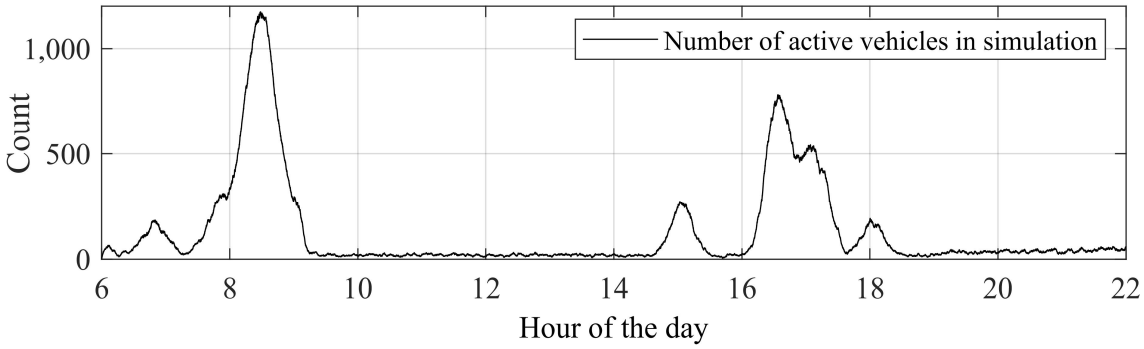

Figure 5.25: Activity profile of the city suburb Hüls

The corresponding distributions for the route lengths and trip durations in Figure 5.26 correspond well for a scenario with the given spatial extent. All the shown measurements refer to the standard models of the simulation environment and serve as references when comparing or changing the driver and vehicle model properties.

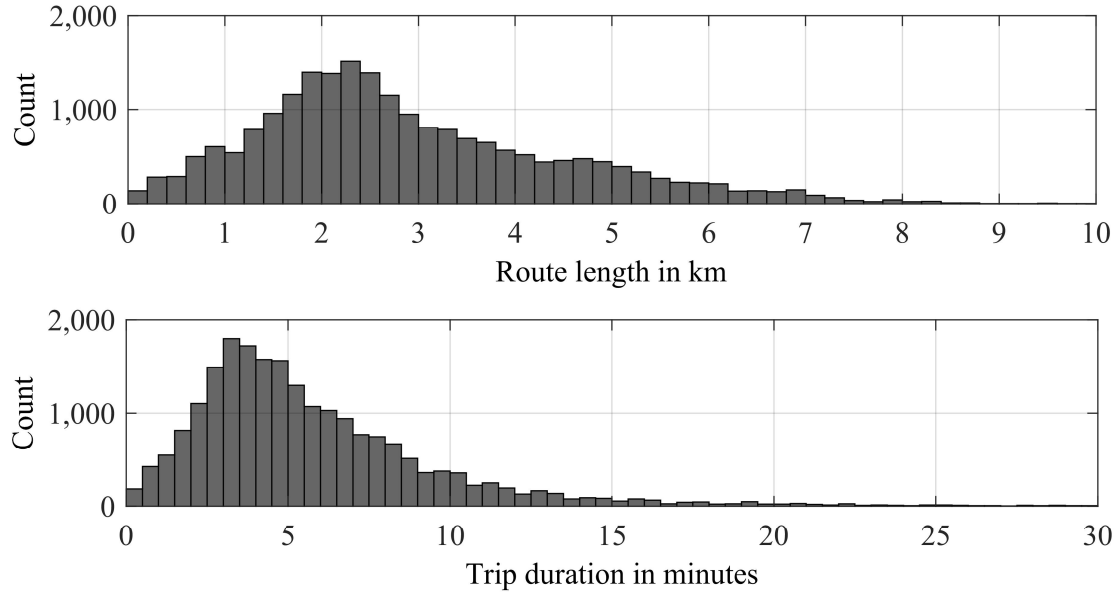

Figure 5.26: Route length and trip duration distributions for the Hüls scenario

5.2.2 Sensor Model Evaluation

Section 4.3.2 implements a virtual sensor model into the simulation as a statistical, mathematical model based on real-world measurement data. As no clear trend towards a specific continuous probability distribution is discernible in the data analysis and model generation for the data set used, particularly for the “wet” and “slippery” clusters, various models are tested and examined for their validity as part of the performed simulation runs. For the actual evaluation, several regions of the generic city scenario network are assigned with weather-related road surface conditions from the environmental model (cf. Section 4.1). Subsequently, vehicles equipped with different WRSCS model types are simulated in the network, recording their simulated measurement data. Finally, the simulated measurement data are compared with the real-world measurement data to evaluate the sensor model's quality.

Figure 5.27 compares the relative deviation of the raw measured values and the filtered measured values and the same characteristic value from measurements collected in the simulation.

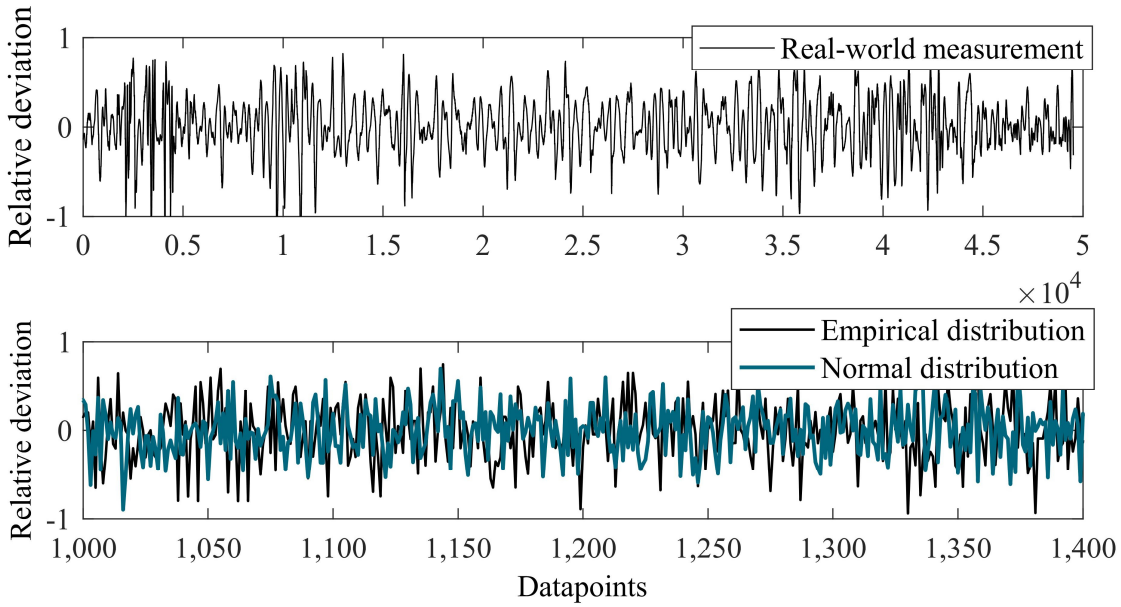

Figure 5.27: Value deviation for the cluster “damp”: real-world (top), simulation (bottom)

Since the actual measured values and the simulated measurement in SUMO differ significantly in the frequency range - the actual measurements are available with a sampling rate of 100 Hz, while the simulated values are recorded only with 1 Hz by default - the plot shown is scaled accordingly. Even if an improved similarity of the courses with the real-world measurement data values is already recognizable here compared to the original equally distributed model, Figure 5.28 shows a comparison of the probability density distributions for the assumed case of normal distribution together with their envelope.

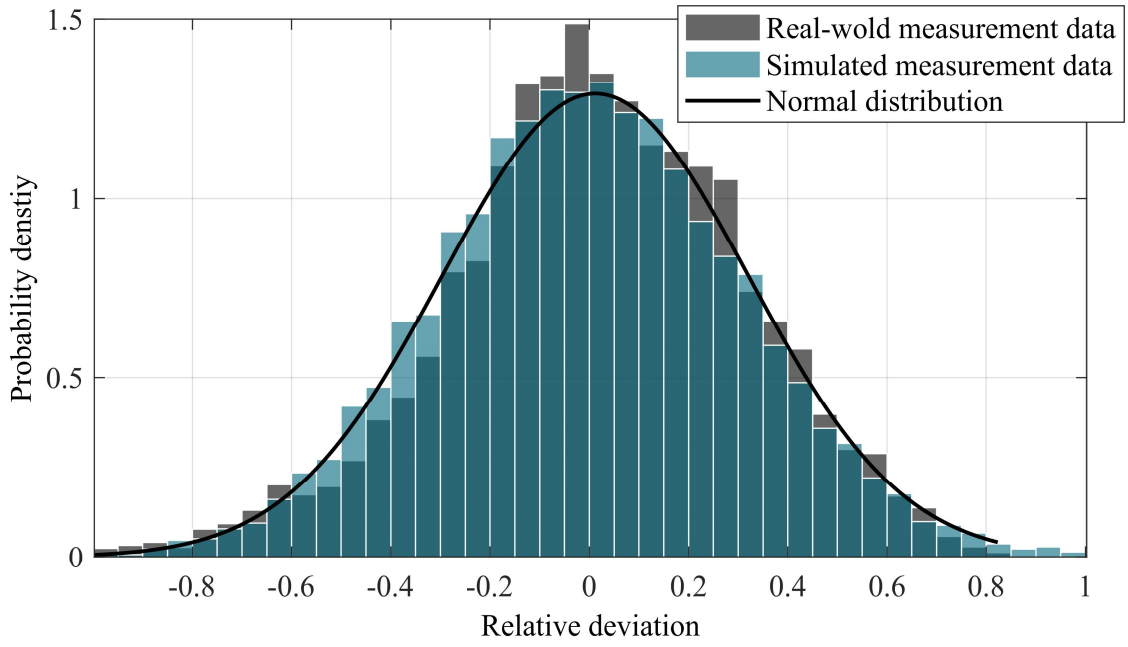

Figure 5.28: Relative deviations for the cluster “damp” for the normal distribution model

As expected, the simulated measured values followed the model specification very well. A possible downside is that this model overrepresents the negative relative deviations between 20 % to approximately 50 %. The consideration of the results in Figure 5.29 shows that this possible weakness can be avoided by implementing the empirical distribution without a fixed distribution function. The graphs show the relative errors of the probability density function of both simulated models related to the respective value of the histogram of the actual measured values. The empirical implementation performs better in comparing the relative errors in the respective 40 classes, with a selected class width of 0.05 in the range of [-1...1].

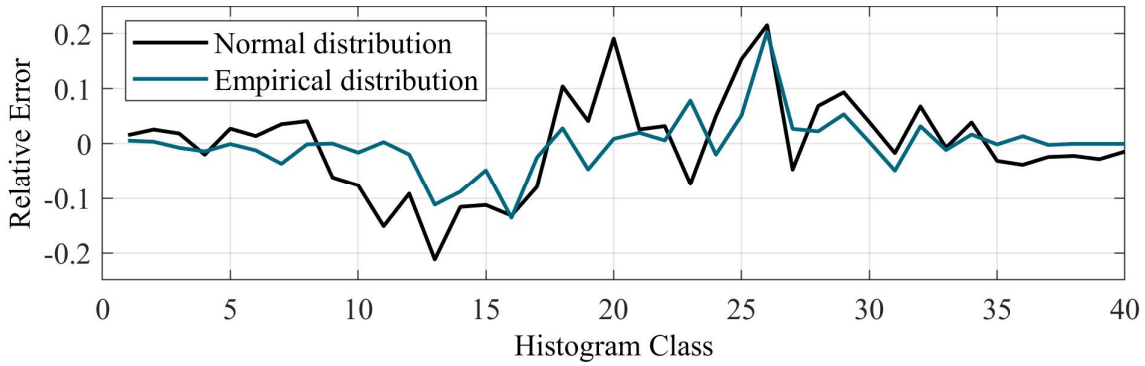

Figure 5.29: Relative errors of both simulated models for the actual measurement of road condition cluster “damp”

The root mean square error RMS(E) for the model of the normal distribution is $RMS_{\text{norm}} = 0.0863$, and for the empirical model, $RMS_{\text{emp}} = 0.0515$ and is thus preferred for this cluster. The analysis of the cluster “wet” shows this assessment even more clearly. The empirical

model also yields better results than the simulation with the normal distribution model when comparing the respective errors of the models in Figure 5.30.

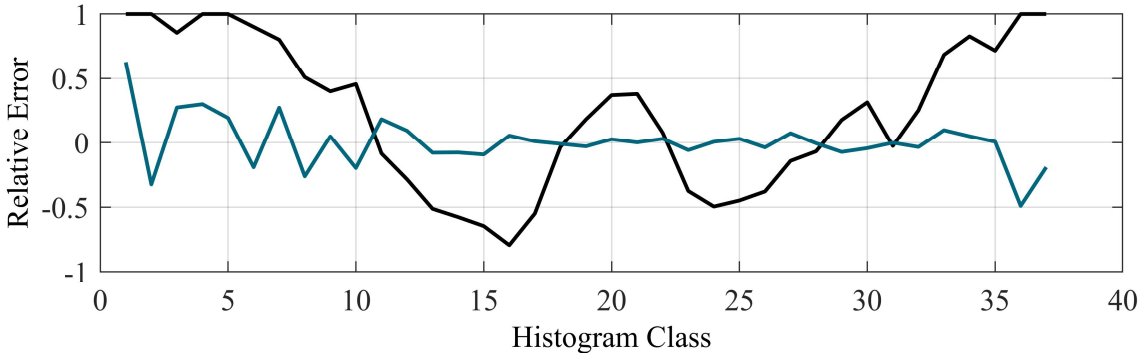

Figure 5.30: Relative errors of both simulated models for the real measurement of road condition cluster “wet”

Again, mathematically, this relationship can be expressed by the RMS of the errors. For the model of normal distribution $RMS_{\text{norm}} = 0.3213$, for the empirical model $RMS_{\text{emp}} = 0.0268$. These results supported the observation of the previous evaluation. Therefore, the empirical distributions are adopted for the sensor model in all road conditions in the simulation environment.

5.2.3 Driver Model Evaluation

The driver model adaptation of Section 4.3.3 to consider a human drivers’ behavior to adapt his speed to the prevailing weather-related road surface conditions is evaluated next within more complex traffic scenarios to ensure the intended behavior when interacting with several vehicles.

The real highway reference scenario from Section 5.2.1.1 is simulated nine times with changing road conditions for each of the two models to evaluate the effectiveness of the modified driver behavior. These included a very wet road surface with a friction value from the lower range of the wetness spectrum and snow-slick road surfaces with friction values from the upper or lower snow spectrum. Since the reference scenario spans twelve hours, this is also chosen in the simulation.

The average speed for each hour in the scenario is then used as the measurement data point to compare this to the expected value of the implemented model. Figure 5.31 shows some of the results for a random selection of the 16 detectors, where the black data points represent the observed average velocities per hour for each of the simulation runs, and the dashed line represents the calculated value according to the linear adaptation model.

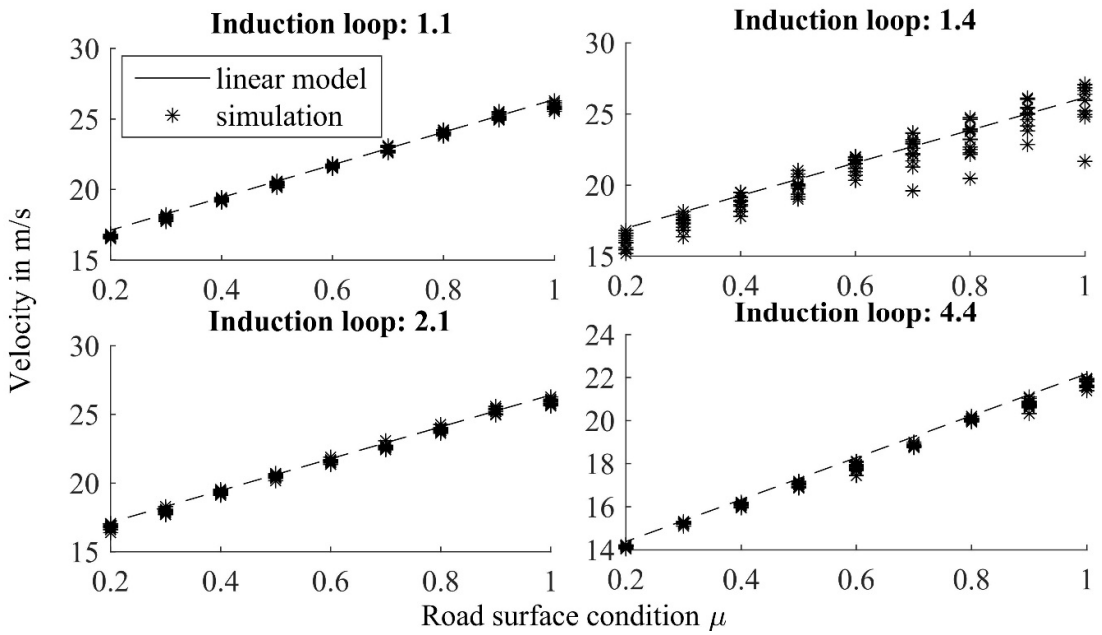

Figure 5.31: Influence of the linear adaptation model for driver behavior in the simulation

Table 5.9 also shows the observed relative velocity decreases for all available induction loop counters. Listed are the respective values for the lower limit (ll.) of the wet friction value range and the upper and lower limits (ul. and ll.) of the snow friction value range. In summary, a speed reduction of 0 – 23.5 % could be determined for wet road surfaces and a speed reduction of 8.6 – 41.9 % for slippery road surfaces, while the observations reported in the literature range from 0 – 30 % in the former case and 10 – 40 % in the latter. It can be concluded that the speed reduction in the simulation based on the given road condition corresponds well to the intended gradient of the implemented model and the corresponding observations reported in the reference literature.

Table 5.9: Observed velocity reduction per counting loop for the linear approach

Road condition	**Induction loop**							
	1.1	1.2	1.3	1.4	2.1	2.2	2.3	2.4
Wet (ll.)	19.1%	19.8%	19.3%	23.5%	19.1%	22.6%	21.7%	19.4%
Snow (ul.)	13.9%	14.4%	14.5%	13.7%	14.5%	8.6%	13.7%	14.1%
Snow (ll.)	32.4%	30.5%	32.3%	35.2%	32.3%	35.7%	41.9%	31.6%
	3.1	3.2	3.3	3.4	4.1	4.2	4.3	4.4
Wet (ll.)	19.3%	19.5%	19.4%	20.1%	19.5%	19.0%	19.60%	19.8%
Snow (ul.)	13.9%	14.1%	14.0%	15.2%	14.2%	13.9%	14.1%	14.8%
Snow (ll.)	32.2%	32.0%	32.5%	31.6%	32.2%	32.2%	32.4%	31.7%

The observed reduction in average speeds in the quadratic model depicted in Figure 5.32 also follows the expectations well.

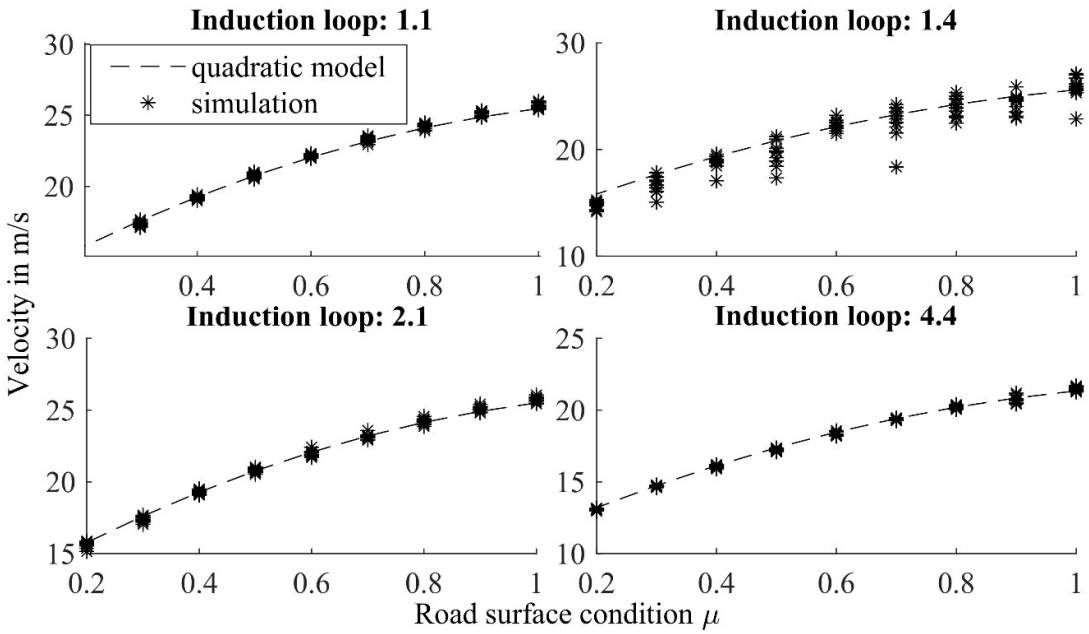

Figure 5.32: Influence of the quadratic model for driver behavior in the simulation

Table 5.10 shows a relative speed reduction of up to 23.6 % in the wet area and a 15.9 – 38.8 % reduction in the snow-equivalent area. It can be concluded that the simulated results of both implementations are well within the limits of the behavior obtained from the studies. Therefore, the quadratic model is selected for the following investigations.

Table 5.10: Observed velocity reduction per counting loop for the quadratic approach

Road condition	**Induction loop**							
	1.1	1.2	1.3	1.4	2.1	2.2	2.3	2.4
Wet (ll.)	21.3%	21.4%	21.1%	22.2%	20.9%	21.7%	23.6%	22.0%
Snow (ul.)	16.3%	16.5%	16.8%	16.5%	16.7%	15.9%	17.4%	16.9%
Snow (ll.)	30.6%	29.6%	30.7%	32.2%	30.8%	27.9%	38.3%	30.3%
	3.1	3.2	3.3	3.4	4.1	4.2	4.3	4.4
Wet (ll.)	21.3%	21.3%	21.5%	22.0%	21.6%	21.0%	21.6%	21.7%
Snow (ul.)	16.6%	16.7%	16.6%	17.8%	16.9%	16.7%	16.7%	17.9%
Snow (ll.)	30.5%	30.4%	30.8%	30.2%	30.6%	31.0%	30.8%	30.0%

5.2.4 Guidance

The subject of the investigation is still the question of the influence of the system in the extended traffic environment. Concerning RQ2 and RQ3, the RSACC and its potential influence on the impact dimension of traffic flow (efficiency) and traffic safety are investigated at this level. For this purpose, the calibrated highway scenario for different days from 2016 from Section 5.2.1.1 is used, each in the daytime period from 7 a.m. - 7 p.m. According to a study by (Robert Bosch

GmbH 2018), the share of newly registered passenger cars with an ACC system in 2016 was already about 19 %, with an upward trend. In order to limit the number of simulation runs, a penetration of 20 % by classic ACC systems is assumed in the reference scenario. Figure 5.33 shows an example of the distribution of vehicle and driver model types in the reference scenario.

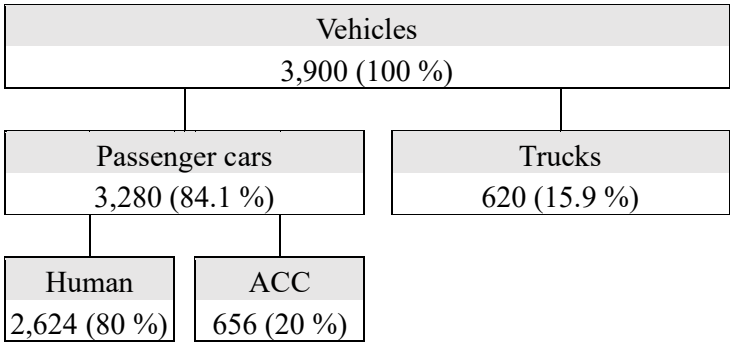

Figure 5.33: Distribution of vehicle and driver types in the reference scenario

While the total number of 3,900 vehicles and the proportions of cars and trucks correspond to the existing measurement data for January 25, 2016, from the data set of (BAST 2018), the further subdivision of the driver models in the scenario follows the just mentioned assumption. Accordingly, the "human" driver model is the driver model introduced in Section 4.3.3 and evaluated in Section 5.2.3. On the other hand, for the ACC model, a classic approach without influence by the road surface condition was initially used in the reference scenario. The behavior of the RSACC is identical to the behavior of the classical ACC in dry conditions. The simulations are performed according to the following pattern. First, the reference scenario is simulated under dry conditions, then under wet ($\mu = 0.65$) and snow-slippery ($\mu = 0.4$) conditions, respectively, with classical ACC and with RSACC. During the simulation runs, relevant key figures, such as the potentially critical situations from a road safety point of view, are recorded, compared, analyzed, and interpreted in each case.

Figure 5.34 shows the result for the absolute number of potentially critical situations for the simulation runs of the first reference scenario. The groups each show two hours and are divided into the dry reference condition, the wet condition, and the smooth road condition. While the human driver type remains unchanged, the proportion of 20 % of automated vehicles is simulated here, each with the state-of-the-art ACC and the RSACC as the driver model. First, the fundamentally jumping increase of potentially critical situations for wet and slippery road surface conditions compared to the dry scenario is explained. To this end, it should be recalled that the reduced coefficient of friction between the road surface and the vehicle's tires also reduces the force that can be transmitted for a braking or evasive maneuver. Accordingly, if the speed or speed difference to distance ratio between two vehicles is the same, a situation must already be classified as potentially critical. The reference scenario shows a total of 269 potentially critical situations with a distribution of 80 % human driver models to 20 % ACC driver models in wet road conditions and a total of 300 in slippery snow conditions. In contrast, an improvement can be observed by replacing the

20 % ACC driver models with the RSACC to 184 potentially critical situations in wet conditions and 248 in slippery conditions. This corresponds to a reduction in absolute numbers of about -31.6 % in wet conditions and about -17.3 % in slippery conditions by this measure alone. Since the simulation is otherwise performed by ceteris paribus, this improvement can be attributed to the improved system alone. However, the first indication of undesired emergence can be observed during the last two hours of this scenario. Since one of the primary functions of the RSACC is to increase the safety distance according to the prevailing road surface conditions, this, in turn, encourages lane changes of other surrounding vehicles, leading to even smaller gaps and thus a negative trend of increasing potentially critical situations again. This phenomenon is looked closer at in the further course of this section.

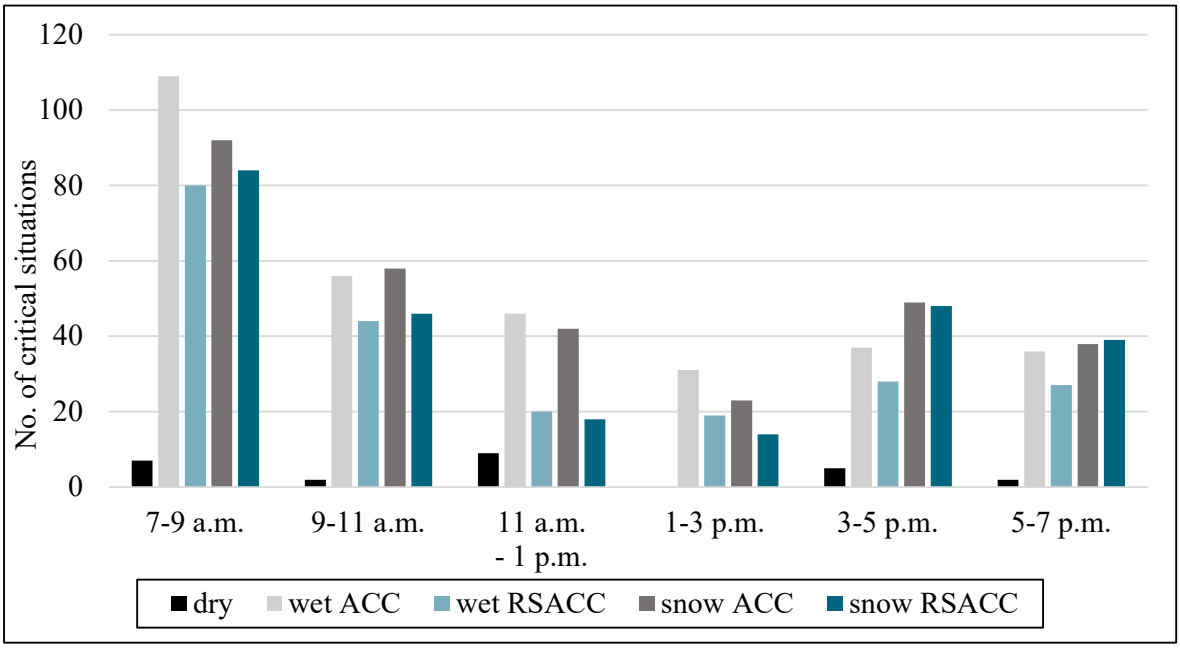

Figure 5.34: Number of potentially critical situations under different conditions in the reference scenario

These simulations are now carried out for increasing penetration of automated vehicles for the ACC without lane condition knowledge and the RSACC, respectively, in order to be able to distinguish more precisely the effects on traffic, i.e., whether knowledge of the surface conditions results in an improvement, or whether full automation would already suffice even without a WRSCS.

Figure 5.35 summarizes the result for wet conditions and shows that an improvement of the selected parameter can indeed be discerned by knowing the road condition for all degrees of penetration. However, with this type of observation, it is not directly possible to determine which driver models are responsible for the actual occurrence of the situation and in what way, which makes a more detailed analysis necessary.

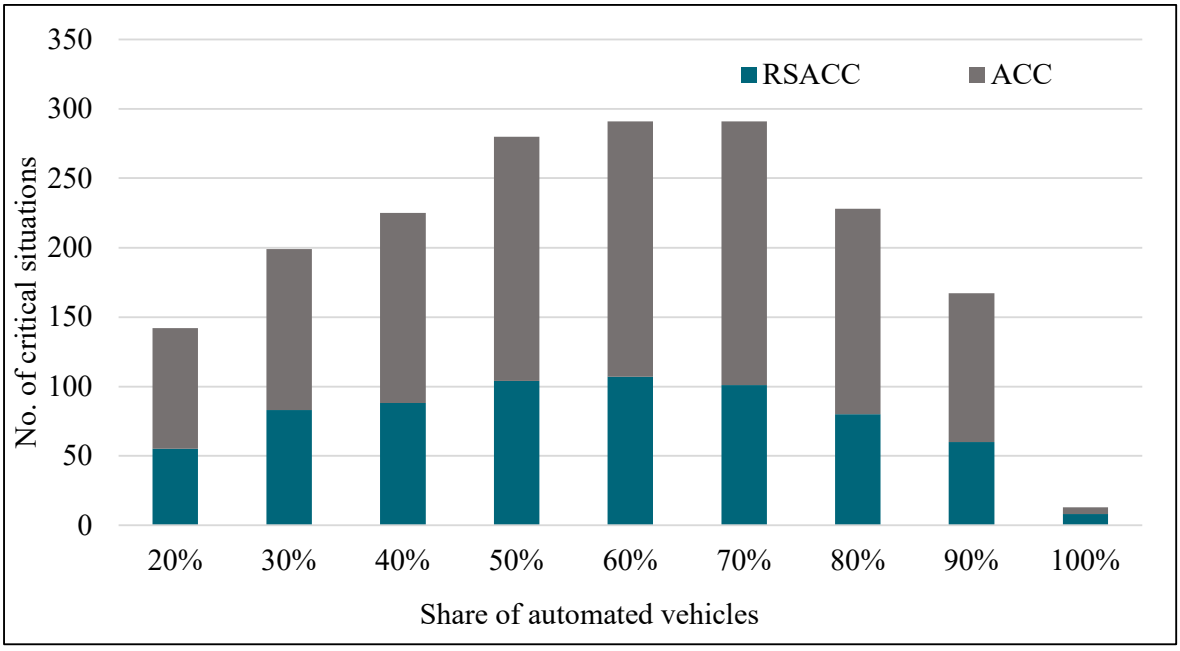

Figure 5.35: Influence of automation on potentially critical traffic situations in wet conditions with and without road condition sensor

First, however, this initial result is checked for plausibility. For this purpose, additional scenarios, one randomly selected day for each month of 2016, are calibrated according to the available traffic data. Subsequently, the simulations are performed for dry, wet, and slippery road conditions, respectively, with the same distribution of driver conditions described above to establish comparability. Table 5.11 summarizes the results for the absolute numbers and relative changes.

Table 5.11: Simulation results for the absolute number of potentially critical driving situations for different scenarios and road conditions

Date	Dry	Wet			Snow		
		ACC	RSACC	Δ %	ACC	RSACC	Δ %
Jan-16	26	269	184	-31.6	300	248	-17.3
Feb-16	28	201	157	-21.9	266	174	-34.6
Mar-16	48	237	178	-24.9	314	217	-30.9
Apr-16	46	285	235	-17.5	294	282	-4.1
May-16	190	758	707	-6.7	939	938	-0.1
Jun-16	36	289	271	-6.2	386	314	-18.7
Jul-16	59	278	224	-19.4	292	219	-25
Aug-16	29	260	210	-19.2	295	212	-28.1
Sep-16	17	295	212	-28.1	361	290	-19.7
Oct-16	67	520	445	-14.4	589	537	-8.8
Nov-16	30	226	188	-16.8	209	156	-25.4
Dec-16	33	267	232	-13.1	337	278	-17.5

Although individual results differ from one another, in summary, however, a trend toward improvement is evident. The simulation runs show a relative reduction of potentially critical driving

situations due to knowledge of the road surface condition of -18.3 % on average for wet conditions and -19.2 % on average for even worse road surface conditions.

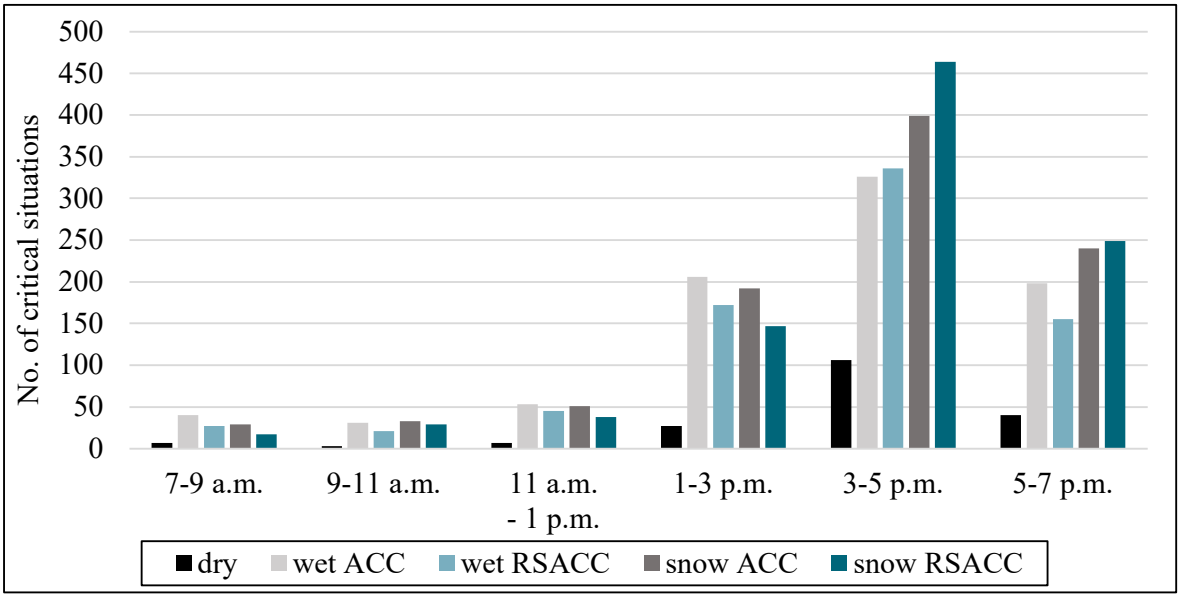

Figure 5.36: Number of potentially critical situations in different conditions in the May scenario

Particularly noteworthy is the result of the simulation of May 2016, which was a Friday with a significantly increased traffic volume compared to the other days due to weekend commuters. The high number of 190 potentially critical situations even during dry weather reflects this overall increased traffic volume. A closer look at Figure 5.36 reveals that the period from 3 p.m. to 5 p.m. is outstandingly critical. This phenomenon is equivalent to the observation in Figure 5.34 above. Due to the high traffic volume, the increased safety distances of the RSACC in the present model lead to a disproportionate increase in the number of lane changes, which result in regular violations of the lane changes and thus in an accumulation of undesirable situations. Figure 5.37 shows the number of observed lane changes over the share of automated vehicles in the simulation.

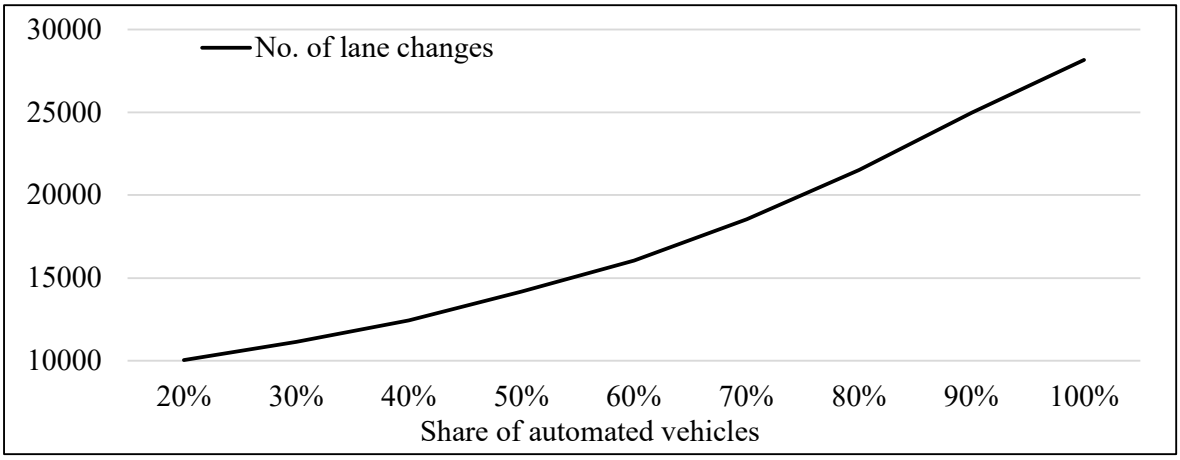

Figure 5.37: Lane change development for increasing shares of automation using RSACC

This behavior was already observed during the calibration phase of the RSACC when it was implemented in SUMO (Weber and Schramm 2020b). Adapting the lateral dynamics and lane change models in traffic simulation is certainly desirable in the future but has not been implemented within the scope of this thesis.

The question of which driver models are responsible for the actual occurrence of the situation and whether this can further support the hypothesis that knowledge of the road surface condition can contribute to handling challenging driving situations in highly automated driving is still open. For this purpose, the shares of the respective driver models are considered in relation to the number of absolute numbers observed in each case for potentially critical situations. Compared to a pure consideration of the absolute numbers, this offers certain advantages because with increasing penetration of the RSACC in the vehicle fleet, the absolute numbers of observed critical situations for this driver model initially increases, simply due to the increased absolute number of correspondingly equipped vehicles. Figure 5.38 shows this situation as an example from 7 a.m. – 9 a.m. for the January scenario. The respective proportions refer to the passenger car vehicle types in the simulation; the simulated proportion of trucks and their driver model always remain unchanged.

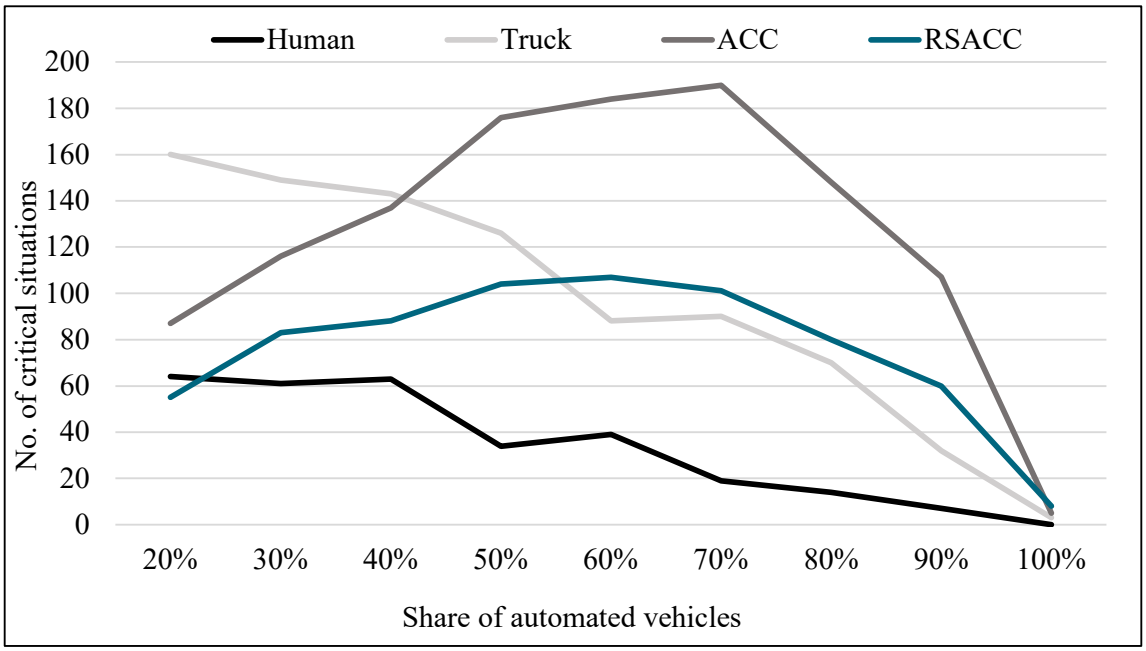

Figure 5.38: Number of potentially critical situations per driver model at increasing shares of automated passenger cars

Three observations are particularly noteworthy here. First, the replacement of the standard ACC by the RSACC causes a decrease in potentially critical driving situations for all vehicle and driver types. For example, the absolute number for ACC compared to the RSACC decreases from 87 to 55. Even the vehicles which are not directly influenced by the system, however, benefit in absolute terms from the equipment of other vehicles in the system, as there is also a decrease in the number of observed potentially critical situations, especially with increasing shares of automated vehicles.

Second, it is also interesting to note that despite a further linear increase in the number of vehicles equipped with RSACC, the number of observed incidents declines sharply above a penetration of 70 % RSACC. This can be explained, among other things, by the fact that both the influence of driving behavior of human driver types, which may not always be rational, apparently decreases significantly from this threshold and a traffic-stabilizing effect of the increasing proportion of highly automated driving vehicles is more apparent. Figure 5.39 supports the observation of such a traffic-stabilizing effect. It shows that speeds increase significantly again on average across all vehicles and all simulations, even in poor weather conditions, with higher proportions of the automated RSACC driving function compared to a standard design with a high proportion of human driver types. One of the reasons for this is that it compensates for an over-adapted, particularly defensive driving style of individual human drivers. Such behavior can have considerable adverse effects, especially in higher traffic volumes, particularly concerning the speeds driven. This trend is observable in the same way in all considered simulation runs.

The third observation worth mentioning is that the number of potentially critical situations for trucks steadily decreases, although the number of truck-type vehicles remains constant. This means that an increased proportion of highly automated vehicles with appropriately equipped systems stabilizes the overall traffic flow and results in an individual improvement in safety for the equipped vehicle and other road users that do not have any improved systems on board.

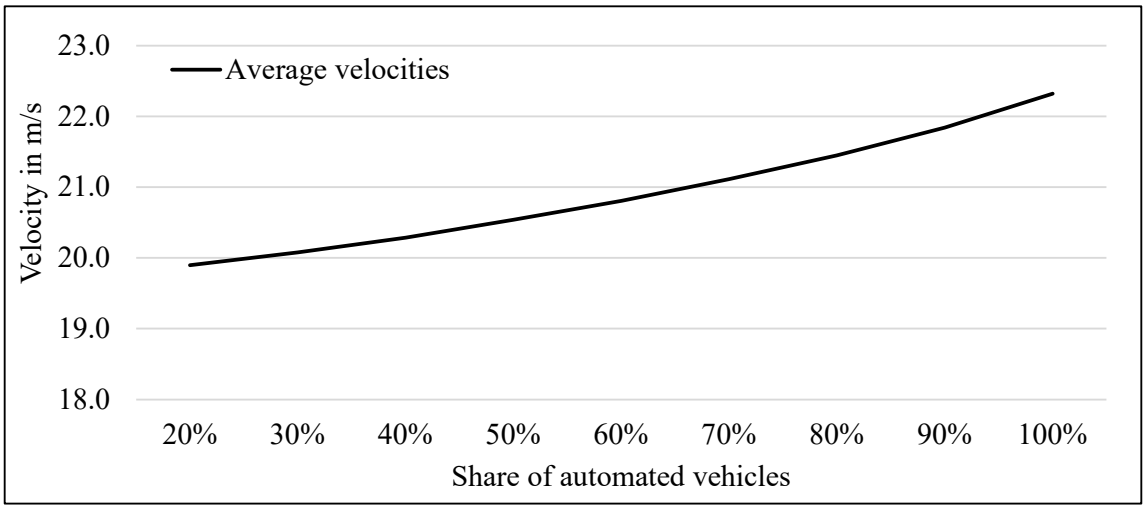

Figure 5.39: Mean average velocities in the entire simulation scenario in wet conditions for increasing shares of automated passenger cars

After describing and interpreting the absolute numbers, it shall be examined whether the changes in the absolute numbers are attributable to a particular system. Figure 5.40 lists the relative proportion of potentially critical driving situations per vehicle with the human driver behavior model for all simulated highway scenarios. For all combinations of ratios between human driver type and RSACC, the relative proportion of human driver type in the potentially critical situations showed a nearly constant trend. The value is about 1.1 % on average across all simulated highway scenarios. In other words, there is about one potentially critical situation for every one hundred vehicles

with human driver type in the simulation, regardless of how many vehicles are equipped in this way in the simulation in absolute.

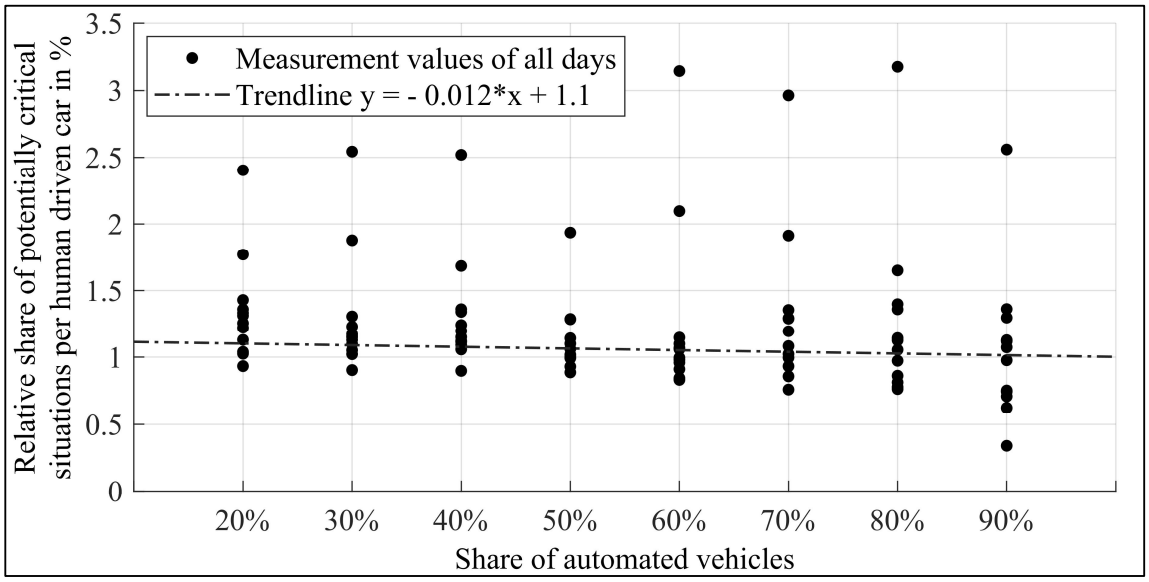

Figure 5.40: Relative share of potentially critical driving situations by vehicles with human driver type to the total number of vehicles with this driver type within the simulation over the share of automated vehicles with the RSACC driving system

On the other hand, in the relative proportion of potentially critical driving situations for vehicles with the automated RSACC driver model, a degressive course of the curves can be seen with increasing penetration of the system in the vehicle fleet in Figure 5.41.

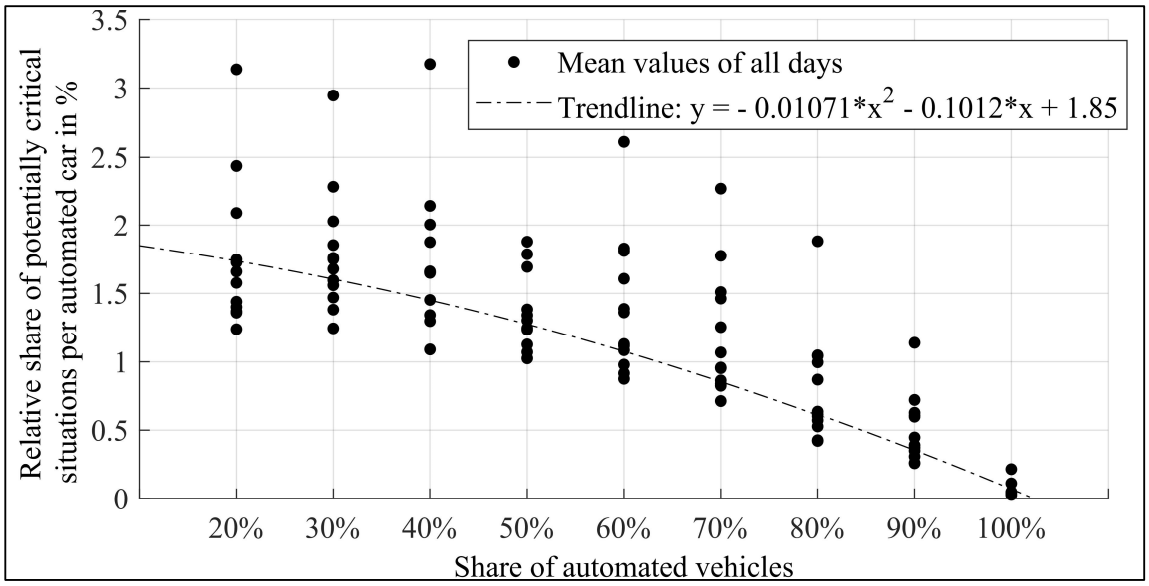

Figure 5.41: Relative share of potentially critical driving situations by vehicles with RSACC driver type to the total number of vehicles with this driver type over the share of automated vehicles within the simulation.

From a ratio of about 50 %, the RSACC reaches the values of the human driver type on average. After that, it even drops to well below 1 %. This peaks at 100 % penetration of simulated passenger cars with RACC at a value of about 0.07 %. The number corresponds to only one potentially critical situation per 1,500 vehicles and is significantly better than standard ACC and better than human driver type. This development is observable in the same way for all tested scenarios.

The results suggest that a positive effect on traffic flow stability and traffic safety at the traffic level can be expected from integrating weather-related road surface condition aware automated driving functions.

5.2.5 Navigation

In order to investigate the effect on the measured variables for answering RQ3 and RQ4 regarding the impact dimensions efficiency and comfort, two variables are varied in the simulations. The first influencing factor is again the road surface condition. Depending on the location and extent of the affected areas, the road surface condition can significantly influence the selection of suitable routes for vehicle navigation. Suitable routes can only be selected in advance if complete information about the existing road conditions is available, making the availability of this information the second interesting investigation factor. Within the simulation, it is assumed that the road conditions of the scenario are known and globally available. However, this data can only be retrieved by those vehicles that have a corresponding communication system. This allows the availability of data to be mapped and varied based on the market penetration of intercommunication-capable vehicles. The two city scenarios serve as simulation scenarios here.

5.2.5.1 Generic City Scenario

Since this scenario involves a small map section, which the size of typical precipitation areas can quickly exceed, it is assumed in the weather conditions that a precipitation area passes by at the upper edge of the map section and covers only a part of the map section the road network. Progressively, this variation is realized between simulation runs in four stages, where 0 %, 25 %, 50 %, and 75 % of the network area lies within the precipitation area, respectively. The second variation parameter within this scenario is the proportion of communication-enabled vehicles. Starting at 0 %, this is increased in steps of 25 % up to penetration of 100 %. The steps are controlled by the configuration data of the vehicle routes and the distribution of vehicle types contained therein. In interaction with all variation stages, which show a precipitation area spreading, the systematic combination of these influence parameters results in 32 simulation runs for the measurement series with 100 and 1,000 vehicles each.

Safety

The driving time in automated driving mode serves as the representative metric for driving safety at the traffic level. This metric is used because increased usability of an automated driving function already creates an intrinsic added value in road safety by reducing or avoiding accidents due to human error. However, since a changing proportion of driving time in automated operation can result either from a reduction in manual driving times or increased route lengths, the change in route length is included in assessing the safety potential. In contrast to the increased driving safety resulting from automated driving, an increased route length is generally considered an additional safety risk. Accident data from the Federal Statistical Office and the Federal Motor Transport Authority provide the basis for this assumption, as in 2019, around 632,254 million kilometers were driven by passenger cars in Germany (KBA 2021), resulting in a total of 300,143 registered accidents with personal injury (Destatis 2020). On average, this means that one accident with personal injury occurs for every 2.1 million kilometers driven. Assuming that accidents in automated driving operations can be reduced by up to 90 %, additional automated driving times are therefore credited a reduced risk factor of only 10 %, while manual driving times are credited a risk factor of 100 % on the overall route length. The resulting risk weighted net route length is then compared across the different simulation runs. A simulation with 0 % communication-enabled vehicles serves as the reference for the percentage developments of the considered metrics in the ensuing investigation since the navigation application does not influence the vehicle routes in these runs.

In the first simulations carried out, in which rain areas in each case cover 25 % of the road network, a positive influence of the vehicle navigation on the driving time in automated driving mode is already noticeable. At the maximum, in these weather conditions, the automated driving time could be increased by 23.35 %, while in this particular example case, the total route length increases by 1.14 %. For the net route length at risk, which comprises the weighted consideration of automated and non-automated driven route sections, this means a reduction of 28.22 %. Further simulation runs also indicate that higher penetrations of communication-enabled vehicles positively affect driving safety, even if the total route length due to navigation increases in the process. The increase in automated driving times exceeds the increase in total route length in all cases, leading to a reduction in the net route length at risk. Figure 5.42 illustrates this observation for the simulation runs with a precipitation area of 25 % and 1,000 simulated vehicles.

For more extensive precipitation-affected areas, an increase in total route lengths of up to 8.32 % is observed. This increase results from more vehicles' overall deviating their route, but the detours also represent potentially longer routes due to the larger precipitation area. Nevertheless, even in these simulation runs, it positively impacts driving safety, as the increased travel time in automated driving reduces the weighted risk on the net route length by up to 14.41 %. This means that a longer route at 10 % risk in automated mode outweighs shorter routes with a larger share of 100 % risk-prone human driving mode from a safety perspective. The increasing route length is also discussed in more detail in evaluating the driving efficiency effects.

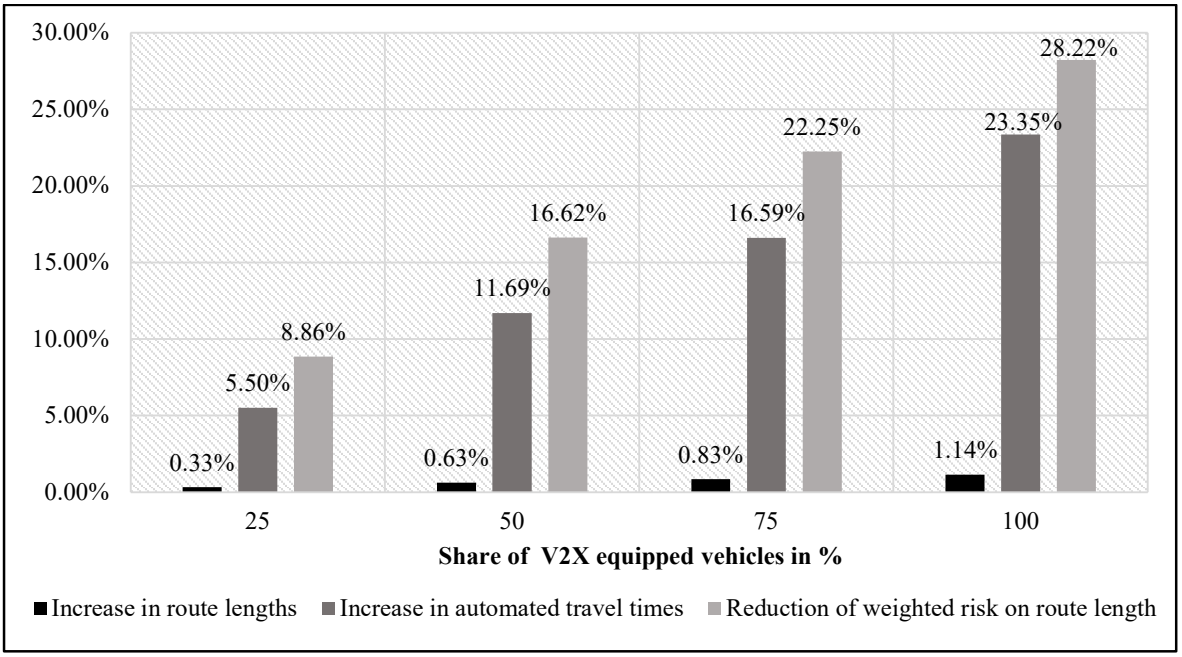

Figure 5.42: Safety relevant results, 25 % precipitation affected area and 1,000 vehicles

Efficiency

Average route length and average travel time are established as the primary metrics to evaluate efficiency. Figure 5.43 shows the increases in route lengths and travel times for the growing proportion of communication-enabled vehicles. The data are based on the simulation runs with 1,000 vehicles and a precipitation spread of 75 %.

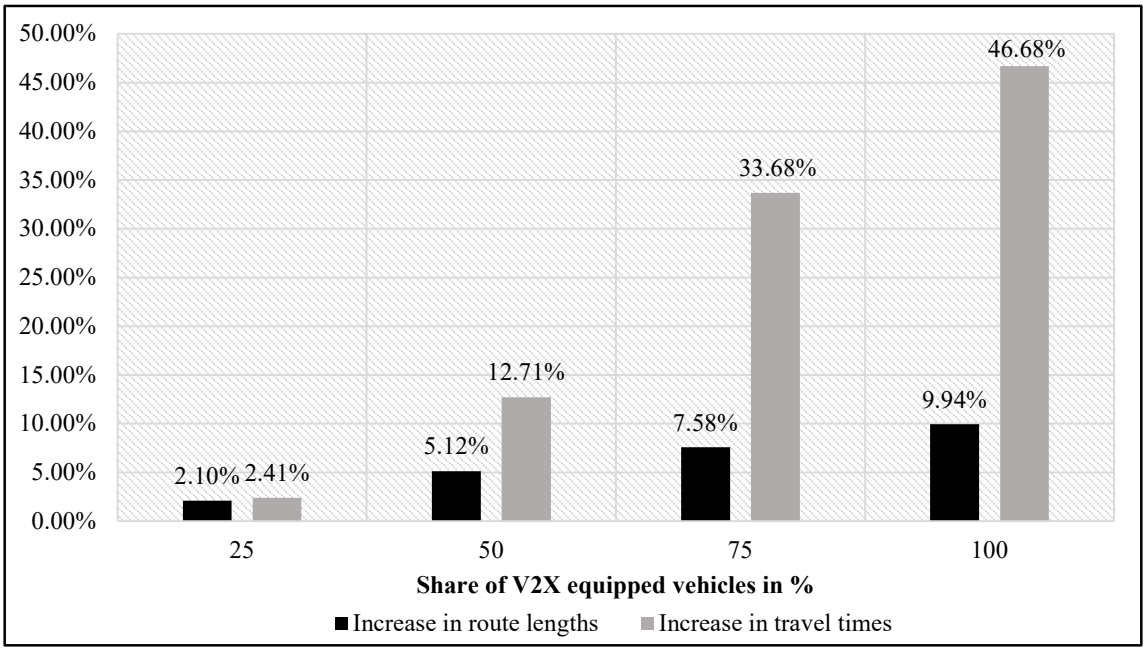

Figure 5.43: Evolution of route lengths and travel times at 75 % precipitation affected area and 1000 vehicles

The evaluation of safety and the evaluation of comfort indicate that the network capacity reaches its limits for a large number of rerouted vehicles. This is implied by the fact that the travel time in the automated driving mode increases significantly compared to the increase in route length in the specific simulation runs. For example, while in simulation runs with 100 vehicles, the increase in route length is in a similar order of magnitude as the increase in travel time, the increase in travel time in scenarios with 1,000 vehicles, and a precipitation area of 75 % reach values that exceed the increase in route length up to four times.

In addition, to further investigate the occurrence of potential traffic congestion, Figure 5.44 aggregates the average speed of all vehicles in the simulation over the simulation time. The graphs qualitatively show that the average speed is subject to only minor fluctuations for 100 communicating vehicles. However, with a traffic volume of 1,000 vehicles, the average speed drops significantly as soon as the road network reaches its capacity limits. The average speed stabilizes at the end of the simulation run when enough vehicles have left the simulation. A closer look at the simulation reveals that the cause of this congestion of the road network is the formation of traffic jams at the edges of the precipitation area. Comparable effects already occur in real traffic today, for example, when many vehicles try to avoid highway congestion using a detour on surrounding local areas.

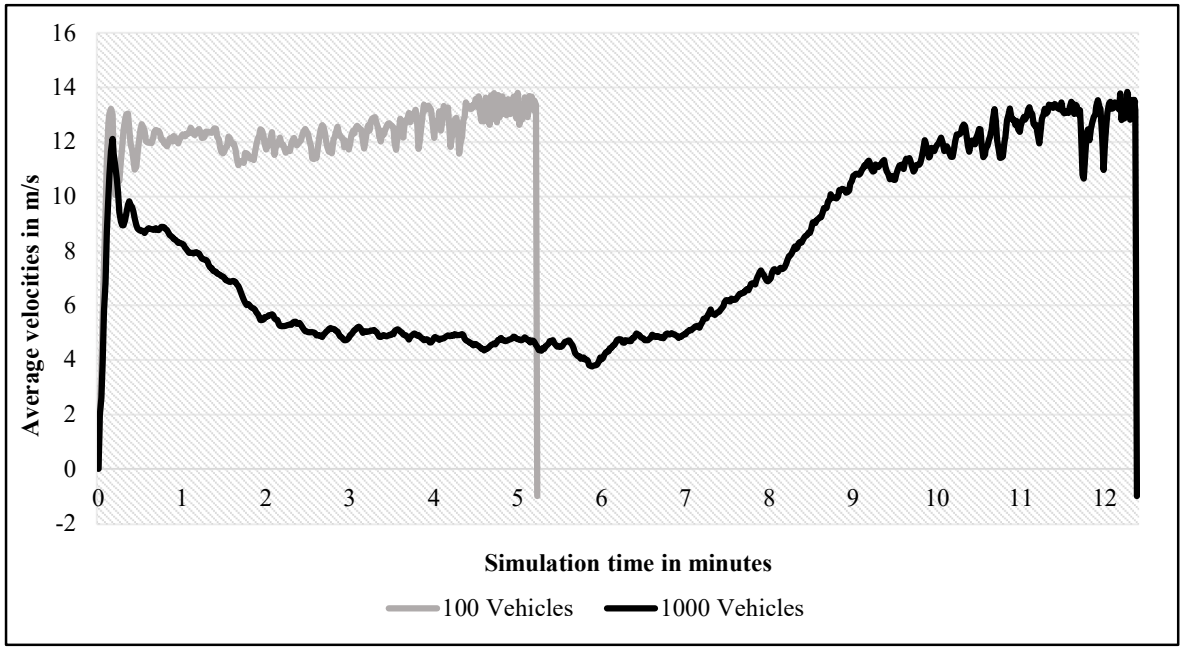

Figure 5.44: Evaluation of network capacity based on average speeds

Although the increased travel time in automated driving is considered here to impact driving comfort positively, the drop in average travel speed and the creation of traffic congestion is considered a negative impact on driving efficiency. Beyond the average travel speed, the increase in route length is vital for the driving efficiency analysis. In evaluating driving safety, it is evident that changes in the original vehicle route to bypass precipitation areas are generally associated with increased route lengths. In evaluating driving safety, the increased proportion in automated driving

is evaluated as a more significant positive impact than the downside due to an increase in route length. However, the increased route length negatively impacts average travel time and overall traffic efficiency. In addition, increased route lengths and possible resulting traffic congestion carry further negative consequences in both economic and environmental terms. For example, in 2015, traffic congestion in the U.S. alone added approximately 11.3 billion liters of fuel and an additional 7 billion hours spent sitting in vehicles (Schrank et al. 2015). Therefore, it remains questionable whether and to what extent societal opinion on climate and environmental policy can be consistent with systems that potentially exacerbate these issues and should be the topic of future research.

5.2.5.2 Realistic City Scenario

Over 24 hours, 25,668 vehicles are simulated in this scenario. Since the first simulation scenario's measurement series already shows that significant measurement results can only be expected at higher penetrations of vehicles capable of communication, this variation is reduced to three levels, 0 %, 50 %, and 100 %. Consequently, in combination with the three weather levels and a reference run, a total of ten simulation runs result for the scenario of the small town of Hüls. The aim is to evaluate and verify the findings obtained in the first scenario in a simulation environment that is closer to reality.

Safety

As in the first scenario, the assessment of driving safety is primarily based on the automated travel time and a weighted evaluation of the route lengths that change due to navigation. Figure 5.45 presents the shares of automated travel time depending on the precipitation area spread and the market penetration of communication-enabled vehicles.

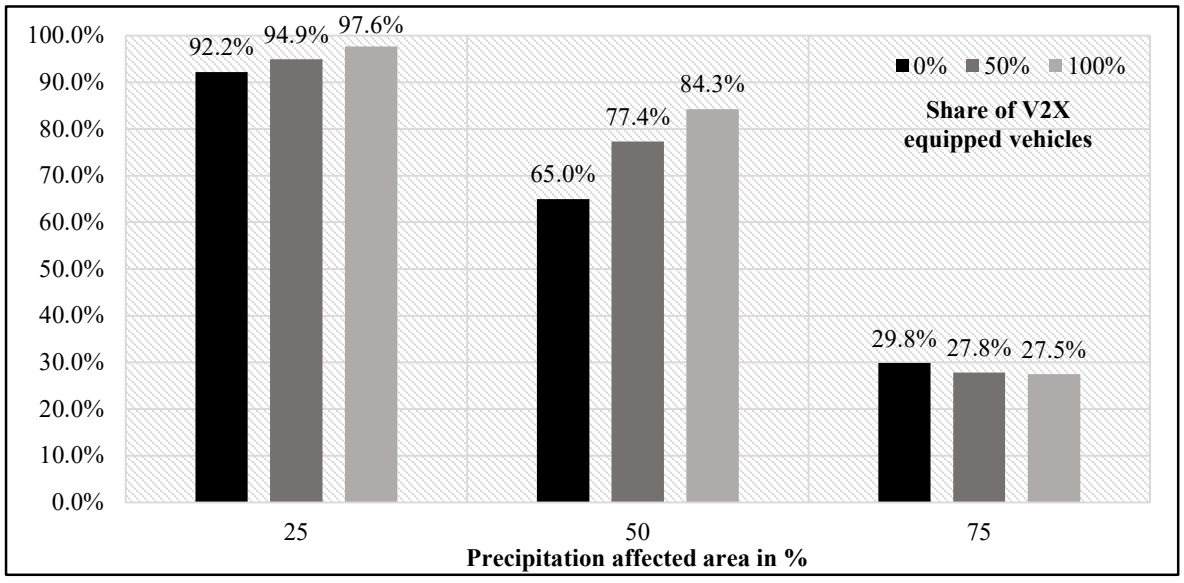

Figure 5.45: Percentages of the automated travel time for the realistic city scenario

In addition, Table 5.12 shows the percentage developments of total route lengths and travel times in relation to the respective reference simulation runs. In the simulation runs with a precipitation area of 25 %, an increase in the automated travel time is also apparent for an increasing proportion of vehicles with communication capability. In the reference run without communication-enabled vehicles, 92.18 % of the total travel time is automated. The automated travel times increase to 94.92 % and 97.64 % for a share of 50 % and 100 % communication-enabled vehicles, respectively, utilizing the developed vehicle navigation. There is a 0.54 % and 0.68 % increase in total route length in these runs when avoiding precipitation. The subsequent analysis of the weighted route lengths shows a corresponding reduction of 1.77 % and 8.24 % so that the influence of vehicle navigation on driving safety is evaluated as positive in both cases.

Table 5.12: Summary of the simulation results concerning safety

V2X equipped vehicles	**Change in route lengths**	**Change in travel times**		**Weighted risk reduction (route)**
		total	automated	
Precipitation affected area 25 %				
50 %	0.54 %	1.76 %	4.79 %	-1.77 %
100 %	0.68 %	8.24 %	14.65 %	-8.24 %
Precipitation affected area 50 %				
50 %	3.63 %	36.27 %	62.29 %	-24.22 %
100 %	6.49 %	82.18 %	136.35 %	-38.07 %
Precipitation affected area 75 %				
50 %	1.01 %	2949 %	2740 %	3.55 %
100 %	-1.10 %	3259 %	3259 %	1.78 %

The simulation runs with a precipitation area spread of 50 % show a picture comparable to the first simulation runs because the travel time in automated driving mode also increases with an increasing proportion of communication-capable vehicles. While only 64.96 % of the travel time in the reference run can be automated, this share increases in simulations with a higher penetration of communication-enabled vehicles to 77.32 % and 84.28 % of the total travel time. Even in these simulation scenarios, the overall increase in route lengths is only a few percent, so a reduction in risk-weighted route length is observed here as well. Furthermore, in these simulation runs, it is noticeable for the first time that the total travel time, as well as the increase in automated travel time, show more significant growths than suggested by the increase in route lengths. For example, the total travel time already increases by 36.27 % for a share of 50 % of communication-enabled vehicles, although the total route length only increases by 3.63 %. This indicates the creation of more minor traffic jams.

Further, this behavior can also be observed in the simulation runs with a precipitation area of 75 %. Contrary to expectations, a decrease in automated travel time is observed in these runs, with increasing numbers of communication-enabled vehicles. Even when considering the route lengths,

which should show further increases due to the bypassing of corresponding areas, decreases are observed compared to the reference scenario. This is because massive traffic jams occur when many vehicles try to bypass the precipitation areas simultaneously. Considering the driving safety for these simulation runs proves to be particularly difficult in this context. However, the claim could be made that participation in traffic jams carries a lower risk for the drivers, the meaningfulness of this evaluation is doubtful. Therefore, the evaluation of driving safety is limited to the simulation runs that did not lead to any traffic conditions, while the exceeding of the network capacity is further investigated in the efficiency consideration.

Comfort

The travel time in automated driving mode and the additional time saved by relieving the driver of the driving task assess the driving comfort. Table 5.13 summarizes the results and shows the average travel times and the travel times in automated and manual operations for all runs of this scenario. As in the evaluation of the first simulation scenario above, it is also observed for these simulation runs that the total travel time always shows an increase as the precipitation area spread increases and the proportion of vehicles with communication capability increases. Already in the evaluation of driving safety, Figure 5.45 above shows that the share of travel time in automated driving mode increases steadily compared to the respective reference runs up to a precipitation area spread of 50 % and a share of 100 % of communication-enabled vehicles.

Table 5.13: Summary of the simulation results concerning comfort

V2X equipped vehicles	**Average travel times in seconds**		
	total	automated	manual
Precipitation affected area 25 %			
0 %	343	316	27
50 %	349	332	18
100 %	372	363	9
Precipitation affected area 50 %			
0 %	343	223	120
50 %	468	362	106
100 %	625	527	98
Precipitation affected area 75 %			
0 %	343	102	241
50 %	10468	2908	7560
100 %	11531	3166	8365

As mentioned in the introduction, the evaluation of these increases is composed of both an increased total driving time and the reduction of manual driving times. For the simulation runs in which only 25 % of the network area is covered by precipitation, the increases in the average

driving time in automated driving mode are around 15 and 46 seconds for a proportion of 50 % and 100 % of vehicles with communication capability. While the first increase is still composed mainly of the reduction of manual travel times, the second increase already results primarily from the increase of the total travel time. Figure 5.46 summarizes these findings graphically, which breaks down the increases in automated travel times as a percentage into the reduction in manual travel times and the increase in total travel time.

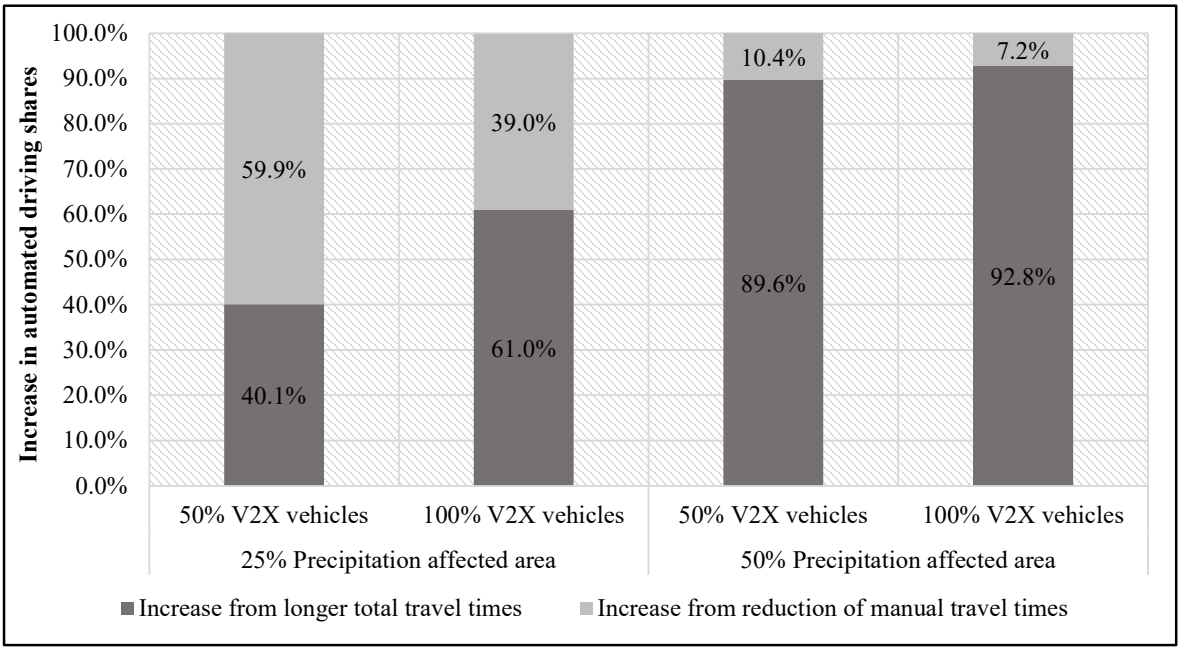

Figure 5.46: Breakdown of the increase in automated travel times

Far more severe congestion conditions occur in the simulation runs with a precipitation area of 75 %. The data in Table 5.13 supports this since both the total travel times and the travel times in manual and automated driving mode show a disproportionately large increase compared to the other simulation runs. The increases in travel times in manual and automated travel modes are primarily linked to whether the vehicles' destination is inside or outside the precipitation areas. Exceeding the network capacity leads to a complete standstill of the traffic, and the influence of the vehicle navigation is evaluated as unfavorable in these simulation runs and further elaborated in the evaluation of the traffic efficiency.

For the comfort aspect, it can be summarized that the reduction of manual travel time is usually accompanied by a proportionally predominant increase in total travel time. Even though the reduction of manual travel times is considered as a positive influence of vehicle navigation on comfort here, this inevitably leads to the further research question of how much additional travel time drivers would accept to reduce a part of their manual travel times.

Efficiency

For evaluating traffic efficiency, both the changes in route lengths traveled and the changes in travel times by the simulated vehicles are evaluated. Table 5.14 lists these two metrics as a function of the proportion of communication-enabled vehicles for all simulation runs. An important observation, which is already apparent in evaluating safety and comfort, is that the network capacity is exceeded when many vehicles deviate from their original route due to the navigation application.

Table 5.14: Summary of the simulation results concerning efficiency

V2X equipped vehicles	**Average metric values**			
	Route lengths in m	Δ length %	Travel times in s	Δ %
Precipitation affected area 25 %				
0 %	2801.0		343.3	
50 %	2816.7	0.54 %	349.4	1.77 %
100 %	2820.6	0.70 %	371.6	8.24 %
Precipitation affected area 50 %				
0 %	2801.0		343.3	
50 %	2902.6	3.63 %	467.9	36.28 %
100 %	2982.9	6.49 %	625.5	82.19 %
Precipitation affected area 75 %				
0 %	2801.0		343.3	
50 %	2829.2	1.01 %	10467.9	2949.12 %
100 %	2770.3	-1.10 %	11530.7	3258.68 %

This is particularly evident in the simulation runs, where 75 % of the network area is affected by precipitation. While the route lengths change by only about 1 % in each case, the total travel time in these runs increases up to 30-times compared to the reference run without communication-enabled vehicles. This drastic increase indicates that in these simulation runs, not only locally increased traffic volumes and minor traffic jams occur, but traffic completely breaks down.

The upper part of Figure 5.47 evaluates the traffic conditions of those simulation runs where the precipitation area covers only 25 % of the network area. Here, a similar course of the graphs shows for all three variations of the penetration rate of communication-capable vehicles. The number of vehicles remains largely uniform throughout the simulation and only takes on short-term peaks during the rush hour periods. While the reference run and the run with a share of 50 % of vehicles capable of communication show an almost identical course, slight overshoots can already be observed at the peak times with a share of 100 % of vehicles capable of communication. This already indicates that the increased traffic volume equalizes more slowly with adaptive vehicle navigation than in the reference run. The lower part of the figure shows the measurement results of the simulation runs at a precipitation area of 75 %. As the percentage of vehicles capable of communication increases, it can be observed in these runs that the number of vehicles in the simulation follows the course of the reference run only at the beginning. With the onset of rush hour

and the associated increased volume of vehicles, massive congestion occurs in these simulation runs using adaptive vehicle navigation. As a result, the traffic situation collapses, and vehicles can no longer leave the simulation because they can no longer reach their specified destinations. Due to the constant addition of vehicles, a complete blockage of the road network occurs.

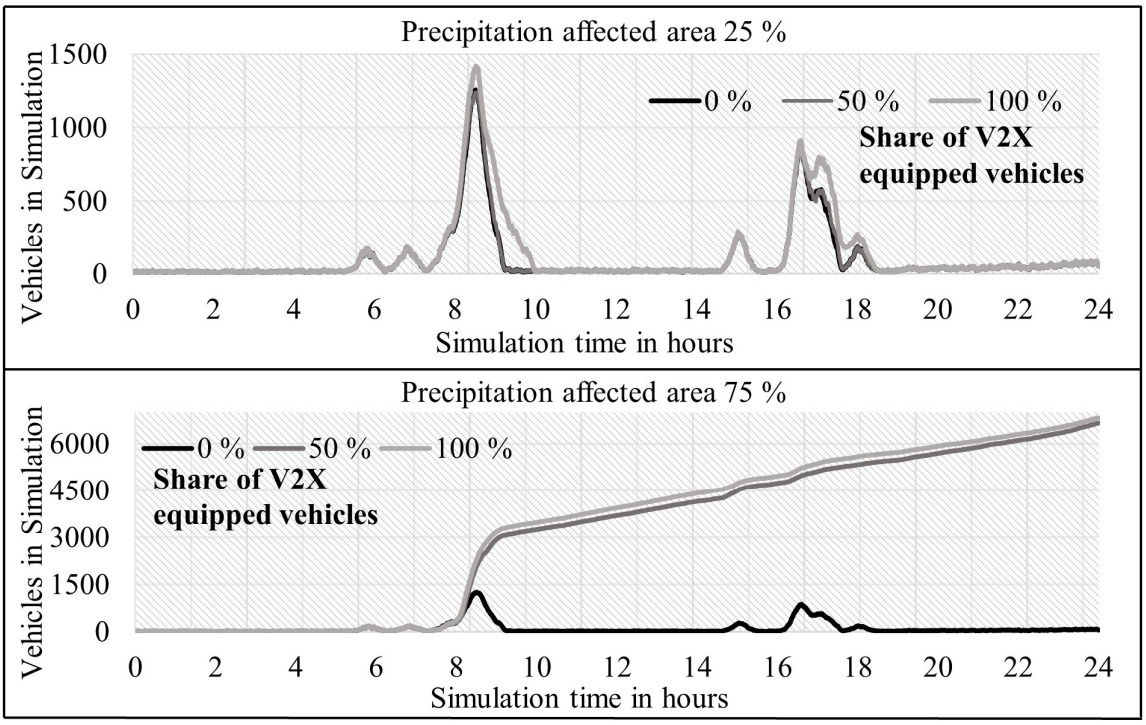

Figure 5.47: Indication of network collapse based on the active vehicles in the simulation

The resulting traffic jams form predominantly at the edges of the precipitation areas, which the vehicles intend to avoid. Due to the repeated occurrence of such traffic conditions, multi-dimensional real-time congestion avoidance is a valuable extension of the navigation application in the future. Such an extension could be implemented, for example, in the form of a continuing iteration of the cost function that considers the last known travel time or the current number of vehicles per route segment up to a complete reevaluation of the boundary conditions. Also problematic is the simulation-related spatial limitation of the available traffic network since this reduces the overall possibilities for alternative routes and amplifies the effect. In the simulation runs where only a few vehicles deviate from their original route, both the route lengths and the total travel times of the vehicles increase. Since the road network does not reach its capacity limits in these runs, a possible increase in maximum capacity due to the increased use of autonomous driving functions, therefore, does not represent any intrinsic added value in terms of efficiency here.

In summary, increasing automated driving times through adaptive navigation leads to increased driving safety and comfort for individual vehicles but may have an inverse correlated effect for overall traffic efficiency for the approach chosen here. An interesting question for further studies would be, for example, whether this effect is counter actable by intelligent dynamic algorithms of a central traffic control unit.

5.3 Discussion of Results

Finally, the results are discussed, particularly regarding the specific research questions from Section 3.4. Overall, the results suggest that the methodology introduced for the holistic consideration of potential is suitable for answering complex questions regarding the effects of future vehicle systems. The approach of relating system variations to a very realistic reference scenario seems to be particularly effective. Since this approach focuses on an a priori consideration of the possible influence of a system, the particular challenge in the preparation of the study lies in the selection and creation of suitable tools. Especially when several different tools interact in a modular way in a larger context, the respective individual limitations and the possibly resulting overall limitations have to be critically considered. In the following subsections, the potential impact dimensions introduced at the beginning will be summarized, critically discussed, and the specific research questions will be answered regarding the weather-related road surface condition sensor under consideration.

5.3.1 Safety

RQ1: Is a positive safety impact at the stabilization level achievable through the system?

On the stabilization level of individual vehicles, an RSCA ABS was investigated to investigate the question. For the longitudinal direction, a reduction of the braking distance of up to 2 % on moist, up to 8 % on wet, and up to 11 % on icy road surfaces was determined in the standard speed ranges for different road types (urban, rural, highway), which coincides with other study results from the literature. Although the reduction in braking distance as a metric indicates a positive influence on safety, it will be briefly explained that further interpretation of this finding is possible upon closer examination. In traffic accident research, models are developed by evaluating real accidents that relate the collision speed to the severity of the accident consequences in the form of so-called Injury Risk Functions (IRF). The injury as such is usually coded in the form of an abbreviated injury scale (AIS) (cf. Table Table 5.15), (Gennarelli and Wodzin 2006).

Table 5.15: Abbreviated Injury Scale

AIS-Code	AIS-Severity
0	Not Injured
1	Minor
2	Moderate
3	Serious
4	Severe
5	Critical
6	Maximum (not treatable)
9	Not Further Specified (NFS)

(Spitzhüttl and Liers 2016) evaluate a real accident database with a sample size of n=138 to create models of injury risk functions for collisions with pedestrians. They use the AIS-based MAIS and PMAIS indicators, which are also frequently used in literature. MAIS denotes the maximum AIS, and PMAIS denotes the probability of injuring at least with the indicated severity. PMAIS2+, for instance, means the probability of injuring at least with MAIS2, i.e., all levels two and above, but not AIS0 and AIS1. Based on the accident data, they create cumulative probability functions in passenger car head-on collisions with injury severity PMAIS2+ (moderate+) and PMAIS3+ (serious+), respectively, shown in Figure 5.48. Both have an offset at 0 kph due to the model assumption of a logistic distribution. The value of the offset results from the observation of injured pedestrians due to collision with low-speed vehicles and with stationary vehicles.

Suppose further an inner-city example situation, where an emergency braking is triggered from an initial speed of 58 kph on a wet road and that a collision with a pedestrian occurs one second later. Within the scope of this thesis, it was determined that the remaining collision speed in this case with the standard ABS is still approx. 43 kph, while the RSCA ABS only has a remaining collision speed of approximately 36 kph due to the optimization. Regarding the IRF, this means that the probability of only minor injuries increases from about 40.6 % to about 54.8 %, while the probability of serious+ injuries decreases from 25.6 % to 15.7 %. Of course, this result applies only to the model used in this case, but it is directly applicable in the same way to similar models, which differ only in their database, but not in their form and methodology.

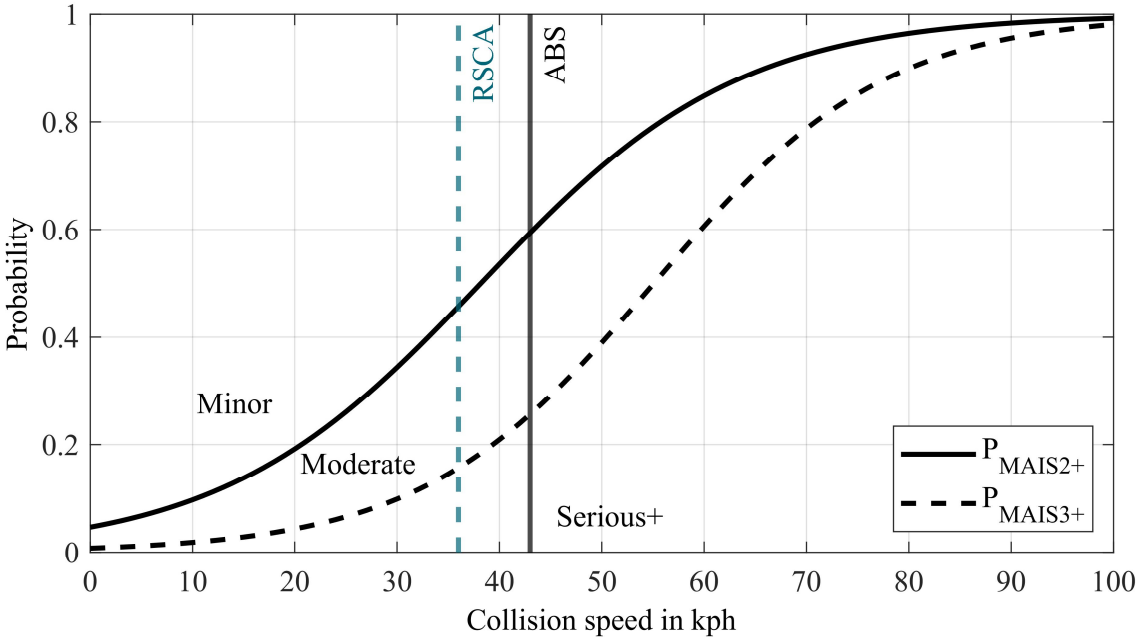

Figure 5.48: IRF for adult pedestrians in head-on passenger car-pedestrian crashes

For the lateral direction, a clear stabilization can be seen through the optimization of the system during maneuver braking in the curve. On the one hand, directly in the characteristic variables such as yaw rate and sideslip angle ratios, and on the other hand, through a reduction in the absolute position deviation from the reference trajectory of about 5 % on average, especially in poor

weather-related road conditions. Thus a positive safety impact can be determined based on objective and standardized characteristic values of this level and based on other derivable variables, such as the consideration of accident consequences.

A positive impact at the stabilization level is achievable in both longitudinal and lateral directions through the use of a weather-related road surface condition sensor.

RQ2: Is a positive safety impact at the guidance level achievable through the WRSCS?

Two systems were investigated in more detail to address this issue: a road surface condition aware ACC (RSACC) and road surface condition aware Emergency Steer and Brake Assist (ESB). Regarding the road surface condition restricted by weather conditions as a starting point for demanding driving situations in the sense of a restriction of the available driving dynamics, it could be shown by the simulations that the RSACC achieves better results on average between 18 % and 20 % concerning the TTC as an evaluation measure in regular driving operation at low penetration rates by a road surface condition sensor by adjusting the safety distance as well as the speed. At very high penetration rates of automated systems in the overall fleet, improvements between 46 % and 53 % could be determined by the RSACC compared to the standard ACC. Concerning the RSCA ESB, it was shown that, on average, an almost 80 % increase in performance could be achieved compared to similar systems without lane condition knowledge, based on the effective avoidability of a collision.

Accordingly, this research question can be answered positively, with the restriction that a positive safety impact only occurs through using the WRSCS system in corresponding ADAS applications.

5.3.2 Efficiency

RQ3: Can the use of a WRSCS lead to an increase in efficiency?

For traffic efficiency, the results show that by knowing the road condition, a stabilizing effect occurs even in worse road conditions due to the better estimation of the driving dynamics limits, described by the increasing mean speed in all scenarios with increasing penetration. On average, the increase in efficiency across all scenarios tested was approximately 12 %.

In addition, efficiency was assessed based on changes in driven route lengths, travel times, and the development of the overall traffic pattern in the context of adaptive navigation. In all simulation runs where vehicle navigation led to increased driving safety and comfort, this was always accompanied by longer travel distances and increased travel times. Therefore, the effect of vehicle navigation on traffic efficiency is estimated to be opposite to the effect on driving safety and comfort. In simulation runs where many vehicles simultaneously tried to avoid or even avoid a rainy area, massive traffic congestion or even a complete standstill of traffic was observed.

While the stabilizing effect in the highway scenarios was an increase in efficiency due to higher average speeds overall, the system had a rather negative effect on efficiency in the urban scenarios due to longer distances, caused in part by more extensive detours and increased congestion induction due to avoidance behavior in certain areas. However, those results yield an opportunity for further research.

Therefore, this research question cannot be answered unambiguously overall.

5.3.3 Comfort

RQ4: Can the WRSCS be expected to have an impact on comfort?

Travel time in automated driving mode was used as a quantifiable metric in the evaluation of driving comfort. This was based on a survey that revealed that the additional time saved by relieving the driver of the driving task is seen as one of the main motivating factors for using an autonomous vehicle. As the penetration of communication-enabled vehicles increases, it is observed across all simulation scenarios that absolute travel time increases in automated driving. However, since absolute travel time alone has little informative value for driving comfort, it was also investigated in what proportion this increase comprises an increased total travel time and a reduction in manual travel times. It was found that the reduction in manual travel times amounted to a maximum of up to 60 %, while in other simulation runs, the reduction in manual travel times only accounted for just under 7 % of the increase in automated travel times. This meant reducing the average manual travel time of about 14 seconds with an additional average total travel time of about 125 seconds on the macroscopic traffic level.

Even if the increase of automated travel time was defined as a positive influence for the driving comfort, the observations lead to the further research question if and how much additional travel time drivers would accept in real traffic to reduce a part of their manual travel time. In addition, an interesting question would also be to what extent the information from the system can have a confidence-increasing effect on the driver as a passenger of automated driving systems through appropriate use in driver information systems and thus directly or indirectly influence the perceived comfort.

Therefore, the answer to RQ4 is clearly yes; a system to detect weather-related road conditions can impact driving comfort.

6 Conclusion and Outlook

This thesis investigates a priori the effectiveness of a weather-related road surface condition sensor on vehicle and traffic level concerning the impact dimensions of safety, efficiency, and comfort. The investigation required an extension of existing methods as none of these take all the addressed levels and dimensions into account. The extended methodology is modular, flexible, and allows the use of different tools and models, some of which are also newly developed. This Chapter briefly summarizes the results obtained and the scientific contributions and shows how the work can be continued in the future.

6.1 Summary

The thesis aims to a priori investigate the potential of a weather-related road surface condition sensor system in the context of future automotive development. For this purpose, an extended general method is derived as an extension to existing approaches, implemented, and successfully applied. Extended applicability characterizes the applied method compared to existing approaches, which is achieved by considering multidimensional aspects in all steps. The actual process includes a detailed system analysis and a stakeholder identification, which allow the formulation of specific research questions in the context of vehicle technology and its potential dimensions - namely safety, efficiency, and comfort. The system analysis showed that a system for detecting weather-related road conditions has a considerable influence on systems at all levels of the vehicle guidance task. Existing assistance systems in all categories can be improved, but a couple of entirely new applications are also conceivable. Several applications were selected for further investigation through stakeholder identification. The aim was to cover as wide an area of application as possible and to avoid organizational and institutional framework conditions as far as possible in order to preserve the scientific approach. These were then investigated in detail using suitable methods and tools, both at the individual vehicle level and at the overall traffic level, within the framework of several simulation studies. For this purpose, some of the tools have to be adapted and entirely newly developed to meet the requirements resulting from the novelty value of the sensor system. Besides the general methodology, this is the core of the scientific contribution of the thesis and will be summarized in more detail in the following subsection. The resulting framework was used to conduct a series of simulation studies on the system's potential impact at both the vehicle and

traffic levels to answer the various specific research questions. It was found that a sensor system for detecting weather-related road conditions has a significant potential to influence safety positively. This relates on the one hand to individual vehicle safety in terms of stabilization, expressed for example, in shorter braking distances and improved lateral stability, and on the other hand to the reduction in the number of safety-critical situations with accident potential at the traffic level through increased safety distances and adapted speeds. A consistently positive impact on comfort was also demonstrated in terms of an increase in automated driving times in which the driver can devote himself to another task and the associated increase in the availability of automated driving functions, which rely on knowledge of the dynamic driving limits. The consideration of efficiency produced an ambivalent result.

On the one hand, the system has been shown to stabilize traffic on highways. However, on the other hand, the increase in the total route length due to the bypassing of bad weather areas results in higher energy consumption and a tendency toward increased congestion in urban areas when many vehicles simultaneously travel on the same alternative routes. This ambivalence forms a good starting point for further future research approaches.

In summary, the central research question in this thesis can be answered as follows:

The systematic and methodical approach described above, applied to the example of a weather-related road surface condition sensor, allows a generalized a priori analysis and evaluation of the potential of future vehicle systems and functions.

6.2 Scientific Contribution

The main scientific contribution is the potential analysis of a weather-related road surface condition sensor regarding future automotive systems. The developed models and tool adaptations considering the WRSCS form the innovative core that can be used without restrictions in the future. These include, as already mentioned at the beginning and explained in detail in the course of the thesis:

- a valid digital sensor model,
- the expansion and optimization of several ADAS with entirely new functionality,
- the development of a weather module as an extension of the environment model,
- the development of a weather-related road surface condition aware driver model,
- the integration of the weather-related road surface condition into the ETSI V2X standard.

The second scientific contribution is the formulation of an extended research method, which enables the potentials and effects of future systems to be investigated a priori and at an early stage of development from different perspectives and concerning general or very specific research questions. Applying the method to the WRSCS shows that different levels and impact dimensions can be investigated side by side both on the vehicle level and the overall traffic level. The modularity also allows the use of optimized and problem-specific selected and adapted tools and thus allows

to achieve meaningful results. The approach also explicitly allows the integration of non-technical models, such as business or economic models, which is a desirable approach for further using the thesis results.

6.3 Outlook

A whole range of possible applications for the various contributions of the thesis has already been outlined in the course of this thesis. Especially the considerable safety potential of a weather-related road surface condition sensor through the integration of the corresponding information in automated vehicle guidance offers a starting point for further developments in this area. The investigated specific ADAS and AD systems, for instance, only represent a single implementation example and control technique, and a further investigation concerning the potential of using different control approaches might be an interesting extension of the present work.

Furthermore, the given research method offers the possibility of taking a more holistic view of issues beyond one-dimensional considerations since the ever-increasing complexity and connectivity of modern technical systems often leads to interdependencies that are often difficult to grasp in advance.

Concerning this thesis, a more detailed consideration of the economic implications of the aspects of safety in particular - for example, full-scale accident consequences up to considerations due to loss of life - and efficiency - for example, the effects and marginal costs due to energy consumption, air pollutants and noise (cf. (Schmid 2005)) and the integration of the corresponding modules into the simulation framework would be desirable in the future. The future challenges can only be considered and dealt with as a holistic problem. The great opportunity for institutional university science remains to play the crucial role at the interface between the various stakeholders of global society and think and act in an interdisciplinary manner.

Appendix

A Model Parameters

All model parameters are derived from literature: (Schuster 1998; Breuer and Bill 2012; Unterreiner 2014; Schramm et al. 2018)

Parameters	Symbol	Unit	Value
Vehicle			
Mass	m_{V}	kg	1506.5
Air drag coefficient	c_{w}	-	0.33
Flow surface	A_{L}	s/m	2.14
Steering ratio	i_{L}	-	16.3
COG height	h_{S}	m	0.5
Distance front axle to cog	l_{v}	m	1.1853
Distance rear axle to cog	l_{h}	m	1.5044
Track width front	s_{v}	m	1.4922
Track width rear	s_{h}	m	1.4874
Height of pivot point to COG	s_{z}	m	0.1
Intertia yaw	$\Theta_{\mathrm{V.zz}}$	kgm^2	2585.6
Inertia pitch	$\Theta_{\mathrm{V.yy}}$	kgm^2	345
Inertia roll	$\Theta_{\mathrm{V.xx}}$	kgm^2	2394.3
Front chassis spring stiffness	$c_{\mathrm{V,f}}$	Ns/m	34900
Rear chassis spring stiffness	$c_{\mathrm{V,r}}$	Ns/m	24600
Front chassis shock absorber stiffness	$d_{\mathrm{V,f}}$	Ns/m	4360
Rear chassis shock absorber stiffness	$d_{\mathrm{V,r}}$	Ns/m	3870
Stabilizer stiffness	$c_{\mathrm{St,f,r}}$	Nm/rad	2882
Drivetrain			
Gear ratio	$i_{\mathrm{G,1}}$	-	3.3
Gear ratio	$i_{\mathrm{G,2}}$	-	1.94
Gear ratio	$i_{\mathrm{G,3}}$	-	1.31
Gear ratio	$i_{\mathrm{G,4}}$	-	1.03
Gear ratio	$i_{\mathrm{G,5}}$	-	0.84
Gear ratio central differential	i_{D}	-	3.68
Coefficient for drive torque split	ξ_{a}	-	0
Engine inertia	Θ_{M}		0.07
Gearbox inertia input side	$\Theta_{\mathrm{V.xx}}$		0.016
Gearbox inertia output side	$\Theta_{\mathrm{V.xx}}$		0.01

Brakes			
Brake pedal ratio	i_{Ped}	-	5
Brake booster ratio	i_{Vs}	-	4.5
Spring constant return spring	$c_{\mathrm{F,Vs}}$	N/m	16000
Vacuum pressure brake booster	$p_{\mathrm{V,ac}}$	Pa	0.9E-5
Area of the brake booster	A_{Vs}	m^2	5.067E-2
Area of brake master cylinder	A_{HZ}	m^2	4.4488E-4
Front brake line length	$l_{\mathrm{Bl,f}}$	m	0.4
Rear brake line length	$l_{\mathrm{Bl,r}}$	m	0.5
Brake line diameter	d_{Bl}	m	0.0025
Brake fluid density	ρ_{Fluid}	kg/m^3	1062
Fluid velocity	v_{Fluid}	m/s	30
Viscosity of brake fluid	ν_{Fluid}	kg/ms	6.4E-6
Area of front/rear brake piston	$A_{\mathrm{BK,f,r}}$	m^2	2.285E-3
Effective front/rear brake radius	$r_{\mathrm{eff,f,r}}$	m	0.07
Friction coefficient of the brake linnings	μ_{lin}	-	0.4
Limiting pressure rear axle	$p_{\mathrm{hyd,h,max}}$	Pa	80E5

Tires			
Tire cross-section	B	mm	205
Height to width ratio	H	%	65
Rim diameter	R	inch	15
Mass of a tire	m_{T}	kg	17
Moment of inertia of the front tire	$\Theta_{\mathrm{T,f}}$	kgm^2	1,7
Moment of inertia of the rear tire	$\Theta_{\mathrm{T,r}}$	kgm^2	2
Vertical stiffness of the front/rear wheels	$c_{\mathrm{z,f,r}}$	N/m	253000
Lateral stress-strain coefficient of the tire tread	k_{α}	N/m^3	12500000
Longitudinal stress-strain coefficient of the tire tread	k_{s}	N/m^3	22508000
Degression parameter	e_{z}	-	0,05
Transition speed for low speed	v_{l}	m/s	6
Transition speed for tire standstill	v_{s}	m/s	0,01
Position of the undeformed tread element	x_{u}	m	2E-6
Damping constant for tire standstill	$d_{\mathrm{s,x/y}}$	Ns/m	1.2E4
Spring constant for tire standstill	$c_{\mathrm{s,x/y}}$	N/m	1.2E6
Inertia factor for front force buildup	$k_{\mathrm{T,f}}$	-	1
Inertia factor for rear force buildup	$k_{\mathrm{T,r}}$	-	1

Environment			
Gravitational acceleration	g	m/s^2	9.81
Air density	ρ_{L}	kg/m^3	1.293
Force factor between road and tire	k_{R}	s/m	0.3
Force factor between road and tire	a	-	0.3
Coefficient of friction road-tire	μ	-	1.2 - 0.2

B Sensor Model Cluster Analysis

In the following, the results of the measured value analysis for the remaining clusters from the sensor modeling in Section 4.3.2 are given.

Damp

Figure B.1 shows that a significantly broader database is available for this cluster. Again, the upper graph shows the measured values of the data cluster "moist" and the corresponding filtered data for a window width of 500 data points. The lower graph shows the corresponding relative deviation from each other.

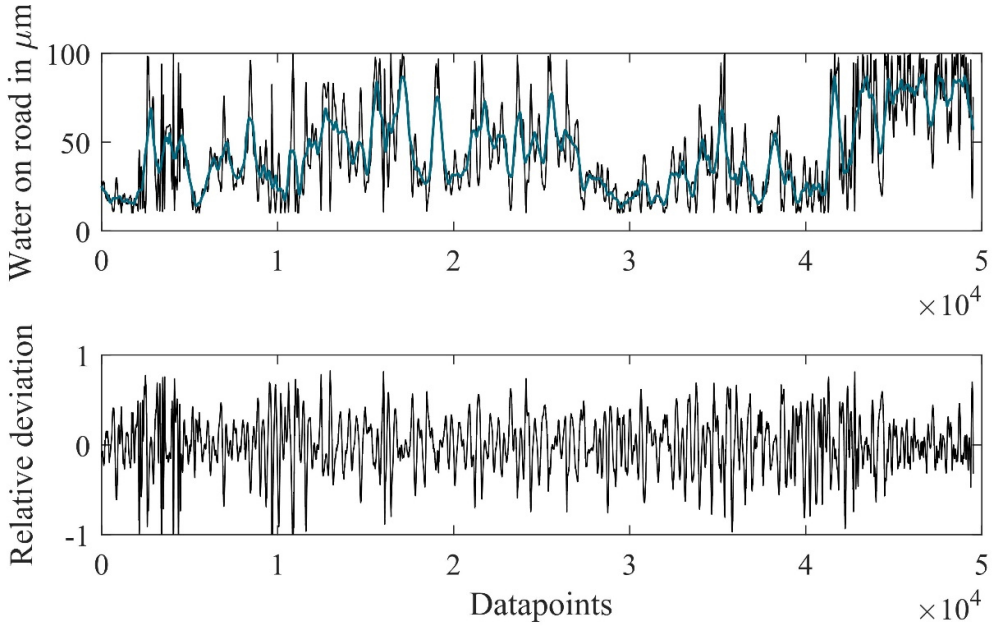

Figure B.0.1: Measured value analysis of cluster “moist”

The graphical preparation of the frequency distribution and the best fits for the probability density distribution is shown in Figure B.0.2. It was found that a normal distribution could rather be assumed in this case, although both forms of distribution could be considered here as well. The respective parameters were k = -0.3537, σ=0.3271 and μ = -0.0869 for the GEV and μ = 0.0121 and σ= 0.3087 for the normal distribution.

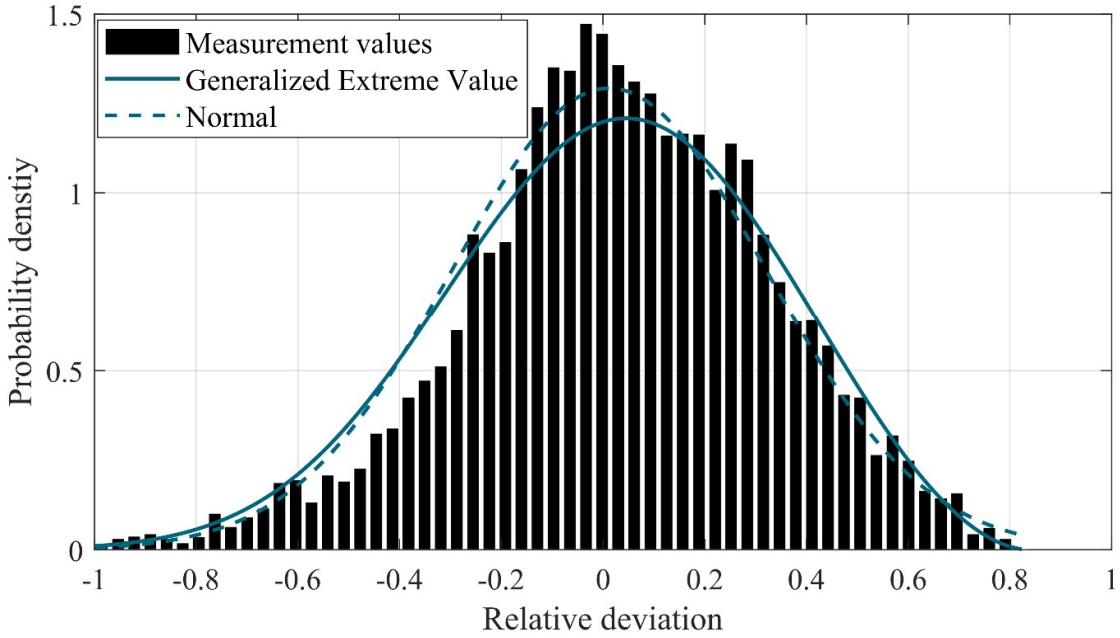

Figure B.0.2: Distributions of the relative measured value deviations of the cluster “damp”

Wet

Figure B.0.3 shows the results of the measured value analysis for the cluster “wet”.

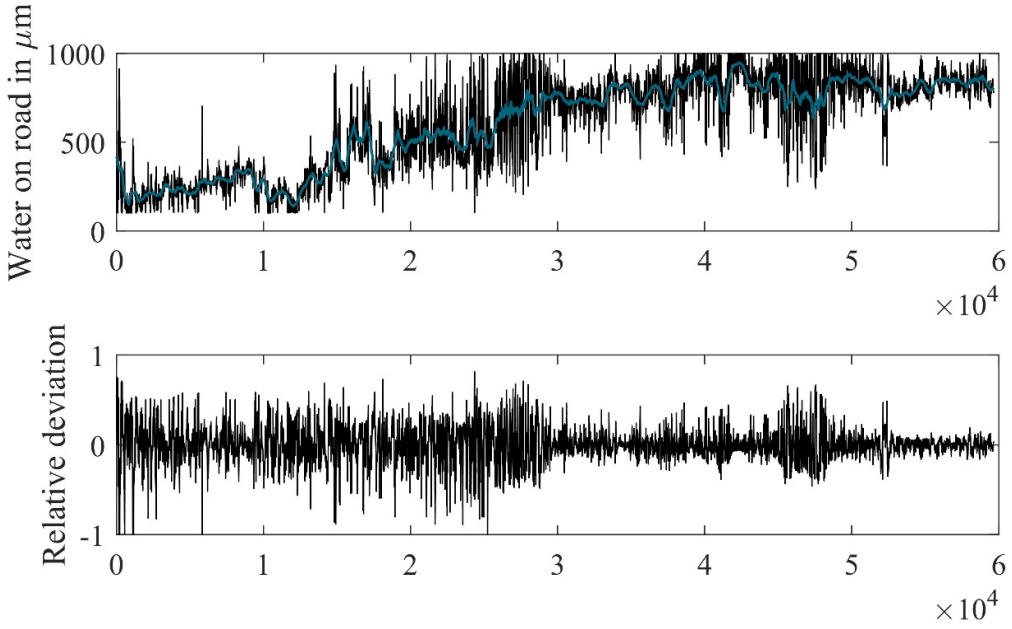

Figure B.0.3: Measured value analysis of cluster “wet”

Like the cluster “damp”, a normal distribution of the relative deviations of the measured values from the real value was more likely to be assumed in this case. However, both sets of parameters

were again extracted: k = -0.2482, σ=0.2201 and μ = -0.0728 for the GEV and μ = 0.0015 and σ= 0.1980 for the normal distribution given in Figure B.0.4.

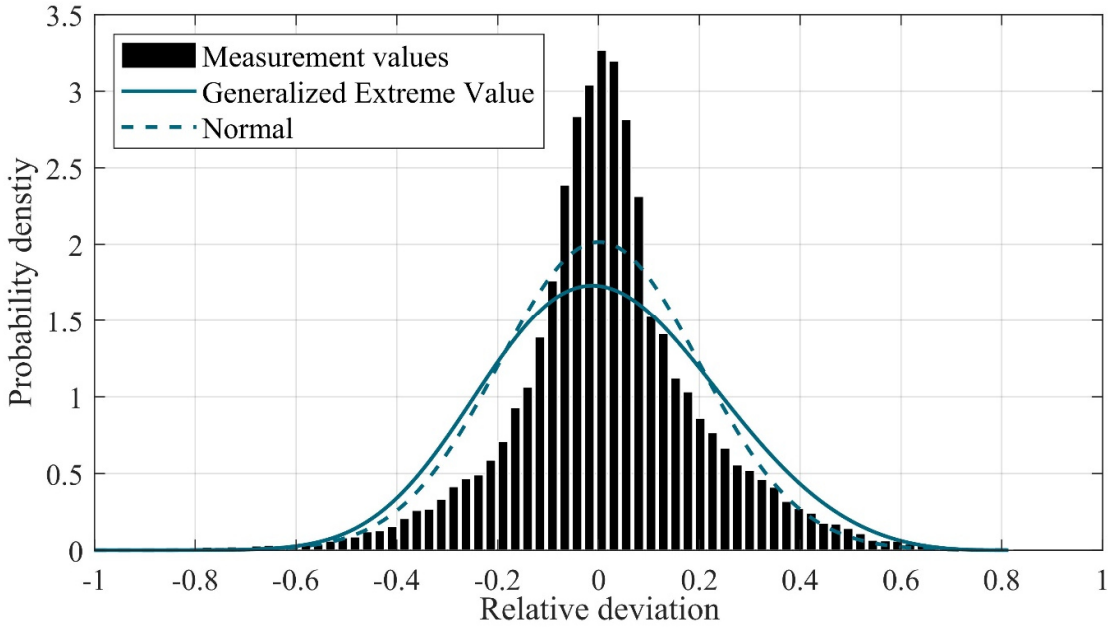

Figure B.0.4: Distributions of the relative measured value deviations of the cluster “wet”

Slippery

Figure B.0.5 shows the results of the measured value analysis for the cluster “slippery”.

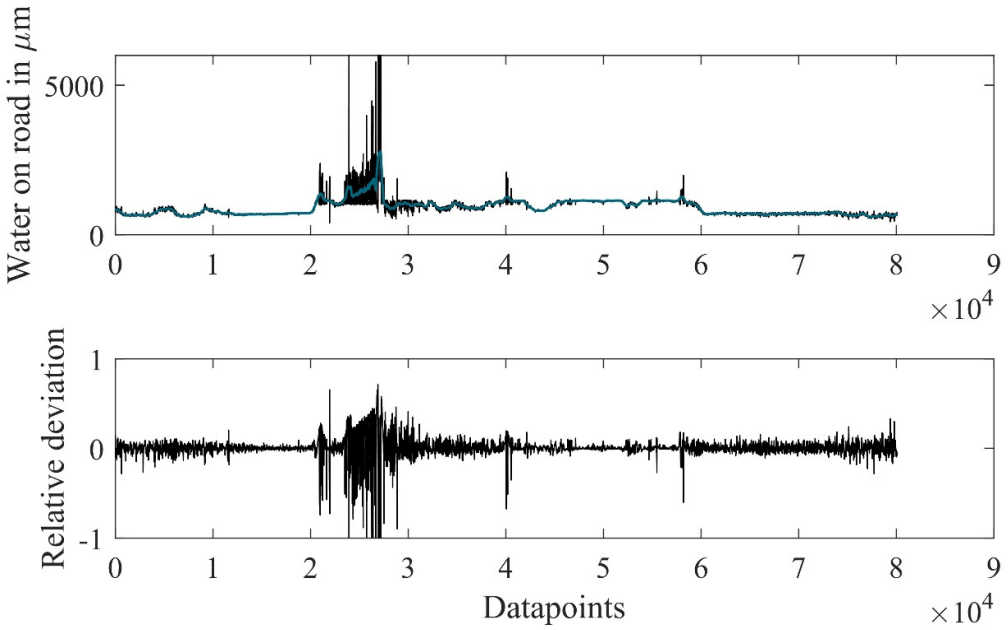

Figure B.0.5: Measured value analysis of cluster “slippery”

The cluster “slippery” is characterized by a relatively high proportion of small relative deviations. In this case, a normal distribution of the relative deviations of the measured values is preferable to a GEV. The respective parameter sets are: k = -0.2635, σ=0.1995 and μ = -0.0449 for the GEV and μ = 0.0005 and σ= 0.1152 for the normal distribution shown in Figure B.0.6.

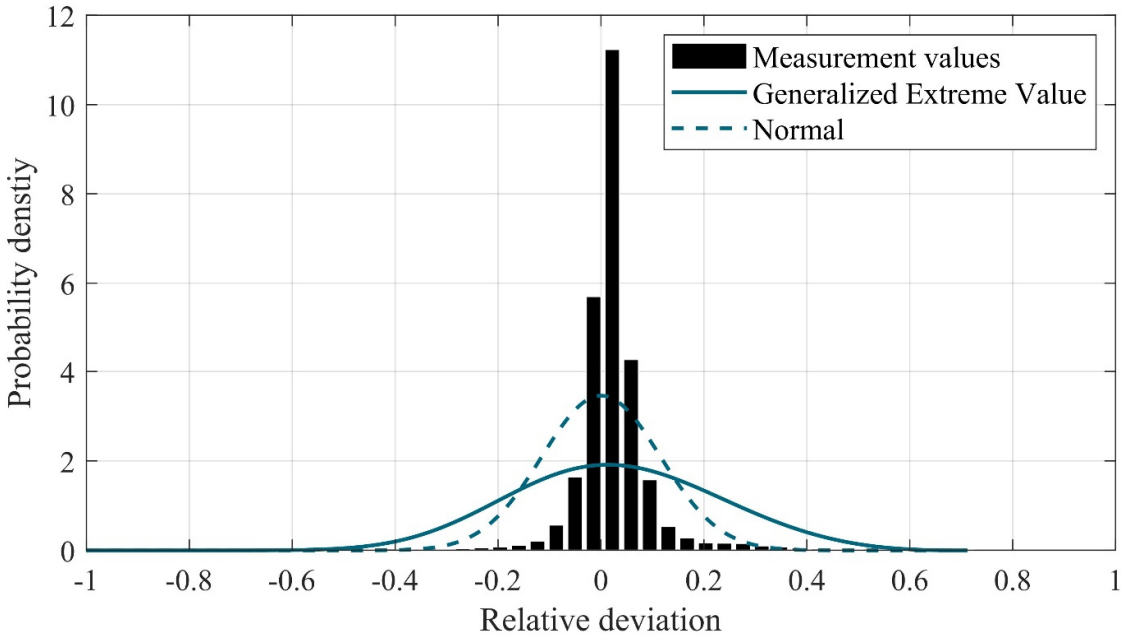

Figure B.0.6: Distributions of the relative measured value deviations of the cluster “wet”

C Overview of selected traffic simulation tools

Tools	Level			Available Models: Car Following								Available Models: Lane Change					Cross Platform		Open Source	
	micro	meso	macro	(Gazis et al. 1961)	(Wiedemann 1974)	(Gipps 1981)	(Fritzsche 1994)	(Krauß 1998)	(Ahmed 1999)	(Toledo et al. 2007)	(Milanés and Shladover 2014)	(Sparmann 1978)	(Gipps 1986)	(Fritzsche 1994)	(Krajzewicz 2009)	(Jakob Erdmann 2014)	yes	no	yes	no
AIMSUN	x	x	x			x							x				x			x
MITSIMlab	x			x					x	x			x					x	x	
PARAMICS	x						x							x				x		x
SUMO	x	x			x	x		x			x				x	x	x		x	
VISSIM	x				x							x						x		x

References

Abdulle, Assyr; Wanner, Gerhard (2002): 200 years of least squares method. In *Elem. Math.* 57 (2), pp. 45–60. DOI: 10.1007/PL00000559.

Adameck, Markus (2011): Magna Electronics Ko-KOMP : Schlussbericht ; Forschungsinitiative KO-FAS. With assistance of TIB-Technische Informationsbibliothek Universitätsbibliothek Hannover, Technische Informationsbibliothek (TIB).

Agarwal, Manish; Maze, Thomas; Souleyrette, Reginald (2005): Impacts of Weather on Urban Freeway Traffic Flow Characteristics and Facility Capacity. In: Proceedings of the 2005 Mid-Continent Transportation Research Symposium. Mid-Continent Transportation Research Symposium. Ames. Iowa State University. Ames: Iowa State University.

Ahmed, Kazi Iftekhar (1999): Modeling Drivers' Acceleration and Lane Changing Behavior. Dissertation. Massachusetts Institute of Technology, Massachusetts. Transportation Systems and Decision Sciences.

Alvarez Lopez, Pablo; Behrisch, Michael; Bieker-Walz, Laura; Erdmann, Jakob; Flötteröd, Yun-Pang; Hilbrich, Robert et al. (2018): Microscopic Traffic Simulation using SUMO. In: 21st IEEE International Conference on Intelligent Transportation Systems (ITSC). Maui, USA, Nov. 4-7: IEEE.

Ammon, Dieter (1997): Modellbildung und Systementwicklung in der Fahrzeugdynamik. Stuttgart: B. G. Teubner.

Arnott, Richard; Small, Kenneth (1994): The Economics of Traffic Congestion. In *American Scientist* 82 (5), pp. 446–455. Available online at http://www.jstor.org/stable/29775281.

Baldessari, Roberto; Bödekker, Bert; Deegener, Matthias; Festag, Andreas; Franz, Walter; Kellum, C. Christopher et al. (2007): CAR 2 CAR Communication Consortium Manifesto; Overview of the C2C-CC System. CAR 2 CAR Communication Consortium.

Barr, Rimon; Haas, Zygmung; van Renesse, R. (2004): JiST/ SWANS; Java in Simulation Time / Scalable Wireless Ad hoc Network Simulator. Cornell University. Cornell. Available online at http://jist.ece.cornell.edu/docs/040309-wnl.pdf, checked on 2/5/2021.

Bartels, Arne; Ruchatz, Thomas (2015): Einführungsstrategie des Automatischen Fahrens. In *at - Automatisierungstechnik* 63 (3), pp. 168–179.

BASt (2012): Technische Lieferbedingungen für Streckenstationen; TLS 2012. Available online at https://www.bast.de/BASt_2017/DE/Publikationen/Regelwerke/Verkehrstechnik/Unterseiten/V5-tls-2012.pdf?__blob=publicationFile&v=1, checked on 5/17/2021.

BAST (2018): Automatische Zählstellen auf Autobahnen und Bundesstraßen, checked on 12/18/2018.

BAST (2021): Fachthemen – Verkehrstechnik - Automatische Zählstellen auf Autobahnen und Bundesstraßen. Available online at https://www.bast.de/BASt_2017/DE/Verkehrstechnik/Fachthemen/v2-verkehrszaehlung/Stundenwerte.html, updated on 1/4/2021, checked on 1/4/2021.

Baur, Mathias (2015): Modellierungsrahmen für Intelligente Verkehrssysteme zur simulationsbasierten Analyse ihrer Wirkungen auf den Straßenverkehr. Dissertation. München, Technische Universität, München. Ingenieurfakultät Bau Geo Umwelt.

Bellem, Hanna; Thiel, Barbara; Schrauf, Michael; Krems, Josef F. (2018): Comfort in automated driving: An analysis of preferences for different automated driving styles and their dependence on personality traits. In *Transportation Research Part F: Traffic Psychology and Behaviour* 55, pp. 90–100. DOI: 10.1016/j.trf.2018.02.036.

Ben Mussa, Sofian Ali; Manaf, Mazani; Ghafoor, Kayhan Zrar; Doukha, Zouina (2015): Simulation tools for vehicular ad hoc networks: A comparison study and future perspectives. In: International Conference on Wireless Networks and Mobile Communications (WINCOM'15). With assistance of Said Amzazi. Marrakech, Morocco, 10/20/2015 - 10/23/2015. Piscataway, NJ: IEEE, pp. 1–8.

Ben-Akiva, Moshe; Koutsopoulos, Haris N.; Toledo, Tomer; Yang, Qi; Choudhury, Charisma F.; Antoniou, Constantinos; Balakrishna, Ramachandran (2010): Traffic Simulation with MITSIMLab. In Jaume Barceló (Ed.): Fundamentals of traffic simulation, vol. 145. 1. Aufl. New York, NY: Springer (International series in operations research management science, 145), pp. 233–268.

Bengler, Klaus; Dietmayer, Klaus; Farber, Berthold; Maurer, Markus; Stiller, Christoph; Winner, Hermann (2014): Three decades of driver assistance systems; Review and future perspectives. In *IEEE Intelligent transportation systems magazine* 6 (4), pp. 6–22.

Benmimoun, Mohamed; Fahrenkrog, Felix; Zlocki, Adrian; Eckstein, Lutz (2011): Incident detection based on vehicle CAN-data within the large scale field operational test "euroFOT". In: 22nd Enhanced Safety of Vehicles Conference. Enhanced Safety of Vehicles Conference. Washington D.C.

Benz, Thomas; Christen, Fréderic; Lerner, Georg; Schulze, Matthias; Vollmer, Dieter (2002): Traffic Effects of Driver Assistance Systems–The Approach within INVENT-VRA. In *Telematik im Kraftfahrzeug*, pp. 1–18.

Boyraz, Emre (2019): Ein Beitrag zur objektiven Bewertung der dynamischen Eigenschaften von Luftfedern. DuEPublico: Duisburg-Essen Publications online, University of Duisburg-Essen, Germany.

Breuel, Gabi (2014): Kooperative Perzeption : Forschungsinitiave Ko-FAS - Verbundprojekt Ko-PER: [Fahrerassistenz und präventive Sicherheit mittels kooperativer Perzeption] : Abschlussbericht Projektpartner Daimler ; Berichtszeitraum: 30.10.2009 bis 30.11.2013. With assistance of Technische Informationsbibliothek (TIB).

Breuer, Bert; Bill, Karlheinz H. (Eds.) (2012): Bremsenhandbuch; Grundlagen, Komponenten, Systeme, Fahrdynamik. 4th ed. Wiesbaden: Springer Vieweg (ATZ / MTZ-Fachbuch).

Brilon, Werner; Geistefeldt, Justin (2010): Überprüfung der Bemessungswerte des HBS für Autobahnabschnitte außerhalb der Knotenpunkte. In *Forschung Strassenbau und Strassenverkehrstechnik* (1033).

Brilon, Werner; Ponzlet, Martin (1996): Variability of Speed-Flow Relationships on German Autobahns. In *Transportation Research Record* 1555 (1), pp. 91–98. DOI: 10.1177/0361198196155500112.

Brustad, Tanita Fossli; Pedersen, Aleksander; Bang, Børre (2020): A field study of sensors for winter road assessment. In *Transportation Research Interdisciplinary Perspectives* 7, p. 100206. DOI: 10.1016/j.trip.2020.100206.

Bundesministerium für Verkehr und digitale Infrastruktur (BMVI) (2015): Verkehrssicherheitsprogramm. Referat La 26. Berlin.

Burckhardt, Manfred (1993): Fahrwerktechnik; Radschlupf-Regelsysteme: Vogel.

Cacciabue, Pietro Carlo (2007): Modelling Driver Behaviour in Automotive Environments; Critical Issues in Driver Interactions with Intelligent Transport Systems. London: Springer.

Chang, Xinjie (1999): Network simulations with OPNET. In Phillip A. Farrington (Ed.): 1999 Winter Simulation Conference proceedings. Phoenix, AZ, USA, 5-8 Dec. 1999. New York: Association for Computing Machinery, pp. 307–314.

Corbridge, Colin (1987): Vibration in vehicles: its effect on comfort. Doctoral. University of Southampton. Institute of Sound and Vibration Research. Available online at https://eprints.soton.ac.uk/52265/.

Cormen, Thomas H.; Leiserson, Charles Eric; Rivest, Ronald Linn; Stein, Clifford (2013): Algorithmen - eine Einführung; Introduction to algorithms. 4., durchgesehene und korrigierte Auflage. München: Oldenbourg Verlag.

Cornet, Andreas; Mohr, Detlev; Weig, Florian; Zerlin, Benno; Hein, Arnt-Philipp (2012): Mobility of the future - Opportunities for automotive OEMs. McKinsey & Company, Inc. Stuttgart, München.

Daimler AG (2017). Available online at http://www.drive-c2x.eu/project, checked on 10/9/2017.

Daimler AG (2020): Mit der Umgebung vernetzt.; Car-to-X Kommunikation geht in Serie. Available online at https://www.daimler.com/innovation/case/connectivity/car-to-x.html, checked on 12/21/2020.

David, F. W.; Nolle, H. (1982): Experimental Modelling in Engineering. Burlington: Elsevier Science. Available online at http://gbv.eblib.com/patron/FullRecord.aspx?p=1837866.

SAE J2945:2017: Dedicated Short Range Communication (DSRC); Systems Engineering Process Guidance for SAE J2945/X Documents and Common Design Concepts.

Deering, Stephen; Hinden, Robert (1998): Internet Protocol, version 6 (IPv6) Specification.

Destatis (2018): Unfallentwicklung auf deutschen Straßen 2017; Begleitmaterial zur Pressekonferenz am 12. Juli 2018 in Berlin. Accident trends on German roads in 2017. Berlin.

Detering, Stefan (2011): Kalibrierung und Validierung von Verkehrssimulationsmodellen zur Untersuchung von Verkehrsassistenzsystemen. Dissertation. Universität Braunschweig. Fakultät für Maschinenbau. Available online at https://publikationsserver.tu-braunschweig.de/receive/dbbs_mods_00038450.

Dijkstra, E. W. (1959): A note on two problems in connexion with graphs. In *Numer. Math.* 1 (1), pp. 269–271. DOI: 10.1007/BF01386390.

DLR (2021): Activity-based Demand Generation - SUMO Documentation. Available online at https://sumo.dlr.de/docs/Demand/Activity-based_Demand_Generation.html, updated on 4/20/2021, checked on 4/20/2021.

Donges, Edmund (1982): Aspekte der aktiven Sicherheit bei der Führung von Personenkraftwagen. In *Automobil-Industrie* 27 (2), pp. 183–190.

Driesch, P.; Weber, T.; Tewiele, S.; Schramm, D. (2019): Energiebedarf von elektrisch und verbrennungsmotorisch angetriebenen Kraftfahrzeugen in Abhängigkeit von Zuladung und Verkehrsumfeld. In Heike Proff (Ed.): Mobilität in Zeiten der Veränderung. Vergangenheit Gegenwart Zukunft. Wiesbaden: Springer Gabler, pp. 297–317.

Dugoff, Howard; Fancher, Paul S.; Segel, Leonard (1969): Tire performance characteristics affecting vehicle response to steering and braking control inputs.

EC (2009): Regulation (EC) No 661/2009 of the European Parliament and of the Council of 13 July 2009 concerning type-approval requirements for the general safety of motor vehicles, their trailers and systems, components and separate technical units; EC. In *Official Journal of the European Communities* 200, pp. 1–24.

Eckert, Alfred; Hartmann, Bernd; Sevenich, Martin; Rieth, P. (2011): Emergency steer & brake assist: a systematic approach for system integration of two complementary driver assistance systems. In. 22nd International Technical Conference on the Enhanced Safety of Vehicles (ESV), pp. 13–16.

Eichhorn, Andreas von (2014): Querverkehrsassistenz unter Berücksichtigung von Unsicherheiten aus Sensorik und Prädiktion. Dissertation. University Duisburg-Essen, Duisburg. Mechatronics.

Elyasi-Pour, Roya (2015): Simulation Based Evaluation of Advanced Driver Assistance Systems. Licentiate. University, Linköping, Norrköping. Department of Science and Technology.

Etemad, Aria (2017): AdaptIVe; Final project results. Wolfsburg ((None)).

EU (2019): REGULATION (EU) 2019/631 OF THE EUROPEAN PARLIAMENT AND OF THE COUNCIL; EU. In *Official Journal of the European Union;* 111, pp. 13–53.

European Commission (EC) (2011): WHITE PAPER; Roadmap to a Single European Transport Area – Towards a competitive and resource efficient transport system. Brussels.

Fagnant, Daniel J.; Kockelman, Kara (2015): Preparing a nation for autonomous vehicles: opportunities, barriers and policy recommendations. In *Transportation Research Part A: Policy and Practice* 77, pp. 167–181. DOI: 10.1016/j.tra.2015.04.003.

Fahrenkrog, Felix (2016): Wirksamkeitsanalyse von Fahrerassistenzsystemen in Bezug auf die Verkehrssicherheit. Dissertation. RWTH Aachen, Aachen. Fakultät für Maschinenwesen.

Festag, Andreas (2015): Standards for vehicular communication—from IEEE 802.11p to 5G. In *e & i Elektrotechnik und Informationstechnik* 132 (7), pp. 409–416. DOI: 10.1007/s00502-015-0343-0.

Festner, Michael (2019): Objektivierte Bewertung des Fahrstils auf Basis der Komfortwahrnehmung bei hochautomatisiertem Fahren in Abhängigkeit fahrfremder Tätigkeiten: Grundlegende Zusammenhänge zur komfortorientierten Auslegung eines hochautomatisierten Fahrstils. DuEPublico: Duisburg-Essen Publications online, University of Duisburg-Essen, Germany.

Fiala, Ernst (2006): Mensch und Fahrzeug; Fahrzeugführung und sanfte Technik. Wiesbaden: Friedr. Vieweg & Sohn Verlag | GWV Fachverlage GmbH Wiesbaden. Available online at http://gbv.eblib.com/patron/FullRecord.aspx?p=748491.

Forkel, Ingo; Riihijärvi, Janne; Gerwig, Olaf (2020): LTE-Mobilfunkversorgung in Deutschland. umlaut. Aachen.

Fritzsche, Hans-Thomas (1994): A model for traffic simulation. In *Traffic Engineering+ Control* 35 (5), pp. 317–321.

Gaitanidou, Evangelia; Bekiaris, Evangelos (2012): Data Analysis Plan for Traffic Efficiency in TeleFOT Project. In *Procedia - Social and Behavioral Sciences* 54, pp. 294–301. DOI: 10.1016/j.sbspro.2012.09.748.

Gasser, Tom M.; Arzt, Clemens; Ayoubi, Mihiar; Bartels, Arne; Eier, Jana; Flemisch, Frank et al. (2012): Rechtsfolgen zunehmender Fahrzeugautomatisierung. BAST. Bergisch-Gladbach (Berichte der Bundesanstalt für Straßenwesen, F 83).

Gazis, Denos C.; Herman, Robert; Rothery, Richard W. (1961): Nonlinear Follow-the-Leader Models of Traffic Flow. In *Operations Research* 9 (4), pp. 545–567. DOI: 10.1287/opre.9.4.545.

Gennarelli, Thomas A.; Wodzin, Elaine (2006): AIS 2005: a contemporary injury scale. In *Injury* 37 (12), pp. 1083–1091. DOI: 10.1016/j.injury.2006.07.009.

Gipps, P. G. (1981): A behavioural car-following model for computer simulation. In *Transportation Research Part B: Methodological* 15 (2), pp. 105–111. DOI: 10.1016/0191-2615(81)90037-0.

Gipps, P. G. (1986): A model for the structure of lane-changing decisions. In *Transportation Research Part B: Methodological* 20 (5), pp. 403–414. DOI: 10.1016/0191-2615(86)90012-3.

Goodwin, Lynette C. (2002): Weather impacts on arterial traffic flow. inc, Mitretek systems. Washingtion.

Greenshields, B. D.; Bibbins, J. R.; Channing, W. S.; Miller, H. H. (1935): A Study of Traffic Capacity. In: Highway Research Board Proceedings (14).

Halfmann, Christoph; Holzmann, Henning (2013): Adaptive Modelle für die Kraftfahrzeugdynamik: Springer-Verlag.

Hart, Peter; Nilsson, Nils; Raphael, Bertram (1968): A Formal Basis for the Heuristic Determination of Minimum Cost Paths. In *IEEE Trans. Syst. Sci. Cyber.* 4 (2), pp. 100–107. DOI: 10.1109/TSSC.1968.300136.

Hartwich, Franziska; Beggiato, Matthias; Krems, Josef F. (2018): Driving comfort, enjoyment and acceptance of automated driving - effects of drivers' age and driving style familiarity. In *Ergonomics* 61 (8), pp. 1017–1032. DOI: 10.1080/00140139.2018.1441448.

Henderson, Thomas R.; Lacage, Mathieu; Riley, George F.; Dowell, Craig; Kopena, Joseph (2008): Network simulations with the ns-3 simulator. In *SIGCOMM demonstration* 14 (14), p. 527.

Hesse, Benjamin (2011): Wechselwirkung von Fahrzeugdynamik und Kfz-Bordnetz unter Berücksichtigung der Fahrzeugbeherrschbarkeit. Universität Duisburg-Essen, Duisburg. Fakultät für Ingenieurwissenschaften. Available online at https://duepublico.uni-due.de/servlets/DocumentServlet?id=27329.

Hiesgen, Gregor (2011): Effiziente Entwicklung eines menschenzentrierten Querführungsassistenzsystems mit einem Fahrsimulator. Universität Duisburg-Essen, Duisburg. Fakultät für Ingenieurwissenschaften. Available online at https://duepublico.uni-due.de/servlets/DocumentServlet?id=27272.

Hiller, Manfred (1983): Mechanische Systeme; Eine Einf. in d. analytische Mechanik u. Systemdynamik. Mit 51 Abb. Berlin, Heidelberg usw.: Springer ((Hochschultext.)).

Hoffmann, Silja (2013): Mikroskopische Modellierung und Bewertung von verkehrssicherheitskritischen Situationen. Dissertation. München, Technische Universität, München. Ingenieurfakultät Bau Geo Umwelt.

ETSI TR 101 607; Intelligent Transport Systems (ITS); Cooperative ITS (C-ITS); Release 1.

ISO/IEC 9075:2016: Information technology; Database languages - SQL.

ISO 15622:2018: Intelligent transport systems - Adaptive cruise control systems - Performance requirements and test procedures.

ISO 22179:2009: Intelligent transport systems — Full speed range adaptive cruise control (FSRA) systems; Performance requirements and test procedures.

ETSI TS 103 097: Intelligent Transport Systems (ITS); Security; Security header and certificate formats.

ETSI TS 102 941:1.2.1: Intelligent Transport Systems (ITS); Security; Trust and Privacy Management.

ETSI TS 101 539-1:V1.1.1, 2013: Intelligent Transport Systems (ITS); V2X Applications; Part 1: Road Hazard Signalling (RHS) application requirements specification. Available online at https://www.etsi.org/deliver/etsi_ts/101500_101599/10153901/01.01.01_60/ts_10153901v010101p.pdf, checked on 5/17/2021.

ETSI EN 302 895:V1.1.1, 2014: Intelligent Transport Systems (ITS); Vehicular Communications; Basic Set of Applications; Local Dynamic Map (LDM). Available online at https://www.etsi.org/deliver/etsi_en/302800_302899/302895/01.01.01_60/en_302895v010101p.pdf, checked on 5/17/2021.

ETSI TS 102 637-1: Intelligent Transport Systems (ITS); Vehicular Communications; Basic Set of Applications; Part 1; Functional Requirements.

ETSI EN 302 637-3:1.2.1: Intelligent Transport Systems (ITS); Vehicular Communications; Basic Set of Applications; Part 3; Specifications of Decentralized Environmental Notification Basic Service.

ETSI EN 302 636: Intelligent Transport Systems (ITS); Vehicular Communications; GeoNetworking.

ETSI EN 302 637-2:1.3.1: Intelligent Transport Systems (ITS);Vehicular Communications; Basic Set of Applications; Part 2: Specification of Cooperative Awareness Basic Service.

Jakob Erdmann (2014): Lane-Changing Model in SUMO. In: SUMO2014, vol. 24: Deutsches Zentrum für Luft- und Raumfahrt e.V (Reports of the DLR-Institute of Transportation Systems Proceedings), pp. 77–88. Available online at https://elib.dlr.de/89233/.

Kanning, Bastian (2020): Sensorsystem zur autonomen Fahrbahnzustandserkennung (SEEROAD) : Schlussbericht : Teilvorhabenbezeichnung: "Elektrodenstrukturen, Sensorelektronik und Sensorintegration" : Laufzeit: 1. März 2017-29.Februar 2020. With assistance of TIB-Technische Informationsbibliothek Universitätsbibliothek Hannover.

KBA (2021): Kraftfahrt-Bundesamt - Inländerfahrleistung - Verkehr in Kilometern - Inländerfahrleistung. Available online at https://www.kba.de/DE/Statistik/Kraftverkehr/VerkehrKilometer/vk_inlaenderfahrleistung/vk_inlaenderfahrleistung_inhalt.htm, updated on 4/27/2021, checked on 4/27/2021.

Kenney, John B. (2011): Dedicated Short-Range Communications (DSRC) Standards in the United States. In *Proceedings of the IEEE* 99 (7), pp. 1162–1182.

Klempau, Frank (2003): Untersuchungen zum Aufbau eines Reibwertvorhersagesystems im fahrenden Fahrzeug. Dissertation. Darmstadt, Technische Universität, Darmstadt. Fachbereich Maschinenbau.

Korte, Matthias (2020): Sensorsystem zur autonomen Fahrbahnzustandserkennung (SEEROAD) : Abschlussbericht : Teilvorhabenbezeichnung: Datenfusionsalgorithmus, Sensordatenplausibilisierung : Laufzeit: 01. März 2017-29.Februar 2020 : Berichtszeitraum: 01. März 2017-29. Februar 2020. Würzburg. Available online at https://www.tib.eu/de/suchen/id/TIBKAT%3A1736562312.

Koskinen, Sami; Peussa, Pertti (Eds.) (2009): FRICTI@N; Final Report - Public. With assistance of Timo Varpula, Matti Kutila, Marco Pesce, Michael Köhler, Thomas Hüsemann, Christian Hartweg et al.

Kraft, Dieter (1988): A Software Package for Sequential Quadratic Programming. With assistance of Forschungsberich Flugmechanik/Flugführung, Institut für Dynamik der Flugsysteme, Abteilung Regelung. Deutsche Forschungs- und Versuchsanstalt fur Luft- und Raumfahrt. Oberpfaffenhofen (Forschungsbericht, 0171-1342).

Krajzewicz, Daniel (2009): Kombination von taktischen und strategischen Einflüssen in einer mikroskopischen Verkehrsflusssimulation. In Thomas Jürgensohn (Ed.): Fahrermodellierung in Wissenschaft und Wirtschaft. 2. Berliner Fachtagung Fahrermodellierung, 19. - 20. Juni 2008. Als. Ms. gedr. Düsseldorf: VDI-Verl. (Fortschritt-Berichte VDI Reihe 22, Mensch-Maschine-Systeme, 28).

Krallmann, Hermann; Bobrik, Annette; Levina, Olga (2013): Systemanalyse im Unternehmen. München: Oldenbourg Wissenschaftsverlag Verlag.

Krauß, Stefan (1998): Microscopic Modeling of Traffic Flow; Investigation of Collision Free Vehicle Dynamics. Köln, Universität zu.

Krefeld (2021): Einwohner | Stadt Krefeld. Available online at https://www.krefeld.de/de/buergerservice/einwohner/, updated on 4/20/2021, checked on 4/20/2021.

Krieger, Karl-Ludwig; Döring, Jakob; Tharmakularajah, Lakshan (2020): Sensorsystem zur autonomen Fahrbahnzustandserkennung (SEEROAD) : Abschlussbericht : Laufzeit: 1. März 2017-29- Februar 2020. Bremen. Available online at https://www.tib.eu/de/suchen/id/TIBKAT%3A1737951398.

Lankes, Erich (2014): Schlussbericht Ko-TAG "Rundumsicherheit" : Forschungsinitiative Ko-FAS - Verbundprojekt Ko-TAG. With assistance of TIB-Technische Informationsbibliothek Universitätsbibliothek Hannover, Technische Informationsbibliothek (TIB).

Leister, Günter (2015): Fahrzeugräder-Fahrzeugreifen; Entwicklung-Herstellung-Anwendung. 2., überarbeitete und ergänzte Auflage. Wiesbaden: Springer Vieweg.

Lengyel, Henrietta; Tettamanti, Tamas; Szalay, Zsolt (2020): Conflicts of Automated Driving With Conventional Traffic Infrastructure. In *IEEE Access* 8, pp. 163280–163297. DOI: 10.1109/ACCESS.2020.3020653.

Ma, Xiaoyi; Hu, Xiaowei; Weber, Thomas; Schramm, Dieter (2021): Experiences with Establishing a Simulation Scenario of the City of Duisburg with Real Traffic Volume. In *Applied Sciences* 11 (3), p. 1193. DOI: 10.3390/app11031193.

Mahrenholz, D.; Ivanov, S. (2004): Real-Time Network Emulation with ns-2. In Stephen J. Turner (Ed.): Proceedings. 8th IEEE International Symposium on Distributed Simulation and Real-Time Applications. Budapest, Hungary, 21-23 Oct. 2004: IEEE Computer Society, pp. 29–36.

Markel, T.; Brooker, A.; Hendricks, T.; Johnson, V.; Kelly, K.; Kramer, B. et al. (2002): ADVISOR: a systems analysis tool for advanced vehicle modeling. In *Journal of Power Sources* 110 (2), pp. 255–266. DOI: 10.1016/S0378-7753(02)00189-1.

Maurer, Markus; Gerdes, J. Christian; Lenz, Barbara; Winner, Hermann (2015): Autonomes Fahren; technische, rechtliche und gesellschaftliche Aspekte: Springer-Verlag.

Maurer, Thomas; Knoop, Steffen; Schramm, Dieter (2012): Barrieren in der Umfelderfassung für autonome Notbrems- und Ausweichsysteme. In Heike Proff, Jörg Schönharting, Dieter Schramm, Jürgen Ziegler (Eds.): Zukünftige Entwicklungen in der Mobilität. Betriebswirtschaftliche und technische Aspekte. Wiesbaden: Springer Gabler, pp. 175–188.

Michon, John A. (1985): A Critical View of Driver Behavior Models; What Do We Know, What Should We Do? In Leonard Evans, Richard C. Schwing (Eds.): Human Behavior and Traffic Safety. N. Boston: Springer US, pp. 485–524.

Milanés, Vicente; Shladover, Steven E. (2014): Modeling cooperative and autonomous adaptive cruise control dynamic responses using experimental data. In *Transportation Research Part C: Emerging Technologies* 48, pp. 285–300. DOI: 10.1016/j.trc.2014.09.001.

Minderhoud, Michiel M.; Bovy, Piet H. L. (2001): Extended time-to-collision measures for road traffic safety assessment. In *Accident Analysis & Prevention* 33 (1), pp. 89–97.

Minnerup, Pascal Marcel (2017): An Efficient Method for Testing Autonomous Driving Software against Nondeterministic Influences. Dissertation. München, Technische Universität, München. Fakultät für Informatik.

Mirgel, Martin; Wruck, Oliver (2021): Geobasis NRW - Produkte und Dienstleistungen. Available online at https://www.bezreg-koeln.nrw.de/brk_internet/geobasis/index.html, updated on 3/19/2021, checked on 4/23/2021.

Mittlböck, Manfred; Atzl, Caroline (2015): Strategien für die Visualisierung und Kommunikation von raumzeitlichen Inhalten mit dynamischen Webkarten. In *AGIT Journal* 1, pp. 566–571.

Mohanadass, Araan (2020): Making the Most of the Energy We Have: Vehicle Efficiency. In Truong Quang Dinh (Ed.): Intelligent and Efficient Transport Systems - Design, Modelling, Control and Simulation: InTech.

National Highway Transportation Safety Agency (NHTSA) (2013): Preliminary statement of policy concerning automated vehicles. National Highway Transportation Safety Agency.

Nelder, J. A.; Mead, R. (1965): A Simplex Method for Function Minimization. In *The Computer Journal* 7 (4), pp. 308–313. DOI: 10.1093/comjnl/7.4.308.

Neubauer, Michael (2015): Verfahren zur Analyse des Nutzens von Fahrerassistenzsystemen mit Hilfe stochastischer Simulationsmethoden. Dissertation. Dresden, Technische Universität, Dresden. Fakultät Machinenwesen.

NHTSA (2016): Federal Automated Vehicles Policy; Accelerating the Next Revolution In Roadway Safety. Available online at https://www.hsdl.org/?view&did=795644, checked on 5/11/2021.

Nobis, Claudia; Kuhnimhof, Tobias (2018): Mobilität in Deutschland - MiD Ergebnisbericht. Studie von infas, DLR, IVT und infas 360 im Auftrag des Bundesministers für Verkehr und digitale Infrastruktur (FE-Nr. 70.904/15).

OpenLayers (2020): OpenLayers - Welcome. Available online at https://openlayers.org/, updated on 12/30/2020, checked on 12/31/2020.

OpenStreetMap (2020): OpenStreetMap. OpenStreetMap Foundation. Available online at https://www.openstreetmap.org/about, updated on 12/31/2020, checked on 12/31/2020.

Otte, Dietmar; Krettek, Christian; Brunner, H.; Zwipp, Hans (2003): Scientific Approach and Methodology of a New In-Depth-Investigation Study in Germany so called GIDAS. In: Proceedings. 18th International Technical Conference on the Enhanced Safety of Vehicles (ESV). Nagoya, Japan, May 19-22. NHTSA.

Ovcharova, Neli (2013): Methodik zur Nutzenanalyse und Optimierung sicherheitsrelevanter Fahrerassistenzsysteme. Dissertation. KIT. Fakultät für Maschinenbau.

Papadoulis, Alkis; Quddus, Mohammed; Imprialou, Marianna (2019): Evaluating the safety impact of connected and autonomous vehicles on motorways. In *Accident; analysis and prevention* 124, pp. 12–22. DOI: 10.1016/j.aap.2018.12.019.

Park, Byungkyu; Won, Jongsun (2006): Microscopic simulation model calibration and validation handbook. With assistance of Traffic Operations Laboratory, Center for Transportation Studies. Virginia Transportation Research Council. Charlottesville (FHWA/VTRC 07-CR6).

ISO 7975:2019: Passenger cars - Braking in a turn; Open-loop test method.

ISO 3888-1:2018: Passenger cars - Test track for a severe lane-change manoeuvre; Part 1: Double lane-change.

DIN 70028:2004: Personenkraftwaten - Messung des Bremsweges bei ABS-Bremsungen geradeaus.

pgRouting (2020): pgRouting Project — Open Source Routing Library. Available online at https://pgrouting.org/, updated on 10/6/2020, checked on 12/31/2020.

Pinter, Krisztian; Szalay, Zsolt; Vida, Gabor (2017): Liability in Autonomous Vehicle Accidents Liability in Autonomous. In *1* 19 (4), pp. 30–35. Available online at http://komunikacie.uniza.sk/index.php/communications/article/view/267.

Pinter, Krisztian; Szalay, Zsolt; Vida, Gabor (2021): Road Accident Reconstruction Using Onboard Data, Especially Focusing on the Applicability in Case of Autonomous Vehicles. In *Period. Polytech. Transp. Eng.* 49 (2), pp. 139–145. DOI: 10.3311/PPtr.13469.

PostGIS (2020): PostGIS — Spatial and Geographic Objects for PostgreSQL. Available online at https://postgis.net/, updated on 12/25/2020, checked on 12/31/2020.

Proff, Heike; Proff, Harald (2008): Dynamisches Automobilmanagement; Strategien für Hersteller und Zulieferer im internationalen Wettbewerb: Springer-Verlag.

Rabsatt, Vince Vincent (2018): Improving Traffic Efficiency and Safety via Vehicular Communications. Dissertation. UCLA, Los Angeles. Computer Science. Available online at https://escholarship.org/uc/item/5t48773h.

Rasmussen, Jens (1983): Skills, rules, and knowledge; signals, signs, and symbols, and other distinctions in human performance models. In *IEEE Trans. Syst., Man, Cybern.* SMC-13 (3), pp. 257–266. DOI: 10.1109/TSMC.1983.6313160.

Reinisch, Philipp (2013): Eine risikoadaptive Eingriffsstrategie für Gefahrenbremssysteme. Duisburg-Essen, Universität, Duisburg. Fakultät für Ingenieurwissenschaften.

Riebl, Raphael; Obermaier, Christina; Neumeier, Stefan; Facchi, Christian (2017): Vanetza: Boosting Research on Inter-Vehicle Communication. In Anatoli Djanatliev, Kai-Steffen Hielscher, Christoph Sommer, David Eckhoff, Reinhard German (Eds.): Proceedings of the 5th GI/ITG KuVS Fachgespräch Inter-Vehicle Communication (FG-IVC 2017). Erlangen, 6-7 April, pp. 37–40.

ISO 611:2003: Road vehicles - Braking of automotive vehicles and their trailers - Vocabulary.

ISO 17287:2003: Road vehicles - Ergonomic aspects of transport information and control systems; Procedure for assessing suitability for use while driving.

ISO 15037-1:2019: Road vehicles - Vehicle dynamics test methods; Part 1: General conditions for passenger cars.

Robert Bosch GmbH (2018): Bosch-Auswertung: Fahrerassistenzsysteme sind weiter stark auf dem Vormarsch. Stuttgart. Available online at https://www.bosch-presse.de/pressportal/de/de/bosch-auswertung-fahrerassistenzsysteme-sind-weiter-stark-auf-dem-vormarsch-148032.html, checked on 4/26/2021.

Robin Chase (2021): Shared Mobility Principles for Livable Cities. Available online at https://www.sharedmobilityprinciples.org/, updated on 1/21/2021, checked on 1/21/2021.

Roth, Martin; Radke, Tobias; Lederer, Matthias; Gauterin, Frank; Frey, Michael; Steinbrecher, Christian et al. (2011): Porsche InnoDrive – An innovative approach for the future of driving. In: 20th Aachen Colloquium Automobile and Engine Technology. Aachen, Oct. 11-12.

Schiller, Thomas; Rothmann, Katherine; Götze, Kristian (2016): Autonomes Fahren in Deutschland – Wie Kunden überzeugt werden. Deloitte Touche Tohmatsu Limited.

Schmid, Stephan (2005): Externe Kosten des Verkehrs: Grenz- und Gesamtkosten durch Luftschadstoffe und Lärm in Deutschland; External costs of transport: marginal and total costs due to air pollutants and noise in Germany. Dissertation. Universität Stuttgart, Stuttgart. Fakultät Maschinenbau.

Schnabel, Werner; Lohse, Dieter; Knote, Thoralf (Eds.) (2011): Straßenverkehrstechnik. 3., vollständig überarb. Aufl. Berlin, Bonn: Beuth; Kirschbaum (Studium, / Schnabel; Lohse ; Bd. 1). Available online at http://www.beuth.de/cmd?level=tpl-langanzeige&websource=vlb&smoid=116949588.

Schnieder, Eckehard; Becker, Uwe (2007): Verkehrsleittechnik; Automatisierung des Straßen- und Schienenverkehrs. Berlin, Heidelberg: Springer-Verlag Berlin Heidelberg (VDI-Buch). Available online at http://site.ebrary.com/lib/alltitles/docDetail.action?docID=10203831.

Schnieder, Eckehard; Schnieder, Lars (2013): Verkehrssicherheit; Maße und Modelle, Methoden und Maßnahmen für den Straßen-und Schienenverkehr: Springer-Verlag.

Schramm, Dieter; Hesse, Benjamin; Maas, Niko; Unterreiner, Michael (2020): Vehicle technology; Technical foundations of current and future motor vehicles. [1. Auflage]. Berlin: De Gruyter Oldenbourg (Graduate).

Schramm, Dieter; Hiller, Manfred; Bardini, Roberto (2018): Vehicle Dynamics; Modeling and Simulation. 2nd. Berlin, Heidelberg: Springer.

Schrank, David; Eisele, Bill; Lomax, Tim; Bak, Jim (2015): 2015 Urban Mobility Scorecard. Available online at https://trid.trb.org/view/1367337.

Schuster, Christian (1998): Strukturvariante Modelle zur Simulation der Fahrdynamik bei niedrigen Geschwindigkeiten. Dissertation. Gerhard-Mercator-Universität, Duisburg. Fachbereich Maschinenbau.

Schweig, Stephan; Liebherr, Magnus; Schramm, Dieter; Brand, Matthias; Maas, Niko (2018): The Impact of Psychological and Demographic Parameters on Simulator Sickness. In. 8th International Conference on Simulation and Modeling Methodologies, Technologies and Applications. Porto, Portugal, 7/29/2018 - 7/31/2018. Porto: SCITEPRESS - Science and Technology Publications, pp. 91–97.

Shimada, Hideki; Yamaguchi, Akihiro; Takada, Hiroaki; Sato, Kenya (2015): Implementation and evaluation of local dynamic map in safety driving systems. In *Journal of Transportation Technologies* 5 (02), p. 102.

Simpson, John Andrew; Weiner, Edmund S. C.; Murry, James Augustus Henry (1989): The Oxford English dictionary. 2. ed. Oxford: Clarendon Press. Available online at http://www.loc.gov/catdir/enhancements/fy0604/88005330-d.html.

Sommer, C.; German, R.; Dressler, F. (2011): Bidirectionally Coupled Network and Road Traffic Simulation for Improved IVC Analysis. In *IEEE Trans. on Mobile Comput.* 10 (1), pp. 3–15. DOI: 10.1109/TMC.2010.133.

Sommerville, Ian (2018): Software Engineering. 10., aktualisierte Auflage. Hallbergmoos: Pearson (it - informatik).

Sparmann, U. (1978): Spurwechselvorgänge auf zweispurigen BAB-Richtungsfahrbahnen: Bundesminister für Verkehr, Abt. Straßenbau (Forschung Straßenbau und Straßenverkehrstechnik). Available online at https://books.google.de/books?id=-dvTSgAACAAJ.

Spitzhüttl, Florian; Liers, Henrik (2016): Methodik zur Erstellung von Verletzungsrisikofunktionen aus Realunfalldaten. Edited by Verband der Automobilindustrie e.V. (VDA). Berlin. Available online at https://www.vda.de/de/services/Publikationen/Publikation.~1492~.html, checked on 5/28/2021.

Stamen Design (2016): maps.stamen.com / toner. Available online at http://maps.stamen.com/toner/#14/51.3782/6.5190, updated on 8/4/2016, checked on 4/23/2021.

IEEE 1609.2:2016: Standard for Wireless Access in Vehicular Environments; Security Services for Applications and Management Messages.

Statistisches Bundesamt (Destatis) (2019): Fachserie Verkehr 8, Reihe 7 Verkehrsunfälle 2018. Wiesbaden.

Statistisches Bundesamt (Destatis) (2020): Fachserie Verkehr 8, Reihe 7 Verkehrsunfälle 2019. Destatis. Wiesbaden.

Stern, Andrew D.; Shah, Vaishali; Goodwin, Lynette; Pisano, Paul (Eds.) (2003): Analysis of weather impacts on traffic flow in metropolitan Washington DC. Washington D.C., 2003. Mitretek Systems, Inc.; Federal Highway Administration.

Stiller, Christoph; León, Fernando Puente; Kruse, Marco (2011): Information fusion for automotive applications – An overview. In *Information fusion* 12 (4), pp. 244–252.

Sugiyama, Yuki; Fukui, Minoru; Kikuchi, Macoto; Hasebe, Katsuya; Nakayama, Akihiro; Nishinari, Katsuhiro et al. (2008): Traffic jams without bottlenecks—experimental evidence for the physical mechanism of the formation of a jam. In *New J. Phys.* 10 (3), p. 33001. DOI: 10.1088/1367-2630/10/3/033001.

SAE J3016:2021: SURFACE VEHICLE RECOMMENDED PRACTICE; Taxonomy and Definitions for Terms Related to Driving Automation Systems for On-Road Motor Vehicles.

Szalay, Zsolt (2021): Next Generation X-in-the-Loop Validation Methodology for Automated Vehicle Systems. In *IEEE Access* 9, pp. 35616–35632. DOI: 10.1109/ACCESS.2021.3061732.

Szalay, Zsolt; Ficzere, Dániel; Tihanyi, Viktor; Magyar, Ferenc; Soós, Gábor; Varga, Pál (2020): 5G-Enabled Autonomous Driving Demonstration with a V2X Scenario-in-the-Loop Approach. In *Sensors (Basel, Switzerland)* 20 (24). DOI: 10.3390/s20247344.

Szalay, Zsolt; Szalai, Metyas; Toth, Balint; Tettamanti, Tamas; Tihanyi, Viktor (2019): Proof of concept for Scenario-in-the-Loop (SciL) testing for autonomous vehicle technology. In: 2019

IEEE International Conference on Connected Vehicles and Expo (ICCVE), 4-8 Nov. 2019: IEEE.

Telpaz, Ariel; Baltaxe, Michael; Hecht, Ron M.; Cohen-Lazry, Guy; Degani, Asaf; Kamhi, Gila (2018): An Approach for Measurement of Passenger Comfort: Real-Time Classification based on In-Cabin and Exterior Data. In. 2018 21st International Conference on Intelligent Transportation Systems (ITSC). Maui, HI, 04.11.2018 - 07.11.2018: IEEE, pp. 223–229.

Toledo, Tomer; Koutsopoulos, Haris N.; Ben-Akiva, Moshe (2007): Integrated driving behavior modeling. In *Transportation Research Part C: Emerging Technologies* 15 (2), pp. 96–112. DOI: 10.1016/j.trc.2007.02.002.

Török, Árpád; Szalay, Zsolt; Uti, Gábor; Verebélyi, Bence (2020): Rerepresenting Autonomated Vehicles in a Macroscopic Transportation Model. In *Periodica Polytechnica Transportation Engineering* 48 (3), pp. 269–275. DOI: 10.3311/PPtr.13989.

RFC 793, 1981: Transmission Control Protocol (TCP). Available online at https://www.rfc-editor.org/rfc/pdfrfc/rfc793.txt.pdf, checked on 5/17/2021.

Transportation Research Board (2000): Highway Capacity Manual 2000. Washington D.C.: Transportation Research Board.

Treiber, Martin; Kesting, Arne (2013): Traffic Flow Dynamics; Data, Models and Simulation, Springer-Verlag Berlin Heidelberg. Berlin Heidelberg: Springer.

Umweltbundesamt (2021): Trends der Niederschlagshöhe. Available online at https://www.umweltbundesamt.de/daten/klima/trends-der-niederschlagshoehe, updated on 9/14/2021, checked on 9/14/2021.

Unterreiner, Michael (2014): Modellbildung und Simulation von Fahrzeugmodellen unterschiedlicher Komplexität. Dissertation. Universität Duisburg-Essen, Duisburg. Fakultät für Ingenieurwissenschaften. Available online at https://duepublico2.uni-due.de/receive/duepublico_mods_00034562.

Unterreiner, Michael (2020): Sensorsystem zur autonomen Fahrbahnzustandserkennung (SEEROAD) : Abschlussbericht : Teilvorhabenbezeichnung: Fahrezugintegration, Verteilung Fahrbahnzustandsinformationen, Fahrzeugvernetzung, Fahr-/Betriebsstrategie : Laufzeit: 1. März 2017-29.Februar 2020. With assistance of TIB-Technische Informationsbibliothek Universitätsbibliothek Hannover.

RFC 768, 1980: User Datagram Protocol (UDP). Available online at https://www.rfc-editor.org/rfc/pdfrfc/rfc768.txt.pdf, checked on 5/17/2021.

SAE J2735:2020: V2X Communications Message Set Dictionary.

van der Zwaag, Marjolein D.; Dijksterhuis, Chris; Waard, Dick de; Mulder, Ben L. J. M.; Westerink, Joyce H. D. M.; Brookhuis, Karel A. (2012): The influence of music on mood and performance while driving. In *Ergonomics* 55 (1), pp. 12–22. DOI: 10.1080/00140139.2011.638403.

Varga, Andras (2010): OMNeT++. In Klaus Wehrle, Mesut Güneş, James Gross (Eds.): Modeling and tools for network simulation. Berlin, Heidelberg: Springer, pp. 35–59.

VDA (2015): Von Fahrerassistenzsystemen zum automatisierten Fahren. Berlin.

Wang, Chao; Quddus, Mohammed A.; Ison, Stephen G. (2009): Impact of traffic congestion on road accidents: a spatial analysis of the M25 motorway in England. In *Accident; analysis and prevention* 41 (4), pp. 798–808. DOI: 10.1016/j.aap.2009.04.002.

Weber, Daniel (2012): Untersuchung des Potenzials einer Brems-Ausweich-Assistenz. Dissertation. KIT, Karlsruhe. Fakultät für Maschinenbau.

Weber, Ingo (2004): Verbesserungspotenzial von Stabilisierungssystemen im Pkw durch eine Reibwertsensorik. Dissertation. Darmstadt, Technische Universität.

Weber, Thomas (2017): Development of a Navigation System for the Simulative Investigation of the Navigation Level Regarding Highly and Fully Automated Driving Operation. Master. University Duisburg-Essen, Duisburg. Mechatronics.

Weber, Thomas; Driesch, Patrick; Schramm, Dieter (2020): Data-Driven BEV Modeling for Realistic Consumption Calculation in Traffic Simulation. In: AmE 2020. Automotive meets Electronics : Beiträge der 11. GMM-Fachtagung, 10.-11. März 2020 in Dortmund. Berlin, Offenbach: VDE VERLAG GMBH (GMM-Fachbericht, 95), pp. 54–59.

Weber, Thomas; Frey, Jan; Schramm, Dieter (2021): Weather Module Extension of a Driving Simulation Environment for ADAS and DAS Research. In: 7th Symposium Driving Simulation 2021. Automotive Solution Center for Simulation e.V. Stuttgart.

Weber, Thomas; Schramm, Dieter (2020a): Sensorsystem zur autonomen Fahrbahnzustandserkennung (SEEROAD) : Abschlussbericht : Teilvorhabenbezeichnung: Fahrzeugmodell, Fahrzeugsimulation : Laufzeit: 1. März 2017-29.Februar 2020. With assistance of TIB-Technische Informationsbibliothek Universitätsbibliothek Hannover.

Weber, Thomas; Schramm, Dieter (2020b): Simulation-based assessment of a road surface condition aware adaptive cruise control. In *IJAMECHS* 8 (4), pp. 166–176. DOI: 10.1504/IJAMECHS.2020.112633.

Weiß, Christian (2017): Sichere Intelligente Mobilität Testfeld Deutschland (simTD); Deliverable D5.5 TP5-Abschlussbericht - Teil A. With assistance of Daimler AG. Sindelfingen (D5.5). Available online at https://www.eict.de/fileadmin/redakteure/Projekte/simTD/Deliverables/simTD-TP5-Abschlussbericht_Teil_A_Manteldokument_V10.pdf, checked on 10/9/2017.

Whitley, Darrell (1994): A genetic algorithm tutorial. In *Stat Comput* 4 (2). DOI: 10.1007/BF00175354.

WHO (2018): Global status report on road safety 2018. World Health Organization. Geneva, Switzerland.

Wiedemann, Rainer (1974): Simulation des Straßenverkehrsflusses. Habilitation. Universität Karlsruhe, Karlsruhe. Institut für Verkehrswesen. Available online at http://worldcatlibraries.org/wcpa/oclc/634105860.

Winner, Hermann; Hakuli, Stephan; Lotz, Felix; Singer, Christina (Eds.) (2015): Handbuch Fahrerassistenzsysteme; Grundlagen, Komponenten und Systeme für aktive Sicherheit und Komfort. 3., überarbeitete und ergänzte Auflage. Wiesbaden: Springer Vieweg (ATZ / MTZ-Fachbuch).

DIN EN 15518-3:2011: Winterdienstausrüstung - Straßenzustands- und Wetterinformationssysteme - Teil 3; Anforderungen an gemessene Werte der stationären Anlagen.

Wu, Cathy; Bayen, Alexandre M.; Mehta, Ankur (2018): Stabilizing Traffic with Autonomous Vehicles. In: 2018 IEEE International Conference on Robotics and Automation (ICRA). 2018 IEEE International Conference on Robotics and Automation (ICRA). Brisbane, QLD, 21.05.2018 - 25.05.2018: IEEE, pp. 1–7.

Xiao, Lin; Wang, Meng; van Arem, Bart (2017): Realistic Car-Following Models for Microscopic Simulation of Adaptive and Cooperative Adaptive Cruise Control Vehicles. In *Transportation Research Record* 2623 (1), pp. 1–9. DOI: 10.3141/2623-01.

Yi, Kyongsu; Woo, Minsu; KIM, Sunga; Lee, Seongchul (1999): A study on a road-adaptive CW/CA algorithm for automobiles using HiL simulations. In *JSME International Journal Series C Mechanical Systems, Machine Elements and Manufacturing* 42 (1), pp. 163–170.

Zeng, X.; Bagrodia, R.; Gerla, M. (1998): GloMoSim: a library for parallel simulation of large-scale wireless networks. In: Proceedings / Twelfth Workshop on Parallel and Distributed Simulation, PADS '98. PADS 98: Parallel and Distributed Simulation '98. Banff, Alta., Canada, 26-29 May 1998. Los Alamitos, Calif.: IEEE Computer Society Press (SIGSIM Newsletter, 28.1998,1), pp. 154–161.

Zhurovskyj, Mychajlo Z.; Pankratova, N. D. (2007): System analysis; Theory and applications ; with 26 tables. Berlin, Heidelberg: Springer (Data and knowledge in a changing world).

Zomotor, Adam; Braess, Hans-Hermann; Rönitz, Rolf (1998): Verfahren und Kriterien zur Bewertung des Fahrverhaltens von Personenkraftwagen. In *ATZ - Automobiltechnische Zeitschrift* 100 (3), pp. 236–243. DOI: 10.1007/BF03223403.

Publications of the Author with Relevance to the Thesis

2021

Weber, Thomas; Frey, Jan; Schramm, Dieter (2021): Integration of Weather in a Driving Simulation Environment for ADAS and ADS Research. [Manuscript submitted for publication]. In: International Journal of Automotive Engineering. ISSN 2185-0992.

Weber, Thomas; Frey, Jan; Schramm, Dieter (2021): Weather Module Extension of a Driving Simulation Environment for ADAS and DAS Research. In: 7th Symposium Driving Simulation 2021. Automotive Solution Center for Simulation e.V. Stuttgart.

Ma, Xiaoyi; Hu, Xiaowei; Weber, Thomas; Schramm, Dieter (2021): Traffic Simulation of Future Intelligent Vehicles in Duisburg City Inner Ring. In *Applied Sciences* 11 (1), p. 29. DOI: 10.3390/app11010029.

Ma, Xiaoyi; Hu, Xiaowei; Weber, Thomas; Schramm, Dieter (2021): Experiences with Establishing a Simulation Scenario of the City of Duisburg with Real Traffic Volume. In *Applied Sciences* 11 (3), p. 1193. DOI: 10.3390/app11031193.

Ma, Xiaoyi; Hu, Xiaowei; Weber, Thomas; Schramm, Dieter (2021): Evaluation of Accuracy of Traffic Flow Generation in SUMO. In *Applied Sciences* 11 (6), p. 2584. DOI: 10.3390/app11062584.

2020

Weber, Thomas; Schramm, Dieter (2020): Simulation-based assessment of a road surface condition aware adaptive cruise control. In IJAMECHS 8 (4), p. 166-176. DOI: 10.1504/IJAMECHS.2020.112633.

Weber, Thomas; Schramm, Dieter (2020): Sensorsystem zur autonomen Fahrbahnzustandserkennung (SEEROAD) : Abschlussbericht : Teilvorhabenbezeichnung: Fahrzeugmodell, Fahrzeugsimulation : Laufzeit: 1. März 2017-29.Februar 2020. With assistance of TIB-Technische Informationsbibliothek Universitätsbibliothek Hannover.

Weber, Thomas; Driesch, Patrick; Schramm, Dieter (2020): Data-Driven BEV Modeling for Realistic Consumption Calculation in Traffic Simulation. In : AmE 2020. Automotive meets Electronics : Beiträge der 11. GMM-Fachtagung, 10.-11. März 2020 in Dortmund. Berlin, Offenbach: VDE VERLAG GMBH (GMM-Fachbericht, 95), pp. 54–59.

Ma, Xiaoyi; Hu, Xiaowei; Thomas, Weber; Dieter, Schramm (2020): Effects of Automated Vehicles on Traffic Flow with Different Levels of Automation. In IEEE Access, p. 1. DOI: 10.1109/ACCESS.2020.3048289.

2019

Weber, Thomas; Driesch, Patrick; Schramm, Dieter (2019): Introducing Road Surface Conditions into a Microscopic Traffic Simulation. In: SUMO User Conference. SUMO User Conference 2019: EasyChair (EPiC Series in Computing), 172-156.

Brisch, Klaus; Eckhardt, Jens; Gelderie, Marcus; Weber, Thomas; Schramm, Dieter; Groß, Daniel et al. (2019): Vernetzte und autonome Mobilität - Herausforderungen für Cybersicherheit und Datenschutz sowie Gewährleistungs- und Haftungsrecht. Edited by eco - Verband der Internetwirtschaft e.V.

Supervised Theses

Bachelor

Frey, Jan (2018): Development of an Optimization Algorithm for Mapping Real Traffic Data in a Traffic Flow Simulation. Bachelor. University Duisburg-Essen, Duisburg. Mechatronics.

Wang, Jie (2017): Implementation and Assessment of a Friction-Dependent ACC in a Driving Simulator. Bachelor. University Duisburg-Essen, Duisburg. Mechatronics.

Zhao, Zijan (2017): Offline Map-Matching of Journey Data for the Improvement of Data Quality. Bachelor. University Duisburg-Essen, Duisburg. Mechatronics.

Master

Frey, Jan (2021): Potentials of Vehicle Networking on the Navigation Level for Automated Driving Operations Based on a Traffic Flow Simulation. Master. University Duisburg-Essen, Duisburg. Mechatronics.

Han, Berhan (2020): Conceptual Design and Implementation of a Decentralized Sensor Data Processing Using the Example of a Filter Algorithm. Master. University Duisburg-Essen, Duisburg. Mechatronics.

Knospe, Max (2018): Development and Simulation of a Friction-Dependent Longitudinal and Lateral Guidance and the Effects on Driver Assistance Systems in Highly Automated Driving. Master. University Duisburg-Essen, Duisburg. Mechatronics.

Bronkalla, Florian (2017): Extension of a Spatial Two-Lane Model by a Complex Tire Model and Simulative Analysis of the Influence of the Road Condition on the Vehicle Dynamics. Master. University Duisburg-Essen, Duisburg. Mechatronics.

DOI: 10.17185/duepublico/75278
URN: urn:nbn:de:hbz:464-20220131-151726-9